# Genetic and Molecular Characterization of New Genes which Influence Germline Apoptosis in *C. elegans*

---

**Dissertation**

zur

Erlangung der naturwissenschaftlichen Doktorwürde

(Dr. sc. nat.)

vorgelegt der

Mathematisch-naturwissenschaftlichen Fakultät

der

**Universität Zürich**

von

**Polina Kamkina**

aus

**der Ukraine**

Promotionskommission

Prof. Dr. Michael Hengartner (Vorsitz und Leitung der Dissertation)

Prof. Dr. Alex Hajnal

Prof. Dr. Barbara Conradt

Prof. Dr. Damian Brunner

Zürich, 2018

*To my parents*

*"The future belongs to those who believe*
*in the beauty of their dreams"*

*Eleanor Roosevelt*

# • Acknowledgements •

I would like to express my deepest gratitude to all people who contributed directly or indirectly to the completion of this tremendous amount of work. This thesis is a result of our combined effort.

Foremost, I would like to thank sincerely my supervisor, Michael Hengartner for the continuous support of my research. Michael encouraged me with challenging and exciting projects so that I could learn the most. Thank you Michael for all those hours we spend on discussing data, planning new experiments and writing manuscripts. Thank you for your patience and wise guidance.

I am very grateful to my thesis committee members Barbara Conradt, Alex Hajnal and Damian Brunner for giving insightful comments and suggestions on my research.

Also, I would like to thank Sabine Schrimpf for being a great supervisor of my Master Thesis and for introducing me into the exciting field of proteomics. Furthermore, the FGCZ provided a lot of framework for the proteomic studies. Here, I would like to acknowledge Jonas Grossmann, Bernd Roschitzki and Claudia Fortes. Additionally, I would like to thank Michael Daube, Sergio Pinto and Xue Zheng for helping me with the daily lab work.

I am also very grateful to the members of Hajnal lab for having me being part of them during the last two years of my PhD. The group has been a source of friendships as well as good advice and collaboration. Thank you for being so kind and friendly.

Special thank you goes to our institute IT Support Werner Wolz who did regular check-ups of my laptop. I would also like to acknowledge our secretaries Angela Lloyd and Martin Daellenbach for being so professional in handling administrative issues.

Importantly, I would like to express the sincere appreciation to my partner, my mother and father, my sister and other relatives for giving me a great backup during this intensive time. Thank you for your unconditional love, dedication, care and encouragement.

# • Table of Contents•

**Acknowledgements** ..... **iv**

**Table of Contents** ..... **v**

**List of Figures, Supplemental Figures and Tables** ..... **viii**

**Abbreviations** ..... **x**

**Summary** ..... **xi**

**Zusammenfassung** ..... **xiii**

**Chapter 1. General Introduction: Apoptosis in *C. elegans*** ..... **1**

1.1 Apoptosis - general features ..... 2

1.2 Somatic cell death during *C. elegans* development ..... 2

1.2.1 Core apoptotic machinery in *C. elegans* ..... 3

1.2.1.1 The CED-3 caspase ..... 3

1.2.1.2 The CED-4 Apaf-1 homolog ..... 6

1.2.1.3 The CED-9 BCL-2 homolog ..... 7

1.2.1.4 The BH3-only protein EGL-1 ..... 9

1.3. Programmed cell death in the *C. elegans* germ line ..... 11

1.3.1 Development of the *C. elegans* germ line ..... 11

1.3.2 Physiological germline apoptosis ..... 13

1.3.2.1 Why do so many apparently healthy germ cells die? ..... 14

1.3.2.2 Regulation of physiological germline apoptosis ..... 15

1.3.3 DNA damage-induced germline apoptosis ..... 16

1.3.3.1 DNA damage checkpoint signaling ..... 17

1.3.3.2 The CEP-1 p53 tumor suppressor homolog ..... 17

1.3.4 Post-transcriptional regulation of germline apoptosis in *C. elegans* ..... 20

1.3.4.1 miRNAs ..... 22

1.3.4.1.1 miRNA biogenesis ..... 23

1.3.4.1.2 Cell-autonomous and circulating miRNAs ..... 25

1.3.4.1.3 miRNA target recognition ..... 26
1.3.4.1.4 miRNA regulation of post-transcriptional gene expression ..... 27
1.4. Overview of my research ..... 29
1.5. References ..... 32

**Chapter 2. *mir-52* is a novel cell-autonomous enhancer of germline apoptosis in *C. elegans* ..... 62**

2.1 Preface ..... 63
2.2 Abstract ..... 65
2.3 Introduction ..... 66
2.4 Results ..... 68
2.4.1 Loss of *mir-52* impairs DNA damage-induced germ cell death ..... 68
2.4.2 Other *mir-51* family members do not affect germ cell apoptosis ..... 69
2.4.3 Apoptotic cell clearance is not affected in *mir-52* compromised worms ..... 69
2.4.4 MAPK signaling is not responsible for *mir-52(n4114)* apoptotic defects upon IR ..... 70
2.4.5 Loss of *mir-52* influences germline apoptosis downstream of or in parallel to *cep-1* ..... 70
2.4.6 *mir-52(n4114)* suppresses germline apoptosis of *ced-9(n1653ts)* ..... 71
2.4.7 *mir-52(n4114)* alters subcellular localization pattern of CED-3::GFP in the germ line 71
2.5 Discussion and Outlook ..... 72
2.6 Materials and Methods ..... 75
2.6.1 *C. elegans* maintenance and strains ..... 75
2.6.2. Generation of transgenic line ..... 75
2.6.3 Apoptotic assays ..... 76
2.6.4 Western blot ..... 76
2.6.5 Microscopy ..... 77
2. 7 Acknowledgements and Funding ..... 77
2.8 Disclosure Declaration ..... 77
2.9 Correspondence ..... 77
2.10 Figure Legends ..... 78
2.11 References ..... 82
2.12 Figures and Tables ..... 89

**Appendix 1. *mir-242(n4605)* and *mir-249(n4983)* influence germline apoptosis in *C. elegans*.....103**

A1.1 Additional miRNA mutants that affect germline apoptosis in *C. elegans*.....104

A1.1.1 *mir-242(n4605)* enhances physiological germline apoptosis.....104

A1.1.2 *mir-249* suppresses DNA damage-induced germ cell death.....104

A1.2. Figure Legends.....106

A1.3. References.....107

A1.4. Figures.....108

**Chapter 3. Upstream regulation of CED-9 during physiological germline apoptosis in *C. elegans*.....112**

3.1 Introduction.....113

3.1.1 *n1653* temperature-sensitive *ced-9 loss-of-function* allele.....113

3.1.2 Experimental design of the forward genetic screens.....114

3.2 Results.....115

3.2.1 Validation of the screening strategy which utilizes tissue-specific *ced-3(RNAi)*.....115

3.2.2 Development of the screening strategy using *Ppie-1::ced-3::gfp::ced-3 3' UTR* transgene.....116

3.2.3 Forward genetic screen using *Ppie-1::ced-3::gfp::ced-3 3' UTR* transgene.....116

3.2.4 Forward genetic screen using tissue-specific *ced-3(RNAi)*.....117

3.3 Discussion.....118

3.4 Figure Legends.....120

3.5 References.....121

3.6 Figures and Tables.....123

**Appendix 2. Quantitative proteome analysis of natural genetic variation in *C. elegans*.....129**

A2.1 Preface.....130

A2.2. Reprint of the research article *Kamkina et al., 2016*.....132

A2.2 Reprint of the research article *Singh et al., 2016*.....144

# • List of Figures, Supplemental Figures and Tables •

## Chapter 1. General introduction: Apoptosis in *C. elegans*

**Fig. 1.1** Germline development and apoptosis…..……..…..30

**Fig. 1.2** miRNA biogenesis……31

## Chapter 2. *mir-52* is a novel cell-autonomous enhancer of germline apoptosis in *C. elegans*

**Fig. 2.1** Loss of *mir-52* impairs DNA damage-induced germ cell death…….……..89

**Fig. 2.2** *mir-52* controls germline apoptosis cell-autonomously……90

**Fig. 2.3** Other *mir-51* family members do not contribute to IR-induced germ cell death…….…91

**Fig. 2.4** Apoptotic cell corpse clearance is normal in *mir-52* mutants……..….92

**Fig. 2.5** *mir-52(n4114)* likely acts independently of the MAPK signaling pathway to control IR-induced germ cell death……...……..93

**Fig. 2.6** Loss of *mir-52* affects germline apoptosis downstream of or in parallel to *cep-1*……94

**Fig. 2.7** CED-3::GFP localization pattern is changed in *mir-52(n4114)* mutant……...…95

**Supplemental Fig. 2.1** The genomic location of *mir-51* family and structure of *mir-52* germline-specific rescue transgene……...…….99

**Supplemental Fig. 2.2** The requirement of *mir-52* for DNA-damage induced germ cell death is temperature dependent…….....……100

**Supplemental Fig. 2.3** *mir-52* tissue-specific rescue of germline apoptosis at 25 ˚C……..101

**Supplemental Fig. 2.4** Physiological germline apoptosis is slightly reduced in *mir-52* and engulfment double mutants……..……102

**Table 2.1** 55 miRNA mutants were analyzed for the defects in germline apoptosis……96

## Appendix 1. *mir-242(n4605)* and *mir-249(n4983)* influence germline apoptosis in *C. elegans*

**Appendix Fig. 1.1** Apoptotic defects in *mir-242(n4605)* and *mir-249(n4983)* worms……..108

**Appendix Fig. 1.2** *mir-242* and *mir-249* are located on the chromosomes IV and X, respectively……..….109

**Appendix Fig. 1.3** *nhr-78* impairs physiological germline apoptosis…….110

**Appendix Fig. 1.4** Apoptotic cell corpse clearance is not affected in *mir-249(n4983)* mutants……..111

## Chapter 3. Upstream regulation of CED-9 during physiological germline apoptosis in *C. elegans*

**Fig. 3.1** Overview of the screening strategies which imply different apoptotic conditions in somatic tissue and germ line……...……..123

**Fig. 3.2** Structure of *opIs535 [Ppie-1::ced-3::gfp::ced-3 3' UTR]* transgene…….……124

**Fig. 3.3** DIC and fluorescence photomicrographs of *ced-9(n1653ts); ced-3(n717)* animals which carry *opIs535 [Ppie-1::ced-3::gfp::ced-3 3' UTR]* transgene……..125

**Fig. 3.4** Workflow of the EMS screens……126

**Table 3.1** Temperature optimization for the screening strategy which utilizes tissue-specific *ced-3(RNAi)*……..127

**Table 3.2** Temperature optimization for the screening strategy using germline-specific expression of a *ced-3::gfp* transgene……..……128

# • Abbreviations •

| | |
|---|---|
| Apaf | Apoptosis activator factor |
| caspase | Cysteine aspartate protease |
| *C. elegans* | *Caenorhabditis elegans* |
| BH | domain Bcl-2 homology domain |
| bp | base pair |
| *D. melanogaster* | *Drosophila melanogaster* |
| DBD | DNA binding domain |
| DSBs | double-strand DNA breaks |
| *E. coli* | *Escherichia coli* |
| *gf* | *gain-of-function* |
| GFP | Green fluorescent protein |
| H | hour |
| IR | ionizing irradiation |
| L1-4 | larval stage 1-4 |
| *lf* | *loss-of-function* |
| min | minutes |
| µl | microlitre |
| miRNA | microRNA |
| ml | millilitre |
| MosSCI | Mos1 transposase-mediated single-copy gene insertion |
| mRNA | messenger RNA |
| mRNP | messenger ribonucleoprotein particle |
| NGM | Nematode growth medium |
| ncRNA | non-coding RNA |
| PS | phosphatidylserine |
| RBP | RNA-binding proteins |
| SILAC | stable isotope labeling by amino acids in cell culture |
| SRM | selected reaction monitoring |
| Unc | uncoordinated |
| UTR | untranslated region |
| UV | ultraviolet irradiation |
| YA | young adult |

# • Summary •

Apoptosis is a form of programmed cell death which involves genetically determined elimination of cells that are no longer needed or potentially dangerous. Apoptotic removal of unwanted cells is crucial for animal development and tissue homeostasis. Malfunction of apoptosis can lead to cancer as well as various neurodegenerative and immune disorders. The first systematic genetic studies to uncover the molecular program promoting cell death were performed in the free-living soil nematode *Caenorhabditis elegans* (*C. elegans*). The resulting work led to the identification of a highly conserved molecular pathway that regulates apoptosis in most animal species, including humans (Chapter 1). Despite much work, several aspects of apoptosis regulation are not resolved yet. In this dissertation, I was mainly interested in the characterization of additional regulatory elements underlining germline apoptosis in *C. elegans*.

Germ cell death is a conserved feature of oocyte development in mammals, insects and nematodes. In *C. elegans* hermaphrodites, more than half of the developing oocytes die, in an apparent stochastic manner, in the absence of any evident apoptotic stimulus in a process that has been called "physiological germ cell death". How physiological germline apoptosis is controlled at the molecular level is currently largely unknown. What makes an apparently healthy germ cell become less preferred than the others? Are there any quality control genes which recognize unfavorable germ cell conditions? To answer these questions, I have developed two synthetic forward screening strategies that employ different apoptotic conditions in somatic tissue and in the germ line, and a hypomorphic *loss-of-function* allele of *ced-9*, a homolog of mammalian BCL-2 (Chapter 3).

Post-transcriptional control of gene expression defines an additional regulatory mode of germ cell death in *C. elegans*. Several RNA-binding proteins were found to influence germline apoptosis; by contrast, potential contribution of microRNAs (miRNAs) is largely unexplored. Through a candidate gene approach, I have identified *mir-52* as a cell-autonomous enhancer of physiological and DNA damage-induced germline apoptosis in *C. elegans* (Chapter 2). *mir-52* is a member of the old and highly conserved *mir-51* miRNA family, which influences germline apoptosis independently of other m*ir-51* family members, underlining its germline-specific functions. *mir-52* likely regulates downstream or in parallel to the p53 tumor suppressor homologue *cep-1*. In addition to my work on *mir-52*, I also identified two other miRNAs, *mir-242* and *mir-249*,

perturbations of which affect physiological and DNA damage-induced germline apoptosis in *C. elegans* (Appendix 1).

Lastly, I was also highly involved in two side projects, which were dealing with the effect of natural variation on gene expression (Appendix 2). In the first project, the quantitative proteome and transcriptome comparison of the two highly divergent *C. elegans* wild-type strains, Bristol (N2) and Hawaii (CB4856) was performed. The main findings here are: i) protein abundance of the two wild-type strains correlates more strongly than the protein abundance *vs* transcript abundance within each wild type; ii) differentially expressed proteins and mRNAs are enriched for genes that function in insulin-signaling and stress-response pathways, which might contribute to the longevity differences observed between N2 and CB4856. In the second collaborative project, the impact of natural genetic variation on signal transduction pathways relevant for cancer progression was analyzed using recombinant inbred lines (RILs) of N2 and CB4856. We found that selected proteins from four cancer signaling pathways (apoptosis, RAS/MAPK, Notch, and Wnt signaling) tend to be upregulated in CB4856 and several RILs relative to N2. Additionally, we detected a distant quantitative trait locus (QTL) on the left arm of chromosome II that affected protein abundance of the apoptotic cell corpse clearance protein PSR-1, and two separate QTLs that influenced developmental apoptosis and DNA damage-induced germ cell death on chromosome IV.

# • Zusammenfassung •

Apoptose ist eine Form des programmierten Zelltods, die zur aktiven Eliminierung von Zellen, welche nicht mehr benötigt werden oder möglicherweise für den Organismus gefährlich sind, führt. Die apoptotische Entfernung unerwünschter Zellen ist entscheidend für die Tierentwicklung und die Gewebehomöostase. Fehler bei der Apoptose können zu Krebs sowie verschiedenen neurodegenerativen und Immunstörungen führen. Erste systematische genetische Studien zur Aufdeckung des molekularen Programms zur Förderung des Zelltods wurden im frei lebenden Fadenwurm *Caenorhabditis elegans* (*C. elegans*) durchgeführt. Die resultierenden Arbeiten führten zur Identifizierung eines hochkonservierten apoptotischen Weges (Kapitel 1). Dennoch sind verschiedene Aspekte der Apoptose-Regulierung bis heute noch nicht gelöst. In dieser Dissertation war ich hauptsächlich an der Charakterisierung zusätzlicher regulatorischer Elemente interessiert, welche die Apoptose in der Keimbahn des *C. elegans* beeinflussen.

Der Keimzelltod ist ein Merkmal der Oozytenentwicklung bei Säugetieren, Insekten und Nematoden. In *C. elegans* Hermaphroditen, sterben mehr als die Hälfte der sich entwickelnden Oozyten auf einer scheinbaren stochastischen Weise, in Abwesenheit eines offensichtlichen apoptotischen Stimulus, in einem Prozess, der "physiologischer Keimzelltod" genannt wurde. Die molekularen Ursachen der physiologischen Apoptose in der Keimbahn zur Zeit sind noch weitgehend unbekannt. Was macht eine scheinbar gesunde Keimzelle weniger bevorzugt als die anderen? Gibt es Qualitätskontrollgene, die ungünstige Keimzellzustände erkennen? Um diese Fragen zu beantworten, habe ich zwei synthetische Forward-Screening-Strategien entwickelt, die unterschiedliche apoptotische Bedingungen in somatischem Gewebe und in der Keimbahn anwenden, kombiniert mit einem hypomorphen Funktionsverlust-Allel vom BCL-2 Homolog *ced-9* (Kapitel 3).

Die posttranskriptionelle Regulation spielt eine wichtige Rolle in der Regulierung des Keimzelltodes in *C. elegans*. Mehrere RNA-bindende Proteine wurden schon identifiziert, welche die Apoptose der Keimbahn beeinflussen. Der potentielle Beitrag von "microRNAs" (miRNAs) ist jedoch bis jetzt nur wenig erforscht worden. In einem Kandidatenscreen habe ich *mir-52* als einen zellautonomen Verstärker der physiologischen und DNA Schaden-induzierten Zelltod in der Keimbahn von *C. elegans* identifiziert (Kapitel 2). *mir-52* ist ein Mitglied der alten und hochkonservierten *mir-51* miRNA Familie, die verschiedene Entwicklungsprozesse reguliert.

*mir-52* beeinflusst Keimbahnapoptose unabhängig von anderen Mitgliedern der Familie, was seine keimzellenspezifischen Funktionen unterzeichnet. *mir-52* beeinflusst die Apoptose der Keimbahn wahrscheinlich stromabwärts oder parallel zum p53-Tumorsuppressor-Homolog *cep-1*. Ich habe auch zwei zusätzliche miRNAs, *mir-242* und *mir-249,* identifiziert, deren Störungen die physiologische und DNA Schaden-induzierten Keimbahn-Apoptose in *C. elegans* beeinflussen (Anhang 1).

Letzlich, war ich auch stark an zwei Nebenprojekten im Bereich der Auswirkungen von der natürlichen genetischen Variation auf die Genexpression ging (Anhang 2). Im ersten Projekt, verglichen wir die quantitative Proteome und Transkriptome der zwei stark divergenten *C. elegans* wildtyp Stämme Bristol (N2) und Hawaii (CB4856). Die Hauptergebnisse sind: i) die Proteinabundanz der zwei Wildtypstämme korreliert stärker als die Proteinabundanz gegenüber der Transkriptabundanz innerhalb jedes Wildtyps; ii) differentiell exprimierte Proteine und mRNAs sind angereichert für Gene, die in Insulinsignal- und Stressreaktionswegen funktionieren, was zu den Langlebigkeitsunterschieden beitragen könnte, die zwischen N2 und CB4856 beobachtet werden. Im zweiten Projekt, haben wir die Auswirkungen der natürlichen genetischen Variation auf Signalwege, die zur Krebsprogression beisteuern, mittels rekombinanter Inzuchtlinien (RILs) von N2 und CB4856 untersucht. Wir fanden heraus, dass ausgewählte Proteine aus vier Krebs-Signalwegen (Apoptose, Ras/MAPK, Notch und Wnt Signal) im Vergleich zu N2 tendenziell in CB4856 und verschiedenen RILs hochreguliert werden. Zusätzlich fanden wir einen Quantitativen Trait Locus (QTL) am linken Arm des Chromosoms II, der die Proteinabundanz des Zell-Kadaver-Beseitigungs-Protein PSR-1 beeinflusst, und zwei separate QTLs auf Chromosome IV, welche die Entwicklung von Apoptose und DNA Schaden-induzierten Keimzelltod beeinflussen.

# • Chapter 1 •

# General Introduction: Apoptosis in *C. elegans*

## 1.1 Apoptosis - general features

Apoptosis is a form of programmed cell death which involves genetically determined elimination of cells that are no longer needed (Lockshin and Williams, 1964). The process of programmed cell death was originally discovered in the mid-nineteenth century (Glucksmann, 1951) and is used to maintain cellular homeostasis during animal development, aging or in response to stress. Malfunction of apoptosis can lead to cancer, many neurodegenerative and immune disorders. Therefore, understanding the regulation of apoptosis is an important step towards treatment development for the pathological conditions.

Apoptotic cells undergo distinct morphological changes including cytoplasm shrinkage, nuclear DNA fragmentation, loss of mitochondrial membrane potential, and phosphatidylserine (PS) exposure on the surface of dying cell (Kerr et al., 1972; Wyllie, 1980; Fadok et al., 1998). Unlike necrotic cell death, which is associated with cells swelling and rapid loss of the membrane integrity, apoptosis generally does not provoke inflammation (Wallach et al., 2014). Apoptotic cells initially maintain their plasma membrane integrity keeping pro-inflammatory intracellular components within dying cells. To prevent secondary necrosis, neighboring cells rapidly ingest apoptotic cells before their disintegration (Kurosaka et al., 2003).

The first systematic genetic studies to uncover the molecular program promoting cell death were performed in the free-living soil nematode *Caenorhabditis elegans* (*C. elegans*, Horvitz, 2003). The resulting work led to the identification of an evolutionary conserved apoptotic pathway. The distinctive characteristics of *C. elegans* biology facilitated these groundbreaking studies. Firstly, programmed cell death is not essential for *C. elegans* viability. Secondly, apoptotic cells can be easily observed using differential interference contrast (DIC) microscopy in living organism, due to their distinctive retractile “button-like” appearance and transparent body of the worm. Thirdly, *C. elegans* has highly invariant pattern of cell divisions (Sulston and Horvitz, 1977; Sulston et al., 1983), the complete knowledge of which enabled analysis of the mutants at single cell level (Sulston and Horvitz, 1981). Lastly, approximately 60% of *C. elegans* genes have human counterparts (Harris et al., 2004)

## 1.2 Somatic cell death during *C. elegans* development

In *C. elegans*, somatic cell death occurs during embryonic and post-embryonic development in highly reproducible manner (Sulston and Horvitz, 1977; Sulston et al., 1983). Out of 1’090

somatic cells generated during the development of *C. elegans* hermaphrodite, 131 cells undergo programmed cell death. The majority of the 131 cells are removed during embryogenesis (Sulston et al., 1983). The rest of the cells die during the larval stage 2 (L2, Sulston and Horvitz, 1977). This process is referred to developmental apoptosis. In adult worms, somatic cells are entirely post-mitotic and thus tolerate high levels of DNA damage without the induction of ectopic cell death.

### 1.2.1 Core apoptotic machinery in *C. elegans*

For majority of the 131 cells, developmental apoptosis is mediated by the core apoptotic machinery, which is highly conserved from *C. elegans* to mammals. It consists of the pro-apoptotic BH3-only protein EGL-1, the anti-apoptotic BCL-2 family member protein CED-9, the Apaf-1 homolog CED-4, and the caspase CED-3. *egl-1* acts upstream of *ced-9* to induce apoptosis, *ced-9* acts upstream of *ced-4* to inhibit apoptosis, *ced-4* acts upstream of *ced-3* to kill cells (Shaham and Horvitz, 1996a; Conradt and Horvitz, 1998).

#### 1.2.1.1 The CED-3 caspase

CED-3 is a human interleukin-1β (ICE) cysteine-dependent, aspartate-specific protease, which triggers intracellular proteolysis cascade cell-autonomously (Yuan and Horvitz, 1990; Yuan et al., 1993; Shaham and Horvitz, 1996a; Xue et al., 1996). It was identified in a screen for the mutants in which most of the 131 cells failed to die (Ellis and Horvitz, 1986). Animals with "undead" cells do not show any obvious morphological or behavioral abnormalities (Ellis and Horvitz, 1986). The undead cells frequently adopt cell fates similar to that of the sister cells (Ellis and Horvitz, 1986). However, their differentiation is less efficient compared to the wild-type counterpart (Ellis and Horvitz, 1986). Overexpression of CED-3 in mammalian cells or in ALM neurons of *C. elegans* triggers ectopic apoptosis (Miura et al., 1993; Shaham and Horvitz, 1996a).

CED-3 is synthesized as a proenzyme/zymogen (proCED-3) which is auto-proteolyticaly cleaved by CED-4 to generate active protease (Xue et al., 1996). Mature CED-3 enzyme contains a large subunit of 17 kDa (p17) and a smaller subunit of 15 kDa (p15) or 13 kDa (p13, Xue et al., 1996). In transgenic worms containing mutant CED-3 protein, which carry missense mutations in the protease domain or has altered cleavage sites of proCED-3, nearly all ALM neurons survive (Shaham et al., 1999). Thus, protease activity of CED-3 and processing of proenzyme are essential for programmed cell death (Shaham et al., 1999; Xue et al., 1996). However, in *ced-3*

mutants with entirely deleted protease domain, including p17 and p15 domains, few cells undergo apoptosis in pharynx, which is completely suppressed in multiple missense *loss-of-function* (*lf*) mutants of *ced-3* (Shaham et al., 1999). This suggests, that some of the developmental cell death can still occur in the absence of CED-3 protease activity (Shaham et al., 1999).

CED-3 expression was identified in nearly all cells of early embryo, and in very few cells of larva and adult using the transgene which carried GFP insertion in *ced*-3 locus (Maurer et al., 2007). Recently, CED-3 perinuclear localization was detected broadly in the embryo using CED-3::GFP translational reporter (Subasic et al., 2016). Additionally, distinct CED-3 expression pattern was observed in the germ line (Subasic et al., 2016, section 3.4). CED-3 was strongly enriched in oocytic nuclei, and weak CED-3 perinuclear localization was identified in the rest of the germ line. Moreover, extensive post-transcriptional regulation of CED-3 expression in the germ line was discovered using the same translational reporter. Similarly, human executioner caspase CASP3 is also broadly regulated at the post-transcriptional level (Subasic et al., 2016).

CED-3 cleaves the substrates preferentially after DEVD sequence (Xue et al., 1996). The downstream targets of CED-3 regulate cellular disassembly process and PS exposure on the surface of the apoptotic cells. Nuclear DNA fragmentation is a hallmark of apoptosis. CED-3 initiates nuclear DNA fragmentation via cleavage of DCR-1 ribonuclease (*C. elegans* Dicer homolog) producing C-terminal cleavage product which generates 3'hydroxyl DNA nicks (tDCR-1, Nakagawa et al., 2010; Ge et al., 2014). Next, multi-nuclease degradosome complex is formed to turn 3'DNA nicks into single-stranded DNA gaps and double-stranded DNA breaks (Conradt et al., 2016). Degradosome consists of mitochondrial endonuclease CPS-6, nuclease factor CRN-1 and mitochondrial non-nuclease worm apoptosis-inducing factor homolog WAH-1 (Parrish et al., 2001, 2003; Wang et al., 2002b). Lastly, DNase II homologs NUC-1, CRN-6, and CRN-7 mediate further degradation of the fragmented nuclear DNA (Wu et al., 2000; Parrish and Xue, 2003; Lai et al., 2009).

Drastic structural rearrangements are observed in mitochondria during apoptosis. They include change in mitochondria size and cristae structure, increase in the outer membrane permeability, and mitochondrial fragmentation (Karbowski et al., 2002; Frezza et al., 2006; Goyal et al., 2007). These structural changes appear to affect the release of the pro-apoptotic factors which then activate the caspase in certain cellular contexts (Frank et al., 2001; Lee et al., 2004b; Frezza et al., 2006), but not in others (Delivani et al., 2006; Parone et al., 2006; Breckenridge et al., 2008;

Estaquier and Arnoult, 2007). In *C. elegans*, mutation in dynamin GTPase DRP-1 inhibits apoptotic mitochondrial fragmentation, which results in accumulation of additional undead cells during development (Jagasia et al., 2005). Other study have shown, however, that in the mutants with highly fragmented mitochondria neither the activation nor kinetics of apoptosis were affected (Breckenridge et al., 2008). Here, weak apoptotic defects were observed only in the sensitized backgrounds when dynamin GTPase DRP-1 or a homolog of human FIS-1 fission protein FIS-2 was mutated. Additionally, the extensive epistasis analysis suggested that *drp-1* and *fis-2* act downstream of *ced-3* independently of each other. Further, the overexpression of *drp-1* did not induce ectopic apoptosis. Finally, it was also shown that CED-3 cleaves DRP-1 *in vitro* which is important for DRP-1 pro-apoptotic functions *in vivo*, but is not essential for its mitochondrial fission function in *C. elegans*. Thus, authors conclude that mitochondrial fission does not activate apoptosis in *C. elegans*, and the primordial function of DRP-1 is to eliminate mitochondria after caspase activation. In mammals, DRP-1 has probably developed additional apoptotic functions mediating the release of pro-apoptotic factors for caspase activation (Breckenridge et al., 2008). Taken together, CED-3 promotes mitochondrial elimination in *C. elegans*.

CED-3 also mediates the inactivation of survival factors. CED-3 cleaves CNT-1 generating N-terminal phosphoinositide (PI)-binding cleavage product, tCNT-1 (Nakagawa et al., 2014). tCNT-1 is then translocated to the plasma membrane and blocks AKT binding to phosphatidylinositol (3, 4, 5)-trisphosphate (PIP3), thereby inhibiting its pro-survival activity (Nakagawa et al., 2010). It was also shown that CED-3 cleaves CED-9 at two sites near its amino terminus, whereas the presence of at least one uncleaved site is important for CED-9 anti-apoptotic function (Xue and Horvitz, 1997). This suggests that pro-survival CED-9 is another CED-3 substrate during the execution phase of apoptosis (Conradt et al., 2016).

PS externalization is a conserved apoptotic event which serves as “eat me” signal and induces engulfment of dying cells (Venegas and Zhou, 2007; Wang et al., 2007; Züllig et al., 2007). CED-3 cleaves Xk-family human homolog CED-8, which controls the timing of programmed cell death (Stanfield and Horvitz, 2000). The CED-8 cleavage induces PS exposure on the surface of the apoptotic cells (Chen et al., 2013). Additionally, WAH-1 binding to phospholipid scramblase SCRM-1 activates its lipid scrambling activity which leads to PS externalization (Wang et al.,

2007). The ectopically exposed PS can also lead to the engulfment of living cells (Darland-Ransom et al., 2008).

Recently, non-apoptotic functions of CED-3 were identified. The long-lived *isp-1* and *nuo-6* mutants have increased mitochondrial reactive oxygen species (mtROC) production (Yang and Hekimi, 2010). It was recently found that *ced-3(lf), ced-4(lf),* and *gain-of-function* (*gf*) of *ced-9* suppress extended lifespan of *isp-1* and *nuo-6* mutants (Yee et al., 2014). *egl-1(lf)* on its turn does not affect the lifespan of mitochondrial mutants. Thus, apoptotic pathway protects animals from mtROC independently of apoptosis (Yee et al., 2014). It was shown that CED-3 and microRNA-induced silencing complex (miRISC) redundantly modulate developmental transitions in *C. elegans* downregulating protein levels of LIN-28 at the end of the L2 stage (Weaver et al., 2014). CED-3 cleaves LIN-28 *in vitro*, which generates truncated protein without the first 31 amino acids. Additionally, CED-3 together with CED-4 promote the regeneration of injured axons independently of CED-9, EGL-1 and another BH3-only domain-containing protein CED-13 (Pinan-Lucarre et al., 2012).

#### 1.2.1.2 The CED-4 Apaf-1 homolog

CED-4 is homologous to mammalian apoptotic adaptor protein Apaf-1 and has pro-apoptotic function (Yuan and Horvitz, 1992; Zou et al., 1997). In *ced-4(lf)* mutants majority of the 131 cells survive (Ellis and Horvitz, 1986). *ced-4* overexpression is sufficient to induce ectopic apoptosis cell-autonomously (Shaham and Horvitz, 1996a). *ced-4* acts upstream of *ced-3*, because killing of ALMs in transgenic lines which overexpress *ced-4* is strongly inhibited by *lf* mutations of *ced-3* (Shaham and Horvitz, 1996a). CED-4 contains an N-terminal CARD domain, a nucleotide-binding domain, a helical domain, and a C-terminal winged-helix domain (Yuan and Horvitz, 1992; Zou et al., 1997; Qi et al., 2010). CARD domain mediated ologomerization of CED-4 results in formation of funnel-shaped octamer/apoptosome, which promotes CED-3 zymogen dimerization and its subsequent auto-catalytic activation (Qi et al., 2010; Huang et al., 2013). Proteolytically cleaved CED-3 dimers associate in pairs to form active tetrameric protease (Huang et al., 2013).

CED-4 polyclonal antibody staining detected the protein associated with mitochondria in almost all cells of the early embryo but not in larvae (Chen et al., 2000). However, CED-4 staining with different antibodies detects the protein in the perinuclear space in the embryo and germ line

(Pourkarimi et al., 2012). In agreement with CED-4 perinuclear localization pattern, downregulation of the nuclear inner membrane protein SUN-1 inhibits CED-4 accumulation at the nuclear periphery (Tzur et al., 2006). In the current model, CED-4 translocates to the perinuclear space and activates CED-3 upon induction of apoptosis. The fact that CED-4 was identified in all embryonic and germ cells at the nuclear periphery independently of apoptosis points towards the existence of the additional unknown mechanisms which regulate CED-4 shuttle from mitochondria to the perinuclear space.

*ced-4* is alternatively spliced generating two different isoforms which have opposite functions in apoptosis (Shaham and Horvitz, 1996b). CED-4S isoform is smaller and has pro-apoptotic function. CED-4L isoform has 24 amino acids insertion between two nucleotide-binding sites and show anti-apoptotic functions (Shaham and Horvitz, 1996b). CED-4L prevents CED-4 octamer formation, which is required for CED-3 activation (Yan et al., 2005; Qi et al., 2010). In *ced-4(n2273)* mutant, which lacks *ced-4S*-specific splice-acceptor site, pro- and anti-apoptotic functions are compromised (Shaham and Horvitz, 1996b). The homolog of serine-arginine-rich (SR) protein kinase SPK-1 promotes splicing of CED-4L and therefore inhibits apoptosis in weak *lf* mutants of *ced-4* (Galvin et al., 2011). Northern blot analysis demonstrated that *ced-4L* transcript is expressed ten times lower than *ced-4S* transcript in whole animal (Shaham and Horvitz, 1996b). However, the isoform-specific expression pattern has not been determined yet.

Under certain circumstances, CED-4 may operate independently of CED-3. *C. elegans* ICD-1 protein, which is similar to human beta-subunit of the nascent polypeptide-associated complex (betaNAC), was implicated in apoptosis (Bloss et al., 2003). During early embryogenesis, loss of ICD-1 induces ectopic cell death, which occurs independently of CED-3, but requires CED-4 (Bloss et al., 2003). ICD-1 contains caspase-cleavage site and caspase recruitment domain, which suggests that anti-apoptotic function of ICD-1 is suppressed by caspases other than CED-3 (Bloss et al., 2003). Additionally, ectopic apoptosis in *pvl-5* mutants is suppressed by *ced-3(lf)* and *ced-9(gf)* mutations, but is independent of *ced-4* (Joshi and Eisenmann, 2004). The molecular identity of *pvl-5* is not known yet (Joshi and Eisenmann, 2004).

#### 1.2.1.3 The CED-9 BCL-2 homolog

CED-9 encodes a homolog of mammalian proto-oncogene BCL-2 and acts cell-autonomously to inhibit apoptosis (Hengartner et al., 1992; Hengartner and Horvitz, 1994a, 1994b; Shaham and

Horvitz, 1996a). CED-9 was originally identified via dominant *gf* allele *n1950*, which blocks apoptosis in the majority of the cells programmed to die (Hengartner et al., 1992). *n1950* allele harbors G169E mutation which results in constitutive overactive gene product (Hengartner and Horvitz, 1994b; Tan et al., 2007). CED-9 physically interacts with CED-4 *in vitro* forming 1:2 CED-9/CED-4 protein complex (Chinnaiyan et al., 1997; Spector et al., 1997; Wu et al., 1997; Yan et al., 2005). Following apoptotic stimuli, CED-9 protein undergoes conformational change which results in CED-4 asymmetric dimer dissociation (Yan et al., 2005), apoptosome formation and subsequent activation of CED-3 caspase (Qi et al., 2010; Huang et al., 2013).

CED-9 protein consists of seven α-helices which constitute four BCL-2 homology regions (BH1 to BH4, Woo et al., 2003). The BH1 domain includes helices α4 and α5; BH2 domain includes helices α6 and α7. α2 helix forms BH3 domain, and α1 helix forms BH4 domain. Like other BCL-2 family members, CED-9 also contains the C-terminal transmembrane (TM) domain, which is required for protein localization to mitochondria. Indeed, GFP-CED-9 fusion protein, which lacks TM domain or is tagged to endoplasmatic reticulum, fails to localize at mitochondria outer membrane, but is able to prevent embryonic lethality of *ced-9(lf)* mutants (Tan et al., 2007). Thus, CED-9 mitochondrial localization is not essential for its anti-apoptotic functions. During apoptosis BCl-2 family members permeabilize the outer mitochondrial membrane by forming pores to release pro-apoptotic factors into the cytoplasm (Basañez et al., 2002). It was recently shown that CED-9 associates with lipid membranes *in vitro* independently of TM domain, which changes membrane permeability for lipid vesicles encapsulated with dyes (Tan et al., 2011). However, little is known whether this pore formation is also required for CED-9 anti-apoptotic functions *in vivo*.

In the screen for the *cis*-dominant suppressors of *ced-9(n1950gf)*, several *ced-9 lf* alleles were isolated (Hengartner et al., 1992). *n2161* is weak *ced-9 lf* allele that results in embryonic lethality mainly due to the excessive cell death. *n1653* is temperature-sensitive *lf* allele that induces excessive apoptosis at 25 ˚C. *n2077* is strong *lf* allele with premature STOP codon which causes very early embryonic arrest without any evidence for ectopic apoptosis. Such phenotypic heterogeneity in *ced-9 lf* alleles might be attributed to the additional non-apoptotic function of CED-9 during animal development (Hengartner et al., 1992). Indeed, the absence of CED-9 results in maternal effect sterility (Hengartner et al., 1992). And, twice as many cells survive in *ced-9(n1950gf)* heterozygotes, mothers of which carried at least one copy of *n1950* allele

(Hengartner et al., 1992). Additionally, CED-9 direct binding protein SPD-5, a centrosome maturation and mitotic spindle assembly factor, is also required for early embryonic development (Dreze et al., 2009).

CED-9 is localized to mitochondria and is expressed in all cells during embryogenesis (Chen et al., 2000; Pourkarimi et al., 2012). Although CED-9 expression was not detected in larvae, several studies suggest that it also acts post-embryonically. Indeed, loss of *ced-9* facilitates ectopic apoptosis of ALM neurons caused by *ced-3* overexpression (Shaham and Horvitz, 1996a).

*ced-9* is derived from polycistronic transcript which also contains *cyt-1*/*mev-1* coding sequences (Hengartner and Horvitz, 1994a; Ishii et al., 1998). *mev-1(kn1)* mutant have increased superoxide production and disrupted mitochondrial membrane potential (Senoo-Matsuda et al., 2001, 2003). Interestingly, *mev-1(kn1)* animals also show increased levels of apoptosis in the germ line and embryos under oxidative stress (Senoo-Matsuda et al., 2003; Du et al., 2015). Moreover, *mev-1(RNAi)* causes early embryonic lethality (Gönczy et al., 2000). Although functions of *ced-9* and *mev-1* are genetically separable (Hengartner and Horvitz, 1994a; Ishii et al., 1998), strong *lf* mutations of *ced-9* might compromise *mev-1* expression possibly through the nonsense mediated mRNA decay.

The genetic analysis suggests that CED-9 might also have minor pro-apoptotic functions (Hengartner and Horvitz, 1994b). In *ced-9(n1950gf)* heterozygotes balanced with wild-type copy of *ced-9*, fewer cells survive compared to animals balanced with the deletion of *ced-9* locus. Thus, wild-type copy of *ced-9* promotes programmed cell death by antagonizing overactive *n1950* copy of *ced-9* (Hengartner and Horvitz, 1994b). Furthermore, double mutants of *ced-9(lf)* and weak *lf* alleles of *ced-3* had more surviving cells compared to weak *ced-3(lf)* mutant alone (Hengartner and Horvitz, 1994b). It was also suggested that CED-9 killing function is activated upon its binding to EGL-1 which induces DRP-1-mediated mitochondrial fragmentation (Jagasia et al., 2005). Taken together, the pro-apoptotic form of CED-9 might help to kill cells that are programmed to die (Hengartner and Horvitz, 1994b; Jagasia et al., 2005).

#### 1.2.1.4 The BH3-only protein EGL-1

EGL-1 encodes a small protein of 91 amino acids similar to BH3-only subfamily of BCL-2 family proteins (Conradt and Horvitz, 1998). EGL-1 is a key activator of apoptosis in somatic

tissues. It was originally defined by *gf* mutations in the screen for egg-laying defective ("Egl") animals (Trent et al., 1983; Desai and Horvitz, 1989). *egl-1(gf)* mutations cause ectopic apoptosis of hermaphrodite-specific neurons (HSN) required for proper egg laying (Ellis and Horvitz, 1986; Trent et al., 1983; Desai and Horvitz, 1989). The inappropriate cell death of HSNs is suppressed by *ced-3(lf), ced-4(lf)* and *ced-9(gf)* mutations (Ellis and Horvitz, 1986; Hengartner et al., 1992).

A small stretch of nine amino acids represents the BH3 domain in EGL-1 coding sequence (Conradt and Horvitz, 1998). EGL-1 binding to CED-9 via BH3 domain at mitochondria induces conformational change of CED-9 and activates apoptosis (Parrish et al., 2000; Yan et al., 2004, 2005). The glycine-to-glutamate substitution in *n1950* allele of *ced-9* blocks interaction between EGL-1 and CED-9 (Parrish et al., 2000).

To identify *egl-1 lf* mutations, dominant suppressor screen was carried out using semi-dominant *egl-1 gf* alleles (Conradt and Horvitz, 1998). The *egl-1 lf* allele *n3082* prevents ectopic cell death of HSNs in *egl-1(gf)* mutatns. *n3082* allele is a five base pair (bp) deletion upstream of the BH3 domain, which generates truncated protein product lacking BH3 domain. *n3082* mutation suppresses *n1084gf* in a semi-dominant manner, because 66% of *egl-1(n1084gf n3082)/ egl-1(n1084gf)* mutants are Egl compared to the hermaphrodites homozygous for both alleles. Additionally, *egl-1(n1084gf n3082)* mediated block of apoptosis is recessive, because *egl-1*(*n1084gf n3082*)/+ heterozygotes have only few extra cells in animal pharynx. *egl-1(n1084gf n3082)* mutation does not prevent ectopic apoptosis caused by c*ed-9(lf),* which indicates, that *egl-1* acts upstream of c*ed-9* (Conradt and Horvitz, 1998).

During *C. elegans* development, *egl-1* expression is upregulated only in the cells which undergo apoptosis (Conradt and Horvitz, 1999). Additionally, CED-9 interaction with EGL-1 was shown to be crucial for EGL-1 synthesis and stabilization in mammalian cells (Peso et al., 1998). Transcriptional upregulation of *egl-1* is regulated by its upstream and downstream *cis*-regulatory sequences (reviewed in Nehme and Conradt, 2009). For example, the transcription factor TRA-1 binds to *egl-1* regulatory site ~5.6 kb downstream of its STOP codon. TRA-1 binding inhibits *egl-1* transcription in HSNs, therefore promoting their survival in *C. elegans* hermaphrodite. In *egl-1 gf* mutants single base pair changes in the regulatory site prevent TRA-1 binding resulting in transcriptional upregulation of *egl-1* (Conradt and Horvitz, 1999). Additionally, asymmetric cell division was attributed to the distinct transcriptional activation pattern of *egl-1* in cells programmed to die. In fact, mutations which affect the asymmetric divisions of mothers of the

cells destined to die, influence the apoptotic fate in daughters (Ou et al., 2010; Gurling et al., 2014; Teuliere et al., 2014). Recently, cell non-autonomous upregulation of *egl-1* transcription was proposed (Jiang and Wu, 2014). Here, secreted LIN-3/EGF was shown to activate LIN-1, which binds to *egl-1* promoter and induces its transcription in apoptotic cells.

## 1.3. Programmed cell death in the *C. elegans* germ line

### 1.3.1 Development of the *C. elegans* germ line

The gonad of *C. elegans* hermaphrodite consists of the two U-shaped arms which meet at a common uterus. The gonad is enclosed by a basement membrane with the five pairs of somatic sheath cells. Most of the germ cells within the gonad share a common cytoplasm, thus forming a syncytium. The adult germ line exhibits distal–to–proximal polarity. Mitotic cells are located at the most distal end of the gonad, whereas meiotic cells are extended proximally. The distal end of each gonad arm is capped by mesenchymal distal tip cell (DTCs).

The remarkable characteristic of germ cells is their ability to recreate the organism. Worm germ cell lineage is established during early embryogenesis prior to hatching. A sequence of unequal divisions of the germline blastomeres P0, P1, P2 and P3 generate the primordial germ cell P4 (Fig. 1.1A). The maternally provided RNA-protein complexes, P granules, are asymmetrically segregated to P4 (Strome and Wood, 1982; Hird et al., 1996; Pitt et al., 2000; Cheeks et al., 2004). Animals with severely compromised P granules have germ cells which express somatic markers and send out neurite-like projections (Updike et al., 2014). P granules include maternally expressed transcripts (class II mRNA), conserved germline helicases GLH-1, GLH-2, GLH-3, and GLH-4, the P granule assembly proteins PGL-1, PGl-2, PGL-3, and meiotic regulators OMA-1 and OMA-2 (Updike and Strome, 2010). The list of P granule components continues to grow, but the majority of them are associated with RNA metabolism. To retain the undifferentiated state of the germline blastomers, maternally provided CCCH-type zinc finger protein PIE-1 mediates global transcriptional repression (Mello et al., 1996). PIE-1 sequesters positive transcription elongation factor b (PTEFb) away from RNA polymerase II (RNAPII) via its carboxy-terminal tail, thereby inhibiting elongation of transcription (Zhang et al., 2003). PIE-1-dependent repression of germ cells lasts until P4 divides into two germline founder cells, Z2 and Z3 at the 100-cell stage embryo (Fig. 1.1A, Mello et al., 1996). After PIE-1 degradation,

the chromatin of Z2 and Z3 becomes more condense, and acquire repressive histone modifications to maintain transcriptionally silent state (Schaner et al., 2003).

Proliferation of Z2 and Z3 starts in response to nutrition at the larval stage 1 (L1). The germline founder cells divide mitotically producing a pool of germline stem cells (GSC). Somatic gonad develops in concert with GSC proliferation. At hatching, Z2 and Z3 are flanked by the somatic gonad precursors, Z1 and Z4 (Fig. 1.1A). Z1 and Z4 give rise to the two mesenchymal distal tip cells (DTCs) and ten proximal cells which rearrange at the late L2 to form somatic gonad primordium. The rapid extension of the gonadal arms lasts until the beginning of the L3 stage. Notch signaling from the DTC together with the PUF family RNA-binding proteins, FBF-1 and FBF-2 control mitotic GSC proliferation (Lamont et al., 2004; Kimble and Crittenden, 2007). FBF-1 and FBF-2, directly repress regulators of the meiotic entry and cell fate specification genes (Crittenden et al., 2002; Eckmann et al., 2004; Thompson et al., 2005; Lee et al., 2006a, 2007a; Kershner and Kimble, 2010). Two types of GSCs exist within the mitotic region (Cinquin et al., 2010). The most distal part of mitotic GSCs is maintained in uniform immature state and is prevented from entering meiosis by Notch signaling form the DTC. The GSCs in the proximal pool are defined as the transit-amplifying cells, which mature gradually while continuing to proliferate mitotically. Thus, the maturation state among the mitotically dividing germ cells varies depending on their position relative to the DTC.

In the beginning of the larval stage 3 (L3), the germ cells that are farthest from the DTC enter meiotic S-phase (Fig. 1.1B). After DNA replication, chromosomes which are normally dispersed around the periphery of the nucleus become polarized and undergo homologous pairing. This region of the germ line is referred to the “transition zone” and corresponds to leptotene and zygotene stages of early meiotic prophase I (Fig. 1.1B). The accumulation pattern of GLD-1 defines a border between mitotic and meiotic region of the germ line. GLD-1 is a KH motif-containing RNA-binding protein (RBP), which acts as a translational repressor of mitosis promoting genes (Francis et al., 1995; Jones and Schedl, 1995; Lee and Schedl, 2001; Marin and Evans, 2003; Biedermann et al., 2009; Wright et al., 2011). In the mitotic region, *gld-1* is post-transcriptionally repressed by FBF proteins(Cinquin et al., 2010; Suh et al., 2009) and GLP-1/Notch receptor (Hansen et al., 2004). As germ cells move away from the DTC, the Notch signaling becomes weak and accumulation of GLD-1 is observed in the germ cell which enter meiosis (Hansen et al., 2004). The GLD-2 is a cytoplasmic poly (A) polymerase which forms a

heterodimer with GLD-3, a Bicaudal-C family RBP, to activate the expression of *gld-1* mRNA (Kadyk and Kimble, 1998; Wang et al., 2002a; Eckmann et al., 2004; Suh et al., 2006b). NOS-3 is a homolog of Drosophila Nanos which acts as a translational regulator (Subramaniam and Seydoux, 1999), and activates the expression of *gld-1* in parallel to GLD-2/GLD-3 heterodimer (Hansen et al., 2004). Upon Notch signaling reduction, the direct reciprocal auto-repression of FBF proteins maintains meiotic germ cell specification (Lamont et al., 2004). Interestingly, miRNAs were also found to be implicated in germ cell proliferation and differentiation (Bukhari et al., 2012; Brown et al., 2017). In the early pachytene region, the synaptonemal complex assembly is completed (Fig. 1.1B). The homologous recombination occurs in the mid pachytene, which is followed by the repair of meiosis-induced DNA double-strand breaks and synaptonemal complex disassembly in the late pachytene and diplotene zones (Fig. 1.1B). During the final stage of prophase I, diakineses, chromosomes of the maturing germ cells condense dramatically in preparation for the first meiotic division. In *C. elegans* hermaphrodite, the germ cells which enter the phachtene region first (at the beginning of the larval stage 4 (L4)) will become sperm (Fig. 1.1B). The germ cells which enter the pachytene region later will differentiate into the oocytes. Oocytes are continuously produced throughout adult life. The regulatory network which controls sperm *vs* oocyte decision includes many of the same regulators used for mitosis *vs* meiosis decision (Kimble and Crittenden, 2007; Ellis and Lin, 2014). Oocytes paused at the diakinesis start their first meiotic division after the ovulation through the spermatheca. Once sperm is depleted, oocytes arrest in the meiotic prophase until insemination occurs. The zygote moves into uterus and goes through the early embryonic development before being extruded through the vulva.

### 1.3.2 Physiological germline apoptosis

Apoptotic removal of superfluous germ cells is a conserved feature of oocyte development in mammals, insects and nematodes. In humans, approximately seven million oocytes are produced during embryogenesis, 99.9% of which die during woman's lifetime (Hsueh et al., 1994). In *Drosophila*, single egg chamber contains 16 germ cells, 15 of which undergo apoptosis after oocyte maturation (Cavaliere et al., 1998). In *C. elegans* hermaphrodites, more than half of the developing oocytes are culled in the late pachytene region of the germ line, in an apparent stochastic manner, in the absence of any evident apoptotic stimulus (Gumienny et al., 1999; Fox et al., 2011). This process is referred to as "physiological germline apoptosis".

#### 1.3.2.1 Why do so many apparently healthy germ cells die?

Apoptotic germ cells might be genetically compromised due to their high proliferation rates. In older women, accumulation of meiotic errors leads to the impaired chromosome segregation in the maturing oocytes with subsequent maternal infertility or chromosomal abnormalities in offspring (Djahanbakhch et al., 2007). The unsynapsed chromosomes trigger germline apoptosis in humans and nematodes (Baudat et al., 2000; Bhalla and Dernburg, 2005). Nevertheless, *ced-4(lf)* and *ced-3(lf)* mutations, which block most of the germ cell death, does not result in high rates of embryonic lethality (Andux and Ellis, 2008). Furthermore, *ced-9(1950gf)* and *egl-1(lf)* mutations, which prevent germline apoptosis in response to DNA damage, do not reduce the quality of the maturing oocytes (Andux and Ellis, 2008). Thus, it is rather unlikely that physiological germline apoptosis functions solely to eliminate defective germ cells.

In *Drosophila* and humans, a number of germ cells are set aside at birth to produce nutrients for growing oocytes. These nurse cells eventually undergo apoptosis once the fate of oocyte is determined. In *C. elegans*, apoptotic germ cells might also function as nurse cells. In fact, quality and size of oocytes decreases in old worms and in mutants with the defective apoptosis (Andux and Ellis, 2008). Similarly, oocyte quality is reduced in mutants with the impaired engulfment, suggesting that removal of apoptotic germ corpses is also important for the development of healthy oocytes (Andux and Ellis, 2008). However, accumulation of the specialized, morphologically distinct nurse cells was not reported in apoptosis defective mutants (Gumienny et al., 1999). Instead, the first ~300 oocytes generated in young *ced-4(lf)* and *ced-3(lf)* animals develop into healthy embryos after fertilization (Andux and Ellis, 2008). Additionally, all pachytene germ cells contribute to the proximal streaming of cytoplasmic materials towards growing oocytes (Wolke et al., 2007). Thus, every germ cell in the pachytene has equal potential to develop into mature oocyte, and none is specifically designed as a nurse cell (Gumienny et al., 1999; Wolke et al., 2007; Andux and Ellis, 2008).

Possibly, certain concentration of the cytoplasmic materials is needed to keep oocyte alive and to generate healthy offspring. To reach this nutrients threshold, transcriptional activity of several germ cells might be needed to secure the survival of a single oocyte. Thus, reducing the germ cell proliferation would not compensate for the intrinsic deficit of the cytoplasmic materials. In mutants with the defective germ cell death, premature depletion of nutrients might contribute to the reduced quality and size of the increased number of oocytes (Andux and Ellis, 2008).

Therefore, germline apoptosis might be used to reduce nutrients competition between the supernumerary germ cells (Andux and Ellis, 2008).

### 1.3.2.2 Regulation of physiological germline apoptosis

The *C. elegans* germ line is a dynamic tissue, and the factors like age of the worm, rates of the germline proliferation and corpse engulfment, and temperature influence basal levels of apoptosis. Dying germ cells are rapidly cellularized away from common syncytium and engulfed by gonadal sheath cells (Wu and Horvitz, 1998). The female germ line is required for apoptosis, whereas the gender of somatic tissue does not influence the apoptotic competency of germ cells (Gumienny et al., 1999). Like somatic cell death, germline apoptosis is also regulated by the core apoptotic machinery. *ced-4(lf)* and *ced-3(lf)* mutants have very few germ cell corpses, whereas increased levels of germline apoptosis are observed in *ced-9(lf)* animals (Gumienny et al., 1999). However, there is no direct link between the transcriptional upregulation of *egl-1* and induction of germline apoptosis under the physiological conditions. *egl-1(lf)* and *ced-9(1950gf)* mutations, which prevents most of the somatic cell death, do not affect physiological germline apoptosis (Gumienny et al., 1999). Additionally, *egl-1* transcription is not upregulated in wild-type worms (Eberhard, 2012). Furthermore, CED-4 does not co-localize with CED-9 at mitochondria in the germ line (Pourkarimi et al., 2012). Thus, the mechanisms which trigger physiological germline apoptosis upstream of *ced-9* are not known yet (Fig. 1.1C). I have addressed this question in details in Chapter 3.

Hypothetically, germ cells might be more susceptible to the subtle fluctuating changes in *egl-1* transcription, while stronger upregulation of *egl-1* is required to induce apoptosis in somatic tissue. Consistent with this hypothesis, the upregulation of *egl-1* transcription is observed in the *ced-9(n1653ts) lf* mutants at 20 ˚C (Eberhard, 2012). Moreover, loss of *egl-1* restores the fertility of *ced-9(n1653ts)* worms at 25 ˚C (Eberhard, 2012). Additional regulatory molecules might amplify subtle changes of *egl-1* transcription or act in parallel to induce apoptosis in the germ line under the physiological conditions.

In *C. elegans*, Ras/MAPK signaling is required for germ cell progression through the pachytene stage (Lee et al., 2007b). The strong *lf* mutations in Ras/MAPK pathway (*let-60 (ras)*, *lin-45 (raf)*, *mek-2* (ERK kinase), *mpk-1* (MAP kinase)) also block constitutive germline apoptosis (Gumienny et al., 1999). *ced-9(lf)* mutation restores germ cell death in *lf* mutants of

Ras/MAPK signaling (Gumienny et al., 1999). Moreover, increased germline apoptosis is observed in mutants with the upregulated Ras/MAPK signaling (*lip-1(lf), gla-3(lf),* Kritikou et al., 2006). Thus, Ras/MAPK signaling is one of the key regulators of physiological germline apoptosis. However, the direct interaction between the components of Ras/MAPK pathway and members of the core apoptotic machinery has not been shown yet. Therefore, Ras/MAPK signaling might also affect physiological germline apoptosis indirectly, by promoting germ cell progression into the apoptosis sensitive stage (Gumienny et al., 1999; Rutkowski et al., 2011).

Several transcription factors (TFs) and RBPs (reviewed in 1.3.4) were shown to regulate physiological gem cell apoptosis. EGL-38 and PAX-2, *C. elegans* homologs of mammalian Pax2/5/8 TFs, promote germ cell survival by directly activating the transcription of *ced-9* (Wang et al., 2004; Park et al., 2006). Conversely, LIN-35, *C. elegans* retinoblastoma susceptibility protein (Rb) homolog, promotes constitutive germline apoptosis by repressing *ced-9* expression (Schertel and Conradt, 2007). Additionally, the reduction of physiological germ cell death was observed in the mutants which lack DP homolog DPL-1 or E2F-like proteins EFL-1 and EFl-2, due to the decreased expression of *ced-4* and *ced-3* (Schertel and Conradt, 2007).

### 1.3.3 DNA damage-induced germline apoptosis

The *C. elegans* germ line is the only adult proliferative tissue, which is continuously optimized to maintain its pluripotency and to respond quickly to alternating intrinsic and environmental stimuli. The stresses like bacterial infection, heat shock, starvation or high glucose diet trigger ectopic germline apoptosis (Aballay and Ausubel, 2001; Salinas et al., 2006; Angelo and Gilst, 2009; Choi, 2011). The exposure to the genotoxic agents such as environmental toxins, ultraviolet (UV) or ionizing irradiation (IR) causes mistakes in DNA replication, miss-incorporation of the nucleotides or double-strand DNA breaks (DSBs). Following DNA damage, mitotic germ cells transiently cease the proliferation to activate DNA repair pathways, but continue to grow, which results in the decreased number of enlarged mitotic germ cells (Fig. 1.1B, Stergiou and Hengartner, 2004). Meiotic germ cells undergo excessive apoptosis in the pachytene region of the germ line (Fig. 1.1B, Gartner et al., 2000; Stergiou et al., 2007; Feng et al., 2017). DNA damage-induced germline apoptosis requires *ced-9, ced-4* and *ced-3,* and is blocked by *egl-1(lf)* and *ced-9(1950gf)* mutations (Fig. 1.1D, Gartner et al., 2000).

#### 1.3.3.1 DNA damage checkpoint signaling

The 9-1-1 DNA damage checkpoint sensors HPR-9, HUS-1 and MRT-2 are recruited to the sites of DNA lesions (Hofmann et al., 2002). The *C. elegans* Rad17 clamp loader homolog, HPR-17 functions in the same DNA damage response pathway as 9-1-1 checkpoint complex (Boerckel et al., 2007). Mutants of 9-1-1 complex and *hpr-17(tm1579)* worms are defective in IR-induced cell cycle arrest and apoptosis (Gartner et al., 2000; Boulton et al., 2002; Hofmann et al., 2002; Boerckel et al., 2007). Another checkpoint sensing factor CLK-2/RAD-5 acts in parallel to 9-1-1 complex localizing to the sites of DSBs (Ahmed et al., 2001; Stergiou and Hengartner, 2004). The members of the phosphatidylinositol 3 kinase (PI3K) family, ATL-1 and ATM-1, activate the effector kinases CHK-1 and CHK-2 (Garcia-Muse and Boulton, 2005), which transduce the DNA damage signal downstream to the p53 tumor suppressor homolog *cep-1* (reviewed in 1.3.3.2, Derry et al., 2001; Schumacher et al., 2001; Stergiou et al., 2007). Remarkably, male germ cells do not undergo apoptosis (Gumienny et al., 1999; Jaramillo-Lambert et al., 2010). The absence of germline apoptosis in males is due to the failure of CED-3 activation, even though the recombination checkpoint cascade is induced following IR or meiotic recombination defects (Jaramillo-Lambert et al., 2010). Interestingly, *C. elegans* homolog of Holiday Junction resolvase GEN-1 promotes germ cell cycle arrest and apoptosis independently of the canonical DNA damage response pathway discussed above (Bailly et al., 2010).

#### 1.3.3.2 The CEP-1 p53 tumor suppressor homolog

In mammals, the p53 family includes three transcription factors, p53, p63, and p73, which have evolved from a common p63/p73-like ancestral protein, as a result of gene duplication events occurred during invertebrate-to-vertebrate transition (Belyi and Levine, 2009). The components of the p53 pathway are mutated in the majority of human cancers (Hollstein et al., 1991; Kandoth et al., 2013). p53 induces cell cycle arrest and apoptosis of damaged cells providing mainly a tumor suppressing function (Kastenhuber and Lowe, 2017). However, there is an increasing evidence that certain p53 mutants may act as oncogenic proteins (Soussi and Wiman, 2015). p53 contains two N-terminal transactivation domains (TA) to recruit the transcription factors, central DNA binding domain (DBD) to recognize the promoter sequences, oligomerization domain (OD) for tetramerization, and short stretch of 30 amino acids to regulate its transcriptional activity (Joerger and Fersht, 2010). Mdm2 is an E3 ubiquitin ligase required for p53 degradation under the physiological conditions (Brooks and Gu, 2006). Upon DNA damage, phosphorylation of p53

and Mdm2 disrupts their association (Levine, 1997; Brooks and Gu, 2006). p53 stabilization activates the transcription of BH3-domain-containing genes *Noxa* and *Puma* to induce apoptosis (Oda et al., 2000; Nakano and Vousden, 2001). p63 and p73 are mainly involved in epithelial development and neuronal differentiation, respectively (Yang et al., 1999, 2000). Several isoforms of p63 and p73 exist depending on the combination of the different N-terminal promoters and C-terminal splicing (Kaghad et al., 1997; Laurenzi et al., 1998; Yang et al., 1998). p63 and p73 are structurally related to p53 and share 55-87% of amino acid sequence homology in DBD (Belyi and Levine, 2009). However, the sterile alpha motif (SAM) domain for protein-protein interactions and transcriptional inhibitory domain (TID) are found exclusively in the C-termini of p63 and p73 (Serber et al., 2002).

In *C. elegans*, CEP-1 is the only member of the p53 family which promotes DNA damage-induced germline apoptosis (Derry et al., 2001; Schumacher et al., 2001). The inactivation of *cep-1* causes a slight reduction in progeny survival following IR (Derry et al., 2001). CEP-1 induces cell cycle arrest only following UV-C treatment, but not in response to IR (Derry et al., 2001; Schumacher et al., 2001; Stergiou et al., 2007). Interestingly, ubiquitous expression of CEP-1::GFP fusion reporter was observed during the entire embryonic development (Derry et al., 2001). Additionally, CEP-1-overexpressing embryos were terminally arrested before hatching with the increased levels of caspase-independent necrotic cell death (Derry et al., 2001). Furthermore, many genes were also shown to be repressed by CEP-1 in the absence of genotoxic stress in the germ line and somatic tissues (Derry et al., 2007). Thus, CEP-1 activity might be carefully regulated during animal development in addition to its function in the germ line.

Initially, CEP-1 was thought to be more related to mammalian p53, due to its role in apoptosis. Consistently, significant overlap between the genes repressed by CEP-1 and human p53 was identified (Derry et al., 2007). However, the phylogenetic and structural analysis suggested that *cep-1* encodes ancestral p63/p73-like gene (Ou et al., 2007; Rutkowski et al., 2010). This hypothesis was further supported by the observation that mammalian p63 monitors the fidelity of the female germ line and induces apoptosis of oocytes in response to DNA damage independently of p53 (Suh et al., 2006a). Moreover, CEP-1-activated genes overlapped significantly with human p63 targets (Derry et al., 2007).

CEP-1 contains conserved DBD, two putative phosphorylation sites, C-terminal non-canonical oligomerization domain (OD) followed by 16-amino-acid linker and SAM domain (Derry et al., 2001; Schumacher et al., 2001; Ou et al., 2007). CEP-1 DBD shares only 15% of amino acid sequence identity with mammalian counterparts (Huyen et al., 2004). The OD of CEP-1 forms dimers and requires additional structural elements in C-terminus to maintain proper conformation (Ou et al., 2007). The C-terminus of CEP-1 can be converted into the tetrameric form by mutations at K544, R551, and E552 residues (Ou et al., 2007).

Like mammalian p53, CEP-1 is phosphorylated by CHK-1 and CHK-2 (Shieh et al., 2000; Schumacher et al., 2001; Stergiou et al., 2007; Jaramillo-Lambert et al., 2010), which leads to the transcriptional upregulation of BH3-only genes *egl-1* and *ced-13* (Hofmann et al., 2002; Schumacher et al., 2005a; Stergiou et al., 2007). *egl-1* and *ced-13* are the strongest *cep-1* dependent genes (Greiss et al., 2008). Interestingly, the majority of the *cep-1* dependent, IR-induced genes are mainly expressed in somatic tissues (Greiss et al., 2008). Furthermore, *cep-1* mutants are hypersensitive to hypoxia- and starvation- induced stresses (Derry et al., 2001).

Several molecules which regulate *cep-1* activity exist. GLD-1 restricts *cep-1* translation to the late pachytene region by binding to its 3'-untranslated region (3'UTR, Schumacher et al., 2005b). In *gld-1(op236)* mutant binding to *cep-1* is compromised, which leads to the increased CEP-1 expression in the distal parts of the germ line and sensitizes germ cells to apoptosis following IR. By contrast, the expression of other GLD-1 targets is not affected in *gld-1(op236)* animals. Another CEP-1 regulatory mode is represented by Ras/MAPK signaling (Rutkowski et al., 2011). The increased activation of MPK-1 sensitizes germ cells to apoptosis following DNA damage. In *lip-1(lf)* mutants, CEP-1 levels are upregulated in early pachytene. Consistently, reduced CEP-1 levels and upregulated levels of GLD-1 were detected in *mpk-1(ga111ts)* untreated worms grown at 25 ˚C. By contrast, GLD-1 levels remained unchanged in *mpk-1(ga111ts)* mutants following IR. Thus, MPK-1 restricts CEP-1 expression to the late pachytene in part by regulating GLD-1 expression, but also via GLD-1 independent mechanism. Additionally, MPK-1 might also directly activate CEP-1 in response to IR. Indeed, MPK-1 is phosphorylated upon DNA damage, and directly interacts with CEP-1 in yeast two-hybrid assay. Further, PRMT-5 negatively regulates DNA damage-induced germline apoptosis (Yang et al., 2009). In *prmt-5(RNAi)* worms, increased levels of germ cell death are observed after IR. PRMT-5 interacts directly with CEP-1 via a cofactor CBP-1, a homolog of mammalian p300/CBP. CBP-1 methylation by PRMT-5

inhibits transcription of *cep-1* to maintain proper expression of *egl-1* and to avoid excessive germ cell apoptosis following DNA damage. Additionally, E3 ubiquitin ligase complex SCF $^{FSN-1}$ negatively regulates CEP-1 transcription and germline apoptosis in response to DNA alkylating agent N-ethyl-N-nitrosourea (ENU, Gao et al., 2008). However, it is not clear whether SCF $^{FSN-1}$ interaction with CEP-1 is direct. Furthermore, HIF-1 downregulates CEP-1 and antagonizes DNA damage-induced germline apoptosis cell-nonautonomously through a secreted neuronal tyrosinase TYR-2 (Sendoel et al., 2010). The inactivation of *tyr-2* restored IR-induced gemline apoptosis in *vhl-1(lf)* mutants, which have increased levels of HIF-1 under normoxic conditions. The ectopic expression of *tyr-2* under the control of germline-specific promoter inhibits DNA damage-induced germline apoptosis.

### 1.3.4 Post-transcriptional regulation of germline apoptosis in *C. elegans*

Post-transcriptional regulation of gene expression covers virtually each step of macromolecule biogenesis in the cell. The interplay between different post-transcriptional mechanisms tremendously influences gene expression. Almost all mRNAs contain sequences that regulate their post-transcriptional expression and localization (Barrett et al., 2012). These regulatory elements are found in introns and exons of pre-mRNA, as well as in coding and non-coding regions of mature transcripts (Hafner et al., 2010; Rosenberg et al., 2015; Weingarten-Gabbay et al., 2016; Wissink et al., 2016). RBPs and non-coding RNAs (ncRNAs) are main post-transcriptional regulatory elements. mRNAs bound by RBPs and ncRNAs form messenger ribonucleoprotein particles (mRNPs), which continuously remodel in response to changes of cellular homeostasis (Tenenbaum et al., 2000; Moore, 2005). *C. elegans* genome contains approximately 1’300 functional ncRNAs and 800 RBPs (Stricklin et al., 2005; Tamburino et al., 2013). Both, ncRNAs and RBPs have on average hundreds of targets, which underline the extent of post-transcriptional regulation on gene expression (Tenenbaum et al., 2000). mRNPs participate in processing of newly synthesized transcripts in the nucleus, export mRNAs to the cytoplasm, ensure translation initiation and elongation, and finally mediate mRNA degradation. Thus revealing mRNP function, assembly and remodeling events is crucial for understanding mRNA regulation. Dysfunction of the post-transcriptional regulation largely contributes to the numerous health disorders (Chatterjee and Pal, 2009; Vaklavas et al., 2017). Additionally, weak correlation between mRNA and proteins levels was observed in several genome-wide studies,

confirming a tremendous impact of post-transcriptional regulation on gene expression (Schwanhäusser et al., 2011; Grün et al., 2014; Kamkina et al., 2016).

Germ cells undergo complex developmental program, progression through which requires accurate spatial and temporal regulation of gene expression. In the *C. elegans* germ line, translational control is a major form of gene expression regulation. The genome-wide analysis of germline-specific genes in *C. elegans* identified a 4-fold enrichment of RNA-binding proteins compared to soma, where gene expression is mostly regulated at the transcriptional level (Wang et al., 2009b). Several studies have also shown that spatio-temporal expression of many genes in the *C. elegans* germ line is regulated mainly by their 3'UTRs (Schumacher et al., 2005b; Merritt et al., 2008; Subasic et al., 2016). The question arise: why translational regulation is extensively utilized in the *C. elegans* germ line? Firstly, germ cells experience strong transcriptional repression of soma-related genes starting from the specification phase (via maternally provided PIE-1) until early embryogenesis (via repressive chromatin modifications). Thus, repressed state of chromatin might be less compatible with the DNA-based regulation mechanisms. Secondly, germ cells go through two distinct types of cell division in a spatially and temporally distinct manner while sharing a common cytoplasm. The continuously moving, quickly dividing germ cells experience a constant change in cytoplasmic stimuli. Translational control offers tight regulation of gene expression, fast response to changing environmental cues, and energy-saving advantage by directly accessing the cytoplasmic pool of pre-made mRNAs.

Because, translational control plays an important role in germline development (Nousch and Eckmann, 2013), one would expect that much of the germline apoptosis is also regulated at the post-transcriptional level. Indeed, many RBPs were identified to influence germ cell death in *C. elegans*. For example, the translation of the executioner caspase *ced-3* is heavily regulated by at least four conserved RBPs to restrict its expression in the germ line (Subasic et al., 2016). GLD-1 inhibits germline apoptosis upstream of the core apoptotic machinery by repressing the translation of *cep-1* (reviewed in 1.3.3.2, Schumacher et al., 2005b). A conserved DEAD-box germline helicase CGH-1 is enriched in P granules and somatic mRNA-protein particles (Navarro et al., 2001). It is required for gametogenesis and also prevents physiological germ cell death (Navarro et al., 2001). Another RBP, CAR-1 interacts with CGH-1 to suppress physiological germline apoptosis (Boag et al., 2005). GLA-3 is a TIS11-like RBP with two CCCH-like zinc-finger domains, which suppresses physiological and DNA damage-induced germ cell death at the

level of MAPK signaling (Kritikou et al., 2006). Additionally, the constitutive P-granule components PGL-1 and PGL-3 were found to inhibit physiological and DNA damage-induced germline apoptosis by repressing protein levels of the Apaf-1 homolog *ced-4* and Sirtuin homolog *sir-2.1* (Min et al., 2016). *Lettre et al.* identified even more RBPs which effect germline apoptosis in *C. elegans* (Lettre et al., 2004).

The microRNA (miRNA) pathway is another form of RNA regulation required for germ cell maintenance in worms, flies and mice. *mir-14* and *bantam* are the first miRNAs identified to influence apoptosis in *D. melanogaster* (Xu et al., 2003; Brennecke et al., 2003). Many miRNAs were reported to regulate cell death in humans (Su et al., 2015). For example, pro-apoptotic *mir-204* directly targets 3'UTR of anti-apoptotic protein BCL-2, and is frequently downregulated in human gastric cancers (GCs, Sacconi et al., 2012). The pro-apoptotic *mir-15a* and *mir-16-1* are downregulated in 65% of B-cell chronic lymphocytic leukemia (CLL) patients (Calin et al., 2002). *mir-15a* and *mir-16-1* inhibit expression of BCL-2 expression and control cell growth (Cimmino et al., 2005). Patients with abdominal aortic aneurysm (AAA) have strongly upregulated levels of anti-apoptotic *mir-504* (Cao et al., 2017), which directly targets tumor suppressor p53 (Hu et al., 2010).

By contrast, very little is known about the impact of miRNAs on the regulation of germ cell death in *C. elegans.* Depletion of miRNA processing enzymes Drosha or Dicer significantly impairs germ cell maturation which cause animal sterility (Knight and Bass, 2001; Denli et al., 2004). Knock-down of two worm Argonaute (AGO) proteins ALG-1 and ALG-2 causes germ cell differentiation defects (Grishok et al., 2001). Genetic studies have identified the highly conserved *mir-34* and members of the *mir-58* family (which are homologous to the *bantam* miRNA in *D. melanogaster*) as positive regulators of IR-induced germline apoptosis (Kato et al., 2009; Subasic et al., 2015). Furthermore, *mir-35* and *mir-58* were recently shown to bind to the 3'UTR of *egl-1* and reduce its expression in mothers of somatic cells fated to die (Sherrard et al., 2017). Thus, it was of my large interest to identify additional miRNA which might influence germline apoptosis in *C. elegans*. I have addressed this question in details in Chapter 2.

#### 1.3.4.1 miRNAs

MicroRNAs (miRNA) are endogenous non-coding RNA molecules of about 22 nucleotides in length that function as key post-transcriptional regulators of gene expression in animals and

plants. Human genome encodes ~2'500 miRNA (Kozomara and Griffiths-Jones, 2014) which regulate up to 60% of all protein coding genes (Friedman et al., 2009). miRNA function in diverse biological processes (Herranz and Cohen, 2010), and are frequently dysregulated in cancer (Lu et al., 2005) and many pathological disorders (Mendell and Olson, 2012). The non-coding gene *lin-4* was the first miRNA discovered in *C. elegans* (Lee et al., 1993; Wightman et al., 1993). *lin-4* antisense base pairing to the 3'UTR of *lin-14* mRNA negatively regulates its protein expression (Wightman et al., 1993), which is required for worm normal progression to the L2 stage (Ruvkun and Giusto, 1989). *lin-4* mediated repression of *lin-14* was largely considered to be a worm-specific phenomenon until the second *C. elegans* miRNA, *let-7,* was discovered seven years later (Reinhart et al., 2000). It became quickly apparent that the sequence and temporal expression pattern of *let-7* are conserved in other animal species (Pasquinelli et al., 2000). Since then, a remarkable variety of non-coding RNAs was identified underscoring the importance of the post-transcriptional events in gene expression (Cech and Steitz, 2014).

#### 1.3.4.1.1 miRNA biogenesis

miRNA genes are mainly transcribed by RNA polymerase II (RNA Pol II) as mono- or poly-cistronic long primary miRNAs (pri-miRNAs, Fig. 1.2, Lee et al., 2002, 2004a; Zhou et al., 2007). Most miRNA genes are located in the non-coding regions of the genome, and are transcribed from their own promoters (Lagos-Quintana et al., 2001; Lau et al., 2001). Other miRNAs are found within the introns of protein-coding genes (Lagos-Quintana et al., 2003; Lai et al., 2003). miRNA promoters do not share a common layout, however several conserved sequence motifs which resemble known *cis*-acting regulatory elements were identified (Ohler et al., 2004; Zhou et al., 2007). The majority of miRNA promoters contain the sequence motif which match the initiator (Inr) element (Zhou et al., 2007). However, the canonical TATA box motif is frequently absent from the putative miRNA core promoters (Ohler et al., 2004; Zhou et al., 2007). The CCCWCCC (W= A or T) conserved motif was found in 1'000 bp region upstream of miRNA fold-backs for the 59 orthologous human/mouse intergenic miRNAs (Ohler et al., 2004). The nematode-specific CTCCGCCC conserved motif was described for all intergenic miRNAs (Ohler et al., 2004). Interestingly, no significant termination motif was found downstream of miRNA fold-backs in nematodes (Ohler et al., 2004). The majority of pri-miRNAs contain a stem-loop structure, 5' 7-methylguanosine cap and a poly (A) tail at 3' end (Lee et al., 2004a). pri-miRNAs are processed in the nucleus into ~70-nucleotide (nt) stem-loop

precursor miRNAs (pre-miRNAs) by Microprocessor heterotrimeric complex which consists of the RNase III endonuclease Drosha and RBP DiGeorge Critical Region 8/Pasha (DGCR8/Pasha, Fig. 1.2, Lee et al., 2003; Denli et al., 2004; Gregory et al., 2004; Han et al., 2004, 2006). The features which specify pri-miRNA for further processing by Microprocessor are different between species. Indeed, most *C. elegans* pri-miRNAs lack the basal UG, the CNNC, and the apical GUG motifs which are found in ~80% of human pri-miRNAs (Auyeung et al., 2013). Additionally, pri-miRNA transcripts that enter miRNA pathway in *C. elegans* failed to do so in human cells (Auyeung et al., 2013).

After processing in the nucleus, pre-miRNAs are translocated to the cytoplasm via a protein complex which consists of karyopherin β family member Exportin 5 and GTP-binding nuclear protein RAN-GTP (Fig. 1.2, Yi et al., 2003; Bohnsack et al., 2004; Lund et al., 2004). In the cytoplasm, pre-miRNAs are further cleaved by RNase III type endonuclease Dicer into ~22 nt double stranded RNA (dsRNA) molecules (Fig. 1.2, Grishok et al., 2001; Hutvágner et al., 2001; Lau et al., 2012). The Dicer PAZ domain anchors simultaneously the 3' overhang and 5' monophosphate of the pre-miRNAs to ensure the correct cleavage of the terminal loop in the RNase III catalytic domain (MacRae et al., 2006, 2007; Park et al., 2011; Fukunaga et al., 2014). Dicer interacts with two RBPs, transactivation response RNA-binding protein (TRBP) and protein activator of PKR (PACT), which facilitate pre-miRNA cleavage and miRNA duplex loading into Argonaute (AGO) protein (Chendrimada et al., 2005; Lee et al., 2006b; Chakravarthy et al., 2010; Fukunaga et al., 2012; Lee and Doudna, 2012; Lee et al., 2013). In mammals, four out of eight AGO paralogues (AGO-1, AGO-2, AGO-3, AGO-4) function in miRNA pathway (Peters and Meister, 2007). In *C. elegans*, 27 Argonaute proteins are expressed, but only two of them (ALG-1 and ALG-2) participate in miRNA-mediated gene silencing (Yigit et al., 2006). AGO family members have paralogue-specific functions. AGO-2 is the only AGO protein with endonuclease activity (Liu et al., 2004). AGO proteins also differ in their capacity to repress target mRNA translation (Wu et al., 2008). In addition, tissue-specific variation in relative abundance of AGO proteins was found suggesting cell-type-dependent specificity of target mRNA repression (Meister et al., 2004; Wu et al., 2008). Finally, different set of miRNAs associate with distinct AGO proteins (Azuma-Mukai et al., 2008; Burroughs et al., 2011). Upon miRNA duplex loading, the endonuclease-deficient AGOs unwind the thermodynamically less stable passenger strand from the mature miRNA to form miRNA-induced silencing complex

(miRISC). miRNA processing is also tightly regulated by RBP at each step of maturation (Kouwenhove et al., 2011).

#### 1.3.4.1.2 Cell-autonomous and circulating miRNAs

Much effort has been made to identify whether miRISC components are associated with certain cellular structures. There is clear evidence that cytoplasmic processing bodies (P-bodies), which function in storage and decay of the repressed mRNAs, are also implicated in miRNA-mediated gene silencing (Eulalio et al., 2007a). The components of miRISC are enriched in cytoplasmic P-bodies (Liu et al., 2005a). The inhibition of miRNA biogenesis results in the disappearance of P-bodies (Jakymiw et al., 2005; Eulalio et al., 2007b). However, knock-down of certain P-body components does not prevent miRNA-mediated repression (Eulalio et al., 2007b). Thus, the formation of large P-body aggregates is rather a consequence than the cause of miRNA-mediated gene silencing (Eulalio et al., 2007b). Stress granules represent another class of cytoplasmic aggregates where miRISC components were found to be accumulated upon global repression of translation (Leung et al., 2006). The components of miRISC were also identified in late endosomes (multivesicular bodies (MVBs), Gibbings et al., 2009; Lee et al., 2009). The impaired maturation of MVBs enhances miRNA-mediated gene silencing (Lee et al., 2009). The impaired formation of MVBs inhibits the repression of target genes (Lee et al., 2009). Thus, it was suggested that MVBs promote continuous assembly and disassembly of miRISC complexes (Gibbings et al., 2009; Lee et al., 2009). Intriguingly, nuclease-resistant circulating miRNAs were discovered in the extracellular environment (Chen et al., 2008; Weber et al., 2010). The circulating miRNAs are frequently packed into the MVB originated exosomes (Valadi et al., 2007). The miRNA content in exosomes was found to be regulated via ceramide-dependent pathway (Kosaka et al., 2010). Several studies have shown that specific concentrations of circulating miRNAs correlated with various types of cancer (Chen et al., 2008; Wang et al., 2009a; Ogata-Kawata et al., 2014). Although, the biological function of extracellular miRNAs remains to be determined, there is increasing evidence that circulating miRNAs might participate in the intercellular communication (Pegtel et al., 2010; Mittelbrunn et al., 2011; Montecalvo et al., 2012).

#### 1.3.4.1.3 miRNA target recognition

Majority of miRNAs bind to the 3'UTRs of target mRNAs. However, targeting at the 5'UTRs and in protein-coding sequences has been reported (Grey et al., 2010; Reczko et al., 2012). miRNA target recognition is based on the "seed" region complementarity (Lewis et al., 2005). The canonical seed region is perfectly complementary to the target mRNA, and covers a continuous stretch of at least six nucleotides (nt) starting from the position two at the 5'-end of the miRNA (Ellwanger et al., 2011). The canonical seed sites are described as a 6-mer (bases 2 to 7), 7-mer-A1 (bases 1 to 7), 7-mer-m8 (bases 1 to 8), and 8-mer (bases 1 to 8) (Bartel, 2009; Ellwanger et al., 2011). The longer canonical seed sites (i.e. 7-mer-A1, 7-mer-m8, and 8-mer) are more evolutionary conserved than the shorter ones (i.e. 6-mer, Ellwanger et al., 2011). The non-canonical seed sites are not perfectly complementary to target mRNA. They include G·U wobble, bulged seed pairing, centered target sites, and seedless elements (Hausser and Zavolan, 2014). In contrast to the canonical seed sites, the non-canonical sites display lower evolutionary conservation (Friedman et al., 2009). In the recent transcriptome-wide studies, which were based on the biochemical isolation of miRNA-mRNA complexes via AGO protein immunoprecipitation, significant portion of non-canonical interactions was identified (Chi et al., 2009; Hafner et al., 2010; Chi et al., 2012; Khorshid et al., 2013; Helwak and Tollervey, 2014). Interestingly, highly abundant miRNAs frequently contain non-canonical sites (Khorshid et al., 2013). The complementary sequences outside of the seed region further stabilize the interaction between miRNA and its target mRNA, particularly when imperfect seed pairing occurs (Brennecke et al., 2005; Grimson et al., 2007).

Approximately 65% of all miRNAs discovered to date are grouped into families based on their seed sequences similarities, origin, evolutionary conservation, and structure of pre-miRNAs (Ding et al., 2011; Burge et al., 2013; Wang et al., 2014). miRNA families are frequently dysregulated in various diseases (Jiang et al., 2009; Ruepp et al., 2010; Ziebarth et al., 2012). miRNA family members have co-related functions due to the overlapping sets of targets. The redundant regulation of target genes maintains cellular homeostasis and counteract disease onset. The relative contribution of individual miRNA family members to target repression remains largely unexplored. miRNA family members frequently have subtle variations in their mature sequences, which increases number of specific targets and refine their repression in different tissues (Roush and Slack, 2008).

#### 1.3.4.1.4 miRNA regulation of post-transcriptional gene expression

The mechanism of the prost-transcriptional target gene repression by miRISC largely depends on the extent of the seed sequence complementarity and on the enzymatic activity of AGO protein. Additionally, miRNAs can function as a "switch" completely suppressing gene expression or as a "fine-tuner" modestly regulating target mRNA (Mukherji et al., 2011). Initial studies suggested that animal miRNAs repress their targets primarily at the level of translation, due to partial seed-target complementarity. miRNAs inhibit translation initiation by interfering with the factors which interact with 5'-cap and poly (A) tail, i.e. eukaryotic translation initiation factor 4G (eIF4G) and poly (A)-binding protein PABPC, respectively (Fig. 1.2, Humphreys et al., 2005; Pillai et al., 2005). miRNAs inhibit translation elongation independently of the 5'-cap through the internal ribosomal entry sites (IRES) causing the premature ribosomal drop-off (Petersen et al., 2006). Recent quantitative genome-wide studies provided strong evidence that animal miRNAs also largely degrade their target mRNAs. In fact, mRNA degradation accounted for up to 80% of changes observed at the protein level in human cell lines (Fig. 1.2, Hendrickson et al., 2009; Guo et al., 2010). Animal miRNAs degrade their target mRNAs predominantly via cellular 5'-to-3' decay pathway. The target mRNAs are first deadenylated by PAN2-PAN3 and CCR4-NOT deadenylase complexes (Wahle and Winkler, 2013), decapped by the decapping enzyme DCP2 (Wang et al., 2002c), and then are degraded in the cytoplasm by major 5'-to-3' exonuclease XRN1 (Bashkirov et al., 1997). In rare cases, where perfect seed-target complementarity is observed, selective incorporation of miRNA duplex into endonuclease-competent AGO-2 results in the cleavage of mRNA (Meister et al., 2004; Yekta et al., 2004). The debate whether mRNA degradation is an independent event is still ongoing. In the current model, miRNAs repress mRNA translation at first and then initiates target mRNA deadenylation and decay (Béthune et al., 2012; Djuranovic et al., 2012; Meijer et al., 2013).

GW182 protein is required for miRNA-mediated gene silencing in animals (Liu et al., 2005b). It acts at the effector step of silencing, downstream of AGO (Eulalio et al., 2008). *C. elegans* contains two GW182 paralogues, AIN-1 and AIN-2 (Ding et al., 2005; Zhang et al., 2007). Several modes of GW182-mediated gene silencing were suggested. GW182 may compete with eIF4G for binding to PABPC, therefore preventing the mRNA circularization and inhibiting translation (Fabian et al., 2009; Zekri et al., 2009). Alternatively, GW182 interaction with

PABPC might provide additional platform for deadenylase binding, therefore exposing target mRNA to the 5'-to-3' decay pathway (Fabian et al., 2009).

Intriguingly, several reports showed that miRNAs not only act as repressors, but can also activate translation (Henke et al., 2008; Ørom et al., 2008). This adds another layer of complexity to the post-transcriptional regulation of gene expression. For example, the change of AGO-2-miRISC function was observed in HEK293 cells at the general growth arrest due to serum deprivation (Vasudevan et al., 2007). However, the mechanisms by which miRNAs might activate translation are not well understood yet.

### 1.4. Overview of my research

In this dissertation, I was mainly interested in the characterization of additional regulatory aspects underlining germline apoptosis in *C. elegans*. As it was discussed above, germ line is the only proliferative and very dynamic tissue in the worm, which is highly susceptible to the subtle changes in animal biology. Thus, weak alterations in germ cell death are readily observable. Moreover, the effect of DNA damage on cell survival can be effectively investigated in the germ line. Although intrinsic noise is higher in the germ line, the members of the core apoptotic machinery rigidly control germ cell death. Nevertheless, several aspects of germline apoptosis regulation are not resolved yet. In fact, induction of the physiological germ cell death occurs through unknown mechanisms. What makes an apparently healthy germ cell become less preferred than the others? Are there any quality control genes which recognize unflavored germ cell conditions? Thus, I have developed two synthetic screening strategies to analyze upstream regulation of CED-9 specifically in the germ line (Chapter 3).

Post-transcriptional control of gene expression defines new regulatory mode of germ cell death in *C. elegans*. Several RBPs influence germline apoptosis; however potential contribution of miRNAs is largely unexplored. I have analyzed 55 single and multiple miRNA mutants for their effect on germ cell death under the physiological conditions and following DNA damage. I have identified *mir-52* as strong suppressor of DNA damage-induced germ cell death in *C. elegans* (Chapter 2). *mir-52* is highly conserved miRNA, which is also frequently miss-regulated in human cancers. *mir-242* and *mir-249* are additional miRNAs, perturbations of which affect physiological and DNA damage-induced germline apoptosis in *C. elegans* (Appendix 1).

I was also highly involved in two side projects, which were dealing with the effect of natural variation on gene expression. These are discussed in details in Appendix 2.

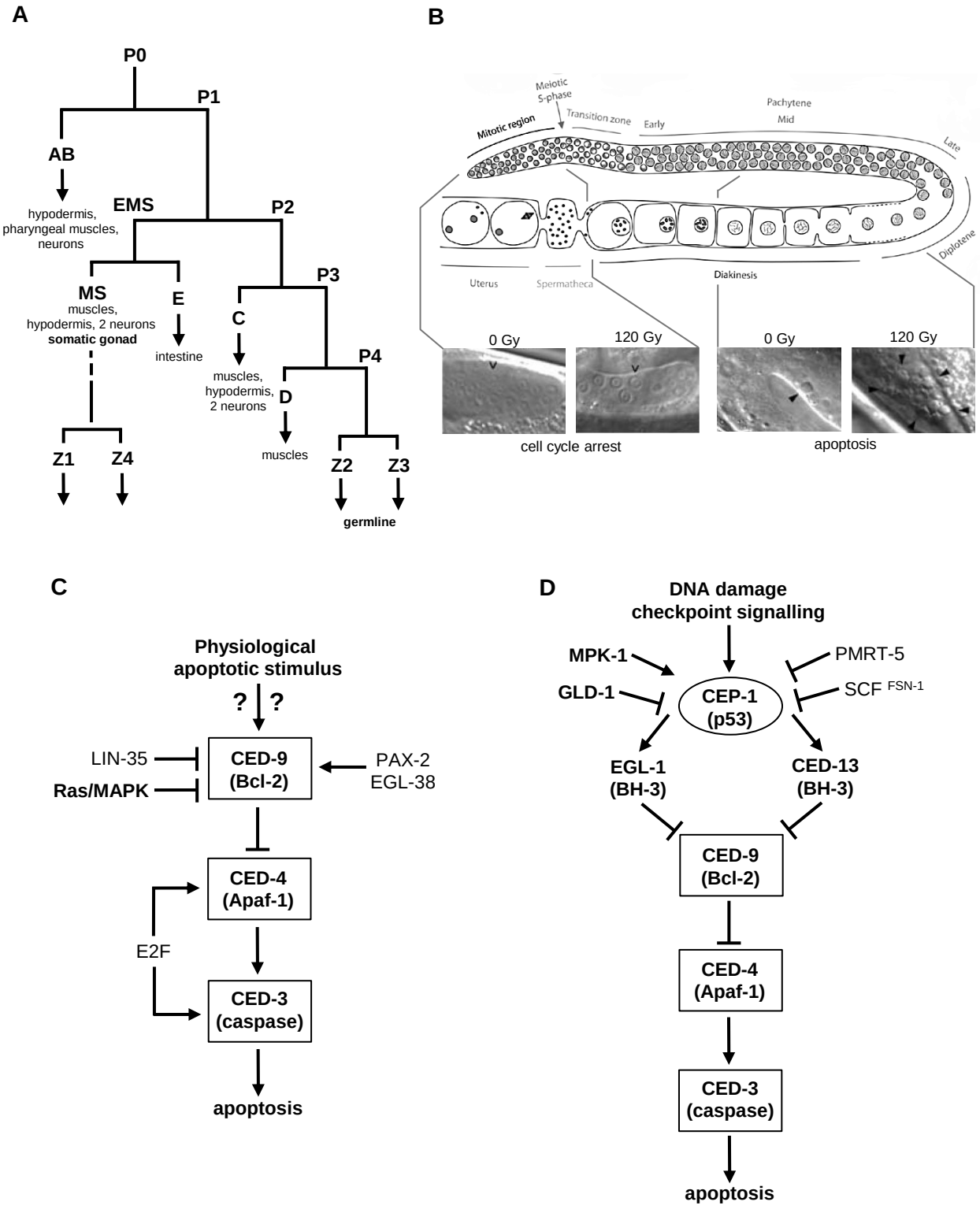


**Fig. 1.1 Germline development and apoptosis.** A. Embryonic origin of the germline (adapted from Strome, 2005; Rose and Gönczy, 2014). B. Schematic representation of adult hermaphrodite gonad with different DNA damage responses in mitotic and meiotic regions (adapted from Stergiou et al., 2004; Hillers et al. 2017). C. Regulation of the physiological germ cell apoptosis (adapted from Gartner et al., 2008). D. Regulation of the DNA damage-induced germline apoptosis (adapted from Gartner et al., 2008).

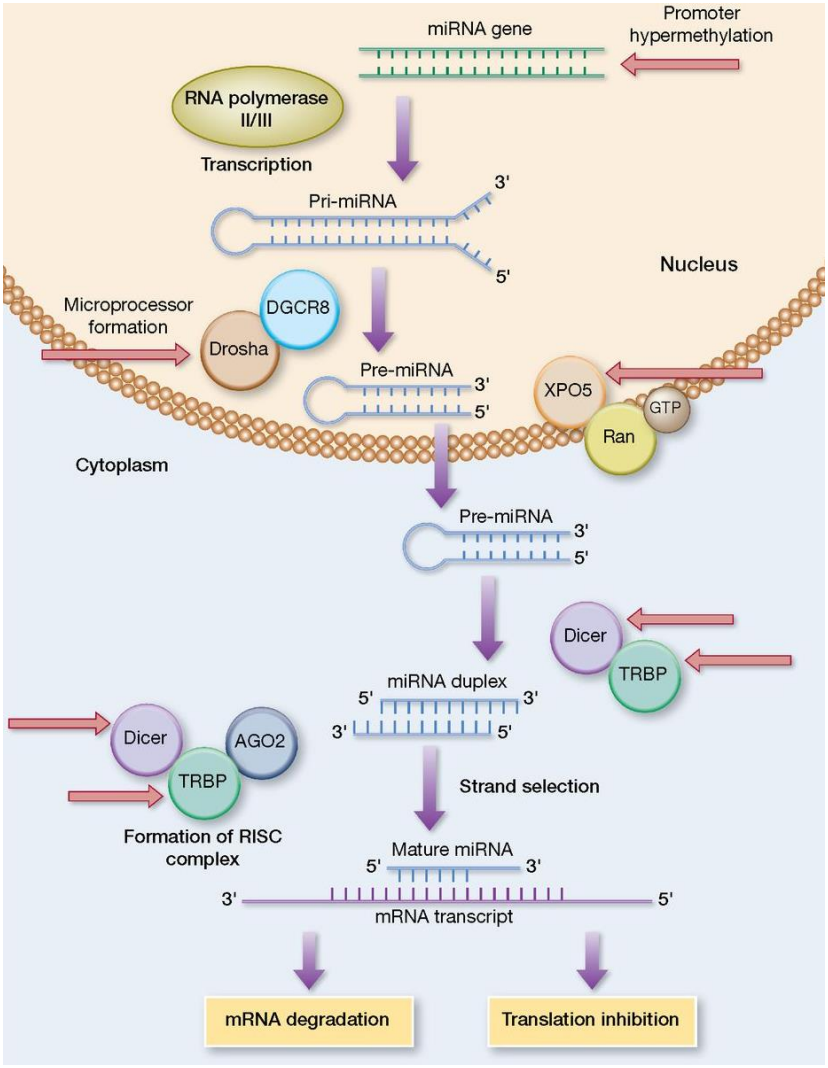


**Fig. 1.2 miRNA biogenesis.** From Mulrane et al., 2013.

## 1.5 References

Aballay, A., and Ausubel, F.M. (2001). Programmed cell death mediated by ced-3 and ced-4 protects Caenorhabditis elegans from Salmonella typhimurium-mediated killing. Proc. Natl. Acad. Sci. U. S. Am. Proc. Natl. Acad. Sci. U. S. Am. 98, 98, 2735, 2735–2739.

Ahmed, S., Alpi, A., Hengartner, M.O., and Gartner, A. (2001). C. elegans RAD-5/CLK-2 defines a new DNA damage checkpoint protein. Curr. Biol. 11, 1934–1944.

Andux, S., and Ellis, R.E. (2008). Apoptosis maintains oocyte quality in aging Caenorhabditis elegans females. PLoS Genet. 4, e1000295.

Angelo, G., and Gilst, M.R.V. (2009). Starvation protects germline stem cells and extends reproductive longevity in C. elegans. Science 326, 954–958.

Auyeung, V.C., Ulitsky, I., McGeary, S.E., and Bartel, D.P. (2013). Beyond secondary structure: primary-sequence determinants license pri-miRNA hairpins for processing. Cell 152, 844–858.

Azuma-Mukai, A., Oguri, H., Mituyama, T., Qian, Z.R., Asai, K., Siomi, H., and Siomi, M.C. (2008). Characterization of endogenous human Argonautes and their miRNA partners in RNA silencing. Proc. Natl. Acad. Sci. 105, 7964–7969.

Bailly, A.P., Freeman, A., Hall, J., Déclais, A.C., Alpi, A., Lilley, D.M., Ahmed, S., and Gartner, A. (2010). The Caenorhabditis elegans homolog of Gen1/Yen1 resolvases links DNA damage signaling to DNA double-strand break repair. PLoS Genet. 6, e1001025.

Barrett, L.W., Fletcher, S., and Wilton, S.D. (2012). Regulation of eukaryotic gene expression by the untranslated gene regions and other non-coding elements. Cell. Mol. Life Sci. 69, 3613–3634.

Bartel, D.P. (2009). MicroRNAs: target recognition and regulatory functions. Cell 136, 215–233.

Basañez, G., Sharpe, J.C., Galanis, J., Brandt, T.B., Hardwick, J.M., and Zimmerberg, J. (2002). Bax-type apoptotic proteins porate pure lipid bilayers through a mechanism sensitive to intrinsic monolayer curvature. J. Biol. Chem. 277, 49360–49365.

Bashkirov, V.I., Scherthan, H., Solinger, J.A., Buerstedde, J.-M., and Heyer, W.-D. (1997). A Mouse cytoplasmic exoribonuclease (mXRN1p) with preference for G4 tetraplex substrates. J. Cell Biol. 136, 761–773.

Baudat, F., Manova, K., Yuen, J.P., Jasin, M., and Keeney, S. (2000). Chromosome synapsis defects and sexually dimorphic meiotic progression in mice lacking Spo11. Mol. Cell 6, 989–998.

Belyi, V.A., and Levine, A.J. (2009). One billion years of p53/p63/p73 evolution. Proc. Natl. Acad. Sci. U. S. A. 106, 17609–17610.

Béthune, J., Artus-Revel, C.G., and Filipowicz, W. (2012). Kinetic analysis reveals successive steps leading to miRNA-mediated silencing in mammalian cells. EMBO Rep. 13, 716–723.

Bhalla, N., and Dernburg, A.F. (2005). A conserved checkpoint monitors meiotic chromosome synapsis in Caenorhabditis elegans. Science 310, 1683–1686.

Biedermann, B., Wright, J., Senften, M., Kalchhauser, I., Sarathy, G., Lee, M.-H., and Ciosk, R. (2009). Translational repression of cyclin E prevents precocious mitosis and embryonic gene activation during C. elegans meiosis. Dev. Cell 17, 355–364.

Bloss, T.A., Witze, E.S., and Rothman, J.H. (2003). Suppression of CED-3-independent apoptosis by mitochondrial βNAC in Caenorhabditis elegans. Nature 424, 1066–1071.

Boag, P.R., Nakamura, A., and Blackwell, T.K. (2005). A conserved RNA-protein complex component involved in physiological germline apoptosis regulation in C. elegans. Dev. Camb. Engl. 132, 4975–4986.

Boerckel, J., Walker, D., and Ahmed, S. (2007). The Caenorhabditis elegans Rad17 Homolog HPR-17 Is Required for Telomere Replication. Genet. Genet. 176, 703–709.

Bohnsack, M.T., Czaplinski, K., and Görlich, D. (2004). Exportin 5 is a RanGTP-dependent dsRNA-binding protein that mediates nuclear export of pre-miRNAs. RNA 10, 185–191.

Boulton, S.J., Gartner, A., Reboul, J., Vaglio, P., Dyson, N., Hill, D.E., and Vidal, M. (2002). Combined functional genomic maps of the C. elegans DNA damage response. Science 295, 127–131.

Breckenridge, D.G., Kang, B.-H., Kokel, D., Mitani, S., Staehelin, L.A., and Xue, D. (2008). Caenorhabditis elegans drp-1 and fis-2 regulate distinct cell-death execution pathways downstream of ced-3 and independent of ced-9. Mol. Cell 31, 586–597.

Brennecke, J., Hipfner, D.R., Stark, A., Russell, R.B., and Cohen, S.M. (2003). bantam encodes a developmentally regulated microRNA that controls cell proliferation and regulates the proapoptotic gene hid in Drosophila. Cell 113, 25–36.

Brennecke, J., Stark, A., Russell, R.B., and Cohen, S.M. (2005). Principles of microRNA–target recognition. PLOS Biol. 3, 3, e85.

Brooks, C.L., and Gu, W. (2006). p53 ubiquitination: Mdm2 and beyond. Mol. Cell 21, 307–315.

Brown, K.C., Svendsen, J.M., Tucci, R.M., Montgomery, B.E., and Montgomery, T.A. (2017). ALG-5 is a miRNA-associated Argonaute required for proper developmental timing in the Caenorhabditis elegans germline. Nucleic Acids Res. 45, 9093–9107.

Bukhari, S.I.A., Vasquez-Rifo, A., Gagné, D., Paquet, E.R., Zetka, M., Robert, C., Masson, J.-Y., and Simard, M.J. (2012). The microRNA pathway controls germ cell proliferation and differentiation in C. elegans. Cell Res. 22, 1034–1045.

Burge, S.W., Daub, J., Eberhardt, R., Tate, J., Barquist, L., Nawrocki, E.P., Eddy, S.R., Gardner, P.P., and Bateman, A. (2013). Rfam 11.0: 10 years of RNA families. Nucleic Acids Res. 41, D226–D232.

Burroughs, A.M., Ando, Y., De, M.H., Tomaru, Y., Suzuki, H., Hayashizaki, Y., and Daub, C.O. (2011). Deep-sequencing of human argonaute-associated small RNAs provides insight into miRNA sorting and reveals argonaute association with RNA fragments of diverse origin. RNA Biol. 8, 158–177.

Calin, G.A., Dumitru, C.D., Shimizu, M., Bichi, R., Zupo, S., Noch, E., Aldler, H., Rattan, S., Keating, M., Rai, K., et al. (2002). Frequent deletions and down-regulation of micro- RNA genes miR15 and miR16 at 13q14 in chronic lymphocytic leukemia. Proc. Natl. Acad. Sci. 99, 15524–15529.

Cao, X., Cai, Z., Liu, J., Zhao, Y., Wang, X., Li, X., and Xia, H. (2017). miRNA-504 inhibits p53-dependent vascular smooth muscle cell apoptosis and may prevent aneurysm formation. Mol. Med. Rep. 16, 2570–2578.

Cavaliere, V., Taddei, C., and Gargiulo, G. (1998). Apoptosis of nurse cells at the late stages of oogenesis of Drosophila melanogaster. Dev. Genes Evol. 208, 106–112.

Cech, T.R., and Steitz, J.A. (2014). The noncoding RNA revolution—trashing old rules to forge new ones. Cell 157, 77–94.

Chakravarthy, S., Sternberg, S.H., Kellenberger, C.A., and Doudna, J.A. (2010). Substrate-specific kinetics of dicer-catalyzed RNA processing. J. Mol. Biol. 404, 392–402.

Chatterjee, S., and Pal, J.K. (2009). Role of 5′- and 3′-untranslated regions of mRNAs in human diseases. Biol. Cell 101, 251–262.

Cheeks, R.J., Canman, J.C., Gabriel, W.N., Meyer, N., Strome, S., and Goldstein, B. (2004). C. elegans PAR proteins function by mobilizing and stabilizing asymmetrically localized protein complexes. Curr. Biol. 14, 851–862.

Chen, F., Hersh, B.M., Conradt, B., Zhou, Z., Riemer, D., Gruenbaum, Y., and Horvitz, H.R. (2000). Translocation of C. elegans CED-4 to nuclear membranes during programmed cell death. Science 287, 1485–1489.

Chen, X., Ba, Y., Ma, L., Cai, X., Yin, Y., Wang, K., Guo, J., Zhang, Y., Chen, J., Guo, X., et al. (2008). Characterization of microRNAs in serum: a novel class of biomarkers for diagnosis of cancer and other diseases. Cell Res. 18, 997–1006.

Chen, Y.Z., Mapes, J., Lee, E.S., Skeen-Gaar, R.R., and Xue, D. (2013). Caspase-mediated activation of Caenorhabditis elegans CED-8 promotes apoptosis and phosphatidylserine externalisation. Nat. Commun. 4, 2726.

Chendrimada, T.P., Gregory, R.I., Kumaraswamy, E., Norman, J., Cooch, N., Nishikura, K., and Shiekhattar, R. (2005). TRBP recruits the Dicer complex to Ago2 for microRNA processing and gene silencing. Nature 436, 740–744.

Chi, S.W., Zang, J.B., Mele, A., and Darnell, R.B. (2009). Argonaute HITS-CLIP decodes microRNA–mRNA interaction maps. Nature 460, 479–486.

Chi, S.W., Hannon, G.J., and Darnell, R.B. (2012). An alternative mode of microRNA target recognition. Nat. Struct. Mol. Biol. 19, 321–327.

Chinnaiyan, A.M., O'Rourke, K., Lane, B.R., and Dixit, V.M. (1997). Interaction of CED-4 with CED-3 and CED-9: A molecular framework for cell death. Science 275, 1122–1126.

Choi, S.S. (2011). High glucose diets shorten lifespan of Caenorhabditis elegans via ectopic apoptosis induction. Nutr. Res. Pract. 5, 214–218.

Cimmino, A., Calin, G.A., Fabbri, M., Iorio, M.V., Ferracin, M., Shimizu, M., Wojcik, S.E., Aqeilan, R.I., Zupo, S., Dono, M., et al. (2005). miR-15 and miR-16 induce apoptosis by targeting BCL2. Proc. Natl. Acad. Sci. U. S. A. 102, 13944–13949.

Cinquin, O., Crittenden, S.L., Morgan, D.E., and Kimble, J. (2010). Progression from a stem cell–like state to early differentiation in the C. elegans germ line. Proc. Natl. Acad. Sci. 107, 2048–2053.

Conradt, B., and Horvitz, H.R. (1998). The C. elegans protein EGL-1 Is required for programmed cell death and interacts with the Bcl-2–like protein CED-9. Cell 93, 519–529.

Conradt, B., and Horvitz, H.R. (1999). The TRA-1A sex determination protein of C. elegans regulates sexually dimorphic cell deaths by repressing the egl-1 cell death activator gene. Cell 98, 317–327.

Conradt, B., Wu, Y.-C., and Xue, D. (2016). Programmed cell death during Caenorhabditis elegans development. Genetics 203, 1533–1562.

Crittenden, S.L., Bernstein, D.S., Bachorik, J.L., Thompson, B.E., Gallegos, M., Petcherski, A.G., Moulder, G., Barstead, R., Wickens, M., and Kimble, J. (2002). A conserved RNA-binding protein controls germline stem cells in Caenorhabditis elegans. Nature 417, 660–663.

Darland-Ransom, M., Wang, X., Sun, C.-L., Mapes, J., Gengyo-Ando, K., Mitani, S., and Xue, D. (2008). Role of C. elegans TAT-1 protein in maintaining plasma membrane phosphatidylserine asymmetry. Science 320, 528–531.

Delivani, P., Adrain, C., Taylor, R.C., Duriez, P.J., and Martin, S.J. (2006). Role for CED-9 and Egl-1 as regulators of mitochondrial fission and fusion dynamics. Mol. Cell 21, 761–773.

Denli, A.M., Tops, B.B.J., Plasterk, R.H.A., Ketting, R.F., and Hannon, G.J. (2004). Processing of primary microRNAs by the Microprocessor complex. Nature 432, 231–235.

Derry, W.B., Putzke, A.P., and Rothman, J.H. (2001). Caenorhabditis elegans p53: Role in apoptosis, meiosis, and stress resistance. Science 294, 591–595.

Derry, W.B., Bierings, R., Iersel, M. van, Satkunendran, T., Reinke, V., and Rothman, J.H. (2007). Regulation of developmental rate and germ cell proliferation in Caenorhabditis elegans by the p53 gene network. Cell Death Differ. 14, 662–670.

Desai, C., and Horvitz, H.R. (1989). Caenorhabditis elegans mutants defective in the functioning of the motor neurons responsible for egg laying. Genet. Genet. 121, 703–721.

Ding, J., Zhou, S., and Guan, J. (2011). miRFam: an effective automatic miRNA classification method based on n-grams and a multiclass SVM. BMC Bioinformatics 12, 843–849

Ding, L., Spencer, A., Morita, K., and Han, M. (2005). The developmental timing regulator AIN-1 interacts with miRISCs and may target the argonaute protein ALG-1 to cytoplasmic P bodies in C. elegans. Mol. Cell 19, 437–447.

Djahanbakhch, O., Ezzati, M., and Zosmer, A. (2007). Reproductive ageing in women. J. Pathol. 211, 219–231.

Djuranovic, S., Nahvi, A., and Green, R. (2012). miRNA-Mediated Gene Silencing by Translational Repression Followed by mRNA Deadenylation and Decay. Science 336, 237–240.

Dreze, M., Charloteaux, B., Milstein, S., Vidalain, P.-O., Yildirim, M.A., Zhong, Q., Svrzikapa, N., Romero, V., Laloux, G., Brasseur, R., et al. (2009). "Edgetic" perturbation of a C. elegans BCL2 ortholog. Nat. Methods 6, 843–849.

Du, H., Wang, M., Wang, L., Dai, H., Wang, M., Hong, W., Nie, X., Wu, L., and Xu, A. (2015). Reproductive toxicity of endosulfan: implication from germ cell apoptosis modulated by mitochondrial dysfunction and genotoxic response genes in Caenorhabditis elegans. Toxicol. Sci. 145, 118–127.

Eberhard, R. (2012). Modulators of DNA damage-induced cell death in Caenorhabditis elegans. University of Zurich.

Eckmann, C.R., Crittenden, S.L., Suh, N., and Kimble, J. (2004). GLD-3 and control of the mitosis/meiosis decision in the germline of Caenorhabditis elegans. Genetics 168, 147–160.

Ellis, H.M., and Horvitz, H.R. (1986). Genetic control of programmed cell death in the nematode C. elegans. Cell 44, 817–829.

Ellis, R.E., and Lin, S.-Y. (2014). The evolutionary origins and consequences of self-fertility in nematodes. F1000Prime Rep 6:62.

Ellwanger, D.C., Büttner, F.A., Mewes, H.-W., and Stümpflen, V. (2011). The sufficient minimal set of miRNA seed types. Bioinformatics 27, 1346–1350.

Estaquier, J., and Arnoult, D. (2007). Inhibiting Drp1-mediated mitochondrial fission selectively prevents the release of cytochrome c during apoptosis. Cell Death Differ. 14, 1086–1094.

Eulalio, A., Izaurralde, E., and Behm-Ansmant, I. (2007a). P bodies: at the crossroads of post-transcriptional pathways. Nat. Rev. Mol. Cell Biol. 8, 9–22.

Eulalio, A., Behm-Ansmant, I., Schweizer, D., and Izaurralde, E. (2007b). P-body formation is a consequence, not the cause, of RNA-mediated gene silencing. Mol. Cell. Biol. 27, 3970–3981.

Eulalio, A., Izaurralde, E., and Huntzinger, E. (2008). GW182 interaction with Argonaute is essential for miRNA-mediated translational repression and mRNA decay. Nat. Struct. Mol. Biol. 15, 346–353.

Fabian, M.R., Mathonnet, G., Sundermeier, T., Mathys, H., Zipprich, J.T., Svitkin, Y.V., Rivas, F., Jinek, M., Wohlschlegel, J., Doudna, J.A., et al. (2009). Mammalian miRNA RISC recruits CAF1 and PABP to affect PABP-dependent deadenylation. Mol. Cell 35, 868–880.

Fadok, V.A., Bratton, D.L., Frasch, S.C., Warner, M.L., and Henson, P.M. (1998). The role of phosphatidylserine in recognition of apoptotic cells by phagocytes. Cell Death Differ. 5, 551–562.

Feng, W.H., Xue, K.S., Tang, L., Williams, P.L., and Wang, J.S. (2017). Aflatoxin B1-induced developmental and DNA damage in Caenorhabditis elegans. Toxins 9, 9.

Fox, P.M., Vought, V.E., Hanazawa, M., Lee, M.-H., Maine, E.M., and Schedl, T. (2011). Cyclin E and CDK-2 regulate proliferative cell fate and cell cycle progression in the C. elegans germline. Development 138, 2223–2234.

Francis, R., Barton, M.K., Kimble, J., and Schedl, T. (1995). gld-1, a tumor suppressor gene required for oocyte development in Caenorhabditis elegans. Genetics 139, 579–606.

Frank, S., Gaume, B., Bergmann-Leitner, E.S., Leitner, W.W., Robert, E.G., Catez, F., Smith, C.L., and Youle, R.J. (2001). The Role of dynamin-related protein 1, a mediator of mitochondrial fission, in apoptosis. Dev. Cell 1, 515–525.

Frezza, C., Cipolat, S., Martins de Brito, O., Micaroni, M., Beznoussenko, G.V., Rudka, T., Bartoli, D., Polishuck, R.S., Danial, N.N., De Strooper, B., et al. (2006). OPA1 controls apoptotic cristae remodeling independently from mitochondrial fusion. Cell 126, 177–189.

Friedman, R.C., Farh, K.K.-H., Burge, C.B., and Bartel, D.P. (2009). Most mammalian mRNAs are conserved targets of microRNAs. Genome Res. 19, 92–105.

Fukunaga, R., Han, B.W., Hung, J.-H., Xu, J., Weng, Z., and Zamore, P.D. (2012). Dicer partner proteins tune the length of mature miRNAs in flies and mammals. Cell 151, 533–546.

Fukunaga, R., Colpan, C., Han, B.W., and Zamore, P.D. (2014). Inorganic phosphate blocks binding of pre-miRNA to Dicer-2 via its PAZ domain. EMBO J. 33, 371–384.

Galvin, B.D., Denning, D.P., and Horvitz, H.R. (2011). SPK-1, an SR protein kinase, inhibits programmed cell death in Caenorhabditis elegans. Proc. Natl. Acad. Sci. 108, 1998–2003.

Gao, M.X., Liao, E.H., Yu, B., Wang, Y., Zhen, M., and Derry, W.B. (2008). The SCFFSN-1 ubiquitin ligase controls germline apoptosis through CEP-1/p53 in C. elegans. Cell Death Differ. 15, 1054–1062.

Garcia-Muse, T., and Boulton, S.J. (2005). Distinct modes of ATR activation after replication stress and DNA double-strand breaks in Caenorhabditis elegans. EMBO J. 24, 4345–4355.

Gartner, A., Boag, P.R., and Blackwell, T.K. (2008). Germline survival and apoptosis. WormBook Online Rev. C Elegans Biol. 1–20.

Gartner, A., Milstein, S., Ahmed, S., Hodgkin, J., and Hengartner, M.O. (2000). A conserved checkpoint pathway mediates DNA damage–induced apoptosis and cell cycle arrest in C. elegans. Mol. Cell 5, 435–443.

Ge, X., Zhao, X., Nakagawa, A., Gong, X., Skeen-Gaar, R.R., Shi, Y., Gong, H., Wang, X., and Xue, D. (2014). A novel mechanism underlies caspase-dependent conversion of the dicer ribonuclease into a deoxyribonuclease during apoptosis. Cell Res. 24, 218–232.

Gibbings, D.J., Ciaudo, C., Erhardt, M., and Voinnet, O. (2009). Multivesicular bodies associate with components of miRNA effector complexes and modulate miRNA activity. Nat. Cell Biol. 11, 1143–1149.

Glucksmann, A. (1951). Cell deaths in normal vertebrate ontogeny. Biol. Rev. Camb. Philos. Soc. 26, 59–86.

Gönczy, P., Echeverri, C., Oegema, K., Coulson, A., Jones, S.J.M., Copley, R.R., Duperon, J., Oegema, J., Brehm, M., Cassin, E., et al. (2000). Functional genomic analysis of cell division in C. elegans using RNAi of genes on chromosome III. Nature 408, 331–336.

Goyal, G., Fell, B., Sarin, A., Youle, R.J., and Sriram, V. (2007). Role of mitochondrial remodeling in programmed cell death in Drosophila melanogaster. Dev. Cell 12, 807–816.

Gregory, R.I., Yan, K., Amuthan, G., Chendrimada, T., Doratotaj, B., Cooch, N., and Shiekhattar, R. (2004). The Microprocessor complex mediates the genesis of microRNAs. Nature 432, 235–240

Greiss, S., Schumacher, B., Grandien, K., Rothblatt, J., and Gartner, A. (2008). Transcriptional profiling in C. elegans suggests DNA damage dependent apoptosis as an ancient function of the p53 family. BMC Genomics 9:334.

Grey, F., Tirabassi, R., Meyers, H., Wu, G., McWeeney, S., Hook, L., and Nelson, J.A. (2010). A viral microRNA down-regulates multiple cell cycle genes through mRNA 5'UTRs. PLoS Pathog. 6, e1000967–e1000967.

Grimson, A., Farh, K.K.-H., Johnston, W.K., Garrett-Engele, P., Lim, L.P., and Bartel, D.P. (2007). MicroRNA targeting specificity in mammals: determinants beyond seed pairing. Mol. Cell 27, 91–105.

Grishok, A., Pasquinelli, A.E., Conte, D., Li, N., Parrish, S., Ha, I., Baillie, D.L., Fire, A., Ruvkun, G., and Mello, C.C. (2001). Genes and mechanisms related to RNA interference regulate expression of the small temporal RNAs that control C. elegans developmental timing. Cell 106, 23–34.

Grün, D., Kirchner, M., Thierfelder, N., Stoeckius, M., Selbach, M., and Rajewsky, N. (2014). Conservation of mRNA and protein expression during development of C. elegans. Cell Rep. 6, 565–577.

Gumienny, T.L., Lambie, E., Hartwieg, E., Horvitz, H.R., and Hengartner, M.O. (1999). Genetic control of programmed cell death in the Caenorhabditis elegans hermaphrodite germline. Development 126, 1011–1022.

Guo, H., Ingolia, N.T., Weissman, J.S., and Bartel, D.P. (2010). Mammalian microRNAs predominantly act to decrease target mRNA levels. Nature 466, 835–840.

Gurling, M., Talavera, K., and Garriga, G. (2014). The DEP domain-containing protein TOE-2 promotes apoptosis in the Q lineage of C. elegans through two distinct mechanisms. Development 141, 2724–2734.

Hafner, M., Landthaler, M., Burger, L., Khorshid, M., Hausser, J., Berninger, P., Rothballer, A., Ascano, M., Jungkamp, A.-C., Munschauer, M., et al. (2010). Transcriptome-wide Identification of RNA-Binding Protein and MicroRNA Target Sites by PAR-CLIP. Cell 141, 129–141.

Han, J., Lee, Y., Yeom, K.-H., Kim, Y.-K., Jin, H., and Kim, V.N. (2004). The Drosha-DGCR8 complex in primary microRNA processing. Genes Dev. 18, 3016–3027.

Han, J., Lee, Y., Yeom, K.-H., Nam, J.-W., Heo, I., Rhee, J.-K., Sohn, S.Y., Cho, Y., Zhang, B.-T., and Kim, V.N. (2006). Molecular basis for the recognition of primary microRNAs by the Drosha-DGCR8 complex. Cell 125, 887–901.

Hansen, D., Wilson-Berry, L., Dang, T., and Schedl, T. (2004). Control of the proliferation versus meiotic development decision in the C. elegans germline through regulation of GLD-1 protein accumulation. Development 131, 93–104.

Harris, T.W., Chen, N., Cunningham, F., Tello-Ruiz, M., Antoshechkin, I., Bastiani, C., Bieri, T., Blasiar, D., Bradnam, K., Chan, J., et al. (2004). WormBase: a multi-species resource for nematode biology and genomics. Nucleic Acids Res. 32, D411–D417.

Hausser, J., and Zavolan, M. (2014). Identification and consequences of miRNA–target interactions — beyond repression of gene expression. Nat. Rev. Genet. 15, 599–612.

Helwak, A., and Tollervey, D. (2014). Mapping the miRNA interactome by cross-linking ligation and sequencing of hybrids (CLASH). Nat. Protoc. 9, 711–728.

Hendrickson, D.G., Hogan, D.J., McCullough, H.L., Myers, J.W., Herschlag, D., Ferrell, J.E., and Brown, P.O. (2009). Concordant regulation of translation and mRNA abundance for hundreds of targets of a human microRNA. PLOS Biol. 7, e1000238.

Hengartner, M.O., and Horvitz, H.R. (1994a). C. elegans cell survival gene ced-9 encodes a functional homolog of the mammalian proto-oncogene bcl-2. Cell 76, 665–676.

Hengartner, M.O., and Horvitz, H.R. (1994b). Activation of C. elegans cell death protein CED-9 by an ammo-acid substitution in a domain conserved in Bcl-2. Nature 369, 318–320.

Hengartner, M.O., Ellis, R., and Horvitz, R. (1992). Caenorhabditis elegans gene ced-9 protects cells from programmed cell death. Nature 356, 494–499.

Henke, J.I., Goergen, D., Zheng, J., Song, Y., Schüttler, C.G., Fehr, C., Jünemann, C., and Niepmann, M. (2008). microRNA-122 stimulates translation of hepatitis C virus RNA. EMBO J. 27, 3300–3310.

Herranz, H., and Cohen, S.M. (2010). MicroRNAs and gene regulatory networks: managing the impact of noise in biological systems. Genes Dev. 24, 1339–1344.

Hillers, K.J., Jantsch, V., Martinez-Perez, E., and Yanowitz, J.L. (2017). Meiosis. Wormbook 1–43.

Hird, S.N., Paulsen, J.E., and Strome, S. (1996). Segregation of germ granules in living Caenorhabditis elegans embryos: cell-type-specific mechanisms for cytoplasmic localisation. Development 122, 1303–1312.

Hofmann, E.R., Milstein, S., Boulton, S.J., Ye, M., Hofmann, J.J., Stergiou, L., Gartner, A., Vidal, M., and Hengartner, M.O. (2002). Caenorhabditis elegans HUS-1 is a DNA damage checkpoint protein required for genome stability and EGL-1-mediated apoptosis. Curr. Biol. 12, 1908–1918.

Hollstein, M., Sidransky, D., Vogelstein, B., and Harris, C.C. (1991). p53 mutations in human cancers. Science 253, 49–53.

Horvitz, H.R. (2003). Nobel lecture. Worms, life and death. Biosci. Rep. 23, 239–303.

Hsueh, A.J.W., Billig, H., and Tsafriri, A. (1994). Ovarian Follicle Atresia: A Hormonally Controlled Apoptotic Process. Endocr. Rev. 15, 707–724.

Hu, W., Chan, C.S., Wu, R., Zhang, C., Sun, Y., Song, J.S., Tang, L.H., Levine, A.J., and Feng, Z. (2010). Negative regulation of tumor suppressor p53 by microRNA miR-504., Negative Regulation of Tumor Suppressor p53 by microRNA miR-504. Mol. Cell 38, 689–699.

Huang, W., Jiang, T., Choi, W., Qi, S., Pang, Y., Hu, Q., Xu, Y., Gong, X., Jeffrey, P.D., Wang, J., et al. (2013). Mechanistic insights into CED-4-mediated activation of CED-3. Genes Dev. 27, 2039–2048.

Humphreys, D.T., Westman, B.J., Martin, D.I.K., and Preiss, T. (2005). MicroRNAs control translation initiation by inhibiting eukaryotic initiation factor 4E/cap and poly(A) tail function. Proc. Natl. Acad. Sci. U. S. A. 102, 16961–16966.

Hutvágner, G., McLachlan, J., Pasquinelli, A.E., Bálint, É., Tuschl, T., and Zamore, P.D. (2001). A cellular function for the RNA-interference enzyme Dicer in the maturation of the let-7 small temporal RNA. Science 293, 834–838.

Huyen, Y., Jeffrey, P.D., Derry, W.B., Rothman, J.H., Pavletich, N.P., Stavridi, E.S., and Halazonetis, T.D. (2004). Structural differences in the DNA binding domains of human p53 and its C. elegans ortholog Cep-1. Structure 12, 1237–1243.

Ishii, N., Fujii, M., Hartman, P.S., Tsuda, M., Yasuda, K., Senoo-Matsuda, N., Yanase, S., Ayusawa, D., and Suzuki, K. (1998). A mutation in succinate dehydrogenase cytochrome b causes oxidative stress and ageing in nematodes. Nature 394, 694–697.

Jagasia, R., Grote, P., Westermann, B., and Conradt, B. (2005). DRP-1-mediated mitochondrial fragmentation during EGL-1-induced cell death in C. elegans. Nature 433, 754–760.

Jakymiw, A., Chan, E.K.L., Hamel, J.C., Fritzler, M.J., Satoh, M., Lian, S., Li, S., and Eystathioy, T. (2005). Disruption of GW bodies impairs mammalian RNA interference. Nat. Cell Biol. 7, 1267–1274.

Jaramillo-Lambert, A., Harigaya, Y., Vitt, J., Villeneuve, A., and Engebrecht, J. (2010). Meiotic errors activate checkpoints that improve gamete quality without triggering apoptosis in male germ cells. Curr. Biol. 20, 2078–2089.

Jiang, H.-S., and Wu, Y.-C. (2014). LIN-3/EGF promotes the programmed cell death of specific cells in Caenorhabditis elegans by transcriptional activation of the pro-apoptotic gene egl-1. PLOS Genet. 10, e1004513.

Jiang, Q., Wang, Y., Hao, Y., Juan, L., Teng, M., Zhang, X., Li, M., Wang, G., and Liu, Y. (2009). miR2Disease: a manually curated database for microRNA deregulation in human disease. Nucleic Acids Res. 37, D98–D104.

Joerger, A.C., and Fersht, A.R. (2010). The Tumor suppressor p53: from structures to drug discovery. Cold Spring Harb. Perspect. Biol. 2, a000919.

Jones, A.R., and Schedl, T. (1995). Mutations in gld-1, a female germ cell-specific tumor suppressor gene in Caenorhabditis elegans, affect a conserved domain also found in Src-associated protein Sam68. Genes Dev. 9, 1491–1504.

Joshi, P., and Eisenmann, D.M. (2004). The Caenorhabditis elegans pvl-5 gene protects hypodermal cells from ced-3-dependent, ced-4-independent cell death. Genet. 167, 673–685.

Kadyk, L.C., and Kimble, J. (1998). Genetic regulation of entry into meiosis in Caenorhabditis elegans. Development 125, 1803–1813.

Kaghad, M., Bonnet, H., Yang, A., Creancier, L., Biscan, J.-C., Valent, A., Minty, A., Chalon, P., Lelias, J.-M., Dumont, X., et al. (1997). Monoallelically expressed gene related to p53 at 1p36, a region frequently deleted in neuroblastoma and other human cancers. Cell 90, 809–819.

Kamkina, P., Snoek, L.B., Grossmann, J., Volkers, R.J.M., Sterken, M.G., Daube, M., Roschitzki, B., Fortes, C., Schlapbach, R., Roth, A., et al. (2016). Natural genetic variation differentially affects the proteome and transcriptome in Caenorhabditis elegans. Mol. Cell. Proteomics 15, 1670–1680.

Kandoth, C., McLellan, M.D., Vandin, F., Ye, K., Niu, B., Lu, C., Xie, M., Zhang, Q., McMichael, J.F., Wyczalkowski, M.A., et al. (2013). Mutational landscape and significance across 12 major cancer types. Nature 502, 333–339.

Karbowski, M., Lee, Y.-J., Gaume, B., Jeong, S.-Y., Frank, S., Nechushtan, A., Santel, A., Fuller, M., Smith, C.L., and Youle, R.J. (2002). Spatial and temporal association of Bax with mitochondrial fission sites, Drp1, and Mfn2 during apoptosis. J. Cell Biol. 159, 931–938.

Kastenhuber, E.R., and Lowe, S.W. (2017). Putting p53 in Context. Cell 170, 1062–1078.

Kato, M., de Lencastre, A., Pincus, Z., and Slack, F.J. (2009). Dynamic expression of small non-coding RNAs, including novel microRNAs and piRNAs/21U-RNAs, during Caenorhabditis elegansdevelopment. Genome Biol. 10, R54.

Kerr, J.F., Wyllie, A.H., and Currie, A.R. (1972). Apoptosis: a basic biological phenomenon with wide-ranging implications in tissue kinetics. Br. J. Cancer 26, 239–257.

Kershner, A.M., and Kimble, J. (2010). Genome-wide analysis of mRNA targets for Caenorhabditis elegans FBF, a conserved stem cell regulator. Proc. Natl. Acad. Sci. 107, 3936–3941.

Khorshid, M., Hausser, J., Zavolan, M., and Nimwegen, E. van (2013). A biophysical miRNA-mRNA interaction model infers canonical and noncanonical targets. Nat. Methods 10, 253–255.

Kimble, J., and Crittenden, S.L. (2007). Controls of germline stem cells, entry into meiosis, and the sperm/oocyte decision in Caenorhabditis elegans. Annu. Rev. Cell Dev. Biol. 23, 405–433.

Knight, S.W., and Bass, B.L. (2001). A role for the RNase III enzyme DCR-1 in RNA interference and germ line development in Caenorhabditis elegans. Science 293, 2269–2271.

Kosaka, N., Iguchi, H., Yoshioka, Y., Takeshita, F., Matsuki, Y., and Ochiya, T. (2010). Secretory mechanisms and intercellular transfer of microRNAs in living Cells. J. Biol. Chem. 285, 17442–17452.

Kouwenhove, M. van, Kedde, M., and Agami, R. (2011). MicroRNA regulation by RNA-binding proteins and its implications for cancer. Nat. Rev. Cancer 11, 644–656.

Kozomara, A., and Griffiths-Jones, S. (2014). miRBase: annotating high confidence microRNAs using deep sequencing data. Nucleic Acids Res. 42, D68–D73.

Kritikou, E.A., Milstein, S., Vidalain, P.-O., Lettre, G., Bogan, E., Doukoumetzidis, K., Gray, P., Chappell, T.G., Vidal, M., and Hengartner, M.O. (2006). C. elegans GLA-3 is a novel component of the MAP kinase MPK-1 signaling pathway required for germ cell survival. Genes Dev. 20, 2279–2292.

Kurosaka, K., Takahashi, M., Watanabe, N., and Kobayashi, Y. (2003). Silent cleanup of very early apoptotic cells by macrophages. J. Immunol. 171, 4672–4679.

Lagos-Quintana, M., Rauhut, R., Lendeckel, W., and Tuschl, T. (2001). Identification of novel genes coding for small expressed RNAs. Science 294, 853–858.

Lagos-Quintana, M., Rauhut, R., Meyer, J., Borkhardt, A., and Tuschl, T. (2003). New microRNAs from mouse and human. RNA 9, 175–179.

Lai, E.C., Tomancak, P., Williams, R.W., and Rubin, G.M. (2003). Computational identification of DrosophilamicroRNA genes. Genome Biol. 4, R42.

Lai, H.J., Lo, S.J., Kage-Nakadai, E., Mitani, S., and Xue, D. (2009). The roles and acting mechanism of Caenorhabditis elegans DNase II genes in apoptotic DNA degradation and development. PLoS ONE 4, e7348.

Lamont, L.B., Crittenden, S.L., Bernstein, D., Wickens, M., and Kimble, J. (2004). FBF-1 and FBF-2 regulate the size of the mitotic region in the C. elegans germline. Dev. Cell 7, 697–707.

Lau, N.C., Lim, L.P., Weinstein, E.G., and Bartel, D.P. (2001). An abundant class of tiny RNAs with probable regulatory roles in Caenorhabditis elegans. Science 294, 858–862.

Lau, P.-W., Guiley, K.Z., De, N., Potter, C.S., Carragher, B., and MacRae, I.J. (2012). The molecular architecture of human Dicer. Nat. Struct. Mol. Biol. 19, 436–440.

Laurenzi, V.D., Costanzo, A., Barcaroli, D., Terrinoni, A., Falco, M., Annicchiarico-Petruzzelli, M., Levrero, M., and Melino, G. (1998). Two new p73 splice variants, γ and δ, with different transcriptional activity. J. Exp. Med. 188, 1763–1768.

Lee, H.Y., and Doudna, J.A. (2012). TRBP alters human precursor microRNA processing in vitro. RNA 18, 2012–2019.

Lee, M.-H., and Schedl, T. (2001). Identification of in vivo mRNA targets of GLD-1, a maxi-KH motif containing protein required for C. elegans germ cell development. Genes Dev. 15, 2408–2420.

Lee, H.Y., Zhou, K., Smith, A.M., Noland, C.L., and Doudna, J.A. (2013). Differential roles of human Dicer-binding proteins TRBP and PACT in small RNA processing. Nucleic Acids Res. 41, 6568–6576.

Lee, M.-H., Hook, B., Lamont, L.B., Wickens, M., and Kimble, J. (2006a). LIP-1 phosphatase controls the extent of germline proliferation in Caenorhabditis elegans. EMBO J. 25, 88–96.

Lee, M.-H., Hook, B., Pan, G., Kershner, A.M., Merritt, C., Seydoux, G., Thomson, J.A., Wickens, M., and Kimble, J. (2007a). Conserved regulation of MAP kinase expression by PUF RNA-binding proteins. PLOS Genet. 3, 2540–2550.

Lee, M.H., Ohmachi, M., Arur, S., Nayak, S., Francis, R., Church, D., Lambie, E., and Schedl, T. (2007b). Multiple functions and dynamic activation of MPK-1 extracellular signal-regulated kinase signaling in Caenorhabditis elegans germline development. Genet. 177, 2039–2062.

Lee, R.C., Feinbaum, R.L., and Ambros, V. (1993). The C. elegans heterochronic gene lin-4 encodes small RNAs with antisense complementarity to lin-14. Cell 75, 843–854.

Lee, Y., Jeon, K., Lee, J.-T., Kim, S., and Kim, V.N. (2002). MicroRNA maturation: stepwise processing and subcellular localization. EMBO J. 21, 4663–4670.

Lee, Y., Ahn, C., Han, J., Choi, H., Kim, J., Yim, J., Lee, J., Provost, P., Rådmark, O., Kim, S., et al. (2003). The nuclear RNase III Drosha initiates microRNA processing. Nature 425, 415–419.

Lee, Y., Kim, M., Han, J., Yeom, K.-H., Lee, S., Baek, S.H., and Kim, V.N. (2004a). MicroRNA genes are transcribed by RNA polymerase II. EMBO J. 23, 4051–4060.

Lee, Y., Hur, I., Park, S.-Y., Kim, Y.-K., Suh, M.R., and Kim, V.N. (2006b). The role of PACT in the RNA silencing pathway. EMBO J. 25, 522–532.

Lee, Y.J., Jeong, S.Y., Karbowski, M., Smith, C.L., and Youle, R.J. (2004b). Roles of the mammalian mitochondrial fission and fusion mediators Fis1, Drp1, and Opa1 in apoptosis. Mol. Biol. Cell 15, 5001–5011.

Lee, Y.S., Pressman, S., Andress, A.P., Kim, K., White, J.L., Cassidy, J.J., Li, X., Lubell, K., Lim, D.H., Cho, I.S., et al. (2009). Silencing by small RNAs is linked to endosomal trafficking. Nat. Cell Biol. 11, 1150–1156.

Lettre, G., Kritikou, E.A., Jaeggi, M., Calixto, A., Fraser, A.G., Kamath, R.S., Ahringer, J., and Hengartner, M.O. (2004). Genome-wide RNAi identifies p53-dependent and -independent regulators of germ cell apoptosis in C. elegans. Cell Death Differ. 11, 1198–1203.

Leung, A.K.L., Calabrese, J.M., and Sharp, P.A. (2006). Quantitative analysis of Argonaute protein reveals microRNA-dependent localization to stress granules. Proc. Natl. Acad. Sci. 103, 18125–18130.

Levine, A.J. (1997). p53, the cellular gatekeeper for growth and division. Cell 88, 323–331.

Lewis, B.P., Burge, C.B., and Bartel, D.P. (2005). Conserved seed pairing, often flanked by adenosines, indicates that thousands of human genes are microRNA targets. Cell 120, 15–20.

Liu, J., Carmell, M.A., Rivas, F.V., Marsden, C.G., Thomson, J.M., Song, J.-J., Hammond, S.M., Joshua-Tor, L., and Hannon, G.J. (2004). Argonaute2 is the catalytic engine of mammalian RNAi. Science 305, 1437–1441.

Liu, J., Valencia-Sanchez, M.A., Hannon, G.J., and Parker, R. (2005a). MicroRNA-dependent localization of targeted mRNAs to mammalian P-bodies. Nat. Cell Biol. 7, 719–723.

Liu, J., Rivas, F.V., Wohlschlegel, J., Iii, J.R.Y., Parker, R., and Hannon, G.J. (2005b). A role for the P-body component GW182 in microRNA function. Nat. Cell Biol. 7, 1261–1266.

Lockshin, R.A., and Williams, C.M. (1964). Programmed cell death—II. Endocrine potentiation of the breakdown of the intersegmental muscles of silkmoths. J. Insect Physiol. 10, 643–649.

Lu, J., Getz, G., Miska, E.A., Alvarez-Saavedra, E., Lamb, J., Peck, D., Sweet-Cordero, A., Ebert, B.L., Mak, R.H., Ferrando, A.A., et al. (2005). MicroRNA expression profiles classify human cancers. Nature 435, nature03702.

Lund, E., Güttinger, S., Calado, A., Dahlberg, J.E., and Kutay, U. (2004). Nuclear export of microRNA precursors. Science 303, 95–98.

MacRae, I.J., Zhou, K., Li, F., Repic, A., Brooks, A.N., Cande, W.Z., Adams, P.D., and Doudna, J.A. (2006). Structural basis for double-stranded RNA processing by Dicer. Science 311, 195–198.

MacRae, I.J., Zhou, K., and Doudna, J.A. (2007). Structural determinants of RNA recognition and cleavage by Dicer. Nat. Struct. Mol. Biol. 14, 934–940.

Marin, V.A., and Evans, T.C. (2003). Translational repression of a C. elegans Notch mRNA by the STAR/KH domain protein GLD-1. Development 130, 2623–2632.

Maurer, C.W., Chiorazzi, M., and Shaham, S. (2007). Timing of the onset of a developmental cell death is controlled by transcriptional induction of the C. elegans ced-3 caspase-encoding gene. Development 134, 1357–1368.

Meijer, H.A., Kong, Y.W., Lu, W.T., Wilczynska, A., Spriggs, R.V., Robinson, S.W., Godfrey, J.D., Willis, A.E., and Bushell, M. (2013). Translational repression and eIF4A2 activity are critical for microRNA-mediated gene regulation. Science 340, 82–85.

Meister, G., Landthaler, M., Patkaniowska, A., Dorsett, Y., Teng, G., and Tuschl, T. (2004). Human Argonaute2 mediates RNA cleavage targeted by miRNAs and siRNAs. Mol. Cell 15, 185–197.

Mello, C.C., Schubert, C., Draper, B., Zhang, W., Lobel, R., and Priess, J.R. (1996). The PIE-1 protein and germline specification in C. elegans embryos. Nature 382, 710–712.

Mendell, J.T., and Olson, E.N. (2012). MicroRNAs in stress signaling and human disease. Cell 148, 1172–1187.

Merritt, C., Rasoloson, D., Ko, D., and Seydoux, G. (2008). 3′ UTRs are the primary regulators of gene expression in the C. elegans germline. Curr. Biol. 18, 1476–1482.

Min, H., Shim, Y.-H., and Kawasaki, I. (2016). Loss of PGL-1 and PGL-3, members of a family of constitutive germ-granule components, promotes germline apoptosis in C. elegans. J. Cell Sci. 129, 341–353.

Mittelbrunn, M., Gutiérrez-Vázquez, C., Villarroya-Beltri, C., González, S., Sánchez-Cabo, F., González, M.Á., Bernad, A., and Sánchez-Madrid, F. (2011). Unidirectional transfer of microRNA-loaded exosomes from T cells to antigen-presenting cells. Nat. Commun. 2:282, ncomms1285.

Miura, M., Zhu, H., Rotello, R., Hartwieg, E.A., and Yuan, J. (1993). Induction of apoptosis in fibroblasts by IL-1β-converting enzyme, a mammalian homolog of the C. elegans cell death gene ced-3. Cell 75, 653–660.

Montecalvo, A., Larregina, A.T., Shufesky, W.J., Stolz, D.B., Sullivan, M.L.G., Karlsson, J.M., Baty, C.J., Gibson, G.A., Erdos, G., Wang, Z., et al. (2012). Mechanism of transfer of functional microRNAs between mouse dendritic cells via exosomes. Blood 119, 756–766.

Moore, M.J. (2005). From birth to death: the complex lives of eukaryotic mRNAs. Science 309, 1514–1518.

Mukherji, S., Ebert, M.S., Zheng, G.X., Tsang, J.S., Sharp, P.A., and Van, A.O. (2011). MicroRNAs can generate thresholds in target gene expression. Nat. Genet. *43*, 854–859.

Mulrane, L., McGee, S.F., Gallagher, W.M., and O'Connor, D.P. (2013). miRNA Dysregulation in Breast Cancer. Cancer Res. 73, 6554–6562.

Nakagawa, A., Shi, Y., Kage-Nakadai, E., Mitani, S., and Xue, D. (2010). Caspase-dependent conversion of Dicer ribonuclease into a death-promoting deoxyribonuclease. Sci. N. Y. N 328, 327–334.

Nakagawa, A., Sullivan, K.D., and Xue, D. (2014). Caspase-activated phosphoinositide binding by CNT-1 promotes apoptosis by inhibiting the AKT pathway. Nat. Struct. Mol. Biol. 21, 1082–1090.

Nakano, K., and Vousden, K.H. (2001). PUMA, a novel proapoptotic gene, is induced by p53. Mol. Cell 7, 683–694.

Navarro, R.E., Shim, E.Y., Kohara, Y., Singson, A., and Blackwell, T.K. (2001). cgh-1, a conserved predicted RNA helicase required for gametogenesis and protection from physiological germline apoptosis in C. elegans. Dev. Camb. Engl. 128, 3221–3232.

Nehme, R., and Conradt, B. (2009). egl-1: a key activator of apoptotic cell death in C. elegans. Oncogene 27, S30–S40.

Nousch, M., and Eckmann, C.R. (2013). Translational control in the Caenorhabditis elegans germ line. In germ cell development in C. Elegans, (Springer, New York, NY), pp. 205–247.

Oda, E., Ohki, R., Murasawa, H., Nemoto, J., Shibue, T., Yamashita, T., Tokino, T., Taniguchi, T., and Tanaka, † Nobuyuki (2000). Noxa, a BH3-only member of the Bcl-2 family and candidate mediator of p53-induced apoptosis. Science 288, 1053–1058.

Ogata-Kawata, H., Izumiya, M., Kurioka, D., Honma, Y., Yamada, Y., Furuta, K., Gunji, T., Ohta, H., Okamoto, H., Sonoda, H., et al. (2014). Circulating exosomal microRNAs as biomarkers of colon cancer. PLOS ONE 9, e92921.

Ohler, U., Yekta, S., Lim, L.P., Bartel, D.P., and Burge, C.B. (2004). Patterns of flanking sequence conservation and a characteristic upstream motif for microRNA gene identification. RNA 10, 1309–1322.

Ørom, U.A., Nielsen, F.C., and Lund, A.H. (2008). MicroRNA-10a binds the 5′UTR of ribosomal protein mRNAs and enhances their translation. Mol. Cell 30, 460–471.

Ou, G., Stuurman, N., D'Ambrosio, M., and Vale, R.D. (2010). Polarized myosin produces unequal-size daughters during asymmetric cell division. Sci. N. Y. N 330, 677–680.

Ou, H.D., Löhr, F., Vogel, V., Mäntele, W., and Dötsch, V. (2007). Structural evolution of C-terminal domains in the p53 family. EMBO J. 26, 3463–3473.

Park, D., Jia, H., Rajakumar, V., and Chamberlin, H.M. (2006). Pax2/5/8 proteins promote cell survival in C. elegans. Development 133, 4193–4202.

Park, J.-E., Heo, I., Tian, Y., Simanshu, D.K., Chang, H., Jee, D., Patel, D.J., and Kim, V.N. (2011). Dicer recognizes the 5′ end of RNA for efficient and accurate processing. Nature 475, 201–205.

Parone, P.A., James, D.I., Cruz, S.D., Mattenberger, Y., Donzé, O., Barja, F., and Martinou, J.-C. (2006). Inhibiting the mitochondrial fission machinery does not prevent Bax/Bak-dependent apoptosis. Mol. Cell. Biol. 26, 7397–7408.

Parrish, J.Z., and Xue, D. (2003). Functional genomic analysis of apoptotic DNA degradation in C. elegans. Mol. Cell 11, 987–996.

Parrish, J., Metters, H., Chen, L., and Xue, D. (2000). Demonstration of the in vivo interaction of key cell death regulators by structure-based design of second-site suppressors. Proc. Natl. Acad. Sci. 97, 11916–11921.

Parrish, J., Li, L., Klotz, K., Ledwich, D., Wang, X., and Xue, D. (2001). Mitochondrial endonuclease G is important for apoptosis in C. elegans. Nature 412, 90–94.

Parrish, J.Z., Yang, C., Shen, B., and Xue, D. (2003). CRN-1, a Caenorhabditis elegans FEN-1 homologue, cooperates with CPS-6/EndoG to promote apoptotic DNA degradation. EMBO J. 22, 22, 3451, 3451–3460.

Pasquinelli, A.E., Reinhart, B.J., Slack, F., Martindale, M.Q., Kuroda, M.I., Maller, B., Hayward, D.C., Ball, E.E., Degnan, B., Müller, P., et al. (2000). Conservation of the sequence and temporal expression of let-7 heterochronic regulatory RNA. Nature 408, 86–89.

Pegtel, D.M., Cosmopoulos, K., Thorley-Lawson, D.A., Eijndhoven, M.A.J. van, Hopmans, E.S., Lindenberg, J.L., Gruijl, T.D. de, Würdinger, T., and Middeldorp, J.M. (2010). Functional delivery of viral miRNAs via exosomes. Proc. Natl. Acad. Sci. 107, 6328–6333.

Peso, L. del, González, V.M., and Núñez, G. (1998). Caenorhabditis elegans EGL-1 disrupts the interaction of CED-9 with CED-4 and promotes CED-3 activation. J. Biol. Chem. 273, 33495–33500.

Peters, L., and Meister, G. (2007). Argonaute proteins: mediators of RNA silencing. Mol. Cell 26, 611–623.

Petersen, C.P., Bordeleau, M.-E., Pelletier, J., and Sharp, P.A. (2006). Short RNAs repress translation after initiation in mammalian cells. Mol. Cell 21, 533–542.

Pillai, R.S., Bhattacharyya, S.N., Artus, C.G., Zoller, T., Cougot, N., Basyuk, E., Bertrand, E., and Filipowicz, W. (2005). Inhibition of translational initiation by let-7 microRNA in human cells. Science 309, 1573–1576.

Pinan-Lucarre, B., Gabel, C.V., Reina, C.P., Hulme, S.E., Shevkoplyas, S.S., Slone, R.D., Xue, J., Qiao, Y., Weisberg, S., Roodhouse, K., et al. (2012). The Core apoptotic executioner proteins CED-3 and CED-4 promote initiation of neuronal regeneration in Caenorhabditis elegans. PLoS Biol. 10, e1001331.

Pitt, J.N., Schisa, J.A., and Priess, J.R. (2000). P granules in the germ cells of Caenorhabditis elegans adults are associated with clusters of nuclear pores and contain RNA. Dev. Biol. 219, 315–333.

Pourkarimi, E., Greiss, S., and Gartner, A. (2012). Evidence that CED-9/Bcl2 and CED-4/Apaf-1 localization is not consistent with the current model for C. elegans apoptosis induction. Cell Death Differ. 19, 406–415.

Qi, S., Pang, Y., Hu, Q., Liu, Q., Li, H., Zhou, Y., He, T., Liang, Q., Liu, Y., Yuan, X., et al. (2010). Crystal structure of the Caenorhabditis elegans apoptosome reveals an octameric assembly of CED-4. Cell 141, 446–457.

Reczko, M., Maragkakis, M., Alexiou, P., Grosse, I., and Hatzigeorgiou, A.G. (2012). Functional microRNA targets in protein coding sequences. Bioinformatics *28*, 771–776.

Reinhart, B.J., Slack, F.J., Basson, M., Pasquinelli, A.E., Bettinger, J.C., Rougvie, A.E., Horvitz, H.R., and Ruvkun, G. (2000). The 21-nucleotide let-7 RNA regulates developmental timing in Caenorhabditis elegans. Nature 403, 901–906.

Rose, L., and Gönczy, P. (2014). Polarity establishment, asymmetric division and segregation of fate determinants in early C. elegans embryos. WormBook Online Rev. C Elegans Biol. 1–43.

Rosenberg, A.B., Patwardhan, R.P., Shendure, J., and Seelig, G. (2015). Learning the sequence determinants of alternative splicing from millions of random sequences. Cell 163, 698–711.

Roush, S., and Slack, F.J. (2008). The let-7 family of microRNAs. Trends Cell Biol. 18, 505–516.

Ruepp, A., Kowarsch, A., Schmidl, D., Buggenthin, F., Brauner, B., Dunger, I., Fobo, G., Frishman, G., Montrone, C., and Theis, F.J. (2010). PhenomiR: a knowledgebase for microRNA expression in diseases and biological processes. Genome Biol. 11, R6.

Rutkowski, R., Hofmann, K., and Gartner, A. (2010). Phylogeny and function of the invertebrate p53 superfamily. Biol. Cold Spring Harb. Perspect. 2, a001131.

Rutkowski, R., Dickinson, R., Stewart, G., Craig, A., Schimpl, M., Keyse, S.M., and Gartner, A. (2011). Regulation of Caenorhabditis elegans p53/CEP-1–dependent germ cell apoptosis by Ras/MAPK signaling. PLOS Genet. 7, e1002238.

Ruvkun, G., and Giusto, J. (1989). The Caenorhabditis elegans heterochronic gene lin-14 encodes a nuclear protein that forms a temporal developmental switch. Nature 338, 313–319.

Sacconi, A., Biagioni, F., Canu, V., Mori, F., Benedetto, A.D., Lorenzon, L., Ercolani, C., Agostino, S.D., Cambria, A.M., Germoni, S., et al. (2012). miR-204 targets Bcl-2 expression and enhances responsiveness of gastric cancer. Cell Death Dis. 3, e423.

Salinas, L.S., Maldonado, E., and Navarro, R.E. (2006). Stress-induced germ cell apoptosis by a p53 independent pathway in Caenorhabditis elegans. Cell Death Differ. 13, 2129–2139.

Schaner, C.E., Deshpande, G., Schedl, P.D., and Kelly, W.G. (2003). A Conserved Chromatin Architecture Marks and Maintains the Restricted Germ Cell Lineage in Worms and Flies. Dev. Cell 5, 747–757.

Schertel, C., and Conradt, B. (2007). C. elegans orthologs of components of the RB tumor suppressor complex have distinct pro-apoptotic functions. Development 134, 3691–3701.

Schumacher, B., Hofmann, K., Boulton, S., and Gartner, A. (2001). The C. elegans homolog of the p53 tumor suppressor is required for DNA damage-induced apoptosis. Curr. Biol. 11, 1722–1727.

Schumacher, B., Schertel, C., Wittenburg, N., Tuck, S., Mitani, S., Gartner, A., Conradt, B., and Shaham, S. (2005a). C. elegans ced-13 can promote apoptosis and is induced in response to DNA damage. Cell Death Differ. 12, 153–161.

Schumacher, B., Hanazawa, M., Lee, M.-H., Nayak, S., Volkmann, K., Hofmann, R., Hengartner, M., Schedl, T., and Gartner, A. (2005b). Translational repression of C. elegans p53 by GLD-1 regulates DNA damage-induced apoptosis. Cell 120, 357–368.

Schwanhäusser, B., Busse, D., Li, N., Dittmar, G., Schuchhardt, J., Wolf, J., Chen, W., and Selbach, M. (2011). Global quantification of mammalian gene expression control. Nature 473, 337–342.

Sendoel, A., Kohler, I., Fellmann, C., Lowe, S.W., and Hengartner, M.O. (2010). HIF-1 antagonizes p53-mediated apoptosis through a secreted neuronal tyrosinase. Nature 465, 577–583.

Senoo-Matsuda, N., Yasuda, K., Tsuda, M., Ohkubo, T., Yoshimura, S., Nakazawa, H., Hartman, P.S., and Ishii, N. (2001). A defect in the cytochrome b large subunit in complex II causes both superoxide anion overproduction and abnormal energy metabolism in Caenorhabditis elegans. J. Biol. Chem. 276, 41553–41558.

Senoo-Matsuda, N., Hartman, P.S., Akatsuka, A., Yoshimura, S., and Ishii, N. (2003). A Complex II Defect Affects Mitochondrial Structure, Leading to ced-3- and ced-4-dependent Apoptosis and Aging. J. Biol. Chem. 278, 22031–22036.

Serber, Z., Lai, H.C., Yang, A., Ou, H.D., Sigal, M.S., Kelly, A.E., Darimont, B.D., Duijf, P.H., Van, H.B., McKeon, F., et al. (2002). A C-terminal inhibitory domain controls the activity of p63 by an intramolecular mechanism. Mol. Cell. Biol. 22, 22, 8601, 8601–8611.

Shaham, S., and Horvitz, H.R. (1996a). Developing Caenorhabditis elegans neurons may contain both cell-death protective and killer activities. Genes Dev. 10, 578–591.

Shaham, S., and Horvitz, H.R. (1996b). An alternatively spliced C. elegans ced-4 RNA encodes a novel cell death inhibitor. Cell 86, 201–208.

Shaham, S., Reddien, P.W., Davies, B., and Horvitz, H.R. (1999). Mutational analysis of the Caenorhabditis elegans cell-death gene ced-3. Genetics 153, 1655–1671.

Sherrard, R., Luehr, S., Holzkamp, H., McJunkin, K., Memar, N., and Conradt, B. (2017). miRNAs cooperate in apoptosis regulation during C. elegans development. Genes Dev. 31, 209–222.

Shieh, S.Y., Ahn, J., Tamai, K., Taya, Y., and Prives, C. (2000). The human homologs of checkpoint kinases Chk1 and Cds1 (Chk2) phosphorylate p53 at multiple DNA damage-inducible sites. Genes Dev. 14, 289–300.

Soussi, T., and Wiman, K.G. (2015). TP53: an oncogene in disguise. Cell Death Differ. 22, 1239–1249.

Spector, M.S., Desnoyers, S., Hoeppner, D.J., and Hengartner, M.O. (1997). Interaction between the C. elegans cell-death regulators CED-9 and CED-4. Nature 385, 653–656.

Stanfield, G.M., and Horvitz, H.R. (2000). The ced-8 gene controls the timing of programmed cell deaths in C. elegans. Mol. Cell 5, 423–433.

Stergiou, L., and Hengartner, M.O. (2004). Death and more: DNA damage response pathways in the nematode C. elegans. Cell Death Differ. 11, 21–28.

Stergiou, L., Doukoumetzidis, K., Sendoel, A., and Hengartner, M.O. (2007). The nucleotide excision repair pathway is required for UV-C-induced apoptosis in Caenorhabditis elegans. Cell Death Differ. 14, 1129–1138.

Stricklin, S.L., Griffiths-Jones, S., and Eddy, S.R. (2005). C. elegans noncoding RNA genes. WormBook Online Rev. C Elegans Biol. 1–7.

Strome, S. (2005). Specification of the germ line. WormBook Online Rev. C Elegans Biol. 1–10.

Strome, S., and Wood, W.B. (1982). Immunofluorescence visualization of germ-line-specific cytoplasmic granules in embryos, larvae, and adults of Caenorhabditis elegans. Proc. Natl. Acad. Sci. U. S. A. 79, 1558–1562.

Su, Z., Yang, Z., Xu, Y., Chen, Y., Yu, Q., Su, Z., Yang, Z., Xu, Y., Chen, Y., and Yu, Q. (2015). MicroRNAs in apoptosis, autophagy and necroptosis. Oncotarget 6, 8474–8490.

Subasic, D., Brümmer, A., Wu, Y., Pinto, S.M., Imig, J., Keller, M., Jovanovic, M., Lightfoot, H.L., Nasso, S., Goetze, S., et al. (2015). Cooperative target mRNA destabilization and translation inhibition by miR-58 microRNA family in C. elegans. Genome Res. 25, 1680–1691.

Subasic, D., Stoeger, T., Eisenring, S., Matia-González, A.M., Imig, J., Zheng, X., Xiong, L., Gisler, P., Eberhard, R., Holtackers, R., et al. (2016). Post-transcriptional control of executioner caspases by RNA-binding proteins. Genes Dev. 30, 2213–2225.

Subramaniam, K., and Seydoux, G. (1999). nos-1 and nos-2, two genes related to Drosophila nanos, regulate primordial germ cell development and survival in Caenorhabditis elegans. Development 126, 4861–4871.

Suh, E.-K., Yang, A., Kettenbach, A., Bamberger, C., Michaelis, A.H., Zhu, Z., Elvin, J.A., Bronson, R.T., Crum, C.P., and McKeon, F. (2006a). p63 protects the female germ line during meiotic arrest. Nature 444, 624–628.

Suh, N., Jedamzik, B., Eckmann, C.R., Wickens, M., and Kimble, J. (2006b). The GLD-2 poly(A) polymerase activates gld-1 mRNA in the Caenorhabditis elegans germ line. Proc. Natl. Acad. Sci. 103, 15108–15112.

Suh, N., Crittenden, S.L., Goldstrohm, A., Hook, B., Thompson, B., Wickens, M., and Kimble, J. (2009). FBF and Its Dual Control of gld-1 Expression in the Caenorhabditis elegans Germline. Genetics 181, 1249–1260.

Sulston, J.E., and Horvitz, H.R. (1977). Post-embryonic cell lineages of the nematode, Caenorhabditis elegans. Dev. Biol. 56, 110–156.

Sulston, J.E., and Horvitz, H.R. (1981). Abnormal cell lineages in mutants of the nematode Caenorhabditis elegans. Dev. Biol. 82, 41–55.

Sulston, J.E., Schierenberg, E., White, J.G., and Thomson, J.N. (1983). The embryonic cell lineage of the nematode Caenorhabditis elegans. Dev. Biol. 100, 64–119.

Tamburino, A.M., Ryder, S.P., and Walhout, A.J.M. (2013). A Compendium of Caenorhabditis elegans RNA Binding Proteins Predicts Extensive Regulation at Multiple Levels. G3 Genes Genomes Genet. 3, 297–304.

Tan, F.J., Fire, A.Z., and Hill, R.B. (2007). Regulation of apoptosis by C. elegans CED-9 in the absence of the C-terminal transmembrane domain. Cell Death Differ. 14, 1925.

Tan, F.J., Zuckerman, J.E., Wells, R.C., and Hill, R.B. (2011). The C. elegans B-cell lymphoma 2 (Bcl-2) homolog cell death abnormal 9 (CED-9) associates with and remodels LIPID membranes. Protein Sci. 20, 62–74.

Tenenbaum, S.A., Carson, C.C., Lager, P.J., and Keene, J.D. (2000). Identifying mRNA subsets in messenger ribonucleoprotein complexes by using cDNA arrays. Proc. Natl. Acad. Sci. 97, 14085–14090.

Teuliere, J., Cordes, S., Singhvi, A., Talavera, K., and Garriga, G. (2014). Asymmetric neuroblast divisions producing apoptotic cells require the cytohesin GRP-1 in Caenorhabditis elegans. Genetics 198, 229–247.

Thompson, B.E., Bernstein, D.S., Bachorik, J.L., Petcherski, A.G., Wickens, M., and Kimble, J. (2005). Dose-dependent control of proliferation and sperm specification by FOG-1/CPEB. Development 132, 3471–3481.

Trent, C., Tsung, N., and Horvitz, H.R. (1983). Egg-laying defective mutants of the nematode Caenorhabditis elegans. Genetics 104, 619–647.

Tzur, Y.B., Margalit, A., Melamed-Book, N., and Gruenbaum, Y. (2006). Matefin/SUN-1 is a nuclear envelope receptor for CED-4 during Caenorhabditis elegans apoptosis. Proc. Natl. Acad. Sci. 103, 13397–13402.

Updike, D., and Strome, S. (2010). P granule assembly and function in Caenorhabditis elegans germ cells., P Granule Assembly and Function in Caenorhabditis elegans Germ Cells. J. Androl. 31, 53–60.

Updike, D.L., Knutson, A.K., Egelhofer, T.A., Campbell, A.C., and Strome, S. (2014). Germ-granule components prevent somatic development in the C. elegans germline. Curr. Biol. 24, 970–975.

Vaklavas, C., Blume, S.W., and Grizzle, W.E. (2017). Translational dysregulation in cancer: molecular insights and potential clinical applications in biomarker development. Front. Oncol. 7, 7, 158–158.

Valadi, H., Ekström, K., Bossios, A., Sjöstrand, M., Lee, J.J., and Lötvall, J.O. (2007). Exosome-mediated transfer of mRNAs and microRNAs is a novel mechanism of genetic exchange between cells. Nat. Cell Biol. 9, 654–659.

Vasudevan, S., Tong, Y., and Steitz, J.A. (2007). Switching from repression to activation: microRNAs can up-regulate translation. Science 318, 1931–1934.

Venegas, V., and Zhou, Z. (2007). Two alternative mechanisms that regulate the presentation of apoptotic cell engulfment signal in Caenorhabditis elegans. Mol. Biol. Cell 18, 3180–3192.

Wahle, E., and Winkler, G.S. (2013). RNA decay machines: deadenylation by the Ccr4–Not and Pan2–Pan3 complexes. Biochim. Biophys. Acta BBA - Gene Regul. Mech. 1829, 561–570.

Wallach, D., Kang, T.-B., and Kovalenko, A. (2014). Concepts of tissue injury and cell death in inflammation: a historical perspective. Nat. Rev. Immunol. 14, 51–59.

Wang, J., Chen, J., Chang, P., LeBlanc, A., Li, D., Abbruzzesse, J.L., Frazier, M.L., Killary, A.M., and Sen, S. (2009a). MicroRNAs in plasma of pancreatic ductal adenocarcinoma patients as novel blood-based biomarkers of disease. Cancer Prev. Res. (Phila. Pa.) 2, 807–813.

Wang, L., Eckmann, C.R., Kadyk, L.C., Wickens, M., and Kimble, J. (2002a). A regulatory cytoplasmic poly(A) polymerase in Caenorhabditis elegans. Nature 419, 312–316.

Wang, Q., Wei, L., Guan, X., Wu, Y., Zou, Q., and Ji, Z. (2014). Briefing in family characteristics of microRNAs and their applications in cancer research. Biochim. Biophys. Acta BBA - Proteins Proteomics 1844, 191–197.

Wang, X., Yang, C., Chai, J., Shi, Y., and Xue, D. (2002b). Mechanisms of AIF-Mediated Apoptotic DNA Degradation in Caenorhabditis elegans. Science 298, 1587–1592.

Wang, X., Greenberg, J.F., and Chamberlin, H.M. (2004). Evolution of regulatory elements producing a conserved gene expression pattern in Caenorhabditis. Evol. Dev. 6, 237–245.

Wang, X., Wang, J., Gengyo-Ando, K., Gu, L., Sun, C.-L., Yang, C., Shi, Y., Kobayashi, T., Shi, Y., Mitani, S., et al. (2007). C. elegans mitochondrial factor WAH-1 promotes phosphatidylserine externalization in apoptotic cells through phospholipid scramblase SCRM-1. Nat. Cell Biol. 9, 541–549.

Wang, X., Zhao, Y., Wong, K., Ehlers, P., Kohara, Y., Jones, S.J., Marra, M.A., Holt, R.A., Moerman, D.G., and Hansen, D. (2009b). Identification of genes expressed in the hermaphrodite germ line of C. elegans using SAGE. BMC Genomics 10, 213.

Wang, Z., Jiao, X., Carr-Schmid, A., and Kiledjian, M. (2002c). The hDcp2 protein is a mammalian mRNA decapping enzyme. Proc. Natl. Acad. Sci. 99, 12663–12668.

Weaver, B.P., Zabinsky, R., Weaver, Y.M., Lee, E.S., Xue, D., and Han, M. (2014). CED-3 caspase acts with miRNAs to regulate non-apoptotic gene expression dynamics for robust development in C. elegans. ELife 3, e04265–e04265.

Weber, J.A., Baxter, D.H., Zhang, S., Huang, D.Y., Huang, K.H., Lee, M.J., Galas, D.J., and Wang, K. (2010). The MicroRNA spectrum in 12 body fluids. Clin. Chem. 56, 1733–1741.

Weingarten-Gabbay, S., Elias-Kirma, S., Nir, R., Gritsenko, A.A., Stern-Ginossar, N., Yakhini, Z., Weinberger, A., and Segal, E. (2016). Systematic discovery of cap-independent translation sequences in human and viral genomes. Science 351, aad4939.

Wightman, B., Ha, I., and Ruvkun, G. (1993). Posttranscriptional regulation of the heterochronic gene lin-14 by lin-4 mediates temporal pattern formation in C. elegans. Cell 75, 855–862.

Wissink, E.M., Fogarty, E.A., and Grimson, A. (2016). High-throughput discovery of post-transcriptional cis-regulatory elements. BMC Genomics 17, 177.

Wolke, U., Jezuit, E.A., and Priess, J.R. (2007). Actin-dependent cytoplasmic streaming in C. elegans oogenesis. Development 134, 2227–2236.

Woo, J.-S., Jung, J.-S., Ha, N.-C., Shin, J., Kim, K.-H., Lee, W., and Oh, B.-H. (2003). Unique structural features of a BCL-2 family protein CED-9 and biophysical characterization of CED-9/EGL-1 interactions. Cell Death Differ. 10, 1310–1319.

Wright, J.E., Gaidatzis, D., Senften, M., Farley, B.M., Westhof, E., Ryder, S.P., and Ciosk, R. (2011). A quantitative RNA code for mRNA target selection by the germline fate determinant GLD-1. EMBO J. 30, 533–545.

Wu, Y.-C., and Horvitz, H.R. (1998). The C. elegans cell corpse engulfment gene ced-7 encodes a protein similar to ABC transporters. Cell 93, 951–960.

Wu, D., Wallen, H.D., and Nuñez, G. (1997). Interaction and regulation of subcellular localization of CED-4 by CED-9. Science 275, 1126–1129.

Wu, L., Fan, J., and Belasco, J.G. (2008). Importance of translation and nonnucleolytic Ago proteins for on-target RNA interference. Curr. Biol. 18, 1327–1332.

Wu, Y.C., Stanfield, G.M., and Horvitz, H.R. (2000). NUC-1, a Caenorhabditis elegans DNase II homolog, functions in an intermediate step of DNA degradation during apoptosis. Genes Dev. 14, 536–548.

Wyllie, A.H. (1980). Glucocorticoid-induced thymocyte apoptosis is associated with endogenous endonuclease activation. Nature 284, 555–556.

Xu, P., Vernooy, S.Y., Guo, M., and Hay, B.A. (2003). The Drosophila microRNA Mir-14 suppresses cell death and is required for normal fat metabolism. Curr. Biol. 13, 790–795.

Xue, D., and Horvitz, H.R. (1997). Caenorhabditis elegans CED-9 protein is a bifunctional cell-death inhibitor. Nature 390, 305–308.

Xue, D., Shaham, S., and Horvitz, H.R. (1996). The Caenorhabditis elegans cell-death protein CED-3 is a cysteine protease with substrate specificities similar to those of the human CPP32 protease. Genes Dev. 10, 1073–1083.

Yan, N., Gu, L., Kokel, D., Chai, J., Li, W., Han, A., Chen, L., Xue, D., and Shi, Y. (2004). Structural, biochemical, and functional analyses of CED-9 recognition by the proapoptotic proteins EGL-1 and CED-4. Mol. Cell 15, 999–1006.

Yan, N., Chai, J., Lee, E.S., Gu, L., Liu, Q., He, J., Wu, J.-W., Kokel, D., Li, H., Hao, Q., et al. (2005). Structure of the CED-4–CED-9 complex provides insights into programmed cell death in Caenorhabditis elegans. Nature 437, 831–837.

Yang, W., and Hekimi, S. (2010). A mitochondrial superoxide signal triggers increased longevity in Caenorhabditis elegans. PLOS Biol. 8, e1000556.

Yang, A., Kaghad, M., Wang, Y., Gillett, E., Fleming, M.D., Dötsch, V., Andrews, N.C., Caput, D., and McKeon, F. (1998). p63, a p53 homolog at 3q27–29, encodes multiple products with transactivating, death-inducing, and dominant-negative activities. Mol. Cell 2, 305–316.

Yang, A., Schweitzer, R., Sun, D., Kaghad, M., Walker, N., Bronson, R.T., Tabin, C., Sharpe, A., Caput, D., Crum, C., et al. (1999). p63 is essential for regenerative proliferation in limb, craniofacial and epithelial development. Nature 398, 714–718.

Yang, A., Walker, N., Bronson, R., Kaghad, M., Oosterwegel, M., Bonnin, J., Vagner, C., Bonnet, H., Dikkes, P., Sharpe, A., et al. (2000). p73-deficient mice have neurological, pheromonal and inflammatory defects but lack spontaneous tumours. Nature 404, 99–103.

Yang, M., Sun, J., Sun, X., Shen, Q., Gao, Z., and Yang, C. (2009). Caenorhabditis elegans protein arginine methyltransferase PRMT-5 negatively regulates DNA damage-induced apoptosis. PLoS Genet. 5, e1000514.

Yee, C., Yang, W., and Hekimi, S. (2014). The intrinsic apoptosis pathway mediates the pro-longevity response to mitochondrial ROS in C. elegans. Cell 157, 897–909.

Yekta, S., Shih, I. -hun., and Bartel, D.P. (2004). MicroRNA-directed cleavage of HOXB8 mRNA. Science 304, 594–596.

Yi, R., Qin, Y., Macara, I.G., and Cullen, B.R. (2003). Exportin-5 mediates the nuclear export of pre-microRNAs and short hairpin RNAs. Genes Dev. 17, 3011–3016.

Yigit, E., Batista, P.J., Bei, Y., Pang, K.M., Chen, C.-C.G., Tolia, N.H., Joshua-Tor, L., Mitani, S., Simard, M.J., and Mello, C.C. (2006). Analysis of the C. elegans argonaute family reveals that distinct Argonautes act sequentially during RNAi. Cell 127, 747–757.

Yuan, J., and Horvitz, H.R. (1990). The Caenorhabditis elegans genes ced-3 and ced-4 act cell autonomously to cause programmed cell death. Dev. Biol. 138, 33–41.

Yuan, J., and Horvitz, H.R. (1992). The Caenorhabditis elegans cell death gene ced-4 encodes a novel protein and is expressed during the period of extensive programmed cell death. Development 116, 309–320.

Yuan, J., Shaham, S., Ledoux, S., Ellis, H.M., and Horvitz, H.R. (1993). The C. elegans cell death gene ced-3 encodes a protein similar to mammalian interleukin-1β-converting enzyme. Cell 75, 641–652.

Zekri, L., Huntzinger, E., Heimstädt, S., and Izaurralde, E. (2009). The silencing domain of GW182 interacts with PABPC1 to promote translational repression and degradation of microRNA targets and is required for target release. Mol. Cell. Biol. 29, 6220–6231.

Zhang, F., Barboric, M., Blackwell, T.K., and Peterlin, B.M. (2003). A model of repression: CTD analogs and PIE-1 inhibit transcriptional elongation by P-TEFb. Genes Dev. 17, 748–758.

Zhang, L., Ding, L., Cheung, T.H., Dong, M.Q., Chen, J., Sewell, A.K., Liu, X., Yates, 3rd JR, and Han, M. (2007). Systematic identification of miRISC proteins, miRNAs, and their mRNA targets in C. elegans by their interactions with GW182 family proteins AIN-1 and AIN-2. Mol. Cell Mol. Cell 28, 98–613.

Zhou, X., Ruan, J., Wang, G., and Zhang, W. (2007). Characterization and Identification of MicroRNA Core Promoters in Four Model Species. PLOS Comput. Biol. 3, e37.

Ziebarth, J.D., Bhattacharya, A., Chen, A., and Cui, Y. (2012). PolymiRTS Database 2.0: linking polymorphisms in microRNA target sites with human diseases and complex traits. Nucleic Acids Res. 40, D216–D221.

Zou, H., Henzel, W.J., Liu, X., Lutschg, A., and Wang, X. (1997). Apaf-1, a human protein homologous to C. elegans CED-4, participates in cytochrome c–dependent activation of caspase-3. Cell 90, 405–413.

Züllig, S., Neukomm, L.J., Jovanovic, M., Charette, S.J., Lyssenko, N.N., Halleck, M.S., Reutelingsperger, C.P.M., Schlegel, R.A., and Hengartner, M.O. (2007). Aminophospholipid translocase TAT-1 promotes phosphatidylserine exposure during C. elegans apoptosis. Curr. Biol. 17, 994–999.

# • Chapter 2 •

# *mir-52* is a novel cell-autonomous enhancer of germline apoptosis in *C. elegans*

## 2.1 Preface

In this chapter, I describe *mir-52* as an additional regulator of germline apoptosis in *C. elegans*. I would like to highlight my contribution to the manuscript together with the contribution of other people involved. I have designed, performed, validated and optimized all apoptosis-related experiments mentioned in the manuscript. Ting Deng did the microinjection of the pPK1045 plasmid. The manuscript was written by me under the guidance of Michael Hengartner. Additional findings on other miRNA mutants, which influence germline apoptosis in *C. elegans*, are described in Appendix 1.

# *mir-52* is as a novel cell-autonomous enhancer of germline apoptosis in *C. elegans*

Polina Kamkina[1,2], Ting Deng[1,2], Andrea Haag[1,2], Alex Hajnal[1] and Michael O. Hengartner[1,*]

[1]Institute of Molecular Life Sciences, University of Zurich, 8057 Zurich, Switzerland

[2]Ph.D. Program in Molecular Life Sciences Zurich, 8057 Zurich, Switzerland

*corresponding author

Michael O. Hengartner
Institute of Molecular Life Sciences
University of Zurich
Winterthurerstrasse 190
CH-8057, Zurich
Switzerland
phone +41 44 635 31 51
e-mail: michael.hengartner@uzh.ch

## 2.2 Abstract

Germline apoptosis is a conserved feature of oocyte development in mammals, insects and nematodes. In the *C. elegans* germ line, post-transcriptional regulation plays a major role in the control of gene expression. However, little is known about the impact of miRNAs on the regulation of germ cell death in *C. elegans.* Here, we show that *mir-52* is required cell-autonomously for DNA damage-induced germline apoptosis. We found that two *mir-52* deletion mutants have strongly reduced levels of germline apoptosis following irradiation (IR). *mir-52* is a member of the old, highly conserved *mir-51* family. Other *mir-51* family members did not display any changes in germ cell death. We also show that *mir-52* promotes IR-induced germline apoptosis downstream or in parallel to *cep-1*. Human homologues of *mir-51* family, mir-100 family, are frequently dysregulated in cancers.

## 2.3 Introduction

Apoptotic removal of unwanted cells is crucial for animal development and tissue homeostasis. Dysregulation of apoptosis can lead to cancer as well as various neurodegenerative and immune disorders. In the *C. elegans* hermaphrodite, 131 out of the 1'090 somatic cells generated die in a highly reproducible manner during development (Sulston and Horvitz, 1977; Sulston et al., 1983). Genetic studies of programmed cell death in *C. elegans* led to the identification of an evolutionarily conserved apoptotic machinery, which consists of the pro-apoptotic BH3-only protein EGL-1, the anti-apoptotic BCL-2 family member CED-9, the Apaf-1 homolog CED-4, and the caspase CED-3 (Yuan and Horvitz, 1990; Hengartner et al., 1992; Yuan and Horvitz, 1992; Yuan et al., 1993; Hengartner and Horvitz, 1994a, 1994b; Xue et al., 1996; Zou et al., 1997; Conradt and Horvitz, 1998; Shaham et al., 1999). In *loss-of-function* (*lf*) mutants of *egl-1*, *ced-4*, and *ced-3*, or in the *gain-of-function ced-9(n1950)*, essentially all of the 131 somatic cells programmed to die survive (Ellis and Horvitz, 1986; Hengartner et al., 1992).

Germline apoptosis is a conserved feature of oocyte development in mammals, insects and nematodes. In *C. elegans* hermaphrodites, more than half of the developing oocytes die, in an apparent stochastic manner, in the absence of any evident apoptotic stimulus in a process that has been called "physiological germ cell death" (Gumienny et al., 1999; Fox et al., 2011). Germ cells can also undergo apoptosis following genotoxic stress such as DNA double-strand breaks (Gartner et al., 2000; Derry et al., 2007; Stergiou et al., 2007). Like somatic cell death, germline apoptosis is also mediated by the core apoptotic machinery (*ced-3*, *ced-4* and *ced-9*, Gumienny et al., 1999). Interestingly, while DNA damage-induced germline apoptosis requires transcriptional upregulation of *egl-1* and another BH3-only gene *ced-13* (which is mediated by p53 tumor suppressor homolog *cep-1*, Gartner et al., 2000; Hofmann et al., 2002; Schumacher et al., 2005a), physiological germ cell death is regulated via a BH3 domain-protein-independent process (Gumienny et al., 1999).

In the *C. elegans* germ line, post-transcriptional regulation plays a major role in the control of gene expression (Nousch and Eckmann, 2013). Indeed, RNA-binding proteins (RBP) are significantly enriched in the germline transcriptome compared to somatic tissues (Wang et al., 2009). Moreover, the spatio-temporal expression of many genes in *C. elegans* germ line is mainly regulated by their 3'-untranslated regions (3'UTRs, Schumacher et al., 2005b; Merritt et al.,

2008; Subasic et al., 2016). Previous studies identified several RBPs that influence germline apoptosis in *C. elegans*. For example, GLD-1 is a KH-motif RBP which represses translation of *cep-1* and *ced-3* and thereby antagonizes germ cell death (Schumacher et al., 2005b; Subasic et al., 2016). GLA-3 is a TIS11-like RBP with two CCCH-like zinc-finger domains, which suppresses physiological and DNA damage-induced germ cell death at the level of MAPK signaling (Kritikou et al., 2006). Additionally, the constitutive P-granule components PGL-1 and PGL-3 were found to inhibit physiological and DNA damage-induced germline apoptosis by downregulating proteins levels of CED-4 and Sirtuin homolog SIR-2.1 (Min et al., 2016).

By contrast, relatively little is known about the potential contribution of microRNAs (miRNAs) to the regulation of germ cell death in *C. elegans*. Genetic studies have identified the highly conserved *mir-34* and members of the *mir-58* family (which are homologous to the *bantam* miRNA in *D. melanogaster*) as positive regulators of IR-induced germline apoptosis (Kato et al., 2009; Subasic et al., 2015). Further, *mir-35* and *mir-58* were recently shown to bind to the 3'UTR of *egl-1* and reduce its expression in mothers of somatic cells fated to die (Sherrard et al., 2017).

The *mir-51* family (mir-100 family in mammals) is an old and highly conserved *C. elegans* miRNA family (Grimson et al., 2008). Members of the mir-100 family are aberrantly expressed in various human cancers and influence many different cellular pathways, including cell cycle progression, metabolism, differentiation, cell survival, migration, and epithelial mesenchymal transition (Li et al., 2015). The dysregulation of mir-100 family members serves as a biomarker for cancers with poor prognosis (Qin et al., 2015). In *C. elegans*, the *mir-51* family includes six miRNAs with a highly conserved seed sequence (Grimson et al., 2008), which are tightly clustered on the chromosomes IV (*mir-51*, *mir-53*, and *mir-52*) and X (*mir-56*, *mir-55*, *mir-54;* Supplemental Fig. 2.1). *mir-51* family members function in diverse developmental processes (Brenner et al., 2012), and deletion of all members of the *mir-51* family is lethal (Alvarez-Saavedra and Horvitz, 2010; Shaw et al., 2010).

Here, we describe *mir-52* as an additional regulator of DNA damage-induced apoptosis in *C. elegans*. We found that two *mir-52* deletion mutants have strongly reduced levels of germline apoptosis following IR, whereas other members of the *mir-51* family did not display any changes in germ cell death. We show that *mir-52* promotes IR-induced germline apoptosis cell-autonomously, downstream or in parallel to *cep-1*.

## 2.4 Results

### 2.4.1 Loss of *mir-52* impairs DNA damage-induced germ cell death

To identify new miRNAs that might influence germline apoptosis in *C. elegans*, we analyzed 55 miRNA mutants (both single and multiple mutants, Table 2.1) for any effect on physiological and DNA damage-induced germ cell death. Two separate *mir-52* deletion mutants, *mir-52(n4114)* and *mir-52(n4100)*, showed a strong reduction in germline apoptosis following IR, while physiological germ cell death (Fig. 2.1A) and somatic cell death (data not shown) were not affected. The *mir-52* alleles *n4100* and *n4114* are 398 bp and 148 bp deletions, which both delete the sequence coding for the mature miRNA (Supplemental Fig. 2.1A). Both alleles also affect *Y37A1B.*330 and *Y37A1B.*335, two small non-coding RNA genes, which are weakly expressed in wild-type embryos (Supplemental Fig. 2.1A, Lee et al., 2017). *Y37A1B.*335 is repressed by *cep-1* following IR, suggesting a potential anti-apoptotic role (Xu et al., 2014). Taking into account the pro-apoptotic nature of *n4100* and *n4114*, we consider it unlikely that loss of *Y37A1B.*335 contributes significantly to the defective apoptotic IR response observed in these mutants. The function of *Y37A1B.*330 is unknown.

*mir-52* mutants reach the L4/YA molt approximately three hours later than the wild type. To check whether the apoptotic defect is also present in older *mir-52* worms, we performed a time-course analysis of germline apoptosis in *mir-52* mutants. We observed a strong reduction of germ cell death post IR in both *mir-52* deletion mutants at all time points tested (Fig. 2.1B). Interestingly, the IR-induced germ cell death defect of *mir-52* mutants is temperature dependent: the reduction in germline apoptosis is weaker at 25 ˚C compared to 15 ˚C and 20 ˚C (Supplemental Fig. 2.2). The molecular basis for this temperature sensitivity is currently unknown.

Several genes expressed in somatic tissues were found to regulate germline apoptosis cell non-autonomously in *C. elegans* (Ito et al., 2010; Sendoel et al., 2010; Al-Amin et al., 2016). *mir-52* was shown to be ubiquitously expressed in somatic tissue throughout animal development (Shaw et al., 2010). Germline expression of *mir-52* was not detected, however multicopy transgenes are often silenced in the *C. elegans* germ line (Shaw et al., 2010). To determine the site of action of *mir-52* in germline apoptosis, we analyzed worms expressing *mir-52* specifically in somatic tissue or in the germ line. The extra chromosomal array *mjEx123*, which restores

pharyngeal attachment to the hypodermis in *mir-51* family mutants (Shaw et al., 2010), failed to rescue the germ cell death defects of *mir-52* mutants (Fig. 2.2A, Supplemental Fig. 2.3A). By contrast, expression of *mir-52* under the control of the germline-specific *mex-5* promoter, restored germline apoptosis following IR (Fig. 2.2B, Supplemental Fig. 2.3B). These observations suggest that *mir-52* is also expressed in germline and controls apoptosis cell-autonomously.

### 2.4.2 Other *mir-51* family members do not affect germ cell apoptosis

The *mir-51* family members have overlapping expression patterns in the soma (Shaw et al., 2010). Moreover, multiple mutants of the family reveal a number of soma-specific synthetic phenotypes (Shaw et al., 2010; Brenner et al., 2012). To examine the possible effect of other *mir-51* family members on germline apoptosis, we analyzed various additional single and multiple mutant combinations. *mir-51 (n4473)*, *mir-53(n4113)* and *mir-54-55-56* showed no changes in germ cell death, with or without IR (Fig. 2.3). Multiple mutants carrying a *mir-52* deletion were generally unhealthy and slow growing. Consistent with the previous observations, the slow growth phenotype was particularly noticeable in *mir-52(n4114); mir-54-55-56(nDf58)* and *mir-53(n4113) mir-52(n4114); mir-54-55-56(nDf58)* mutants (Alvarez-Saavedra and Horvitz, 2010; Shaw et al., 2010). The exact staging of these worms was difficult, thus they were not pursued further. The allelic combination *mir-51(n4473) mir-52(n4114); mir-54-55-56(nDf58)* was lethal. We found that *mir-51(n4473) mir-52(n4114)* and *mir-53(n4113) mir-52(n4114)* worms had apoptotic levels comparable to those found in the *mir-52(n4114)* single mutant. All other multiple mutants of the family showed no changes in germline apoptosis (Fig. 2.3). Thus, while there is extensive redundancy between *mir-51* family for the reported somatic phenotypes, DNA damage-induced germ cell apoptosis appears to rely solely on *mir-52*.

### 2.4.3 Apoptotic cell clearance is not affected in *mir-52* compromised worms

Formally, the reduced number of germ cell corpses observed in *mir-52* mutants following IR could be the result not of a defect in cell death, but rather due to faster corpse clearance. To distinguish between these two possibilities, we crossed *mir-52(n4114)* with mutants impaired in one of the two parallel engulfment pathways, i.e. *ced-1(e1735)* and *ced-12(k149)* (Gumienny et al., 2001; Zhou et al., 2001). No change in somatic cell corpse clearance was observed in *ced-1(e1735); mir-52(n4114)* and *ced-12(k149); mir-52(n4114)* animals (Fig. 2.4B). By contrast, germline apoptosis was slightly reduced in both double mutants, compared to the corresponding

*ced-1(e1735)* and *ced-12(k149)* single mutants (Fig. 2.4A, Supplemental Fig. 2.4) following IR and in non-irradiated animals. Given that loss of *mir-52* reduced germ cell corpse numbers in both main engulfment pathway mutants, it is unlikely that *mir-52(lf)* promotes engulfment, as its effect should have been abrogated in at least one of the two pathway mutants. We suspect that *mir-52* mutants might in fact also have a weak defect in physiological germ cell death (as hinted in Fig. 2.2A, Fig. 2.3 ) which becomes more obvious in *mir-52* and engulfment double mutants due to excessive number of germ cell corpses (Fig. 2.4A, Supplemental Fig. 2.4). Taken together, our data show that loss of *mir-52* weakly affects physiological and strongly blocks DNA damage-induced germline apoptosis.

### 2.4.4 MAPK signaling is not responsible for *mir-52(n4114)* apoptotic defects upon IR

Previous studies have shown that Ras/MAPK signaling is required for physiological (Gumienny et al., 1999) and DNA damage-induced (Rutkowski et al., 2011; Eberhard et al., 2013) germline apoptosis. Thus, we first asked whether the upregulation of Ras/MAPK signaling would rescue IR response defect of *mir-52(n4114)* mutant. Double mutants of *mir-52* and mutants with upregulated MAPK signaling, i.e. *let-60(ga89ts)*, *let-60(n1046gf)*, *lip-1(zh15)*, *gla-3(op216)* showed increased germ cell death following IR compared to *mir-52(n4114)* alone (Fig. 2.5A, Han et al., 1990; Eisenmann and Kim, 1997; Berset et al., 2001; Kritikou et al., 2006). However, this suppression was not complete, as the double mutants had less corpses than the corresponding *let-60(ga89ts)*, *let-60(n1046gf)*, *lip-1(zh15)*, and *gla-3(op216)* single mutants.

Next, we examined whether the apoptotic defects in *mir-52(n4114)* might be due to reduced MPK-1 phosphorylation. While total MPK-1 levels were slightly downregulated in *mir-52* mutants, levels of the activated germline-specific isoform MPK-1B (Lee et al., 2007) were slightly increased in *mir-52(n4114)* animals, both with and without IR (Fig. 2.5B). The increase in activated MPK-1B signal in *mir-52* mutant might be a compensatory response to the slightly reduced total MAPK protein abundance. Our observations make it unlikely that the apoptotic defects in *mir-52(n4114)* mutants are due to defective Ras/MAPK signaling.

### 2.4.5 Loss of *mir-52* influences germline apoptosis downstream of or in parallel to *cep-1*

We next asked whether the defects in *mir-52(n4114)* IR response were due to reduced activation of *cep-1*. The RNA-binding protein GLD-1 represses the translation of *cep-1* (Schumacher et al., 2005b). The *gld-1 lf* allele *op236* causes a mild overexpression of *cep-1* resulting in an increased

basal level of germ cell apoptosis and increased sensitivity to IR. In *gld-1(op236); mir-52(n4114)* double mutants, germ cell death was strongly reduced at 20 ˚C compared to that in *gld-1(op236)* single mutant with and without IR (Fig. 2.6A). At 25 ˚C, the suppression of germline apoptosis was observed in young worms without IR (Fig. 2.6A). Thus, the overexpression of *cep-1* did not rescue the apoptotic defects of *mir-52(n4114)*. This suggests that loss of *mir-52* affects germline apoptosis downstream of *cep-1* or in parallel to it.

### 2.4.6 *mir-52(n4114)* suppresses germline apoptosis of *ced-9(n1653ts)*

Finally, we examined whether *mir-52* influences the components of the core apoptotic machinery. We built the double mutant between *mir-52(n4114)* and temperature-sensitive *ced-9* hypomorphic allele *n1653* and analyzed it for the alterations in germ cell death. As previously noticed with the engulfment double mutants, we observed that *ced-9(n1653ts); mir-52(n4114)* animals had decreased levels of germ cell death even in the absence of external DNA damage, suggesting that loss of *mir-52* results directly or indirectly in a weak defect of physiological germ cell death (Fig. 2.6B). The IR-dependent increase of germline apoptosis in the double mutant was weaker that in the *ced-9(n1653ts)* single mutant (Fig. 2.6B), suggesting that loss of *mir-52* might be able to affect germ cell death either independently or downstream of *ced-9*. A major caviat of this conclusion is that *ced-9(n1653ts)* is not a null allele, and the results from the double mutant must thus be interpreted with great caution.

### 2.4.7 *mir-52(n4114)* alters subcellular localization pattern of CED-3::GFP in the germ line

We also asked whether suppression in germline apoptosis in *mir-52(n4114)* mutants is accompanied by any changes in the expression pattern of CED-3 caspase. Interestingly, we observed less punctuate distribution pattern of CED-3::GFP around the perinuclear space in the germline of *ced-3(n717) mir-52(n4114)* double mutants carrying translational *ced-3::gfp* wild-type reporter, *opIs461* (Fig. 2.7B, Subasic et al., 2016). However, the potential contribution of this change to the observed apoptotic phenotype remains to be investigated.

## 2.5 Discussion and Outlook

We undertook a reverse genetic screen to identify additional miRNAs that affect germ cell death in *C. elegans*. We found that the highly conserved miRNA *mir-52* is required for DNA damage-induced germline apoptosis. *mir-52* deletion mutants have strongly reduced levels of germ cell death following IR. Applying tissue-specific rescue transgenes, we demonstrated that *mir-52* acts cell-autonomously to promote germline apoptosis following IR. In addition to the IR-response defect, we also observed a weak suppression of physiological germline apoptosis in *mir-52* mutants. The phenotype was confirmed in *mir-52* and engulfment double mutants. Thus, *mir-52* slightly enhances germline apoptosis under physiological conditions, and its pro-apoptotic function becomes more evident upon increased DNA damage. Interestingly, the suppression of germline apoptosis was much weaker in *mir-52* mutants grown at 25 ˚C. Given that temperature-induced changes in gene expression and function were reported previously in *C. elegans* (Mertensk̈otter et al., 2013; Zhang et al., 2015; Chen et al., 2016), it is conceivable that such alterations could counterbalance the loss of *mir-52* at higher temperature. The genome-wide analysis of altered gene expression in *mir-52* mutants at different temperatures would probably reveal molecular nature of the detected temperature sensitivity.

The *mir-51* family members have overlapping functions in the soma (Shaw et al., 2010; Brenner et al., 2012). We analyzed multiple mutants of the *mir-51* family for the defects in germline apoptosis and concluded that *mir-52* regulates germline apoptosis independently of other *mir-51* family members. Such differences in regulation suggest distinct functions of the *mir-51* family in the germ line and somatic tissue. It should be noted, however, that mutants carrying simultaneous deletions of *mir-52* and *mir-54-55-56* were not analyzed due to their extreme slow growing phenotype (Alvarez-Saavedra and Horvitz, 2010; Shaw et al., 2010). The contribution of *mir-51* family members to the range of developmental processes was deduced as *mir-52* ≅ *mir-54-55-56* > *mir-51* > *mir-53* (Alvarez-Saavedra and Horvitz, 2010). We did not observed any changes of germline apoptosis in *mir-54-55-56* mutants alone. Nevertheless, a weak contribution of *mir-54-55-56* to the apoptotic phenotype observed in *mir-52* mutants following IR cannot be excluded. To confirm that *mir-54-55-56* function exclusively in somatic tissue, germline-specific rescue of *mir-54-55-56* in *mir-52(n4114)* animals could be used.

Many genes and regulatory pathway are known to influence germ cell death in *C. elegans*. Upregulation of RAS/MAPK signaling partially rescued apoptotic response in *mir-52* mutants,

Moreover, phosphorylated MPK-1 levels in whole worm protein extracts were slightly increased in *mir-52(n4114)* worms. Thus, it is rather unlikely that the apoptotic defects in *mir-52(n4114)* mutants were caused by defective Ras/MAPK signaling. To support the data explicitly, quantification of RAS/MAPK signaling might be performed using dissected gonads of *mir-52* mutants.

DNA damage checkpoint signaling triggers apoptosis of meiotic germ cells via *cep-1*. In *mir-52* mutants, suppression of germ cell death upon IR was not caused by a reduced activation of *cep-1* itself, because *cep-1* overexpression failed to rescue the apoptotic defects of *mir-52(n4114)*. We will next analyze whether loss of *mir-52* might specifically alter transcriptional upregulation of *cep-1* downstream targets *egl-1* and *ced-13*. Notably, several molecules were shown to promote mitotic germ cell cycle arrest and apoptosis independently of the canonical DNA damage response pathway (Deng et al., 2008; Greiss et al., 2008; Bailly et al., 2010). Thus, we cannot exclude that *mir-52* might affect germline apoptosis at the level of DNA damage checkpoint signaling independently of *cep-1*. To examine whether apoptotic defects in *mir-52* mutants were caused by the inability to respond to DNA damage, size and number of the mitotic germ cells will be quantified. *rad-51*, the *C. elegans* homolog of bacterial RecA, which interacts with members of DNA damage checkpoint signaling for proper meiotic recombination (Alpi et al., 2003). Downregulation of *rad-51* results in accumulation of unprocessed double strand breaks in meiotic germ cells (Gartner et al., 2000). Hence, *rad-51(RNAi)* might be also used to analyze whether DNA damage checkpoint signaling is compromised in *mir-52* mutants.

We observed weak suppression of germline apoptosis in *ced-9(n1653ts); mir-52(n4114)* double mutants without IR, further confirming that *mir-52* also influences physiological germline apoptosis. The reduction of germ cell death in *ced-9(n1653ts); mir-52(n4114)* animals was even stronger following DNA damage, suggesting that loss of *mir-52* might affect germline apoptosis either independently or downstream of *ced-9*. Importantly, *n1653ts* is a hypomorpic *loss-of-function* allele. Therefore, the observed phenotype might be also caused by altered signal transduction downstream of the compromised DNA damage check point signaling or other upstream regulatory pathway, independently of *cep-1*. To narrow down the site of action of *mir-52*, we will examine the brood size of *mir-52* and *ced-9* double mutants using the strong *ced-9 lf* allele, *n2161*.

In addition to the apoptotic defect, *mir-52* mutants also showed a more diffuse distribution pattern of CED-3::GFP (i.e. reduce intensity of perinuclear patches). A perinuclear localization was also reported for CED-4, both in somatic tissues and in the germ line (Pourkarimi et al., 2012). Moreover, perinuclear CED-4 increased in germ cells following IR (Deng et al., 2008; Greiss et al., 2008; Pourkarimi et al., 2012). However, the increased accumulation of CED-4 in response to apoptotic stimuli was not sufficient to trigger germ cell death (Pourkarimi et al., 2012). Thus, altered localization pattern of CED-3 in *mir-52* mutants might have apoptosis-specific as well as apoptosis independent function. Because *ced-3* auto-proteolytic activation is dependent on *ced-4*, we will also examine CED-4 localization pattern in *mir-52* mutants. Notably, mRNAs for members of the core apoptotic machinery do not have obvious *mir-52* binding sites. Therefore, we assume that the effect of *mir-52* deletion on CED-3 localization and suppression of germline apoptosis in *ced-9(n1653ts)* worms might be indirect.

Hypoxia-inducible factor 1 (HIF-1) inhibits germline apoptosis following IR (Sendoel et al., 2010). Under normoxic conditions, HIF-1 is targeted for proteolytic degradation via hydroxylation of specific proline residues by the *egl-9*, prolyl hydroxylase (Epstein et al., 2001; Jiang et al., 2001). In *egl-9(lf)* mutants, HIF-1 accumulates in a manner similar to that observed under hypoxic conditions (Epstein et al., 2001). The 3'UTR of *egl-9* carries a very good candidate *mir-52* binding site (Friedman et al., 2009; Jan et al., 2011). Taking into account apoptosis the suppressive nature of HIF-1, it would be interesting to analyze the expression of *egl-9* in *mir-52* mutants in response to IR. Remarkably, hypoxia-dependent downregulation of mir-100 was observed in bladder cancer cell lines and in breast cancer tumor samples in humans (Blick et al., 2013). Moreover, transfection of bladder cancer cell lines with a mir-100 mimic under hypoxic conditions reduced cell growth (Blick et al., 2013).

Taken together, our data suggest that *mir-52* is a cell-autonomous enhancer of physiological and DNA damage-induced germline apoptosis. Other members of the *mir-51* family do not appear to affect germ cell death. *mir-52* likely influences germline apoptosis downstream or in parallel to *cep-1*. However, further investigations will be needed to uncover the exact mode of action of *mir-52*.

## 2.6 Materials and Methods

### 2.6.1 *C. elegans* maintenance and strains

All strains were grown at 20 ˚C (unless indicated otherwise) on NGM agar plates seeded with *E. coli* OP50 strain according to standard procedures (Brenner, 1974). The Bristol N2 strain was used as the wild type.

The following alleles and transgenes were used in this study: LGI: *gla-3(op216)*, *cep-1(gk138)*, *ced-1(e1735)*, *ced-12(k149)*, *gld-1(op236)*; LGII: *opIs537 [Pmex-5::mir-52 (promoterless)]* (this study); LGIII: *mpk-1(ga111)*, *ced-4(n1162)*; LGIV: *mir-52(n4114)*, *mir-52(n4100)*, *mir-51(n4473)*, *mir-53(n4113)*, *mir-51 mir-53(nDf67)*, *let-60(n1046)*, *let-60(ga89)*, *lip-1(zh15)*, *ced-3(n717)*; LGX: *mir-54-55-56(nDf58)*. All mutations are described in WormBase (http://www.wormbase.org, Stein et al., 2001). In addition, the multicopy transgene *opIs461 [$P_{ced-3}$::ced-3::gfp::ced-3(3′ UTR)]* (Subasic et al., 2016) and extrachromosomal arrays *mjEx123 [mir-52 (genomic) + $P_{dlg-1}$::dlg-1-mcherry)]* (Shaw et al., 2010) were used.

### 2.6.2. Generation of transgenic line

The single-copy insertion allele *opIs537* was generated by Mos1 transposase-mediated single-copy gene insertion (MosSCI, Frøkjær-Jensen et al., 2012) using EG6699 strain [*ttTi5605*; *unc-119(ed3)*]. The germline-specific *mir-52* rescue plasmid was constructed using MultiSite Gateway cloning (Life Technologies). The *mir-52* promoterless 1’233 base pairs (bp) fragment was amplified using the primers 5´-GGGGACAAGTTTGTACAAAAAA GCAGGCTTACTACTACTACTCCTACAACTACAA-3´ and 5´-GGGGACCACTTTGTAC AAGAAAGCTGGGTGCTGTAAAATATATCATTCCAGTGAA-3´ primers and inserted into the pDONR 221 vector. The p2R-P3 vector includes a non-coding 127 bp sequence from chromosome IV amplified with 5´-GGGGACAGCTTTCTTGTACAAAGTGGTTACCAATTCT TATTAAATAAACAAA-3´ and 5´-GGGGACAACTTTGTATAATAAAGTTGGAGGTTTGG AGCCAACAGGCGTGTGG-3´ primers. A pDONR P4 P1R vector carrying genomic 488 bp promoter fragment immediately upstream of the *mex-5* start codon (kind gift from B. Conradt) was recombined with the pDONR 221 and p2R-P3 vectors according to the manufacturer’s instructions to generate the pPK1045 plasmid.

### 2.6.3 Apoptotic assays

Apoptotic corpses were quantified as previously described (Sulston and Horvitz, 1977; Gumienny et al., 1999) at 20 ˚C (unless indicated otherwise). The starting point for adulthood was defined when the majority (~80%) of the bleach-synchronized animals passed L4/YA molt (14h post "Christmas tree" vulva in wild-type worms under standard conditions). To analyze DNA damage-induced germ cell death, worms were irradiated with 60 Gy (X-ray, Rad Source 2000) at the L4/YA molt. Animals were anesthetized in a drop of 5mM levamisole, and apoptotic corpses were counted using differential interference contrast (DIC) microscopy. For the temperature sensitivity assays, worms were shifted to 15 ˚C or 25 ˚C as L1 larvae. *gla-3(op216)* was used as a positive control for the increased number of germ cell corpses with and without IR; *cep-1(gk138)* was used as a negative control for the reduced number of germ cell corpses following IR.

### 2.6.4 Western blot

Bleach-synchronized gravid worms (18h post L4/YA molt) were irradiated with 0 Gy, 60 Gy and collected 4h later. Gravid adults were washed three times in M9 buffer and frozen in liquid nitrogen. To extract proteins, worms were sonicated on ice for 10min at 320 W power (30s sonication + 1 min break) using UCD-200 Bioruptor Standart sonicator (Diagenode) in the freshly prepared RIPA buffer (50mM Tris-HCl, pH 8, 150mM NaCl, 0.5% deoxycholate, 1% NP40, 0.1% SDS, 1 tablet/10ml PhosStop EASYpack phosphatase inhibitor (Roche), 1 tablet/10mL Complete Mini protease inhibitor (Roche)) in the ratio of 1 : 2 (worms : buffer). Protein concentration was determined using Pierce™ 660-nm protein assay (ThermoFisher). Protein samples were boiled in Laemmli buffer for 10 min. 20 µg of protein extracts were resolved on a 4%-12% Bis-Tris NuPage gel and transferred to PVDF membrane using a wet blot chamber (Invitrogen, XCell II™ Blot). The membranes were blocked with 5% milk in PBST for 1h and probed with phosphorylated ERK (M8159, Sigma-Aldrich, 1:5000, mouse), ERK (M5670, Sigma-Aldrich, 1:500, rabbit), and α-tubulin (T6074, Sigma-Aldrich, 1:3000, mouse) specific antibodies. Secondary antibodies were anti-mouse HRP (A9044, Sigma-Aldrich, 1:3000) and anti-rabbit HRP (A0545, Sigma-Aldrich, 1:1000). Primary antibodies were incubated over night at 4 ˚C. Secondary antibodies were incubated for 1h at room temperature. The relative band

intensities were quantified using FUSION SL (Vilber) image analyzer, FusionCapt Advance software, and normalized to tubulin.

### 2.6.5 Microscopy

Fluorescent images were acquired on Leica DM6000 B (Leica Microsystems) microscope equipped with Leica DFC360 FX camera (pixel size: 6.45µm x 6.45µm) controlled by LAS AF6000 imaging software (Leica Microsystems). Fluorescent images were acquired with the same exposure times, intensities, and gain for all samples. Images were enhanced for brightness and contrast to the same extent with ImageJ (Collins, 2007) and Photoshop (Adobe Systems).

## 2.7 Acknowledgements and Funding

We would like to thank Robert Horvitz and *Caenorhabditis* Genetics Center (CGC) for the miRNA strains used in the screen, Barbara Conradt for the pDONR P4 P1R vector carrying *mex-5* promoter, Xue Zheng for the help with performing primary miRNA screen, members of the Hengartner and Hajnal labs for the critical discussions on the project. This work was supported by the Swiss National Science Foundation (Sinergia grant: CRSII3_141942, Apoptosis grant: 31003A_143932) and the Kanton of Zurich. The funders had no role in study design, data collection and analysis, decision to publish, or preparation of the manuscript.

## 2.8 Disclosure Declaration

The authors disclose no financial or any other conflict of interest.

## 2.9 Correspondence

requests for materials should be addressed to M.O.H.
(michael.hengartner@imls.uzh.ch)

## 2.10 Figure Legends

**Fig. 2.1 Loss of *mir-52* impairs DNA damage-induced germ cell death.** A. Germline apoptosis is strongly reduced upon IR in *mir-52(n4114)* and *mir-52(n4100)* animals. Young adults were irradiated with 60 Gy and analyzed 24h later (n=30 animals/genotype). B. IR-induced germ cell death is also impaired in older *mir-52* deletion mutants. Young adults were irradiated, and analyzed at the indicated time points post L4/YA molt (n=30 animals/genotype). Solid lines represent the data of the untreated worms; dashed lines represent the data of the irradiated worms. Data shown are average number of apoptotic cells ± standard deviation (SD) for three replicates. *P*-values in (A) were generated using Benjamini-Hochberg corrected paired *t*-test between mutants and wild type, where ** represents the *p*-value < 0.01.

**Fig. 2.2 *mir-52* controls germline apoptosis cell-autonomously.** A. Soma-specific *mir-52* expression from the extrachromosomal array *mjEx123* did not rescue DNA damage-induced germline apoptotic defects of *mir-52(n4114)* animals. B. Germline-specific rescue of *mir-52, opIs537*, restored wild-type levels of germ cell death following IR. Number of germ cell corpses were quantified during physiological (0 Gy) and DNA damage-induced (60 Gy) germline apoptosis in worms irradiated at young adult stage and analyzed 24h later (n=30 animals/genotype). Data shown are average number of germ cell corpses ± SD for three replicates. *P*-values were generated using Benjamini-Hochberg corrected paired *t*-test, where * represents the *p*-value < 0.05, **- *p*-value < 0.01.

**Fig. 2.3 Other *mir-51* family members do not contribute to IR-induced germ cell death.** Germ cell corpses were scored with and without IR in single and multiple mutants of *mir-51* family. Young adults were irradiated with 60 Gy and analyzed 24h later (n=30 animals/genotype). Data shown are average number of germ cell corpses ± SD for three replicates. *P*-values were generated using Benjamini-Hochberg corrected paired *t*-test, where ** represents the *p*-value < 0.01.

**Fig. 2.4 Apoptotic cell corpse clearance is normal in *mir-52* mutants.** A. Germ cell corpses are slightly reduced in engulfment competent and IR-defective *mir-52* mutants. Young adults were irradiated with 60 Gy and analyzed 12h later (n=30 animals/genotype). B. Somatic cell corpse clearance is not affected in *mir-52* mutants. Cell corpses were quantified in the head region of freshly hatched L1 larvae (n=25 animals/genotype). Data shown are average number of germ cell

corpses ± SD for three replicates. *P*-values in (A) were generated using Benjamini-Hochberg corrected paired *t*-test, where * represents the *p*-value < 0.05, **- *p*-value < 0.01.

**Fig. 2.5 *mir-52(n4114)* likely acts independently of the MAPK signaling pathway to control IR-induced germ cell death.** A. Activated MAPK signaling pathway does not fully rescue the apoptotic defects of *mir-52(n4114)*. Quantification of germ cell corpses during physiological (0 Gy) and DNA damage-induced (60 Gy) apoptosis was performed in the double mutants of *mir-52* and mutants with upregulated MAPK signaling. Young adults were irradiated with 60 Gy and analyzed 24h later (n=30 animals/genotype). Data shown are average number of germ cell corpses ± SD for three replicates. B. Total MPK-1 levels are slightly reduced and phosphorylated MPK-1 levels are slightly increased in *mir-52(n4114)* worms. Western blot analysis of Ras/MAPK signaling in *mir-52(n4114)* mutants with (60 Gy) and without (0 Gy) IR was performed using monoclonal anti-P-ERK and anti-ERK antibodies. *mpk-1(ga111)* served as negative control, and α-tubulin - as internal loading control. Data are representative of average band intensities compared to N2 ± SD for three replicates (a.u. - arbitrary units). Benjamini-Hochberg corrected *P*-values in (A) were generated using paired *t*-test, where * represents the *p*-value < 0.05, **- *p*-value < 0.01.

**Fig. 2.6 Loss of *mir-52* affects germline apoptosis downstream of or in parallel to *cep-1*.** A. *mir-52(n4114)* suppresses increased germ cell death due to *cep-1* overexpression. Quantification of germ cell corpses during physiological (0 Gy) and DNA damage-induced (60 Gy) apoptosis was performed in synchronized worms at the indicated temperature and time post L4/YA molt (n=30 animals/genotype). B. *ced-9(n1653ts); mir-52(n4114)* animals show reduced levels of germline apoptosis at the physiological conditions and in response to DNA damage. Data shown are average number of germ cell corpses ± SD for three replicates. Benjamini-Hochberg corrected *P*-values were generated using paired *t*-test, where * represents the *p*-value < 0.05, **- *p*-value < 0.01.

**Fig. 2.7 CED-3::GFP localization pattern is changed in *mir-52(n4114)* mutant.** Fluorescence photomicrographs of *ced-3(n717) mir-52(n4114)* worms which carry *opIs461 [$P_{ced-3}$::ced-3::gfp::ced-3(3′ UTR)]* transgene are shown. *ced-3(n717); opIs461* animals were used as a control. Synchronized worms were analyzed in triplicates 24h post L4/YA molt (n=10

animals/genotype) during physiological (0 Gy) and DNA damage-induced (60 Gy) apoptosis at 20 ˚C. Scale bar - 10µm.

**Table 2.1 55 miRNA mutants were analyzed for the defects in germline apoptosis.** Number of germ cell corpses was quantified in 55 miRNA mutants once or twice in the primary screen. Selected candidates were then analyzed in triplicates in the secondary screen. Quantification of germ cell corpses during physiological (0 Gy) and DNA damage-induced (60 Gy) apoptosis was performed in synchronized worms at 20 ˚C, 24h post L4/YA molt (n=20 animals/genotype). "snoRNA" stands for small nucleolar RNAs, non-coding RNAs are marked with "ncRNA", "PC" represents protein coding genes.

**Supplemental Fig. 2.1 The genomic location of *mir-51* family and structure of *mir-52* germline-specific rescue transgene.** A. *mir-51* family members are tightly clustered on the chromosomes IV and X. B. Fragment of pPK1045 plasmid, which carries *Pmex-5::mir-52* rescue transgene.

**Supplemental Fig. 2.2 The requirement of *mir-52* for DNA-damage induced germ cell death is temperature dependent.** Apoptotic defects in *mir-52* mutants are strong at 15 ˚C (A), but at 25 ˚C, loss of *mir-52* only partially prevents IR-induced germ cell death (B). Quantification of germ cell corpses during physiological (0 Gy) and DNA damaged-induced (60 Gy) apoptosis was performed in synchronized worms at the indicated time post L4/YA molt for the corresponding temperatures (n=30 animals/genotype). Data shown are average number of germ cell corpses ± SD for three replicates. Benjamini-Hochberg corrected *P*-values were generated using paired *t*-test, where * represents the *p*-value < 0.05. Samples marked with "n.d." were not scored.

**Supplemental Fig. 2.3 *mir-52* tissue-specific rescue of germline apoptosis at 25 ˚C.** A. Somatic *mir-52* expression partially rescues the defects of DNA damage-induced germline apoptosis in *mir-52(n4114)* worms at 25 ˚C. B Gemline-specific expression of *mir-52* fully rescues the defects of germline apoptosis following IR at 25 ˚C. Synchronized worms at the indicated time post L4/YA molt for the corresponding temperatures were analyzed (n=30 animals/genotype). Data shown are average number of germ cell corpses ± SD for three replicates. Benjamini-Hochberg corrected *P*-values were generated using paired *t*-test, where * represents the *p*-value < 0.05. Samples marked with "n.d." were not scored.

**Supplemental Fig. 2.4 Physiological germline apoptosis is slightly reduced in *mir-52* and engulfment double mutants.** Number of germ cell corpses was quantified in synchronized worms 24h post L4/YA molt (n=30 animals/genotype) during physiological (0 Gy) germline apoptosis at 20 ˚C. Data shown are average number of germ cell corpses ± SD for three replicates. *P*-values were generated using Benjamini-Hochberg corrected paired *t*-test, where * represents the *p*-value < 0.05, **- *p*-value < 0.01.

## 2.11 References

Al-Amin, M., Min, H., Shim, Y.-H., and Kawasaki, I. (2016). Somatically expressed germ-granule components, PGL-1 and PGL-3, repress programmed cell death in C. elegans. Sci. Rep. 6, srep33884.

Alpi, A., Pasierbek, P., Gartner, A., and Loidl, J. (2003). Genetic and cytological characterization of the recombination protein RAD-51 in Caenorhabditis elegans. Chromosoma *112*, 6–16.

Alvarez-Saavedra, E., and Horvitz, H.R. (2010). Many families of C. elegans microRNAs are not essential for development or viability. Curr. Biol. CB 20, 367–373.

Bailly, A.P., Freeman, A., Hall, J., Déclais, A.C., Alpi, A., Lilley, D.M., Ahmed, S., and Gartner, A. (2010). The Caenorhabditis elegans homolog of Gen1/Yen1 resolvases links DNA damage signaling to DNA double-strand break repair. PLoS Genet. *6*, e1001025.

Berset, T., Hoier, E.F., Battu, G., Canevascini, S., and Hajnal, A. (2001). Notch inhibition of RAS signaling through MAP kinase phosphatase LIP-1 during C. elegans vulval development. Science 291, 1055–1058.

Blick, C., Ramachandran, A., Wigfield, S., McCormick, R., Jubb, A., Buffa, F.M., Turley, H., Knowles, M.A., Cranston, D., Catto, J., et al. (2013). Hypoxia regulates FGFR3 expression via HIF-1α and miR-100 and contributes to cell survival in non-muscle invasive bladder cancer. Br. J. Cancer *109*, 50–59.

Brenner, S. (1974). The Genetics of Caenorhabditis elegans. Genetics 77, 71–94.

Brenner, J.L., Kemp, B.J., and Abbott, A.L. (2012). The mir-51 family of microRNAs functions in diverse regulatory pathways in Caenorhabditis elegans. PLOS ONE 7, e37185.

Chen, Y.-C., Chen, H.-J., Tseng, W.-C., Hsu, J.-M., Huang, T.-T., Chen, C.-H., and Pan, C.-L. (2016). A C. elegans thermosensory circuit regulates longevity through crh-1/CREB-dependent flp-6 neuropeptide signaling. Dev. Cell *39*, 209–223.

Collins, T.J. (2007). ImageJ for microscopy. BioTechniques 43, 25–30.

Conradt, B., and Horvitz, H.R. (1998). The C. elegans protein EGL-1 Is required for programmed cell death and interacts with the Bcl-2–like protein CED-9. Cell 93, 519–529.

Deng, X., Yin, X., Allan, R., Lu, D.D., Maurer, C.W., Haimovitz-Friedman, A., Fuks, Z., Shaham, S., and Kolesnick, R. (2008). Ceramide biogenesis is required for radiation-induced apoptosis in the germ line of C. elegans. Sci. N. Y. N *322*, 110–115.

Derry, W.B., Bierings, R., Iersel, M. van, Satkunendran, T., Reinke, V., and Rothman, J.H. (2007). Regulation of developmental rate and germ cell proliferation in Caenorhabditis elegans by the p53 gene network. Cell Death Differ. 14, 662–670.

Eberhard, R., Stergiou, L., Hofmann, E.R., Hofmann, J., Haenni, S., Teo, Y., Furger, A., and Hengartner, M.O. (2013). Ribosome synthesis and MAPK activity modulate ionizing radiation-induced germ cell apoptosis in Caenorhabditis elegans. PLOS Genet. 9, e1003943.

Eisenmann, D.M., and Kim, S.K. (1997). Mechanism of activation of the Caenorhabditis elegans ras homologue let-60 by a novel, temperature-sensitive, gain-of-function mutation. Genet. 146, 553–565.

Ellis, H.M., and Horvitz, H.R. (1986). Genetic control of programmed cell death in the nematode C. elegans. Cell 44, 817–829.

Epstein, A.C.R., Gleadle, J.M., McNeill, L.A., Hewitson, K.S., O'Rourke, J., Mole, D.R., Mukherji, M., Metzen, E., Wilson, M.I., Dhanda, A., et al. (2001). C. elegans EGL-9 and mammalian homologs define a family of dioxygenases that regulate HIF by prolyl hydroxylation. Cell *107*, 43–54.

Fox, P.M., Vought, V.E., Hanazawa, M., Lee, M.-H., Maine, E.M., and Schedl, T. (2011). Cyclin E and CDK-2 regulate proliferative cell fate and cell cycle progression in the C. elegans germline. Development 138, 2223–2234.

Friedman, R.C., Farh, K.K.-H., Burge, C.B., and Bartel, D.P. (2009). Most mammalian mRNAs are conserved targets of microRNAs. Genome Res. *19*, 92–105.

Frøkjær-Jensen, C., Davis, M.W., Ailion, M., and Jorgensen, E.M. (2012). Improved Mos1-mediated transgenesis in C. elegans. Nat. Methods 9, 117–118.

Gartner, A., Milstein, S., Ahmed, S., Hodgkin, J., and Hengartner, M.O. (2000). A conserved checkpoint pathway mediates DNA damage–induced apoptosis and cell cycle arrest in C. elegans. Mol. Cell 5, 435–443.

Greiss, S., Hall, J., Ahmed, S., and Gartner, A. (2008). C. elegans SIR-2.1 translocation is linked to a proapoptotic pathway parallel to cep-1/p53 during DNA damage-induced apoptosis. Genes Dev. *22*, 2831–2842.

Grimson, A., Srivastava, M., Fahey, B., Woodcroft, B.J., Chiang, H.R., King, N., Degnan, B.M., Rokhsar, D.S., and Bartel, D.P. (2008). Early origins and evolution of microRNAs and Piwi-interacting RNAs in animals. Nature 455, 1193-1197.

Gumienny, T.L., Lambie, E., Hartwieg, E., Horvitz, H.R., and Hengartner, M.O. (1999). Genetic control of programmed cell death in the Caenorhabditis elegans hermaphrodite germline. Development 126, 1011–1022.

Gumienny, T.L., Brugnera, E., Tosello-Trampont, A.-C., Kinchen, J.M., Haney, L.B., Nishiwaki, K., Walk, S.F., Nemergut, M.E., Macara, I.G., Francis, R., et al. (2001). CED-12/ELMO, a novel member of the CrkII/Dock180/Rac pathway, is required for phagocytosis and cell migration. Cell 107, 27–41.

Han, M., Aroian, R.V., and Sternberg, P.W. (1990). The let-60 locus controls the switch between vulval and nonvulval cell fates in Caenorhabditis elegans. Genet. 126, 899–913.

Hengartner, M.O., and Horvitz, H.R. (1994a). Activation of C. elegans cell death protein CED-9 by an ammo-acid substitution in a domain conserved in Bcl-2. Nature 369, 318–320.

Hengartner, M.O., and Horvitz, H.R. (1994b). C. elegans cell survival gene ced-9 encodes a functional homolog of the mammalian proto-oncogene bcl-2. Cell 76, 665–676.

Hengartner, M.O., Ellis, R., and Horvitz, R. (1992). Caenorhabditis elegans gene ced-9 protects cells from programmed cell death. Nature 356, 494–499.

Hofmann, E.R., Milstein, S., Boulton, S.J., Ye, M., Hofmann, J.J., Stergiou, L., Gartner, A., Vidal, M., and Hengartner, M.O. (2002). Caenorhabditis elegans HUS-1 Is a DNA Damage Checkpoint Protein Required for Genome Stability and EGL-1-Mediated Apoptosis. Curr. Biol. 12, 1908–1918.

Ito, S., Greiss, S., Gartner, A., and Derry, W.B. (2010). Cell-nonautonomous regulation of C. elegans germ cell death by kri-1. Curr. Biol. 20, 333–338.

Jan, C.H., Friedman, R.C., Ruby, J.G., and Bartel, D.P. (2011). Formation, regulation and evolution of *Caenorhabditis elegans* 3′UTRs. Nature *469*, 97–101.

Jiang, H., Guo, R., and Powell-Coffman, J.A. (2001). The Caenorhabditis elegans hif-1 gene encodes a bHLH-PAS protein that is required for adaptation to hypoxia. Acad. Sci. U. S. Am. *98*, 7916–7921.

Kato, M., Paranjape, T., Ullrich, R., Nallur, S., Gillespie, E., Keane, K., Esquela-Kerscher, A., Weidhaas, J.B., and Slack, F.J. (2009). The mir-34 microRNA is required for the DNA damage response in vivo in C. elegans and in vitro in human breast cancer cells. Oncogene 28, 2419–2424.

Kritikou, E.A., Milstein, S., Vidalain, P.-O., Lettre, G., Bogan, E., Doukoumetzidis, K., Gray, P., Chappell, T.G., Vidal, M., and Hengartner, M.O. (2006). C. elegans GLA-3 is a novel component of the MAP kinase MPK-1 signaling pathway required for germ cell survival. Genes Dev. 20, 2279–2292.

Lee, M.-H., Hook, B., Pan, G., Kershner, A.M., Merritt, C., Seydoux, G., Thomson, J.A., Wickens, M., and Kimble, J. (2007). Conserved Regulation of MAP Kinase Expression by PUF RNA-Binding Proteins. PLOS Genet. 3, 2540–2550.

Lee, R.Y.N., Howe, K.L., Harris, T.W., Arnaboldi, V., Cain, S., Chan, J., Chen, W.J., Davis, P., Gao, S., Grove, C., et al. (2017). WormBase 2017: molting into a new stage. Nucleic Acids Res. 46, 869–874.

Li, C., Gao, Y., Zhang, K., Chen, J., Han, S., Feng, B., Wang, R., and Chen, L. (2015). Multiple roles of microRNA-100 in human cancer and its therapeutic potential. Cell. Physiol. Biochem. 37, 2143–2159.

Merritt, C., Rasoloson, D., Ko, D., and Seydoux, G. (2008). 3′ UTRs are the primary regulators of gene expression in the C. elegans germline. Curr. Biol. 18, 1476–1482.

Mertenskötter, A., Keshet, A., Gerke, P., and Paul, R.J. (2013). The p38 MAPK PMK-1 shows heat-induced nuclear translocation, supports chaperone expression, and affects the heat tolerance of Caenorhabditis elegans. Cell Stress Chaperones *18*, 293–306.

Min, H., Shim, Y.-H., and Kawasaki, I. (2016). Loss of PGL-1 and PGL-3, members of a family of constitutive germ-granule components, promotes germline apoptosis in C. elegans. J. Cell Sci. 129, 341–353.

Nousch, M., and Eckmann, C.R. (2013). Translational control in the Caenorhabditis elegans germ line. Germ cell development in C. elegans, (Springer, New York, NY), 205–247.

Pourkarimi, E., Greiss, S., and Gartner, A. (2012). Evidence that CED-9/Bcl2 and CED-4/Apaf-1 localization is not consistent with the current model for C. elegans apoptosis induction. Cell Death Differ. *19*, 406–415.

Qin, C., Huang, R.-Y., and Wang, Z.-X. (2015). Potential role of miR-100 in cancer diagnosis, prognosis, and therapy. Tumor Biol. 36, 1403–1409.

Rutkowski, R., Dickinson, R., Stewart, G., Craig, A., Schimpl, M., Keyse, S.M., and Gartner, A. (2011). Regulation of Caenorhabditis elegans p53/CEP-1–dependent germ cell apoptosis by Ras/MAPK signaling. PLOS Genet. 7, e1002238.

Schumacher, B., Schertel, C., Wittenburg, N., Tuck, S., Mitani, S., Gartner, A., Conradt, B., and Shaham, S. (2005a). C. elegans ced-13 can promote apoptosis and is induced in response to DNA damage. Cell Death Differ. 12, 153–161.

Schumacher, B., Hanazawa, M., Lee, M.-H., Nayak, S., Volkmann, K., Hofmann, R., Hengartner, M., Schedl, T., and Gartner, A. (2005b). Translational repression of C. elegans p53 by GLD-1 regulates DNA damage-induced apoptosis. Cell 120, 357–368.

Sendoel, A., Kohler, I., Fellmann, C., Lowe, S.W., and Hengartner, M.O. (2010). HIF-1 antagonizes p53-mediated apoptosis through a secreted neuronal tyrosinase. Nature 465, 577–583.

Shaham, S., Reddien, P.W., Davies, B., and Horvitz, H.R. (1999). Mutational analysis of the Caenorhabditis elegans cell-death gene ced-3. Genetics 153, 1655–1671.

Shaw, W.R., Armisen, J., Lehrbach, N.J., and Miska, E.A. (2010). The Conserved miR-51 microRNA family is redundantly required for embryonic development and pharynx attachment in Caenorhabditis elegans. Genetics 185, 897–905.

Sherrard, R., Luehr, S., Holzkamp, H., McJunkin, K., Memar, N., and Conradt, B. (2017). miRNAs cooperate in apoptosis regulation during C. elegans development. Genes Dev. 31, 209–222.

Stein, L., Sternberg, P., Durbin, R., Thierry-Mieg, J., and Spieth, J. (2001). WormBase: network access to the genome and biology of Caenorhabditis elegans. Nucleic Acids Res. 29, 82–86.

Stergiou, L., Doukoumetzidis, K., Sendoel, A., and Hengartner, M.O. (2007). The nucleotide excision repair pathway is required for UV-C-induced apoptosis in Caenorhabditis elegans. Cell Death Differ. 14, 1129–1138.

Subasic, D., Brümmer, A., Wu, Y., Pinto, S.M., Imig, J., Keller, M., Jovanovic, M., Lightfoot, H.L., Nasso, S., Goetze, S., et al. (2015). Cooperative target mRNA destabilization and translation inhibition by miR-58 microRNA family in C. elegans. Genome Res. 25, 1680–1691.

Subasic, D., Stoeger, T., Eisenring, S., Matia-González, A.M., Imig, J., Zheng, X., Xiong, L., Gisler, P., Eberhard, R., Holtackers, R., et al. (2016). Post-transcriptional control of executioner caspases by RNA-binding proteins. Genes Dev. 30, 2213–2225.

Sulston, J.E., and Horvitz, H.R. (1977). Post-embryonic cell lineages of the nematode, Caenorhabditis elegans. Dev. Biol. 56, 110–156.

Sulston, J.E., Schierenberg, E., White, J.G., and Thomson, J.N. (1983). The embryonic cell lineage of the nematode Caenorhabditis elegans. Dev. Biol. 100, 64–119.

Wang, X., Zhao, Y., Wong, K., Ehlers, P., Kohara, Y., Jones, S.J., Marra, M.A., Holt, R.A., Moerman, D.G., and Hansen, D. (2009). Identification of genes expressed in the hermaphrodite germ line of C. elegans using SAGE. BMC Genomics 10, 213.

Xu, D., Wei, G., Lu, P., Luo, J., Chen, X., Skogerbø, G., and Chen, R. (2014). Analysis of the p53/CEP-1 regulated non-coding transcriptome in C. elegans by an NSR-seq strategy. Protein Cell 5, 770–782.

Xue, D., Shaham, S., and Horvitz, H.R. (1996). The Caenorhabditis elegans cell-death protein CED-3 is a cysteine protease with substrate specificities similar to those of the human CPP32 protease. Genes Dev. 10, 1073–1083.

Yuan, J., and Horvitz, H.R. (1990). The Caenorhabditis elegans genes ced-3 and ced-4 act cell autonomously to cause programmed cell death. Dev. Biol. 138, 33–41.

Yuan, J., and Horvitz, H.R. (1992). The Caenorhabditis elegans cell death gene ced-4 encodes a novel protein and is expressed during the period of extensive programmed cell death. Development 116, 309–320.

Yuan, J., Shaham, S., Ledoux, S., Ellis, H.M., and Horvitz, H.R. (1993). The C. elegans cell death gene ced-3 encodes a protein similar to mammalian interleukin-1β-converting enzyme. Cell 75, 641–652.

Zhang, B., Xiao, R., Ronan, E.A., He, Y., Hsu, A.L., Liu, J., and Xu, X.Z. (2015). Environmental Temperature Differentially Modulates C. elegans Longevity through a Thermosensitive TRP Channel. Cell Rep. *11*, 1414–1424.

Zhou, Z., Hartwieg, E., and Horvitz, H.R. (2001). CED-1 Is a transmembrane receptor that mediates cell corpse engulfment in C. elegans. Cell 104, 43–56.

Zou, H., Henzel, W.J., Liu, X., Lutschg, A., and Wang, X. (1997). Apaf-1, a human protein homologous to C. elegans CED-4, participates in cytochrome c–dependent activation of caspase-3. Cell 90, 405–413.

## 2.12 Figures and Tables

Figure 2.1, *Kamkina et. al.*

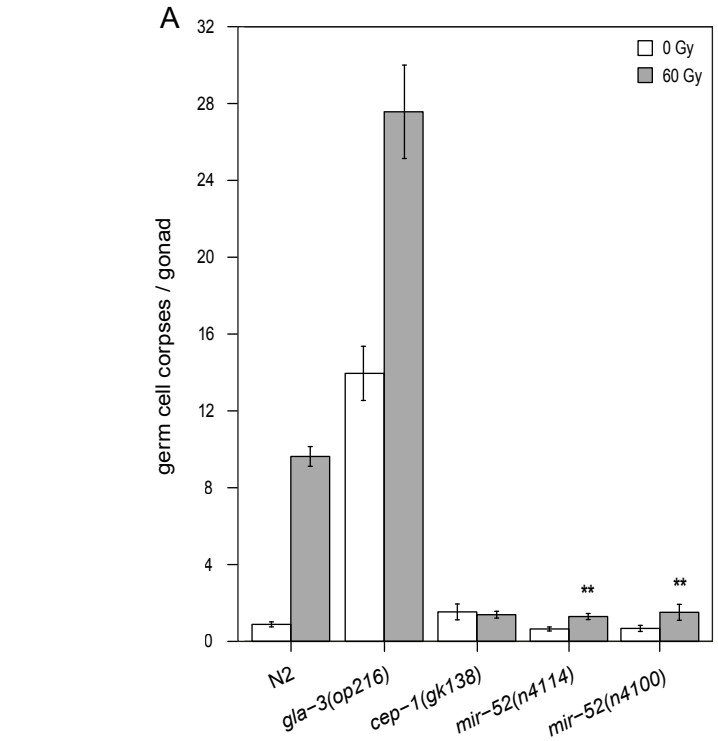


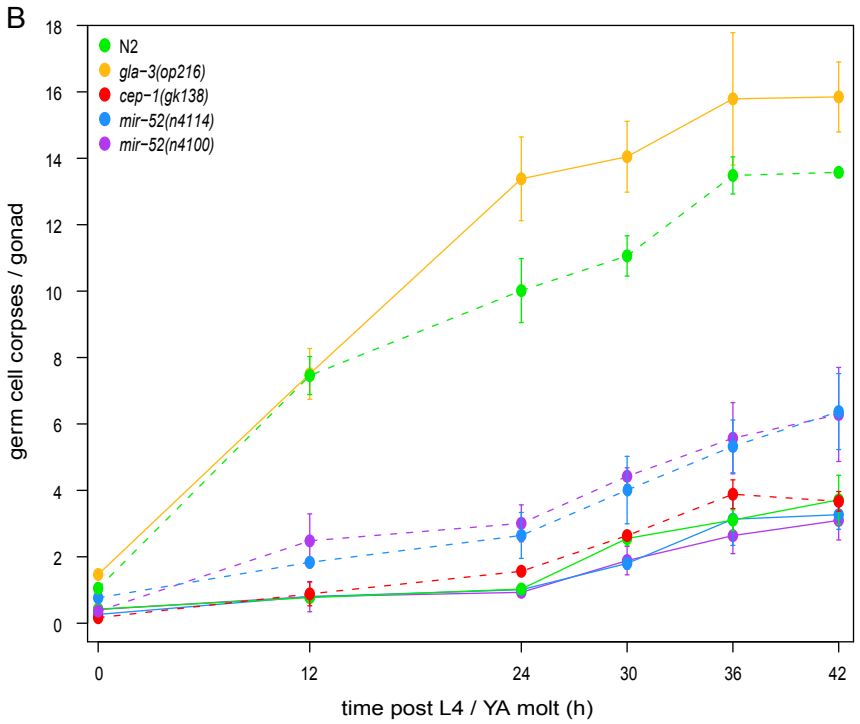

Figure 2.2, *Kamkina et. al.*

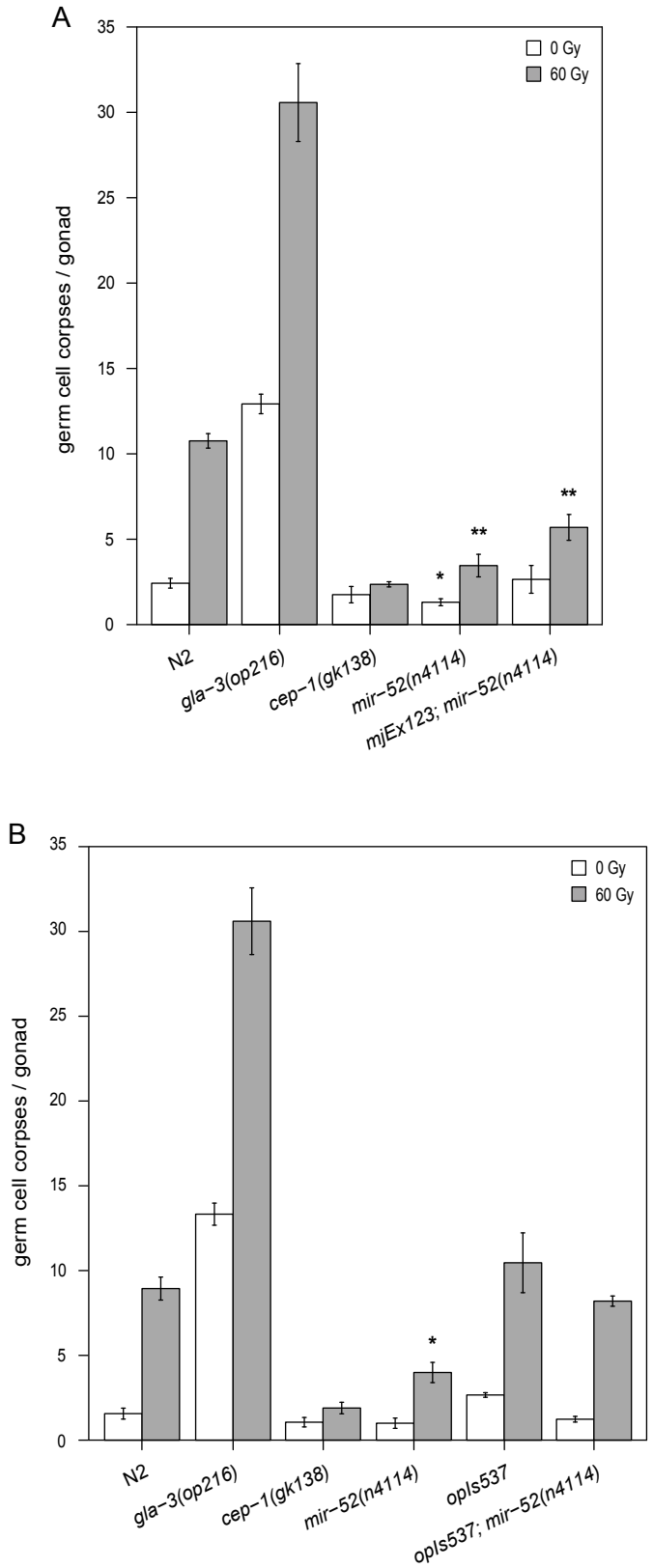

Figure 2.3, *Kamkina et. al.*

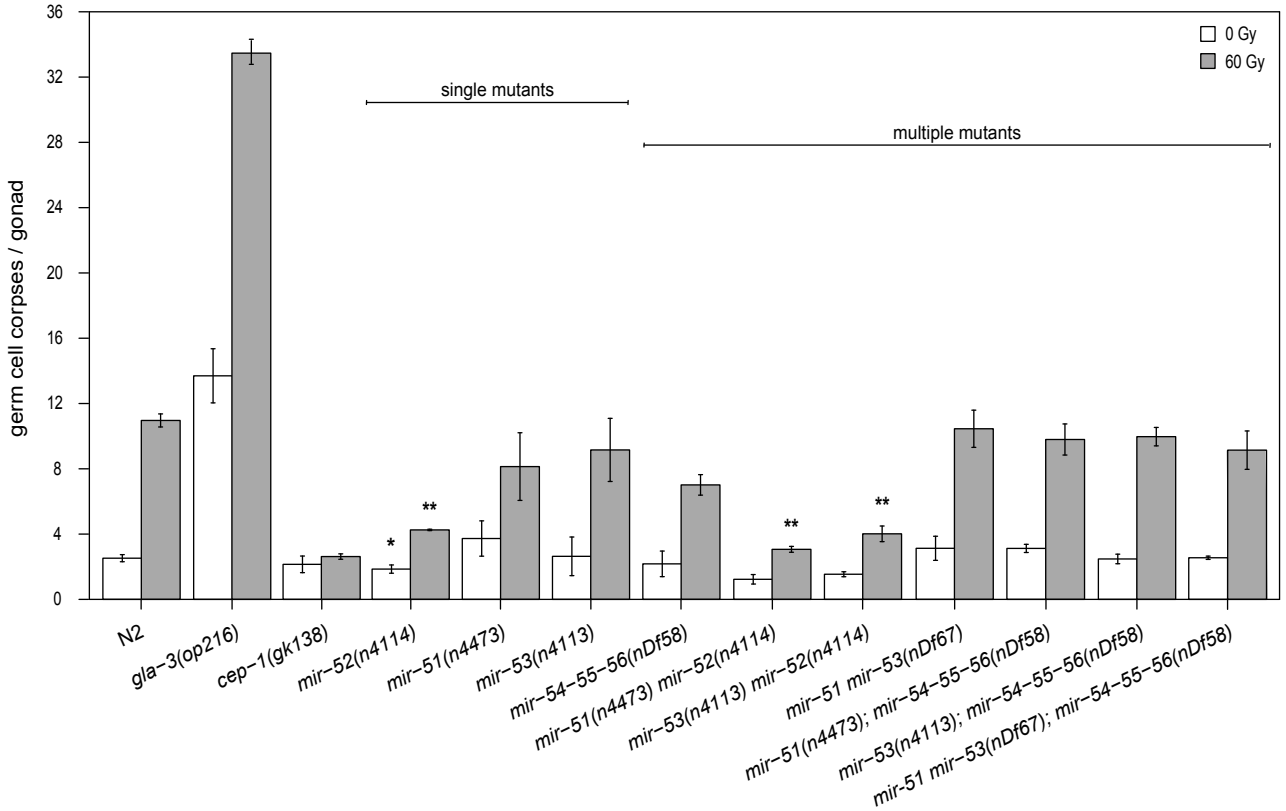

Figure 2.4, *Kamkina et. al.*

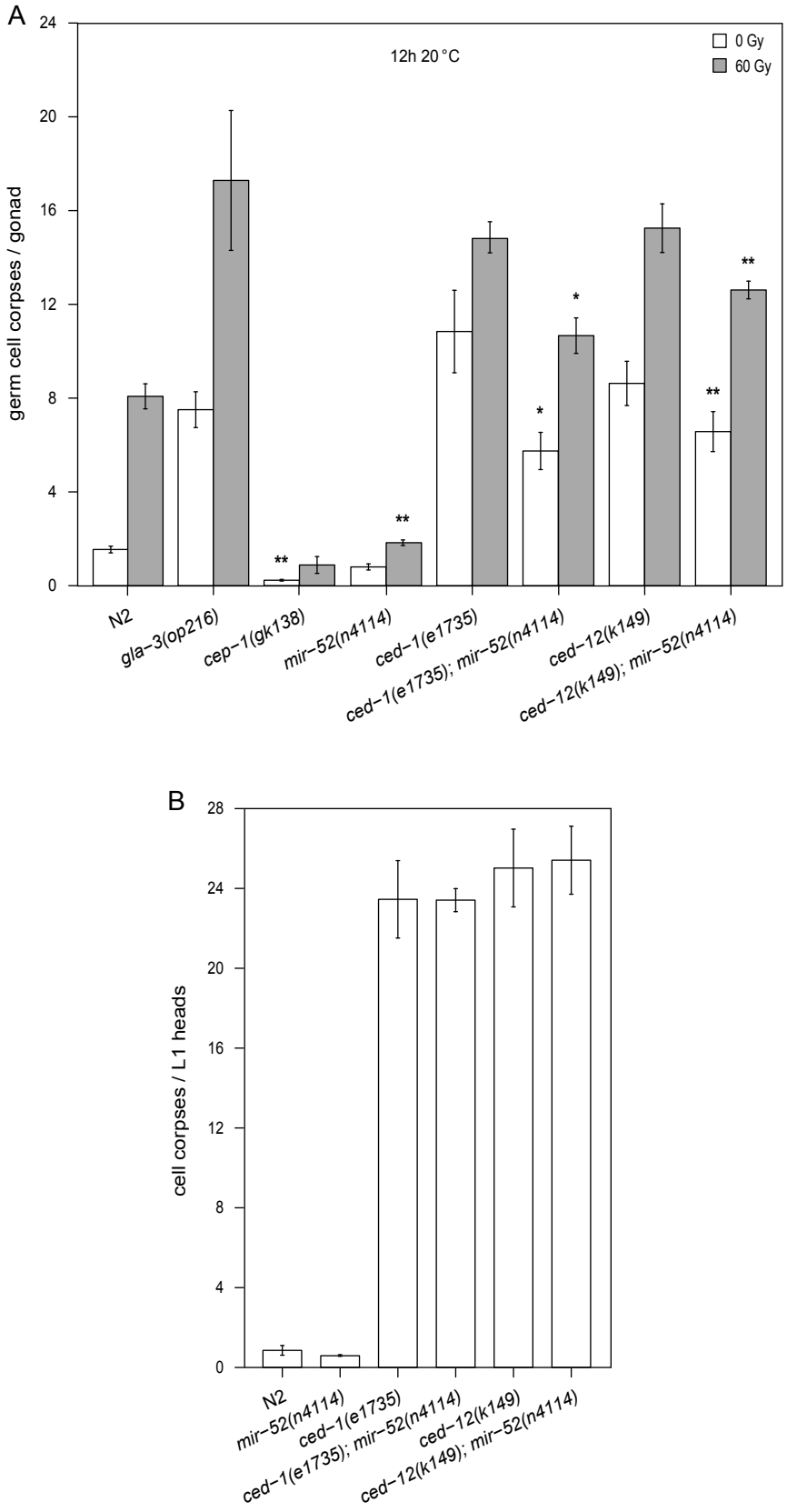

Figure 2.5, *Kamkina et. al.*

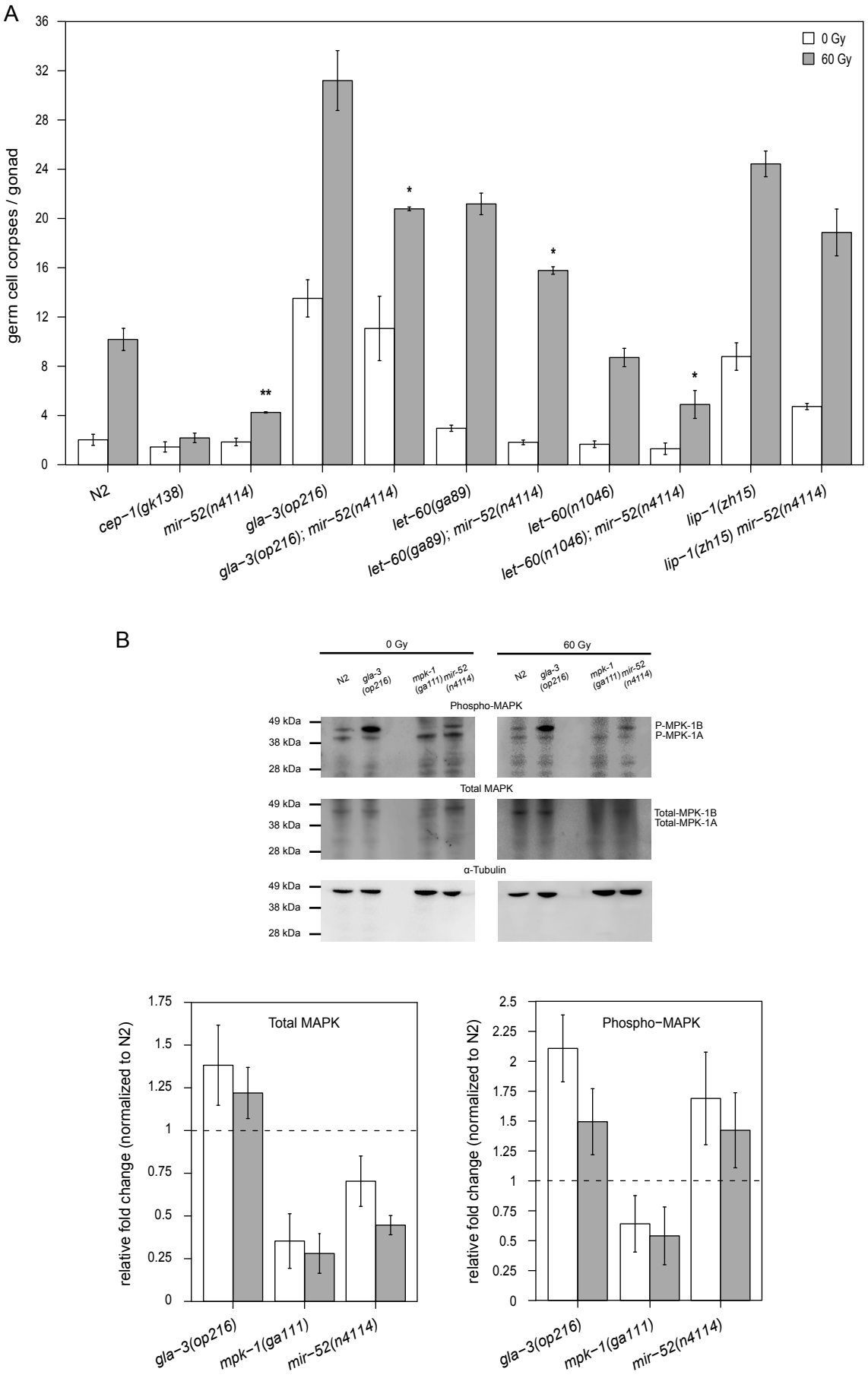

Figure 2.6, *Kamkina et. al.*

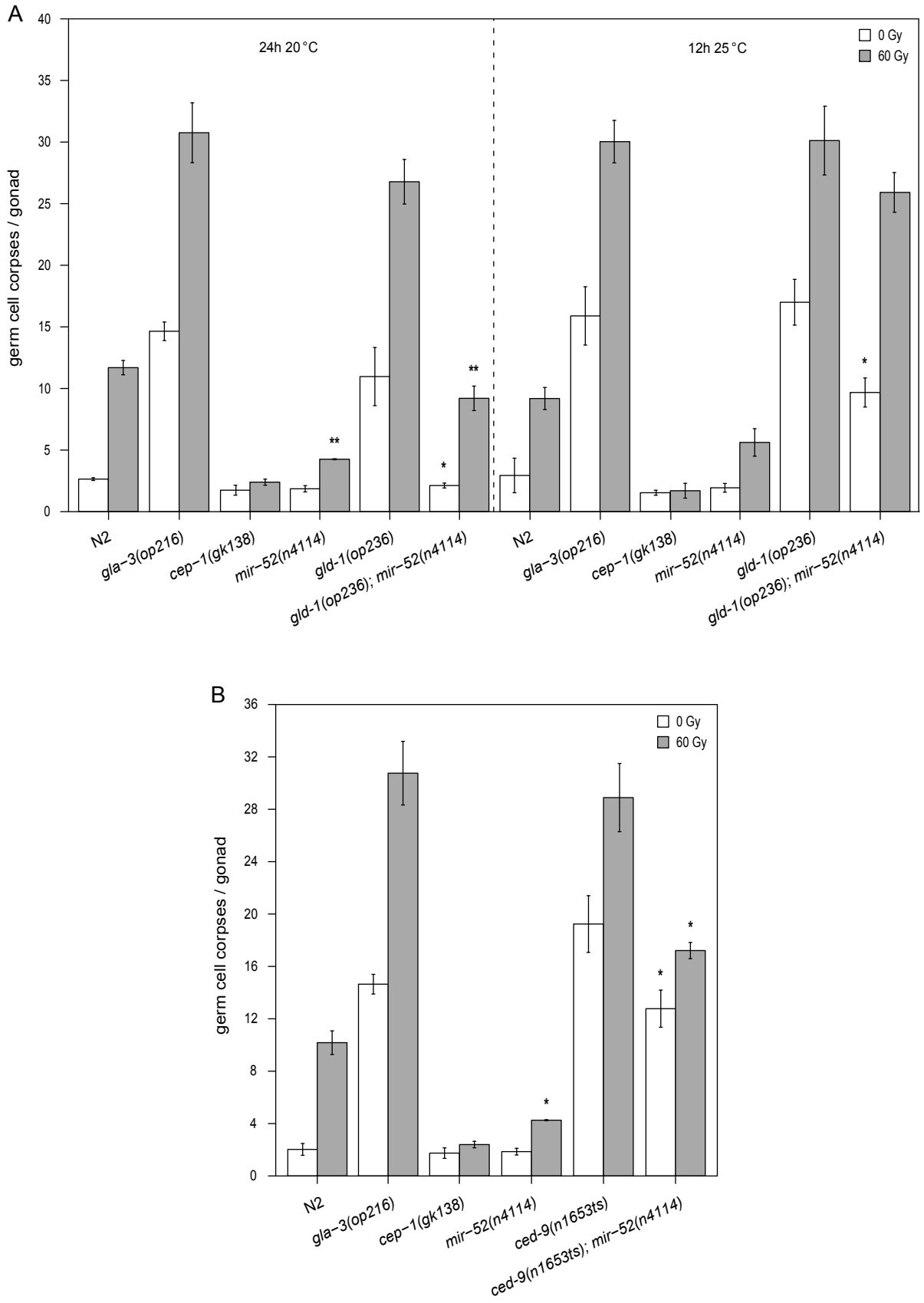

Figure 2.7, *Kamkina et. al.*

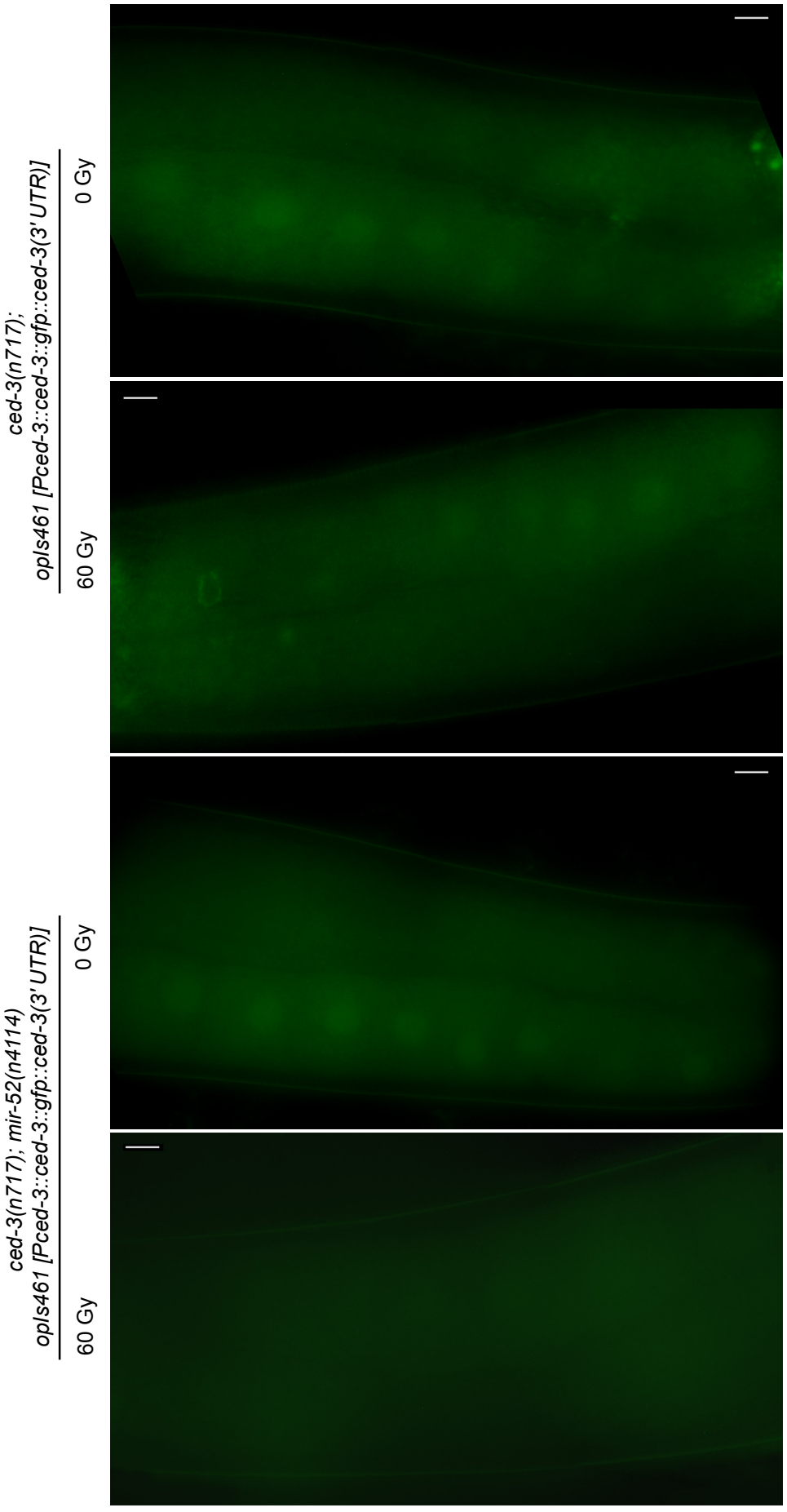

Table 2.1, *Kamkina et. al.*

| Strain | miRNAs analyzed | Alleles | Other genes affected | Primary screen | | | | | | Secondary screen | | | | | | | | | |
|---|---|---|---|---|---|---|---|---|---|---|---|---|---|---|---|---|---|---|---|
| | | | | 0 Gy | | | 60 Gy | | | 0 Gy | | | | | 60 Gy | | | | |
| | | | | 1st | 2nd | Mean | 1st | 2nd | Mean | 1st | 2nd | 3rd | Mean | SD | 1st | 2nd | 3rd | Mean | SD |
| VC576 | *mir-1* | *gk276 I* | *T09B4.14* (ncRNA) | 0.70 | --- | **0.70** | 2.64 | --- | **2.64** | --- | --- | --- | **---** | --- | --- | --- | --- | **---** | --- |
| MT16762 | *mir-256* | *n4471 V* | *mec-1* | 2.40 | --- | **2.40** | 4.60 | --- | **4.60** | --- | --- | --- | **---** | --- | --- | --- | --- | **---** | --- |
| MT14445 | *mir-1; mir-256* | *n4102 I; n4471 V* | Chr. I: *T09B4.14* (ncRNA), *T09B4.17* (ncRNA), Chr. V: *mec-1* | 0.79 | 0.88 | **0.83** | 2.35 | 1.31 | **1.83** | --- | --- | --- | **---** | --- | --- | --- | --- | **---** | --- |
| VC1051 | *mir-34* | *gk437 I* | --- | 1.00 | 0.75 | **0.88** | 2.70 | 3.48 | **3.09** | --- | --- | --- | **---** | --- | --- | --- | --- | **---** | --- |
| MT13406 | *mir-34* | *n4276 X* | --- | 2.60 | --- | **2.60** | 6.12 | --- | **6.12** | --- | --- | --- | **---** | --- | --- | --- | --- | **---** | --- |
| MT14752 | *mir-35-44; nEx1188 [mir-35 mir-45 (genomic) + sur-5::GFP]* | *nDf50 nDf49 II; nEx1188* | *F54D5.12* (PC), *Y62F5A.15* (ncRNA), *Y62F5A.9* (ncRNA), *Y62F5A.14* (ncRNA), *ZK930.12* (ncRNA), *ZK930.15* (snoRNA) | 1.00 | 1.80 | **1.40** | 4.28 | 5.24 | **4.76** | --- | --- | --- | **---** | --- | --- | --- | --- | **---** | --- |
| MT13372 | *mir-42-44* | *nDf49 II* | *ZK930.12* (ncRNA), *ZK930.15* (snoRNA) | 4.05 | | **4.05** | 6.00 | | **6.00** | 4.50 | 0.83 | 3.22 | **2.85** | 1.52 | --- | --- | --- | **---** | --- |
| MT14117 | *mir-2; mir-42-44* | *n4108 I; nDf49 II* | Chr. I: *ppfr-1* ; Chr. II: *ZK930.12* (ncRNA), *ZK930.15* (snoRNA) | 1.40 | 2.05 | **1.73** | 6.68 | 5.44 | **6.06** | --- | --- | --- | **---** | --- | --- | --- | --- | **---** | --- |
| MT14875 | *mir-61 mir-250* | *nDf59 V* | *sel-11* | 1.10 | --- | **1.10** | 4.36 | --- | **4.36** | --- | --- | --- | **---** | --- | --- | --- | --- | **---** | --- |
| MT17431 | *mir-42-44; mir-61 mir-250; mir-247 mir-797* | *nDf49 II; nDf59 V; n4505 X* | Chr. II: *ZK930.12* (ncRNA), *ZK930.15* (snoRNA); Chr. V: *sel-11* | 0.75 | --- | **0.75** | 1.28 | --- | **1.28** | --- | --- | --- | **---** | --- | --- | --- | --- | **---** | --- |
| MT17848 | *mir-2; mir-42-44; mir-61, mir-250; mir-247, mir-797* | *n4108 I; nDf49 II; nDf59 V; n4505 X* | Chr. I: *ppfr-1* ; Chr. II: *ZK930.12* (ncRNA), *ZK930.15* (snoRNA); Chr. V: *sel-11* | 0.65 | --- | **0.65** | 0.68 | --- | **0.68** | --- | --- | --- | **---** | --- | --- | --- | --- | **---** | --- |
| MT14993 | *mir-46; mir-47* | *n4475 III; gk167 X* | Chr. III: *ZK525.4* (ncRNA) | 2.30 | 2.20 | **2.25** | 5.28 | 9.64 | **7.46** | 2.68 | 2.59 | 2.54 | **2.60** | 0.06 | 4.46 | 5.14 | 5.11 | **4.90** | 0.32 |
| MT12956 | *mir-49* | *n4103 X* | --- | 0.90 | --- | **0.90** | 5.40 | --- | **5.40** | --- | --- | --- | **---** | --- | --- | --- | --- | **---** | --- |
| MT15501 | *mir-83* | *n4638 IV* | *C06A6.9* (ncRNA) | 1.65 | --- | **1.65** | 3.76 | --- | **3.76** | --- | --- | --- | **---** | --- | --- | --- | --- | **---** | --- |
| MT13433 | *mir-45* | *n4280 II* | *top-2* , *ZK930.13* (ncRNA) | 1.35 | --- | **1.35** | 3.96 | --- | **3.96** | --- | --- | --- | **---** | --- | --- | --- | --- | **---** | --- |
| MT12945 | *mir-52* | *n4100 IV* | *Y37A1B.335* (ncRNA), *Y37A1B.330* (ncRNA) | 0.20 | --- | **0.20** | 0.72 | --- | **0.72** | 0.47 | 0.46 | 0.87 | **0.60** | 0.19 | 1.57 | 0.34 | 2.06 | **1.32** | 0.72 |
| MT12990 | *mir-52* | *n4114 IV* | *Y37A1B.335* (ncRNA), *Y37A1B.330* (ncRNA) | 0.60 | --- | **0.60** | 1.56 | --- | **1.56** | 0.33 | 0.86 | 0.35 | **0.51** | 0.24 | 1.41 | 1.77 | 1.17 | **1.45** | 0.25 |
| MT14767 | *mir-54-56* | *nDf58 X* | *F09A5.11* (ncRNA) | 0.80 | --- | **0.80** | 1.64 | --- | **1.64** | --- | --- | --- | **---** | --- | --- | --- | --- | **---** | --- |

Table 2.1 continued, *Kamkina et. al.*

| Strain | miRNAs analyzed | Alleles | Other genes affected | Primary screen | | | | | | Secondary screen | | | | | | | | | |
|---|---|---|---|---|---|---|---|---|---|---|---|---|---|---|---|---|---|---|---|
| | | | | 0 Gy | | | 60 Gy | | | 0 Gy | | | | | 60 Gy | | | | |
| | | | | 1st | 2nd | Mean | 1st | 2nd | Mean | 1st | 2nd | 3rd | Mean | SD | 1st | 2nd | 3rd | Mean | SD |
| MT17429 | *mir-53 mir-51* | *nDf67 IV* | *F36H1.17* (ncRNA), *alh-3* | 0.60 | --- | **0.60** | 3.36 | --- | **3.36** | --- | --- | --- | **---** | --- | --- | --- | --- | **---** | --- |
| MT17137 | *mir-51; mir-54-56* | *n4473 IV; nDf58 X* | Chr. IV: *F36H1.17* (ncRNA), *alh-3* ; Chr. X: *F09A5.11* (ncRNA) | 0.40 | --- | **0.40** | 1.44 | --- | **1.44** | --- | --- | --- | **---** | --- | --- | --- | --- | **---** | --- |
| MT17136 | *mir-53 mir-51; mir-54-56* | *nDf67 IV; nDf58 X* | Chr. IV: *F36H1.17* (ncRNA), *alh-3* ; Chr. X: *F09A5.11* (ncRNA) | 1.15 | --- | **1.15** | 0.84 | --- | **0.84** | --- | --- | --- | **---** | --- | --- | --- | --- | **---** | --- |
| MT17143 | *mir-53 mir-51 mir-52/nT1[qIs51] (IV;V); mir-54-56* | *nDf67 n4114/nT1[qIs51] (IV;V); nDf58 X* | Chr. IV: *F36H1.17* (ncRNA), *alh-3, Y37A1B.335* (ncRNA), *Y37A1B.330* (ncRNA); Chr. X: *F09A5.11* (ncRNA) | 0.65 | --- | **0.65** | 0.56 | --- | **0.56** | --- | --- | --- | **---** | --- | --- | --- | --- | **---** | --- |
| MT15024 | *mir-58.1* | *n4640 IV* | *Y67D8A.6* (ncRNA), *Y67D8A.2* (PC) | 1.00 | --- | **1.00** | 2.56 | --- | **2.56** | --- | --- | --- | **---** | --- | --- | --- | --- | **---** | --- |
| MT15563 | *mir-80; mir-58.1; mir-81, mir-82* | *nDf53 III; n4640 IV; nDf54 X* | Chr. III: *K01F9.6* (ncRNA), Chr. IV: *Y67D8A.6* (ncRNA), *Y67D8A.2* (PC), Chr. X: *T07D1.2(* PC) | 0.55 | 0.40 | **0.48** | 1.68 | 1.08 | **1.38** | --- | --- | --- | **---** | --- | --- | --- | --- | **---** | --- |
| MT14935 | *mir-59* | *n4604 IV* | --- | 3.00 | 4.20 | **3.60** | 6.16 | 6.32 | **6.24** | --- | --- | --- | **---** | --- | --- | --- | --- | **---** | --- |
| VT1289 | *mir-63* | *n4568 X* | --- | 1.80 | --- | **1.80** | 3.48 | --- | **3.48** | --- | --- | --- | **---** | --- | --- | --- | --- | **---** | --- |
| MT16495 | *mir-64-66, mir-229* | *nDf63 III* | *gcn-1* | 0.44 | 0.70 | **0.57** | 2.25 | 1.85 | **2.05** | --- | --- | --- | **---** | --- | --- | --- | --- | **---** | --- |
| SX79 | *mir-64 mir-229; mir-228; mir-124* | *nDf52 II; n4382 IV; n4255 IV* | Chr. II: *gcn-1* Chr. IV: *21ur-11442, 21ur-9840, 21ur-6620, 21ur-8162, T12E12.44* (ncRNA) *C29E6.8* (ncRNA), *trpa-1* | 2.00 | 0.85 | **1.43** | 4.20 | 2.60 | **3.40** | --- | --- | --- | **---** | --- | --- | --- | --- | **---** | --- |
| MT14765 | *mir-68* | *n4569 IV* | --- | 1.25 | --- | **1.25** | 2.92 | --- | **2.92** | --- | --- | --- | **---** | --- | --- | --- | --- | **---** | --- |
| VT1362 | *mir-70* | *n4109 V* | *pmp-5* | 1.60 | --- | **1.60** | 3.24 | --- | **3.24** | --- | --- | --- | **---** | --- | --- | --- | --- | **---** | --- |
| MT17428 | *mir-72; mir-73 mir-74* | *n4130 II; nDf47 X* | *Chr. II: pqn-42* ; *Chr. X: T24D8.14* (ncRNA), *T24D8.16* (ncRNA) | 1.80 | --- | **1.80** | 2.44 | --- | **2.44** | --- | --- | --- | **---** | --- | --- | --- | --- | **---** | --- |
| SX34 | *mir-71; mir-72; mir-73 mir-74* | *n4105 I; n4130 II; nDf47 X* | *Chr. I: F16A11.6(* ncRNA), *ppfr-1; Chr. II: pqn-42, Chr. X: T24D8.14* (ncRNA), *T24D8.16* (ncRNA) | 3.70 | 2.05 | **2.88** | 5.28 | 3.68 | **4.48** | --- | --- | --- | **---** | --- | --- | --- | --- | **---** | --- |
| MT14448 | *mir-79; mir-75* | *n4126 I; n4472 X* | Chr. I: *C12C8.6* (ncRNA) | 2.60 | 1.85 | **2.23** | 2.36 | 2.92 | **2.64** | --- | --- | --- | **---** | --- | --- | --- | --- | **---** | --- |
| MT14451 | *mir-76* | *n4474 I* | *C44B11.4* (PC) | 1.55 | --- | **1.55** | 3.12 | --- | **3.12** | --- | --- | --- | **---** | --- | --- | --- | --- | **---** | --- |
| MT16311 | *mir-77* | *n4286 II* | *T21B4.20* (snoRNA) | 1.10 | --- | **1.10** | 3.36 | --- | **3.36** | --- | --- | --- | **---** | --- | --- | --- | --- | **---** | --- |
| MT15021 | *mir-78* | *n4637 IV* | *21ur-9765, 21ur-9780, 21ur-10635, 21ur-1935, 21ur-14536, 21ur-10414* | 1.55 | --- | **1.55** | 4.12 | --- | **4.12** | --- | --- | --- | **---** | --- | --- | --- | --- | **---** | --- |
| MT16336 | *mir-86 mir-8211* | *n4607 III* | *Y56A3A.7* (PC) | 0.60 | --- | **0.60** | 3.60 | --- | **3.60** | --- | --- | --- | **---** | --- | --- | --- | --- | **---** | --- |
| MT15981 | *mir-87; mir-233* | *n4104 V; n4761 X* | Chr. V: *F10C2.11* (ncRNA), *kup-1* , Chr. X: *W03G11.4* (PC) | 1.20 | 1.55 | **1.38** | 3.36 | 2.84 | **3.10** | --- | --- | --- | **---** | --- | --- | --- | --- | **---** | --- |

Table 2.1 continued, *Kamkina et. al.*

| Strain | miRNAs analyzed | Alleles | Other genes affected | Primary screen | | | | | | Secondary screen | | | | | | | | | |
|---|---|---|---|---|---|---|---|---|---|---|---|---|---|---|---|---|---|---|---|
| | | | | 0 Gy | | | 60 Gy | | | 0 Gy | | | | | 60 Gy | | | | |
| | | | | 1st | 2nd | Mean | 1st | 2nd | Mean | 1st | 2nd | 3rd | Mean | SD | 1st | 2nd | 3rd | Mean | SD |
| MT15517 | *mir-233* | *n4761 X* | *W03G11.4* (PC) | 1.80 | --- | **1.80** | 5.12 | --- | **5.12** | --- | --- | --- | **---** | --- | --- | --- | --- | **---** | --- |
| MT14449 | *mir-232* | *nDf56 IV* | *F13H10.5* (PC) | 0.50 | 0.81 | **0.66** | 2.70 | 2.90 | **2.80** | --- | --- | --- | **---** | --- | --- | --- | --- | **---** | --- |
| MT15019 | *mir-357 mir-358* | *nDf60* | *symk-1* , *F25G6.1* (PC) | 2.75 | --- | **2.75** | 5.72 | --- | **5.72** | --- | --- | --- | **---** | --- | --- | --- | --- | **---** | --- |
| MT14588 | *mir-234* | *n4520 II* | *C13B4.6* (ncRNA) | 0.60 | --- | **0.60** | 3.88 | --- | **3.88** | --- | --- | --- | **---** | --- | --- | --- | --- | **---** | --- |
| MT17997 | *mir-235* | *n4504 I* | --- | 0.60 | --- | **0.60** | 2.00 | --- | **2.00** | 1.47 | 1.58 | 2.73 | **1.93** | 0.57 | --- | --- | --- | **---** | --- |
| MT16061 | *mir-238; mir-239.2 mir-239.1* | *n4112 III; nDf62 X* | Chr. X: *C34E11.9* (ncRNA), *C34E11.20* (snoRNA) | 0.95 | 1.85 | **1.40** | 4.20 | 5.00 | **4.60** | --- | --- | --- | **---** | --- | --- | --- | --- | **---** | --- |
| MT15873 | *mir-240 mir-786 mir-8203* | *n4541 X* | --- | 0.85 | --- | **0.85** | 4.04 | --- | **4.04** | --- | --- | --- | **---** | --- | --- | --- | --- | **---** | --- |
| MT14936 | *mir-242* | *n4605 IV* | *nhr-78* | 8.00 | --- | **8.00** | 5.64 | --- | **5.64** | 5.53 | 4.96 | 5.83 | **5.44** | 0.36 | 7.26 | 8.69 | 8.57 | **8.17** | 0.65 |
| MT16337 | *mir-245* | *n4798 I* | *F55D12.8* (ncRNA) | 1.00 | --- | **1.00** | 3.08 | --- | **3.08** | --- | --- | --- | **---** | --- | --- | --- | --- | **---** | --- |
| MT16848 | *mir-249* | *n4983 X* | --- | 0.50 | --- | **0.50** | 0.36 | --- | **0.36** | 0.91 | 0.46 | 1.03 | **0.80** | 0.25 | 1.92 | 2.51 | 3.00 | **2.48** | 0.44 |
| MT16335 | *mir-251* | *n4606 X* | --- | 0.85 | --- | **0.85** | 2.16 | --- | **2.16** | --- | --- | --- | **---** | --- | --- | --- | --- | **---** | --- |
| MT16317 | *mir-252; mir-251* | *n4570 II; n4606 X* | Chr. II: *W02B12.17* (ncRNA), *W02B12.18* (ncRNA), *W02B12.13* (PC) | 1.30 | 0.85 | **1.08** | 3.40 | 3.64 | **3.52** | --- | --- | --- | **---** | --- | --- | --- | --- | **---** | --- |
| MT16060 | *mir-253* | *nDf64 V* | *F44E7.14* (ncRNA), *F44E7.13* (ncRNA), *F44E7.5* (PC), *F44E7.15* (ncRNA) | 4.35 | --- | **4.35** | 4.60 | --- | **4.60** | --- | --- | --- | **---** | --- | --- | --- | --- | **---** | --- |
| MT16762 | *mir-256* | *n4471 V* | *mec-1* | 2.40 | --- | **2.40** | 4.60 | --- | **4.60** | --- | --- | --- | **---** | --- | --- | --- | --- | **---** | --- |
| MT14682 | *mir-257* | *n4548 V* | --- | 2.50 | --- | **2.50** | 3.76 | --- | **3.76** | --- | --- | --- | **---** | --- | --- | --- | --- | **---** | --- |
| MT15023 | *mir-268* | *n4639 V* | *C06H2.10* (ncRNA), *glb-3* | 0.85 | --- | **0.85** | 3.04 | --- | **3.04** | --- | --- | --- | **---** | --- | --- | --- | --- | **---** | --- |
| MT16316 | *mir-355* | *n4618 II* | --- | 0.89 | --- | **0.89** | 2.24 | --- | **2.24** | --- | --- | --- | **---** | --- | --- | --- | --- | **---** | --- |

Supplemental Figure 2.1, *Kamkina et. al.*

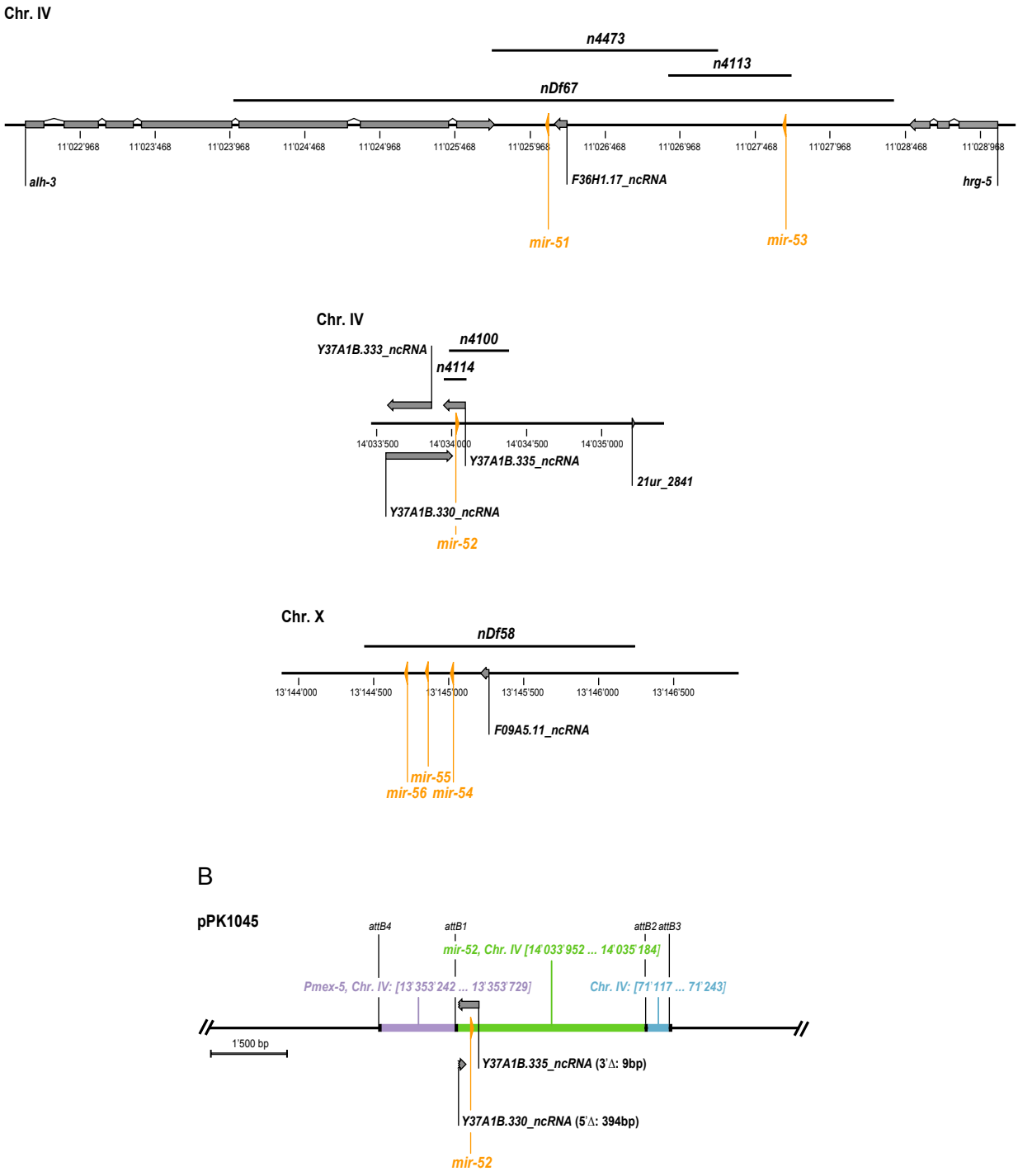

Supplemental Figure 2.2, *Kamkina et. al.*

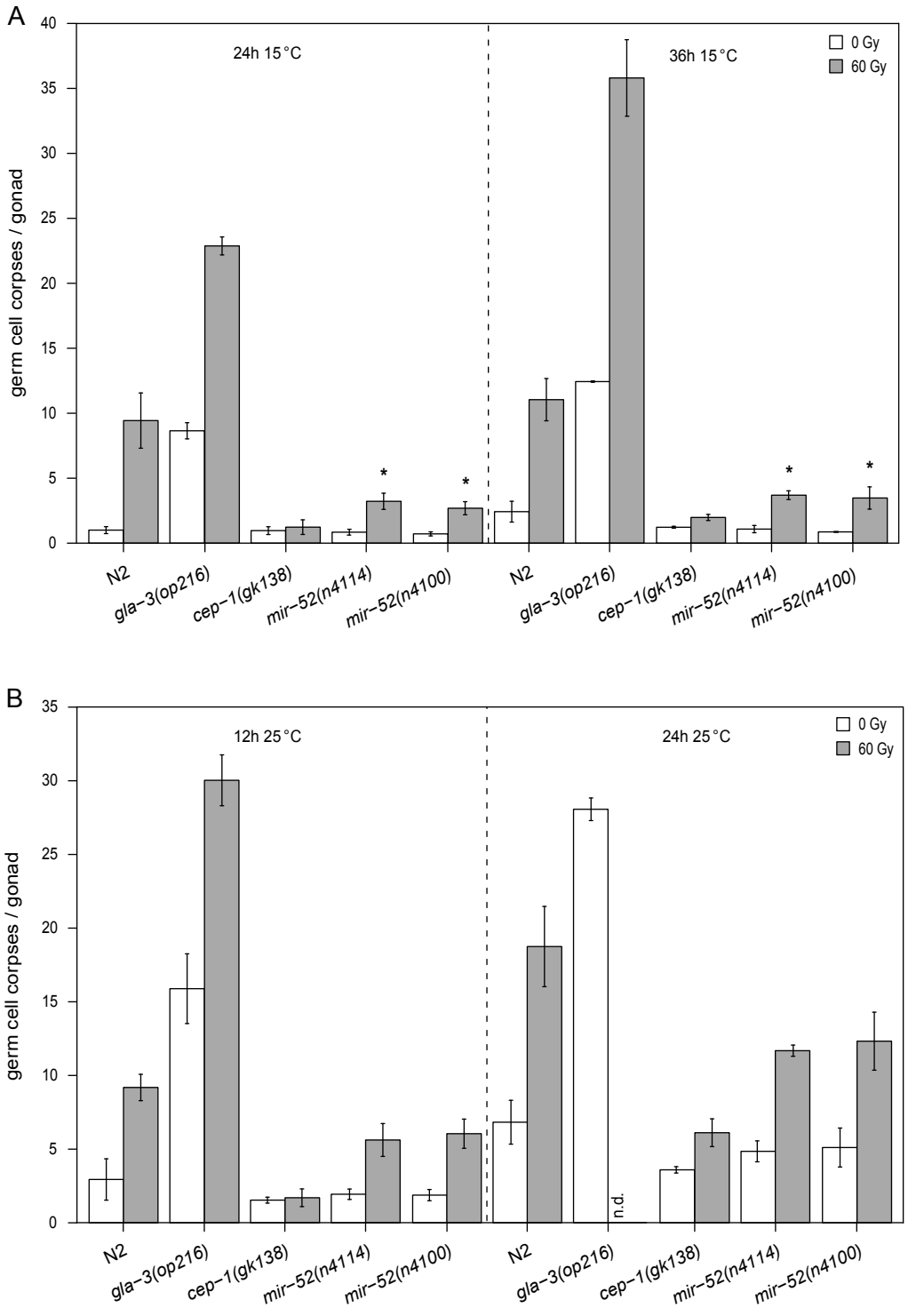

Supplemental Figure 2.3, *Kamkina et. al.*

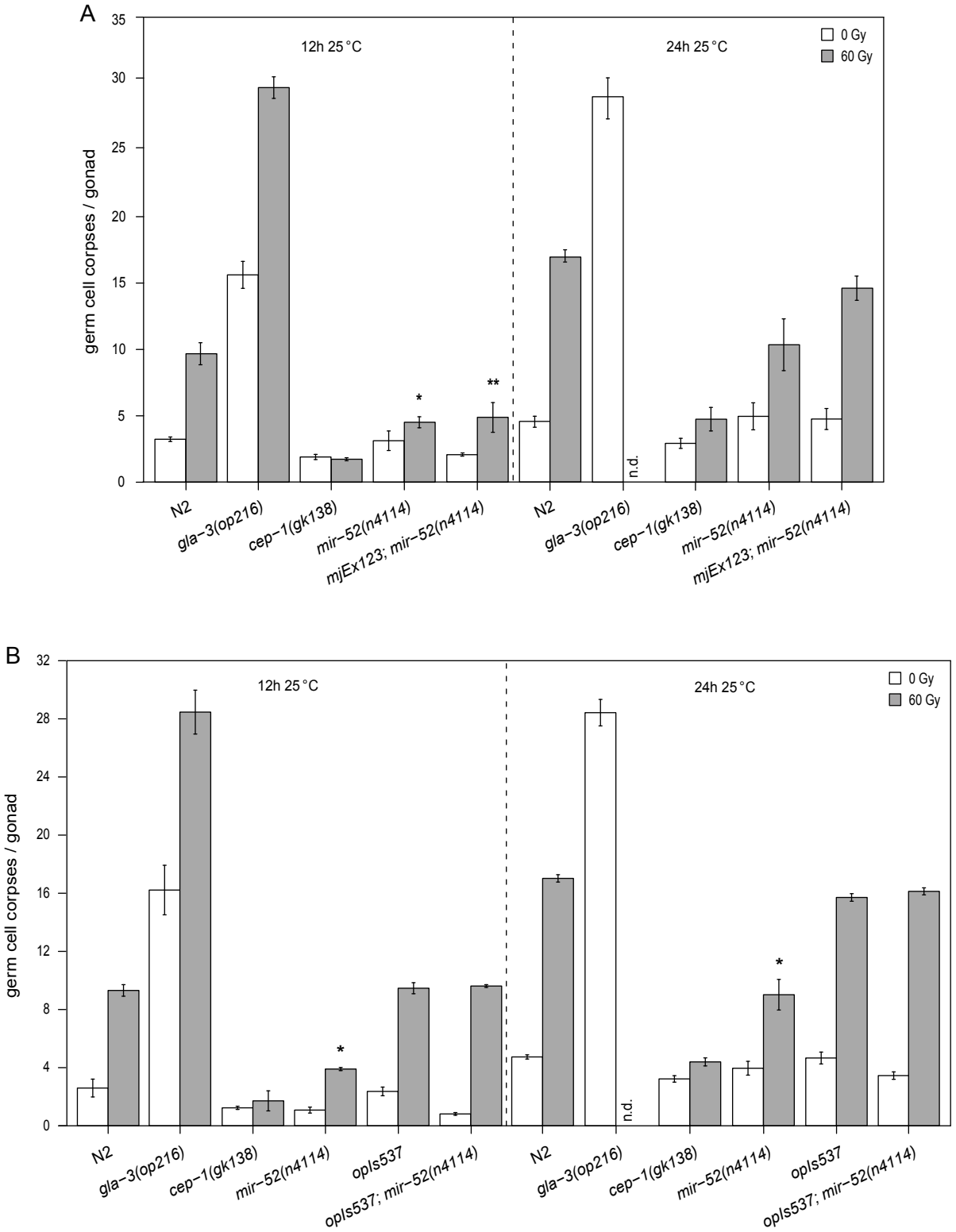

Supplemental Figure 2.4, *Kamkina et. al.*

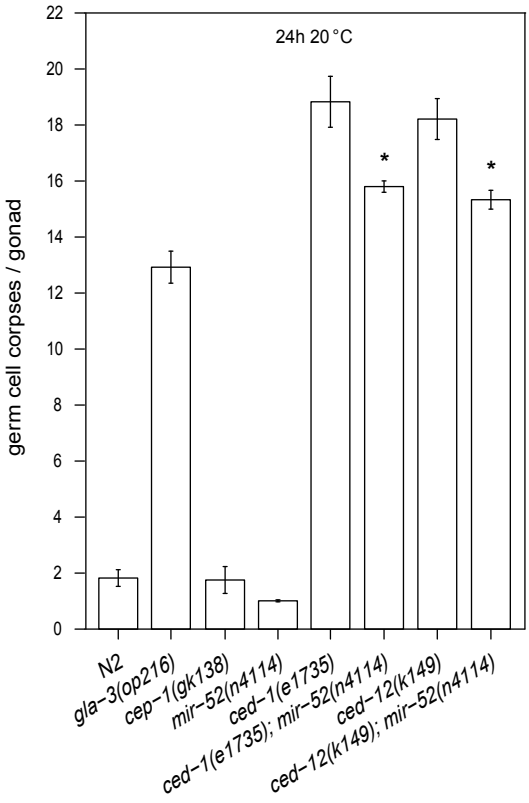

# • Appendix 1 •

# *mir-242(n4605)* and *mir-249(n4983)* influence germline apoptosis in *C. elegans*

## A1.1 Additional miRNA mutants that affect germline apoptosis in *C. elegans*

In the screen of 55 miRNA mutants (Chapter 2), I have also observed the differences in germline apoptosis of *mir-242(n4605)* and *mir-249(n4983)* worms compared to the wild type (Table 2.1, Appendix Fig. 1.1). Thus, I have decided to examine these miRNAs further.

### A1.1.1 *mir-242(n4605)* enhances physiological germline apoptosis

The *mir-242(n4605)* mutants show increased number of germ cell corpses at the physiological conditions (Appendix Fig. 1.1). This apoptotic phenotype was also confirmed in the time-course experiment (Appendix Fig. 1.1B). *n4605* allele is 949 bp deletion which removes complete sequence of *mir-242* itself and the last exon of *nhr-78* (Appendix Fig. 1.2). Thus, I have examined the contribution of *nhr-78* to the apoptotic phenotype observed in *mir-242(n4605)* mutants. Upon *nhr-78 (RNAi),* increased levels of the physiological germline apoptosis were detected (Appendix Fig. 1.3A). The apoptotic phenotype of *nhr-78 (RNAi)* was also confirmed in the backcrossed *nhr-78(gk827629)* mutant (Appendix Fig. 1.3B). Like in *mir-242(n4605)* deletion mutant, levels of the DNA damage-induced germ cell death were not changed in *nhr-78(gk827629)* worms (Appendix Fig. 1.3B). Given the similarity of the apoptotic phenotypes observed in *mir-242(n4605)* and *nhr-78(gk827629)* mutants, *mir-242* was not analyzed further. *nhr-78*, however, might be an interesting candidate for future investigations.

### A1.1.2 *mir-249* suppresses DNA damage-induced germ cell death

*mir-249* is another miRNA, perturbation of which mostly affects DNA damage-induced germline apoptosis (Appendix Fig. 1.1). *n4983* allele is a 735 bp deletion, which removes complete sequence coding for the mature *mir-249* (Appendix Fig. 1.2). The increased levels of germ cell death following IR were observed in young and older *mir-249(n4983)* worms, although the phenotype was rather weak (Appendix Fig. 1.1B). Interestingly, I have also observed higher number of germ cell corpses in older *mir-249(n4983)* animals at the physiological conditions (Appendix Fig. 1.1B). Probably, weak perturbations of the physiological germline apoptosis in *mir-249(n4983)* mutants are amplified with the age of the worm and become even more obvious upon extensive DNA damage. To test whether the increased number of germ cell corpses in *mir-249(n4983)* worms following IR was due to the defects in cell death or engulfment, I crossed *mir-249(n4983)* with mutants impaired in one of the two parallel engulfment pathways, i.e. *ced-1(e1735)* and *ced-12(k149)* (Zhou et al., 2001; Gumienny et al., 2001). No change in somatic

cell corpse clearance was observed in *ced-1(e1735); mir-249(n4983)* and *ced-12(k149); mir-249(n4983)* double mutants (Appendix Fig. 1.4B). By contrast, germline apoptosis was slightly increased in both double mutants following IR compared to the corresponding *ced-1(e1735)* and *ced-12(k149)* single mutants (Appendix Fig. 1.4A). Thus, I conclude that *mir-249* suppresses physiological and DNA damage-induced germline apoptosis in engulfment-independent manner. Because apoptotic phenotype of *mir-249(n4983)* mutant is rather weak, I have decided to follow only *mir-52*, which was identified as a strong enhancer of DNA damage-induced germline apoptosis (Chapter 2).

## A1.2. Figure Legends

**Appendix Fig. 1.1 Apoptotic defects in *mir-242(n4605)* and *mir-249(n4983)* worms.** A. Germline apoptosis is upregulated in *mir-242(n4605)* and *mir-249(n4983)* animals at the physiological conditions or following IR, respectively. Young adults were irradiated with 60 Gy and analyzed 24h later (n=30 animals/genotype). B. Time-course analysis of germline apoptosis in *mir-242(n4605)* and *mir-249(n4983)* mutants. Young adults were irradiated, and analyzed at the indicated time points post L4/YA molt (n=30 animals/genotype). Solid lines represent the data of the untreated worms; dashed lines represent the data of the irradiated worms. Data shown are average number of apoptotic cells ± standard deviation (SD) for three replicates. *P*-values in (A) were generated using Benjamini-Hochberg corrected paired *t*-test, where * represents the *p*-value < 0.05, **- the *p*-value < 0.01, and ****- the *p*-value < 0.0001.

**Appendix Fig. 1.2 *mir-242* and *mir-249* are located on the chromosomes IV and X, respectively.**

**Appendix Fig. 1.3 *nhr-78* impairs physiological germline apoptosis.** A. Upon *nhr-78 (RNAi)*, increased number of germ cell corpses is observed at the physiological conditions. "*nhr-78 (RNAi) 1"* stands for the RNAi clone from Ahringer library (Kamath and Ahringer, 2003), *"nhr-78 (RNAi) 2"* stands for the RNAi clone from ORFeome library (Reboul et al., 2003). Synchronized L1 worms were fed with ds RNA-expressing bacteria until 24h post L4/YA molt as described previously (Kamath et al., 2000), and analyzed for the changes in germ cell death. B. Physiological germline apoptosis is also upregulated in *nhr-78(gk827926)* mutant. Data shown are average number of apoptotic cells ± standard deviation (SD) for three replicates. *P*-values were generated using Benjamini-Hochberg corrected paired *t*-test, where * represents the *p*-value < 0.05, **- the *p*-value < 0.01, and ***- the *p*-value < 0.001.

**Appendix Fig. 1.4 Apoptotic cell corpse clearance is not affected in *mir-249(n4983)* mutants.** A. Number of germ cell corpses is increased in both *ced-1(e1735); mir-249(n4983)* and *ced-12(k149); mir-249(n4983)* double mutants following IR. Young adults were irradiated with 60 Gy and analyzed 12h later (n=30 animals/genotype). B. Somatic cell corpse clearance is not affected in *mir-249* mutants. Cell corpses were quantified in the head region of freshly hatched L1 larvae (n=25 animals/genotype). *P*-values in (A) were generated using Benjamini-Hochberg corrected paired *t*-test, where * represents the *p*-value < 0.05.

## A1.3. References

Gumienny, T.L., Brugnera, E., Tosello-Trampont, A.-C., Kinchen, J.M., Haney, L.B., Nishiwaki, K., Walk, S.F., Nemergut, M.E., Macara, I.G., Francis, R., et al. (2001). CED-12/ELMO, a novel member of the CrkII/Dock180/Rac pathway, is required for phagocytosis and cell migration. Cell 107, 27–41.

Kamath, R.S., and Ahringer, J. (2003). Genome-wide RNAi screening in Caenorhabditis elegans. Methods 30, 313–321.

Kamath, R.S., Martinez-Campos, M., Zipperlen, P., Fraser, A.G., and Ahringer, J. (2000). Effectiveness of specific RNA-mediated interference through ingested double-stranded RNA in Caenorhabditis elegans. Genome Biol. 2, research0002.

Reboul, J., Vaglio, P., Rual, J.-F., Lamesch, P., Martinez, M., Armstrong, C.M., Li, S., Jacotot, L., Bertin, N., Janky, R., et al. (2003). C. elegans ORFeome version 1.1: experimental verification of the genome annotation and resource for proteome-scale protein expression. Nat. Genet. 34, 35-41.

Zhou, Z., Hartwieg, E., and Horvitz, H.R. (2001). CED-1 is a transmembrane receptor that mediates cell corpse engulfment in C. elegans. Cell 104, 43–56.

## A1.4 Figures

Appendix Figure 1.1, *Kamkina et. al.*

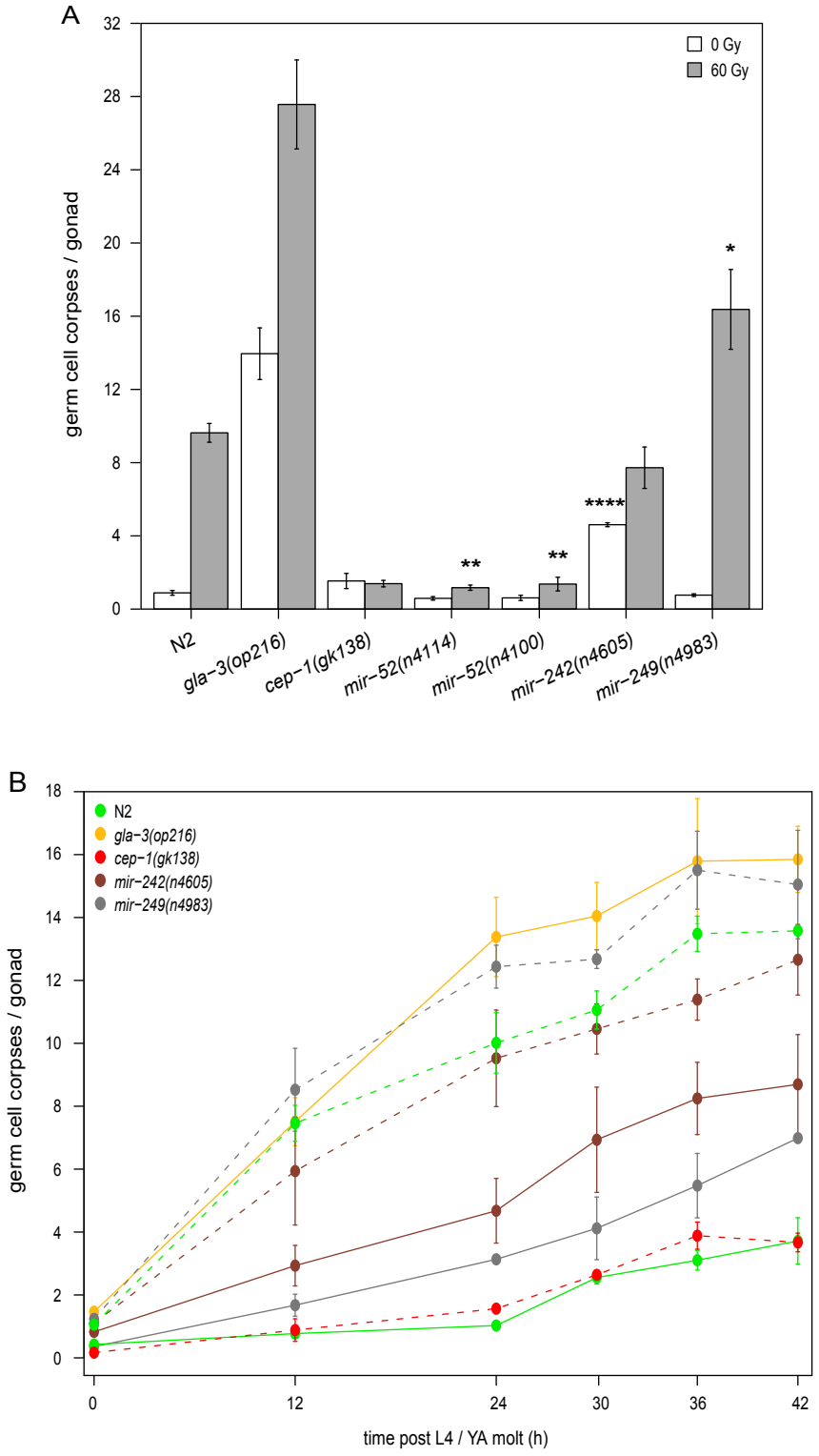

Appendix Figure 1.2, *Kamkina et. al.*

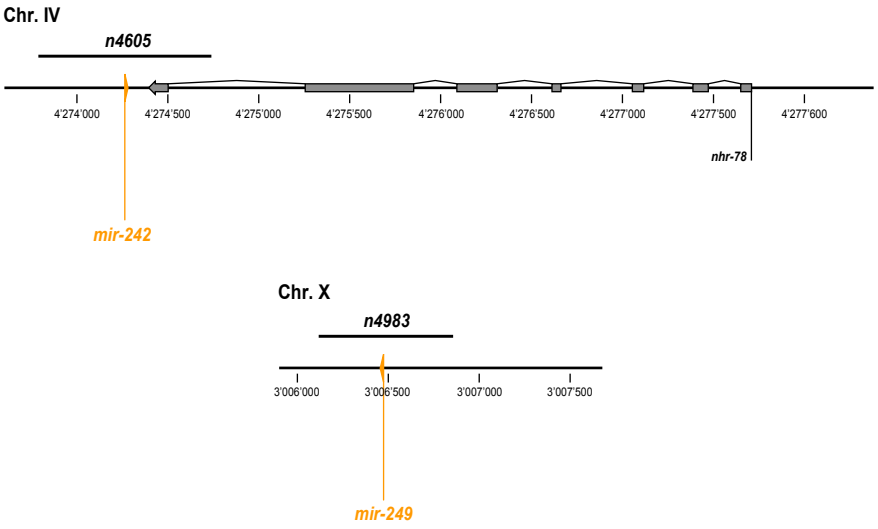

Appendix Figure 1.3, *Kamkina et. al.*

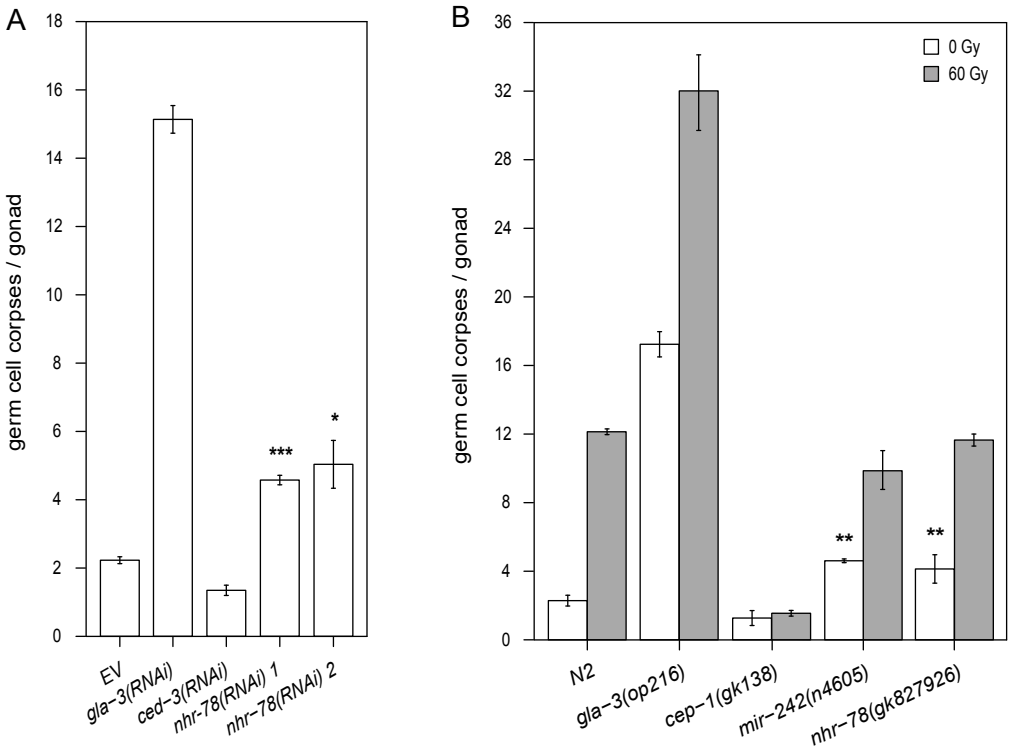

Appendix Figure 1.4, *Kamkina et. al.*

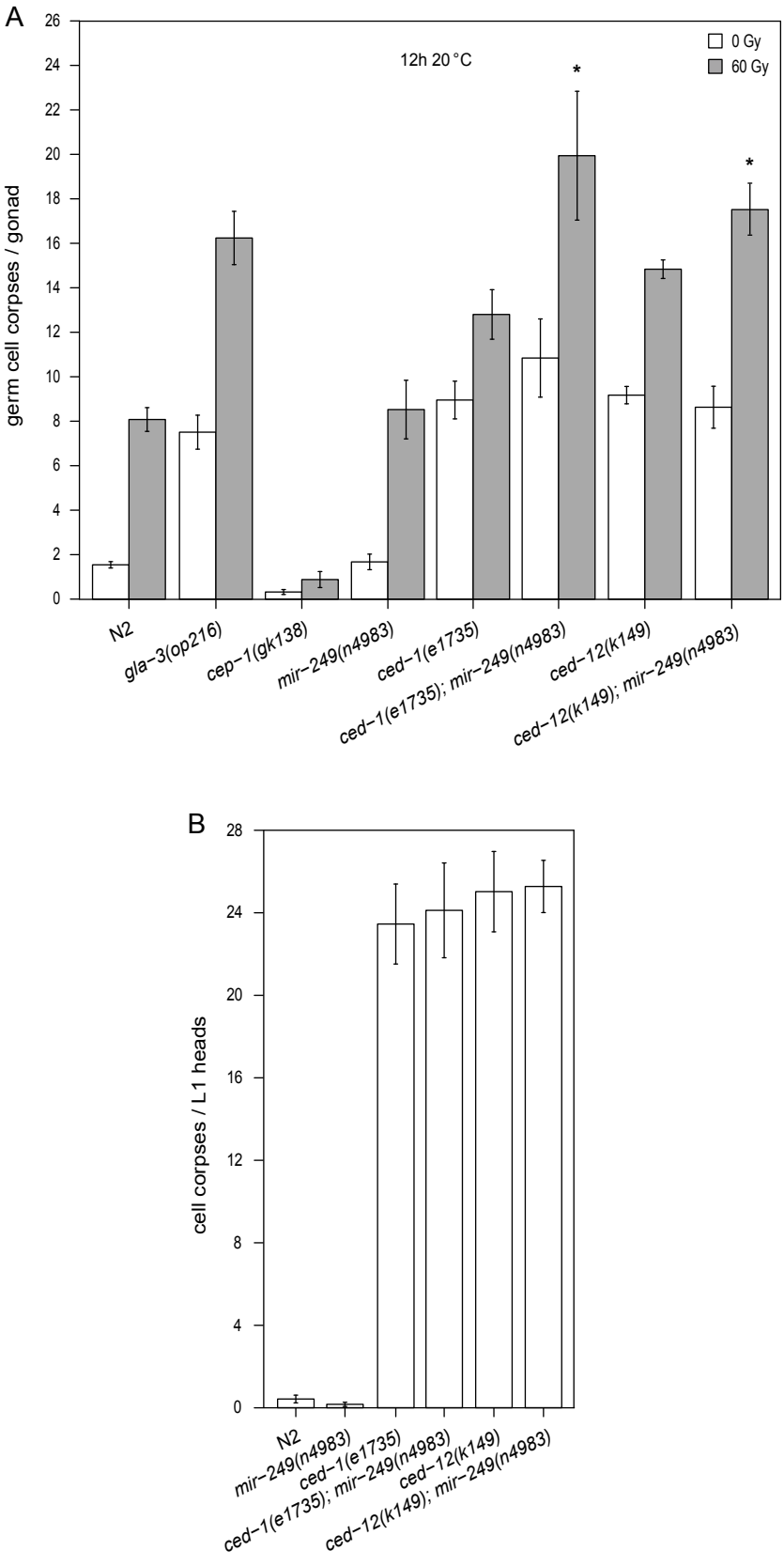

# • Chapter 3 •

# Upstream regulation of CED-9 during physiological germline apoptosis in *C. elegans*

## 3.1 Introduction

In *C. elegans,* the majority of the generated germ cells die during oocyte development, in the absence of any obvious external apoptotic stimulus in a process that has been called "physiological germ cell death". *egl-1(lf)* and *ced-9(1950gf)* mutations, which prevent most of the somatic cell deaths and DNA damage induced germline apoptosis, have little effect on physiological germ cell death (Gumienny et al., 1999). According to the current model, cell survival is largely regulated by the direct interaction of CED-9 with CED-4 at mitochondria, which prevents the auto-catalytic activation of CED-3 (reviewed in Chapter 1). Strikingly, CED-4/CED-9 co-localization at mitochondria was not detected in the germline. Instead, perinuclear accumulation of CED-4 was found in healthy as well as apoptotic germ cells (Pourkarimi et al., 2012). Additionally, a CED-9 protein which is defective in CED-4 binding rescues embryonic lethality of *ced-9(n2161)* mutants (Dreze et al., 2009). Therefore, CED-9 anti-apoptotic function does not exclusively correlate with CED-4 sequestration in the germline, and physiological germline apoptosis is genetically separable from that observed in somatic tissue or in response to DNA damage. In order to investigate additional mechanisms which trigger physiological germline apoptosis upstream of CED-9, I have established two synthetic forward screening strategies that employ tissue-specific apoptotic conditions and *n1653* temperature-sensitive *lf* allele of *ced-9*.

### 3.1.1 *n1653* temperature-sensitive *ced-9 loss-of-function* allele

The *ced-9(lf)* mutants are embryonic lethal due to excessive cell death (Hengartner et al., 1992). *ced-9(lf)* mutants derived from *ced-9(lf)/+* heterozygous mothers hatch and grow to normal sizes, but lay very few eggs, which barely hatch or are arrested at the L1 stage (Hengartner et al., 1992). Thus, genetic analysis using strong *lf* mutants of *ced-9* is relatively difficult. *n1653* is a hypomorphic temperature-sensitive allele originally isolated in a screen for mutants with absent or defective HSNs (Desai and Horvitz, 1989). The *n1653* point mutation changes the tyrosine at position 149 in the alpha-helical structure α4, near the beginning of the BH1 domain into an asparagine (Woo et al., 2003). The Y149 residue is crucial for the proper CED-9 tertiary structure formation, and the Y149N (*n1653ts*) mutation disrupts CED-4/CED-9 interaction (Yan et al., 2004; Dreze et al., 2009). *ced-9(n1653ts)* animals show moderately increased levels of apoptosis at lower temperatures and become sterile at 25 ˚C (Hengartner et al., 1992; Eberhard, 2012).

Interestingly, some of the excessive apoptosis in *ced-9(n1653ts)* animals is dependent on *cep-1* (Eberhard, 2012). Therefore, *n1653ts* might be an attractive allele to study additional regulatory aspects of germline apoptosis.

### 3.1.2 Experimental design of the forward genetic screens

A *n1653* temperature-sensitive suppressor screen has been previously performed in the lab (M. O. Hengartner unpublished data). However, only *lf* mutations in *ced-4* and *ced-3* were isolated. We hypothesized that the strong requirement of CED-9 for somatic tissue survival overshadows its function in the germline. I thus decided to uncouple apoptotic conditions in somatic tissue and germline of *ced-9(n1653ts)* mutants, such that excessive cell death only happens in the germline. In this screen, restored animal fertility at the restrictive temperature is utilized as the selection marker. Two different experimental designs were developed for the screen: first set-up is based on the tissue-specific *ced-3 (RNAi)*; second set-up implies germline-specific expression of *ced-3* translational reporter.

*mut-7(pk204)* animals are RNAi-defective in the germline (Ketting et al., 1999). In *mut-7(pk204) ced-9(n1653ts)* double mutants, suppression of apoptosis by *ced-3(RNAi)* is restricted to somatic tissue. In the germline, however, the apoptotic machinery remains active causing animal sterility at the restrictive temperature. Following ethyl methane sulfonate (EMS) exposure, these worms should become fertile again only in the presence of additional, apoptosis-suppressive mutation (Fig. 3.1A).

Another strategy to overcome strong somatic requirement of CED-9 implies the generation of the transgenic line carrying translational reporter of *ced-3* driven by the germline-specific promoter *pie-1* (*Ppie-1::ced-3::gfp::ced-3 3' UTR*) in *ced-9(n1653ts); ced-3(n717)* background. Here, *ced-3(lf)* compensates for the loss of CED-9 in somatic tissue, whereas in the germline, wild-type copy of CED-3 causes excessive cell death at the restrictive temperature. After EMS treatment, F2 animal carrying a mutation which suppresses germ cell death should produce viable progeny (Fig. 3.1B).

## 3.2 Results

### 3.2.1 Validation of the screening strategy which utilizes tissue-specific *ced-3(RNAi)*

Several aspects of the experimental design using *mut-7(pk204) ced-9(n1653ts)* double mutant and *ced-3(RNAi)* have to be considered. I have examined optimal restrictive temperature conditions for *mut-7(pk204) ced-9(n1653ts)* animals. According to the published data, *mut-7(pk204)* worms are also temperature-sensitive and become sterile at 23 ˚C due to defects in sperm (Ketting et al., 1999). However, the *mut-7(pk204)* strain available in our lab becomes sterile only at 25 ˚C (Table 3.1). Additionally, viability of the wild-type worms was also partially compromised at 25 ˚C compared to that at the standard conditions (20 ˚C, Table 3.1). Therefore, I have analyzed fertility at a slightly lower temperature, i.e. 24 ˚C (Table 3.1). The wild-type animals had similar offspring number at 20 ˚C and 24 ˚C. Next, I checked whether *ced-9(n1653ts)* mutants remain sterile at 24 ˚C. Although the fertility of *ced-9(n1653ts)* animals was slightly higher at 24 ˚C, total offspring number was by far much lower than that in the wildtype. *mut-7(pk204)* worms also had increased numbers of the offspring at 24 ˚C. By contrast, *mut-7(pk204) ced-9(n1653ts)* double mutants remained sterile at 24 ˚C. Of note, the temperature sensitivity of *mut-7(pk204) ced-9(n1653ts)* double mutant at 24 ˚C was stronger than that observed in *ced-9(n1653)* animals. The survival of the worms was comparable, independently of the *E. coli* strains used at the respective temperatures (Table 3.1). Thus, 24 ˚C is the optimal restrictive temperature for the screen.

*par-1(RNAi)* is an established essay for the RNAi efficacy in the germline (Tijsterman et al., 2002). *ced-9(n1653ts)* and wild-type worms were less viable upon *par-1(RNAi)* at 20 °C and 24 °C (Table 3.1). As expected, *mut-7(pk204)* worms and *mut-7(pk204) ced-9(n1653ts)* double mutants were resistant to *par-1(RNAi)* (Table 3.1). Thus, *par-1(RNAi)* can be used as a control to exclude mutations which would restore RNAi sensitivity in the germline after EMS exposure.

The efficiency of *ced-3(RNAi)* is another factor which determines the success of the screening strategy using *mut-7(pk204) ced-9(n1653ts)* worms. I have examined whether *ced-9(n1653ts)* mutants become fertile upon *ced-3(RNAi)* at 24 ˚C (Table 3.1). Indeed, downregulation of *ced-3* reduced embryonic lethality of *ced-9(n1653ts)* worms. *ced-3(RNAi)* in *mut-7(pk204)* worms and *mut-7(pk204) ced-9(n1653ts)* double mutants was restricted to somatic tissue (Table 3.1). It

should be mentioned however, that bacterial contamination of the RNAi plates could strongly compromise the screen by diluting the effect of *ced-3* downregulation.

### 3.2.2 Development of the screening strategy using *Ppie-1::ced-3::gfp::ced-3 3' UTR* transgene

It took quite an effort to generate an integrated transgenic line which carries a translational reporter of *ced-3*. The seven bombardments and 308 microinjections of the corresponding vectors yielded 17 lines, most of which had *Ppie-1::ced-3::gfp::ced-3 3' UTR* transgene as an extrachromosomal array (Fig. 3.2). The integrated lines were either silenced or had incorrect fragment orientation. Ultimately, two integrated lines could be generated, one of which was GFP-positive (*opIs535*). To my knowledge, it is the only known single-copy caspase transgenic line with germline-specific expression in *C. elegans*.

In *ced-9(n1653ts); ced-3(n717)* double mutants carrying this *ced-3* reporter, the number of extra surviving cells in pharynx was comparable to that in *ced-3(n717)* worms at 20 ˚C and 24 ˚C (M. O. Hengartner personal communication, data not shown), suggesting that, as expected, the transgene is not expressed in somatic tissues. Furthermore, GFP fluorescence was observed only in adult *ced-9(n1653ts); ced-3(n717)* germlines (Fig. 3.3). Interestingly, CED-3::GFP showed a patchy perinuclear localization pattern in mitotic and meiotic germ cells (Fig. 3.3). Additionally, CED-3 was strongly enriched in the nuclei of the maturing oocytes (Fig. 3.3).

Next, I analyzed the temperature sensitivity of *ced-9(n1653ts); ced-3(n717)* double mutants which carry the *opIs535* transgene. *ced-3(n717)* and *ced-9(n1653ts); ced-3(n717)* animals were fertile at the restrictive temperature (Table 3.2). By contrast, *opIs535; ced-9(n1653ts); ced-3(n717)* worms were sterile at 24 ˚C (Table 3.2). Taken together, my data suggests that a screening strategy which implements germline-specific expression of *ced-3::gfp* transgene would be a robust approach to study regulation of physiological germline apoptosis. Therefore, I have decided to use this experimental set-up for the screen.

### 3.2.3 Forward genetic screen using *Ppie-1::ced-3::gfp::ced-3 3' UTR* transgene

I have performed the screen twice for approximately 44'000 (24'000 and 20'000) haploid genomes using *opIs535 [Ppie-1::ced-3::gfp::ced-3 3' UTR]; ced-9(n1653ts); ced-3(n717)* strain. As was described above, these worms should become fertile again at the restrictive temperature

in the presence of additional apoptosis suppressive mutations. The screen was performed according to the protocol described previously with minimal adjustments (Fig. 3.4, Brenner, 1974; Kutscher and Shaham, 2014). In short, EMS-exposed young adults (P0 generation) were allowed to recover for four hours on OP50 plates at 15 ˚C. The P0 worms were then transferred every eight hours to the fresh OP50 plates for the next two days and kept at 20 ˚C. The screening plates were moved to the restrictive temperature (24 ˚C) once worms in the F2 generation reached the L4 stage, and examined for restored fertility ten days later.

Surprisingly, no positive identifications were obtained after EMS treatment. The wild-type worms kept at the same restrictive temperature were fertile. I also noticed that some F2 worms were uncoordinated (Unc) or had protruding vulva (Pvl) confirming that EMS treatment worked.

### 3.2.4 Forward genetic screen using tissue-specific *ced-3(RNAi)*

In parallel, I also performed a screen of ~10’000 genomes using *mut-7(pk204) ced-9(n1653ts)* double mutant and *ced-3(RNAi)*. The screen was performed as described above, except that *ced-3(RNAi)* plates were continuously used (Fig. 3.4). Again, although the mutagenesis was also successful in this case, I did not find any plates with fertile animals at 24 ˚C.

### 3.3 Discussion

Mutations in *ced-4* and *ced-3* have previously been isolated in EMS suppression screens of *ced-9(n1653ts)* animals (M. O. Hengartner unpublished data). Therefore, I certainly expected to recover such mutations in my experimental set-ups too. Unfortunately, this was not the case, independently of the methodology I have used. Given the presence of Unc and Pvl worms in the F2 generation, it is strikingly unusual that no apoptosis-specific perturbations were obtained in these screens. There is no obvious explanation for this finding.

Besides *ced-4* and *ced-3,* additional candidates could have been expected to be identified in my screens. *ced-9* expression levels might be important to establish the germ cell sensitivity to apoptosis. Indeed, EGL-38 and PAX-2, *C. elegans* homologs of the mammalian Pax2/5/8 transcription factors (TFs), promote germ cell survival by directly activating the transcription of *ced-9* (Wang et al., 2004; Park et al., 2006). Conversely, LIN-35, the *C. elegans* retinoblastoma susceptibility protein (Rb) promotes physiological germline apoptosis by repressing *ced-9* expression (Schertel and Conradt, 2007). Moreover, in *lin-45(lf); ced-9(n1653ts)* double mutants, physiological germline apoptosis is reduced at the restrictive temperature. Thus, it is conceivable that additional TFs or RBPs might regulate expression of *ced-9* during physiological germline apoptosis.

*egl-1(lf)* mutation suppresses physiological germline apoptosis in *ced-9(n1653ts)* worms, but not in other *ced-9(lf)* mutants (Gumienny et al., 1999; Eberhard, 2012). I assume that in strong *ced-9(lf)* mutants, CED-9 cannot bind to CED-4 independently of its interaction with EGL-1. In *ced-9(n1653ts)* worms, however, weak interaction between CED-9 and CED-4 might be sufficient to prevent germ cell death in *egl-1(lf)* mutants. Therefore, I also expected to identify additional mutations which enhance CED-4/CED-9 interaction in my screens.

The *C. elegans* germline is a highly proliferative tissue. In older women, accumulation of meiotic errors leads to impaired chromosome segregation in maturing oocytes with subsequent maternal infertility or chromosomal abnormalities in offspring (Djahanbakhch et al., 2007). In *C. elegans*, the unsynapsed chromosomes or mistakes in DNA repair trigger excessive germline apoptosis (Boulton et al., 2004; Bhalla and Dernburg, 2005). Germ cells that undergo apoptosis under the physiological conditions might be also genetically compromised due to their high proliferative rate. Indeed, several genome integrity checkpoint genes are involved in the regulation of DNA damage-induced germline apoptosis (reviewed in 1.3.3.1). However, germ cell specification for

apoptosis might also be a result of pleiotropic germ cell defects, because *ced-9(1950gf)* and *egl-1(lf)* mutations, which prevent germline apoptosis in response to DNA damage, do not reduce the quality of the maturing oocytes under the physiological conditions (Andux and Ellis, 2008).

Due to the lack of germ cell apoptosis, *ced-4(lf)* and *ced-3(lf)* mutants have increased number of total germ cells, which is however accompanied by a reduction in size and quality of oocytes resulting in a higher incidence of dead eggs compared to wild-type worms (Andux and Ellis, 2008). I suspect that a certain nutrients threshold might be required to keep oocytes alive and generate healthy offspring. Hence, germline apoptosis might be used to reduce nutrients competition between supernumerary germ cells (Andux and Ellis, 2008). The insulin signaling pathway might be a good candidate to monitor nutrient availability in the germline. In fact, insulin-like receptor DAF-2 was shown to promote DNA damage-induced apoptosis independently of its function in dauer formation through Ras/MAPK signaling (Perrin et al., 2013).

Importantly, genes which regulate germline apoptosis upstream of CED-9 may also play a role in animal development or contribute to oocyte fertilization. Thus, their mutation would promote embryonic survival or increase oocyte fertilization rates. Lastly, false positives, for example mutations that silence transgene expression in the germline or restore RNAi sensitivity in the germline should also have been picked up in the screens.

I am convinced that further variation on the experimental conditions would optimize the screening strategies described above for their successful implementation in the analysis of CED-9 upstream regulation during physiological germline apoptosis in *C. elegans*.

### 3.4 Figure Legends

**Fig. 3.1 Overview of the screening strategies which imply different apoptotic conditions in somatic tissue and germ line.** A. In *mut-7(pk204) ced-9(n1653ts)* animals, *ced-3(RNAi)* reduces somatic cell death. In the germ line, by contrast, the apoptotic machinery remains active because of the *mut-7* mutation and causes animal sterility at the restrictive temperature. Following EMS exposure, F2 animals carrying a mutation which reduces germ cell death become fertile again. B. In *ced-9(n1653ts); ced-3(n717)* double mutants, somatic cell death is prevented by *ced-3(lf)* allele. In the germline, CED-3 expression from the *Ppie-1::ced-3::gfp::ced-3 3' UTR* transgene allows excessive apoptosis. After EMS, a homozygous mutation which suppresses germ cell death restores animal fertility at the restrictive temperature.

**Fig. 3.2 Structure of *opIs535 [Ppie-1::ced-3::gfp::ced-3 3' UTR]* transgene.** The depicted fragment was inserted either in pCG150 vector used for bombardment or in pCFJ150 vector used for MosSCI microinjection.

**Fig. 3.3 DIC and fluorescence photomicrographs of *ced-9(n1653ts); ced-3(n717)* animals which carry *opIs535 [Ppie-1::ced-3::gfp::ced-3 3' UTR]* transgene.** Adult worms, L3 larva and 44-100 cell embryos are represented. Scale bar - 10µm.

**Fig. 3.4 Workflow of the EMS screens.** EMS-exposed young adults (P0 generation) were allowed to recover for 4h on OP50 plates at 15 ˚C. The P0 worms were then transferred every 8h to the fresh OP50 plates (d=150mm) for the next two days and kept at 20 ˚C. Plates were moved to the restrictive temperature (24 ˚C) once worms in the F2 generation reached the L4 stage. Animals fertility was examined after ten days. For *mut-7(pk204) ced-9(n1653ts)* double mutants, *ced-3(RNAi)* plates (d=150mm) were used instead.

**Table 3.1 Temperature optimization for the screening strategy which utilizes tissue-specific *ced-3(RNAi)*.** Ten L4 worms were transferred to the corresponding RNAi or OP50 NGM plates, grown at the represented temperatures and number of worms per plate was quantified ten days later. *unc-22(RNAi)* was used as positive control. "EV" stands for empty L4440 vector.

**Table 3.2 Temperature optimization for the screening strategy using germline-specific expression of a *ced-3::gfp* transgene.** Ten L4 worms were transferred to an OP50 NGM plate, grown at the represented temperatures and the number of worms per plate was quantified ten days later.

### 3.5 References

Andux, S., and Ellis, R.E. (2008). Apoptosis maintains oocyte quality in aging Caenorhabditis elegans females. PLoS Genet. 4, e1000295.

Bhalla, N., and Dernburg, A.F. (2005). A conserved checkpoint monitors meiotic chromosome synapsis in Caenorhabditis elegans. Science 310, 1683–1686.

Boulton, S.J., Martin, J.S., Polanowska, J., Hill, D.E., Gartner, A., and Vidal, M. (2004). BRCA1/BARD1 orthologs required for DNA Repair in Caenorhabditis elegans. Curr. Biol. 14, 33–39.

Brenner, S. (1974). The Genetics of Caenorhabditis Elegans. Genetics 77, 71–94.

Desai, C., and Horvitz, H.R. (1989). Caenorhabditis elegans mutants defective in the functioning of the motor neurons responsible for egg laying. Genet. 121,703–721.

Djahanbakhch, O., Ezzati, M., and Zosmer, A. (2007). Reproductive ageing in women. J. Pathol. 211, 219–231.

Dreze, M., Charloteaux, B., Milstein, S., Vidalain, P.-O., Yildirim, M.A., Zhong, Q., Svrzikapa, N., Romero, V., Laloux, G., Brasseur, R., et al. (2009). “Edgetic” perturbation of a C. elegans BCL2 ortholog. Nat. Methods 6, 843–849.

Eberhard, R. (2012). Modulators of DNA damage-induced cell death in Caenorhabditis elegans. University of Zurich.

Gumienny, T.L., Lambie, E., Hartwieg, E., Horvitz, H.R., and Hengartner, M.O. (1999). Genetic control of programmed cell death in the Caenorhabditis elegans hermaphrodite germline. Development 126, 1011–1022.

Hengartner, M.O., Ellis, R., and Horvitz, R. (1992). Caenorhabditis elegans gene ced-9 protects cells from programmed cell death. Nature 356, 494–499.

Ketting, R.F., Haverkamp, T.H.A., van Luenen, H.G.A.M., and Plasterk, R.H.A. (1999). mut-7 of C. elegans, required for transposon silencing and RNA interference, is a homolog of Werner Syndrome Helicase and RNaseD. Cell 99, 133–141.

Kutscher, L.M., and Shaham, S. (2014). Forward and reverse mutagenesis in C. elegans. WormBook Online Rev. C Elegans Biol. 1–26.

Park, D., Jia, H., Rajakumar, V., and Chamberlin, H.M. (2006). Pax2/5/8 proteins promote cell survival in C. elegans. Development 133, 4193–4202.

Perrin, A.J., Gunda, M., Yu, B., Yen, K., Ito, S., Forster, S., Tissenbaum, H.A., and Derry, W.B. (2013). Noncanonical control of C. elegans germline apoptosis by the insulin/IGF-1 and Ras/MAPK signaling pathways. Cell Death Differ. 20, 97–107.

Pourkarimi, E., Greiss, S., and Gartner, A. (2012). Evidence that CED-9/Bcl2 and CED-4/Apaf-1 localization is not consistent with the current model for C. elegans apoptosis induction. Cell Death Differ. 19, 406–415.

Schertel, C., and Conradt, B. (2007). C. elegans orthologs of components of the RB tumor suppressor complex have distinct pro-apoptotic functions. Development 134, 3691–3701.

Tijsterman, M., Okihara, K.L., Thijssen, K., and Plasterk, R.H.A. (2002). PPW-1, a PAZ/PIWI Protein required for efficient germline RNAi, is defective in a natural isolate of C. elegans. Curr. Biol. 12, 1535–1540.

Woo, J.-S., Jung, J.-S., Ha, N.-C., Shin, J., Kim, K.-H., Lee, W., and Oh, B.-H. (2003). Unique structural features of a BCL-2 family protein CED-9 and biophysical characterization of CED-9/EGL-1 interactions. Cell Death Differ. 10, 1310–1319.

Yan, N., Gu, L., Kokel, D., Chai, J., Li, W., Han, A., Chen, L., Xue, D., and Shi, Y. (2004). Structural, Biochemical, and Functional Analyses of CED-9 Recognition by the Proapoptotic Proteins EGL-1 and CED-4. Mol. Cell 15, 999–1006.

## 3.6 Figures and Tables

Figure 3.1

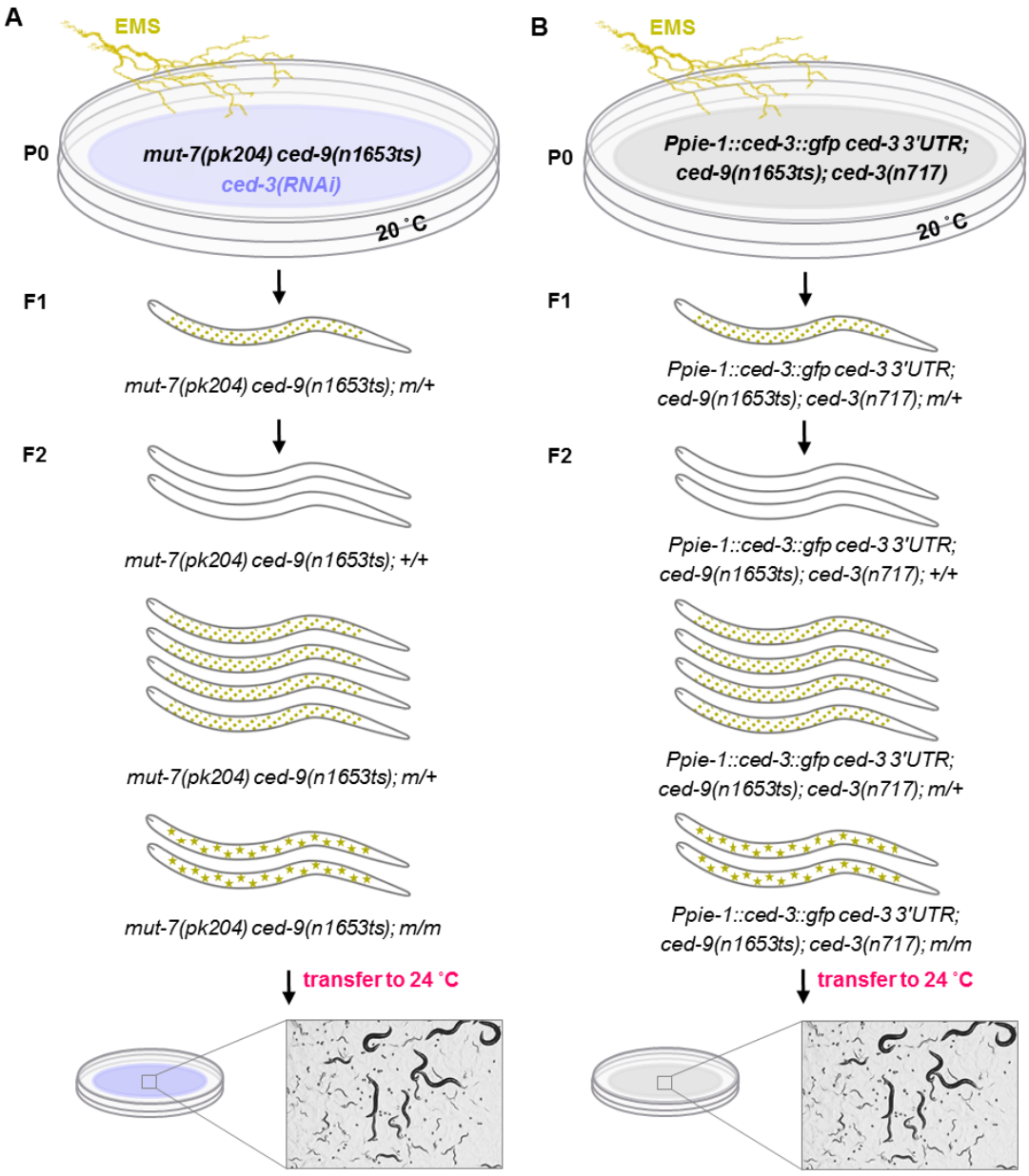

Figure 3.2

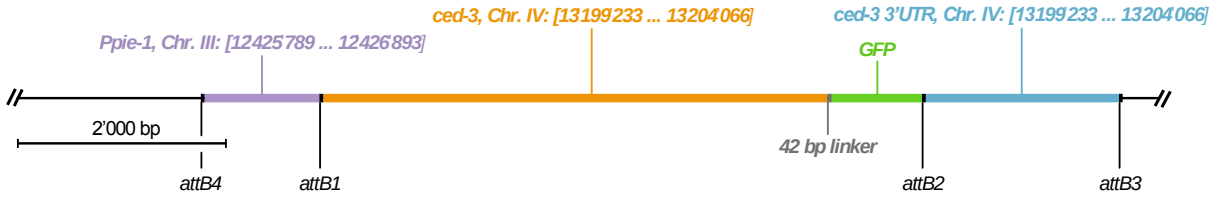
ced-3, Chr. IV: [13199233 ... 13204066]
ced-3 3'UTR, Chr. IV: [13199233 ... 13204066]
Ppie-1, Chr. III: [12425789 ... 12426893]
GFP
2'000 bp
42 bp linker
attB4
attB1
attB2
attB3

Figure 3.3

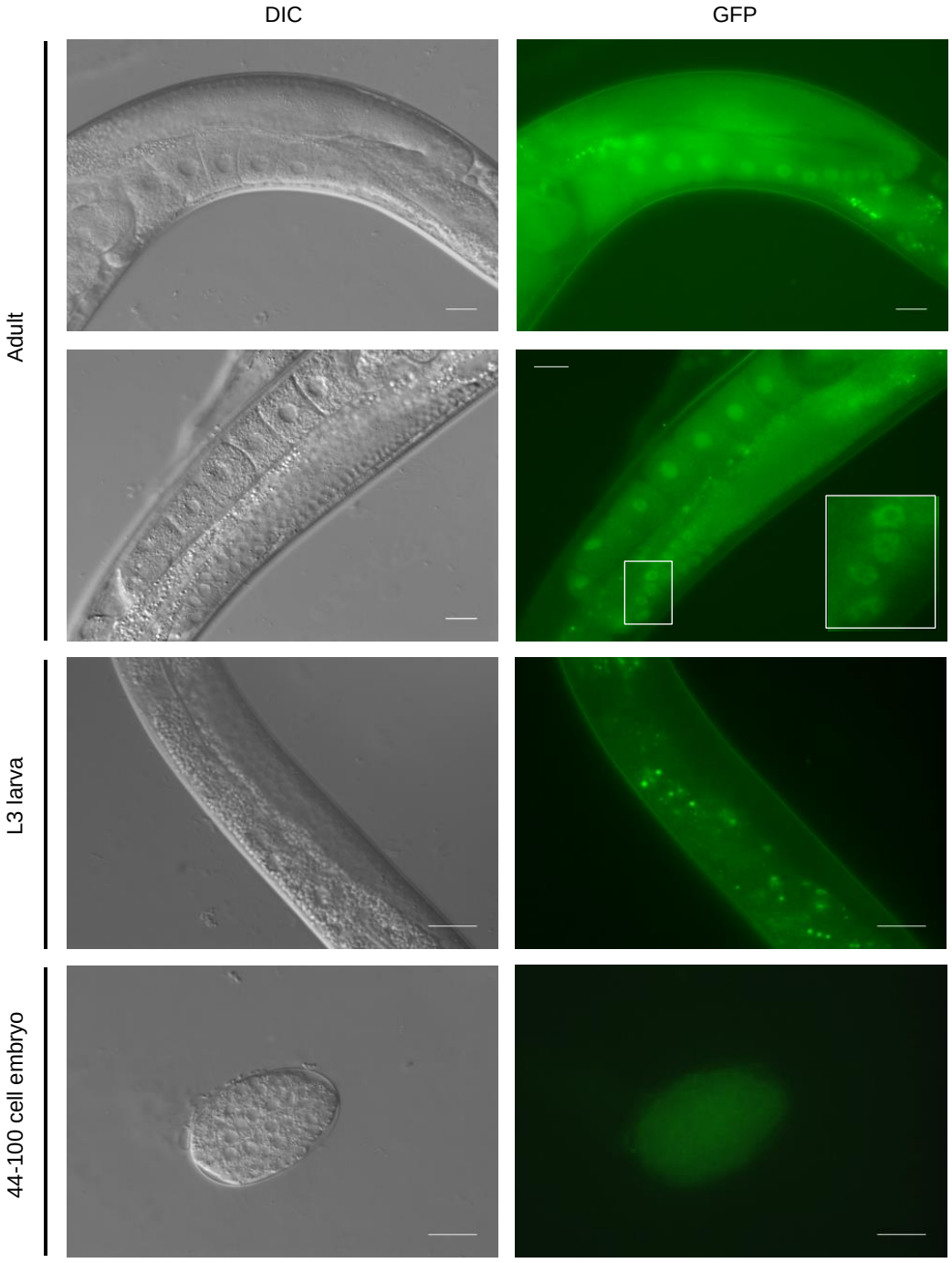

Figure 3.4

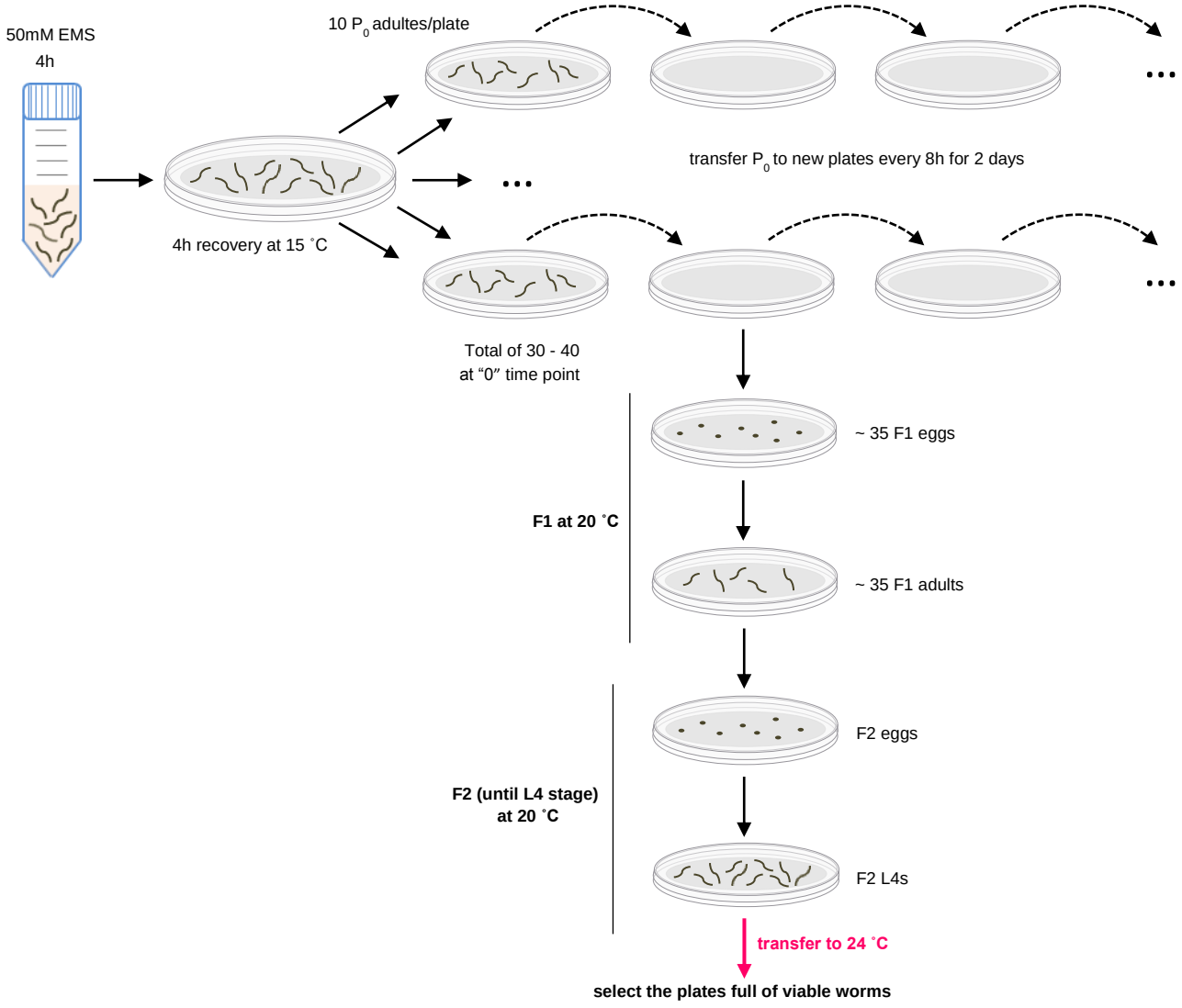
50mM EMS
4h
10 P0 adultes/plate
4h recovery at 15 ˚C
transfer P0 to new plates every 8h for 2 days
Total of 30 - 40
at "0" time point
~ 35 F1 eggs
F1 at 20 ˚C
~ 35 F1 adults
F2 eggs
F2 (until L4 stage)
at 20 ˚C
F2 L4s
transfer to 24 ˚C
select the plates full of viable worms

Table 3.1

| Treatment | t ˚C | # of worms | | | |
|---|---|---|---|---|---|
| | | **N2** | ***ced-9(n1653ts)*** | ***mut-7(pk204)*** | ***mut-7(pk204) ced-9(n1653ts)*** |
| OP50 | 20 | ~ 4'880 | ~ 2'020 | ~ 3'040 | ~ 1'340 |
| HT115 (DE3): EV | | ~ 4'720 | ~ 2'380 | ~ 2'800 | ~ 1'560 |
| *unc-22(RNAi)* | | ~ 1'200, Unc | ~ 1'960, Unc | ~ 2'000, Unc | ~ 1'250, Unc |
| *par-1(RNAi)* | | 88 | 30 | ~ 2'440 | ~ 1'160 |
| *ced-3(RNAi)* | | ~ 4'800 | ~ 3'640 | ~ 3'120 | ~ 1'010 |
| OP50 | 24 | ~ 4'000 | 23 | ~ 320 | 5 |
| HT115 (DE3): EV | | ~4'000 | 13 | ~ 220 | 5 |
| *unc-22(RNAi)* | | ~ 3500, Unc | 12, Unc | ~ 260, Unc | 3, Unc |
| *par-1(RNAi)* | | 16 | 1 | ~ 250 | 4 |
| *ced-3(RNAi)* | | ~ 4'000 | ~ 880 | ~ 280 | 3 |
| OP50 | 25 | ~ 1'600 | 1 | 0 | 0 |
| HT115 (DE3): EV | | ~ 1'000 | 0 | 0 | 0 |
| *unc-22(RNAi)* | | ~ 1'450, Unc | 0 | 0 | 0 |
| *par-1(RNAi)* | | 0 | 0 | 0 | 0 |
| *ced-3(RNAi)* | | ~ 1'200 | 90 | 0 | 0 |

Table 3.2

| Genotype | t ˚C / # of worms | |
|---|---|---|
| | **20** | **24** |
| N2 | ~ 5'200 | ~ 4'350 |
| *ced-9(n1653ts)* | ~ 2'700 | 18 |
| *ced-3(n717)* | ~ 5'500 | ~ 4'000 |
| *ced-9(n1653ts); ced-3(n717)* | ~ 4'000 | ~ 3'620 |
| *Ppie-1::ced-3::gfp::ced-3 3'UTR; ced-9(n1653ts); ced-3(n717)* | ~ 3'000 | 23 |

# • Appendix 2 •

# Quantitative proteome analysis of natural genetic variation in *C. elegans*

## A2.1 Preface

In this section, I would like to present two side projects which were dealing with the effect of natural variation on gene expression. In the first project, the quantitative proteome and transcriptome comparison of the two highly divergent *C. elegans* wild-type strains, Bristol (N2) and Hawaii (CB4856) was performed. I was responsible for all the work related to proteomics in this manuscript. I have quantified the proteomes of N2 and CB4856 using a mass spectrometric approach called "stable isotope labeling by amino acids in cell culture" (SILAC). Jonas Grossmann performed the correction of the mass spectrometric data to account for arginine-to-proline conversion. Of the total 3'238 quantified proteins, 129 (5.2%) proteins were significantly differentially expressed between the two wild-type strains. The differentially expressed proteins were enriched for the genes that function in insulin-signaling and stress-response pathways. The quantitative transcriptome comparison was performed by Basten Snoek. Of all the genes, 1'532 genes (7.4%) were differentially expressed at the mRNA level. The differentially expressed genes were also strongly enriched in expression quantitative trait loci (eQTLs) associated with aging. Additionally, we observed that the protein abundance of the two wild-type strains correlated more strongly than the protein abundance *vs* transcript abundance within each wild type. Our results suggest that at least a subset of our differentially expressed genes might contribute to the longevity differences of N2 and CB4856. This study was recently published in the MCP journal (*Kamkina et al.,* Molecular and Cellular Proteomics 2016 15: 1670-1680) under the title "Natural genetic variation differentially affects the proteome and transcriptome in *C. elegans*".

In the second project, the impact of natural genetic variation on cancer progression was analyzed using recombinant inbred lines (RILs) of N2 and CB4856. In particularly, expression of the 44 genes involved in four cancer signaling pathways (RAS/MAPK, Notch, Wnt signaling and apoptosis) was quantified using another mass spectrometric approach called "selected reaction monitoring" (SRM) and microarrays in four RILs and parental strains. I was heavily involved in the initial phase of the SRM method development. To identify and quantify targeted proteins of interest, I have selected three-to-five signature proteotypic peptides (PTPs) with the best mass spectrometric responses. I have also generated the signature spectral library and identified the elution/retention times of the selected PTPs. Finally, I have developed the offline reversed phase-high pressure liquid chromatography (RP-HPLC) peptide fractionation protocol for total

worm protein extracts. We found that quantified proteins tend to be upregulated in CB4856 and RILs relative to N2. Additionally, we detected a distant protein QTL on the left arm of chromosome II that affected protein abundance of the phosphatidylserine receptor protein PSR-1, and two separate QTLs on chromosome IV that influenced developmental apoptosis and DNA damage-induced germ cell death. This study was also recently published in the PLOS ONE journal (*Singh et al.,* PLOS ONE 11: e0149418) under the title "Natural genetic variation influences protein abundances in *C. elegans* developmental signalling pathways". Both projects were supported by European Community Health Seventh Framework Programme FP7/2007-2013 under Grant PANACEA 222936, the Swiss National Science Foundation, and the Kanton of Zurich.

## A2.2 Reprint of the research article *Kamkina et al., 2016*

This section contains a reprint of the research article entitled "Natural genetic variation differentially affects the proteome and transcriptome in *C. elegans*" published in Molecular and Cellular Proteomics journal on March 4, 2016 (volume 15, issue 5, pages: 1670-1680). The supplemental materials and tables are available at the online version of the research article under: http://www.mcponline.org/content/15/5/1670/suppl/DC1

MCP MOLECULAR & CELLULAR PROTEOMICS ASBMB

Research



# Natural Genetic Variation Differentially Affects the Proteome and Transcriptome in *Caenorhabditis elegans*

**Polina Kamkina‡§¶, L. Basten Snoek¶‖, Jonas Grossmann**, Rita J. M. Volkers‖, Mark G. Sterken‖, Michael Daube‡, Bernd Roschitzki**, Claudia Fortes**, Ralph Schlapbach**, Alexander Roth‡, Christian von Mering‡, Michael O. Hengartner‡, Sabine P. Schrimpf‡ ‡‡, and Jan E. Kammenga‖‡‡**

**Natural genetic variation is the raw material of evolution and influences disease development and progression. An important question is how this genetic variation translates into variation in protein abundance. To analyze the effects of the genetic background on gene and protein expression in the nematode *Caenorhabditis elegans*, we quantitatively compared the two genetically highly divergent wild-type strains N2 and CB4856. Gene expression was analyzed by microarray assays, and proteins were quantified using stable isotope labeling by amino acids in cell culture. Among all transcribed genes, we found 1,532 genes to be differentially transcribed between the two wild types. Of the total 3,238 quantified proteins, 129 proteins were significantly differentially expressed between N2 and CB4856. The differentially expressed proteins were enriched for genes that function in insulin-signaling and stress-response pathways, underlining strong divergence of these pathways in nematodes. The protein abundance of the two wild-type strains correlates more strongly than protein abundance *versus* transcript abundance within each wild type. Our findings indicate that in *C. elegans* only a fraction of the changes in protein abundance can be explained by the changes in mRNA abundance. These findings corroborate with the observations made across species.** ***Molecular & Cellular Proteomics 15: 10.1074/mcp.M115.052548, 1670–1680, 2016.***

Natural genetic variation in gene expression shapes the diversity in phenotypic traits and is the raw material for evolutionary processes (1). Variation in gene expression can be very extensive across individuals with different genotypes. The additive effects (narrow-sense heritability) of independent loci on gene expression variation can reach 35% in humans (2). The broad-sense heritable variation in gene expression has been estimated to be up to 70% in the nematode *Caenorhabditis elegans* (3, 4) and up to 80% in yeast (5). This high heritability and the ability to construct genetically segregating populations facilitate mapping of gene expression regulation and subsequent detection of expression quantitative trait loci (eQTL)[1] (5–11). eQTLs are genomic regions containing a polymorphism associated with variation in transcript abundance between genotypes (12). eQTL analysis provides insight into the underlying genetic architecture of complex traits and is valuable for the identification of pathways and gene networks (10, 13–15). A key question is whether gene expression variation is translated into variation at the proteome level and whether it affects functionally relevant proteins. Genetic model species provide an ideal platform to explore the relationship between gene expression variation and variation at the proteome level due to their tractability. Although it is well established that there is a correlation between transcript and protein abundances, the relationship between natural variation in gene expression and variation in protein abundance is less well understood. The proteome provides information required to understand the functioning of cells (16), and combined with natural genetic variation, it allows for mapping of protein expression regulators (17). In yeast, gene expression variation in 354 genes between genetically different strains was found to lead to variation in protein abundance for a limited set of proteins reflecting mainly transcription-independent mechanisms (18). In mice, the natural variation of transcript abundance and protein levels among inbred strains correlates slightly (0.27) (19). Over half of the identified eQTLs in yeast contributed to changes in protein levels of regulated genes, but several protein-QTLs did not correlate with their cognate transcript levels (20).

From the ‡Institute of Molecular Life Sciences, University of Zurich, 8057 Zurich, Switzerland; §Ph.D. Program in Molecular Life Sciences Zurich, 8057 Zurich, Switzerland; ‖Laboratory of Nematology, Wageningen University, Wageningen 6708 PB, The Netherlands; **Functional Genomics Center Zurich, University of Zurich and Swiss Federal Institute of Technology Zurich, 8057 Zurich, Switzerland

Received June 10, 2015, and in revised form, February 22, 2016
Published, MCP Papers in Press, March 4, 2016, DOI 10.1074/mcp.M115.052548

[1] The abbreviations used are: eQTL, expression quantitative trait loci; FDR, false discovery rate; GO, gene ontology; IBAQ, intensity-based absolute quantification; L4, larval stage 4; SILAC, stable isotope labeling by amino acids in cell culture; ACN, acetonitrile.

MCP MOLECULAR & CELLULAR PROTEOMICS ASBMB



*C. elegans* is an ideal model organism to analyze the effect of the genetic background on its transcriptome (8, 9, 21–23) and proteome because comprehensive proteome catalogues have been generated (24, 25). The quantitative proteome comparison in *C. elegans* and *Drosophila melanogaster* showed that the interspecies' protein abundance correlation was higher than the intraspecies' correlation between protein and mRNA abundance. This suggests that protein levels are under evolutionary selection acting post-transcriptionally (26). In a recent interspecies comparison of the two nematodes *C. elegans* and *Caenorhabditis briggsae*, the protein and transcript changes were found to be conserved throughout development (27).

To complete these comparative interspecies expression analyses with an intraspecies analysis and to investigate the effect of natural genetic variation from the transcriptome to the proteome, the genetically highly divergent *C. elegans* wild-type strains, N2 (isolated in Bristol, UK) and CB4856 (from Hawaii), were compared quantitatively. Transcriptome data were acquired by microarray analysis, and for quantitative proteome analysis, the SILAC labeling method was used, which was recently established for *C. elegans* (28, 29). We analyzed animals at the developmental larval stage 4 (L4), because at this stage the largest differences in gene expression levels were detected between N2 and CB4856 (3, 4, 30–32). The genomes of these two wild-type strains, as well as polymorphisms between them, have been characterized extensively (33–40). These genetic polymorphisms often lead to gene expression differences, which are playing a role in a whole range of phenotypic differences between N2 and CB4856, such as life history traits (4, 41–44), behavior (40, 45–49), and life span (9, 41, 50). Here, we asked whether natural genetic variation causes variation in protein levels between N2 and CB4856 and whether it is related to variation in transcript abundance.

Using SILAC on three independent biological replicates, we quantified a total of 3,238 proteins, 2,485 proteins were identified in at least two biological replicates. We found 129 proteins to be significantly differentially expressed between N2 and CB4856 with at least a 1.3-fold change in abundance and a $p$ value $< 0.000457$. They were enriched for genes that function in insulin-signaling and stress-response pathways, underlining strong divergence of these pathways in nematodes. The protein abundance of the two wild-type strains correlated more strongly than the protein abundance *versus* transcript abundance within each wild type.

## EXPERIMENTAL PROCEDURES

*C. elegans Strains and Culture Conditions*—The two *C. elegans* wild-type strains N2 (Bristol) and CB4856 (Hawaii) were grown at 20 °C on 9-cm NGM agar plates without peptone (3 g/liter NaCl, 20 g/liter bacto-agar, 5 mg/liter cholesterol, 25 mM $K_2PO_4$, 1 mM $MgSO_4$, 1 mM $CaCl_2$) and with a lawn of *Escherichia coli* (OP50 strain) bacteria.

*Transcriptome Comparison*—For RNA isolation we used a Maxwell® 16 AS2000 instrument with a Maxwell® 16 LEV simplyRNA tissue kit (both from Promega Corp., Madison, WI). The mRNA isolation was preceded by a modified lysis step. In short, 200 μl of homogenization buffer, 200 μl of lysis buffer, and 10 μl of a 20 mg/ml stock solution of proteinase K were added to each sample. The samples were then incubated for 10 min at 65 °C, 1000 rpm in a Thermomixer (Eppendorf, Hamburg, Germany). After cooling on ice for 1 min, the samples were pipetted into the cartridges, and the protocol as recommended by Promega was continued. After mRNA isolation, the "Two-color Microarray-based Gene Expression Analysis, Low Input Quick Amp Labeling" protocol, version 6.0, was followed, starting from step 5 (4, 30, 31).

The microarrays used were *C. elegans* (V2) Gene Expression Microarray 4×44K slides, manufactured by Agilent Technologies, Santa Clara, CA. mRNA isolation, labeling with cyanine-3 and cyanine-5, and hybridization were performed as recommended by Agilent. The microarrays were scanned using an Agilent High Resolution C Scanner, using the settings as recommended. Data were extracted with the Agilent Feature Extraction Software version 10.5, following the manufacturer's guidelines.

For processing the data of the RNA microarrays, the "Limma" package for the "R" environment was used. No background correction of the RNA-array data was performed as recommended by Ref. 51. For the "within-array normalization of the RNA-array data" the Loess method was used, and for the "between-array normalization" the Quantile method was used. The obtained normalized intensities were used for further analysis.

*SILAC Labeling*—*E. coli* AT713 strain (lysine/arginine auxotrophic; *E. coli* Genetic Stock Center, CGSC number 4529, Yale) was grown in M9 Minimal Salts Medium (30.0 g of $Na_2HPO_4$, 15.0 g of $KH_2PO_4$, 2.5 g of NaCl, 5.0 g of $NH_4Cl$, $H_2O$ to 1 liter) supplemented with 150 mg/liter of either light (Arg-0, Lys-0) or heavy amino acids (Arg-10, Lys-8; Cambridge Isotope Laboratories). The cultures were kept for 2 days at 37 °C on a Lab-Therm Kühner orbital shaker at 230 rpm with a shaking diameter of 5 cm and harvested at an $A_{600}$ between 1.5 and 3.0. Bacteria were pelleted at 1,800 × *g* for 15 min at 4 °C; the supernatant was aspirated, and aliquots of 50 ml were frozen at −20 °C.

Adult N2 and CB4856 worms were bleached, and ~20,000 larval stage 1 animals were transferred to NGM plates freshly seeded with light or heavy labeled bacteria at 20 °C. For the first biological replicate, CB4856 animals were fed with heavy labeled AT713. For the second and third replicates, N2 animals were fed with heavy labeled AT713. Nematode populations were grown for two generations, and proteins were isolated from animals at L4. To determine the labeling efficiency, N2 heavy protein extracts were analyzed on an LTQ Orbitrap XL mass spectrometer (Thermo Scientific). The mgf files were searched against the *C. elegans* 6,239 database (07/03/2010, database (07/03/2010, Functional Genomics Center Zurich), using the Mascot software. The library was downloaded from the UniProt database, contains 24,362 entries, and was supplemented inhouse with 259 common MS contaminants. In total, 3,908 assigned peptide spectrum matches were analyzed with a score higher than 30, which yielded 1,562 peptides. Of these, 1,552 (99.6%) peptides were heavy labeled.

*Protein Isolation, SDS-PAGE, Protein Digestion*—To extract proteins, worm samples were homogenized with glass beads (G1277 acid-washed beads, diameter of 212–300 μm, Sigma-Aldrich) in freshly prepared cell lysis buffer (8 M urea, 5% 1 M Tris-HCl, pH 8.3) in a ratio of 1:1:2 (worms/beads/buffer) at 4 °C for 30 s at 5 m/s four times (FastPrep®-24, MP Biomedicals). The lysates were centrifuged three times at 20,000 × *g* for 10 min at room temperature to remove debris. Protein concentration in the supernatant was determined using the Bradford reagent (Sigma-Aldrich), and 1 μg of each protein sample was checked for equimolarity by SDS-PAGE.

MCP MOLECULAR & CELLULAR PROTEOMICS ASBMB



The L4 animal lysates of N2 and CB4856 were combined in a 1:1 ratio. Protein disulfide bridges were reduced with 5 mM dithiothreitol (DTT) at 60 °C for 30 min and alkylated with 15 mM iodoacetamide in the dark at 37 °C for 1 h. 600 μg of proteins were digested with trypsin (modified sequencing grade porcine, Promega) in a ratio of 1:50 w/w overnight at 37 °C. Samples were kept frozen at −20 °C until further processing.

*HPLC Fractionation of Peptides and ZipTip C18 Sample Clean Up*— Peptide samples were dried in a SpeedVac concentrator and resuspended in solvent A (5% ACN, 20 mM $K_2HPO_4$, pH 11) to a final urea concentration below 2 M. The pH was adjusted to 11 with 20% KOH, and the peptides were loaded on a 150 × 4.6-mm YMC Triart C18 column filled with 5 μm of silica beads (YMC Europe GmbH) at a flow rate of 1 ml/min using an Agilent 1100 liquid chromatography system (Agilent Technologies Inc.). Peptides were separated by a linear gradient from 2 to 50% of solvent B (50% ACN, 20 mM $K_2HPO_4$, pH 11) within 50 min. In total, 47 fractions were collected and pooled into 10 fractions based on the intensity measured by a UV-light detector at 214 nm. The reproducibility of the separation was controlled by running twice a self-mixed standard peptide mixture (adrenocorticotropin(1–16), angiotensinogen(1–14), bradykinin(2–9), leu-enkephalin, substance P, and vasopressin). Pooled fractions were vacuum-centrifuged until complete dryness and resuspended in 50 μl of 5% ACN, 0.1% TFA. Salts were removed using ZipTip $C_{18}$ pipette tips (Millipore Corp.), and the peptides were eluted with 15 μl of 60% ACN, 0.1% TFA. Samples were dried and re-dissolved in 12 μl of 3% ACN, 0.1% formic acid to a final peptide concentration of 0.4 μg/μl.

*LC-MS/MS Analysis*— LC-MS/MS was performed on a reversed-phase nano-LC system (Eksigent) at pH 3. Peptides were separated on a self-packed reverse-phase column (75 μm × 10 cm) packed with C18 beads (Magic C18, AQ, 3 μm, 200 Å, Bischoff GmbH, Leonberg, Germany) at a flow rate of 200 nl/min. The column was equilibrated with 95% solvent A (0.1% formic acid in water) and 5% solvent B (0.1% formic acid in ACN). Peptides were eluted using the following gradient: 0–1 min; 5–9% B, 1–56 min; 9–40% B, 56–60 min; 40–50% B and 60–64 min; 50–95% B. Peptides were analyzed on an LTQ Orbitrap XL mass spectrometer in the data-dependent acquisition mode. High accuracy mass spectra were acquired in the mass range of 300–1,800 *m/z*. In parallel, up to six data-dependent MS/MS were recorded in the linear ion trap of the most intense ions with charge state 2+, 3+, and 4+ using collision-induced dissociation. Target ions already selected for MS/MS were dynamically excluded for 60 s. Each sample was measured twice. The second analysis was performed with an exclusion list containing all precursor values of the first analysis with an elution time window of ±2.5 min.

*MaxQuant Analysis*— Data acquired on the LTQ Orbitrap XL MS were analyzed with MaxQuant version 1.3.0.5 (Max Planck Institute of Biochemistry Munich (52), searching the *C. elegans* 6,239 database at the Functional Genomics Center Zurich, Zurich. Search parameters were as follows: cysteine carbamidomethylation as fixed modification, protein N-terminal acetylation and methionine oxidation as variable modifications; SILAC labeling (Arg-10, Lys-8) as heavy labels; enzyme trypsin; two missed cleavages were allowed; and a minimum of six amino acids per identified peptide were required. The precursor ion mass tolerance was set to 20 ppm, and the fragment mass tolerance was set to 0.5 Da. The peptide FDR was set to 1%; protein FDR was set to 5%. In total, 40 raw data files were generated for every biological replicate and combined for database searching with the match between runs set to 2 min. Proteins with all shared peptides were combined into one protein group. The "Majority Protein IDs" column was used for protein assignments. The annotated MS/MS spectra with the lowest posterior error probability for single peptide identifications were extracted from 2,485 protein dataset using R package protViz (53) and are shown in supplemental Figs. S3–S5. The lists of corresponding single peptides are included in supplemental Tables S6–S8 for all three replicates.

*Correction of Arginine-to-Proline Conversion*— To estimate the effect of the arginine-to-proline conversion, all raw files were analyzed with the Progenesis QI for Proteomics software (Nonlinear Dynamics). The MS1 *m/z* feature maps filtered for the charge states from 2 to 7 were generated using the automatic method for peak picking with a sensitivity value of 5. The number of fragment ion counts was limited to 200, and deisotoping and charge deconvolution were applied. The generated mgf files were searched against the *C. elegans* database with Mascot for the identification of heavy proline peaks. The precursor mass tolerance was set to 10 ppm, and the fragment ion mass tolerance was set to 0.6 Da. Only fully tryptic termini with two missed cleavages were considered. The isotopic labeling of arginine (Arg-10) and lysine (Lys-8), heavy proline (Pro-6), heavy glutamate (Glu-6) labels and methionine oxidation were set as variable modifications. Cysteine carbamidomethylation was set as fixed modification. The analysis yielded 301 peptides with heavy proline and heavy arginine and/or heavy lysine. Based on this, the contribution of the heavy proline signal to the heavy arginine-lysine signal was estimated to 20% on average for peptides carrying one proline (supplemental Fig. 1*A*). This contribution to the signal intensity was proportional to the number of prolines per peptide (supplemental Fig. 1, *A* and *B*). Using a Perl script kindly provided by Jacob D. Jaffe (Broad Institute, Cambridge, MA), new protein group log2 heavy/light (H/L) ratios were calculated. In a first step, the intensity values of heavy peptides with prolines were corrected by adding to the measured signal intensity a value, which corresponds to 20% × *n* of heavy peptides abundance, where *n* is the number of prolines in the peptide. In a second step, adjusted peptide log2 H/L ratios were built and combined into the protein groups based on the MaxQuant protein group identifications. For each protein group median log2 H/L ratios were calculated. The protein group log2 H/L median ratios were calculated separately for each biological replicate; median was normalized to 1 and used for further analysis (supplemental Table 2). The effect of the arginine-to-glutamate conversion was negligible, because only 15 peptides identified had a heavy glutamate with heavy arginine and/or heavy lysine. Corrected peptide intensity values were used to calculate the corrected iBAQ values (intensity-based absolute quantification). The *C. elegans* database was digested *in silico* with trypsin using the Skyline software (version 1305, MacCoss Lab (54)), and the number of tryptic peptides per protein was extracted. The length of the peptides ranged from 6 to 30 amino acids; the N-terminal amino acids and potential ragged ends were not excluded. Using an in-house R function, corrected intensities of peptides per protein were summed up and divided by the corresponding number of tryptic peptides. Heavy and light iBAQ values were calculated separately and normalized using an intersect of 0 and slopes of 1.01896, 1.00456, and 1.00487 for the first, second, and third replicates, respectively. The proline corrected log2 iBAQ and protein abundance ratios correlated well with the uncorrected ratios (0.66 and 0.71, respectively), and the correlations for the differentially expressed proteins were even stronger (~0.9, supplemental Fig. 1, *C* and *D*). Proline corrected heavy and light peptide intensities correlated well between the replicates ($r \geq 0.74$, see supplemental Fig. 2).

*Experimental Design and Statistical Rationale*— mRNAs were quantified in three biological replicates. In total, six worm samples were analyzed, three for each strain (N2 and CB4856). Gene expression differences between the genotypes were determined by a linear model using "log2 hybridization intensities ~ genotype + error." Correction for multiple testing was done using a permutation determined threshold (3, 4, 31, 55). For each probe the values were

MCP MOLECULAR & CELLULAR PROTEOMICS ASBMB



permuted once and analyzed by the same model. The FDR rate was set to a ratio of false to true positives of 0.013, which occurred at $p <= 0.0032$ ($-\log10(p) = 2.5$). False positive was the number of genes with a significant $p$ value from the permuted set, and true positives were the number of genes with significant values from the original set. Proteins were quantified in three biological replicates, including label switching. For every biological replicate, two biochemical and two technical replicates were analyzed. In total, six combined protein samples were measured. To identify proteins that are differentially expressed between N2 and CB4856, SILAC data were filtered for proteins that were quantified at least twice with at least a 1.3-fold difference in abundance (the biological significance of the 1.3-fold change cutoff has been shown by Ref. 56, and a $p$ value < 0.000457 (z-test, permutation determined threshold with the FDR cutoff of 0.05)).

*Enrichment Analysis*—The enrichment analyses were undertaken using the following databases with annotations. Gene ontologies were downloaded from Ensemble (version 83) using the BioMart package in R. The enrichment of GO terms was analyzed using the topGO package from the bioconductor suite in R (58). GO terms with less than two annotated genes were excluded from the analysis. The enrichments were computed using the Fisher test. The elim algorithm was applied to account for the underlying GO graph topology (57). The anatomy terms, protein domains, and gene classes were obtained via WormMart of the WS220 WormBase release. Genes from WormBook chapters were obtained from the 2012 version of WormBook. eQTLs (8, 9) were obtained from WormQTL (21–23). KEGG pathways were obtained from release 65.0 of the Kyoto Encyclopedia of Genes and Genomes. These were tested for the enrichments by a hypergeometric test using R. Specific gene sets were obtained from supplementary data of the following papers: the aging set (59); DAF-16 sets (60, 61); and the DAF-16/PQM-1 set (62). The enrichments for specific gene sets were performed using Benjamini-Hochberg multiple testing corrected two-sided Fisher exact (aging and DAF-16 datasets) and hypergeometric tests (DAF-16/PQM-1 dataset). Note that the hypergeometric test and one-sided Fisher exact test are basically the same tests (63).

*Data Storage*—The transcript profiles and protein levels were stored in WormQTL (21–23) and can be accessed on line.

The MS proteomics data have also been deposited to the ProteomeXchange Consortium (64) via the PRIDE partner repository with the dataset identifier PXD002010.

## RESULTS

*Transcriptome Comparison*—As the strongest mRNA expression differences between N2 and CB4856 were observed at stage L4 (3, 4, 30–32), we measured the genome-wide transcription levels of three biological replicates of L4 stage synchronized larvae using microarrays. We found 1,532 genes to be differentially expressed (7.4%, $-\log10(p) > 2.5$; FDR = 0.013) of which 712 showed higher expression in CB4856 and 820 higher expression levels in N2 (Fig. 1). Differentially expressed genes were enriched for groups of genes involved in binding of proteins, sugars, and DNA, like f-box, *math/bath/btb*, *clec*, and *nhr* genes (supplemental Table 4) as observed previously (3, 4, 32). These groups of genes are highly polymorphic between wild isolates (4, 33, 34). No major differences in genes linked to L4 development (30) could be detected between CB4856 and N2. We identified specific enrichments between the genes expressed higher in N2 compared with CB4856 (supplemental Table 4). For example, the

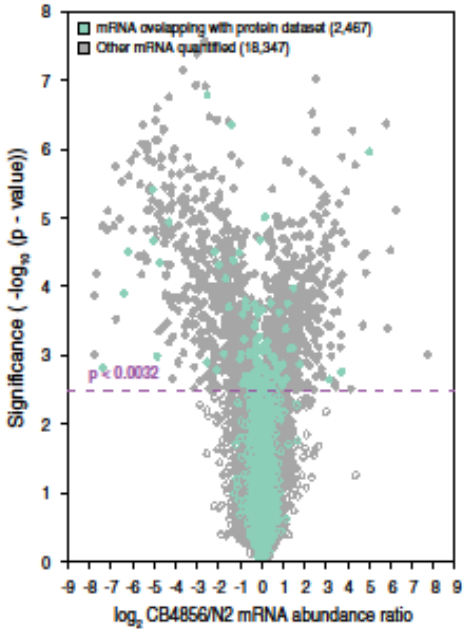


FIG. 1. **Volcano plot of mRNAs abundance differences between N2 and CB4856.** Differentially expressed mRNAs (1,532; 7.4%) are shown in *solid gray* and *green dots* (threshold: $p < 0.003$, FDR = 0.013, indicated by the *violet line*). Unique mRNAs overlapping with the protein dataset (2,467; 11.9%) are shown in *green*, and genes for which only mRNA was quantified (18,347; 88.1%) are shown in *gray*.

GO-term "monooxygenase activity" was specifically enriched for genes expressed higher in CB4856. Because many of the gene expression differences between CB4856 and N2 are caused by their genetic differences, most of these will also be present in recombinant offspring. The loci causal for gene expression differences can be observed as eQTLs, which yield information about the genetic and regulatory architecture of gene expression. As expected, the group of 1,532 genes differentially expressed between CB4856 and N2 was highly enriched for genes with eQTLs that were previously identified in these recombinant inbred line populations (6, 8, 9) (928/1,532; $p << 10^{-100}$ (8), 431/1,532; $p << 10^{-100}$ (9)). To investigate whether these mRNA expression level differences are also found on the protein level, we measured protein abundance in both strains.

*Protein Abundances Are Very Similar in N2 and CB4856*—We quantitatively compared protein abundances between the two *C. elegans* wild-type strains N2 and CB4856 in the L4 stage using SILAC and mass spectrometry. Protein extracts were analyzed in three biological replicates, including label switching. Almost complete labeling (99.6%) of the second generation L4 worms was observed. In total, we quantified 3,238 distinct proteins, ranging from 2,536 to 2,622 proteins

MCP MOLECULAR & CELLULAR PROTEOMICS ASBMB



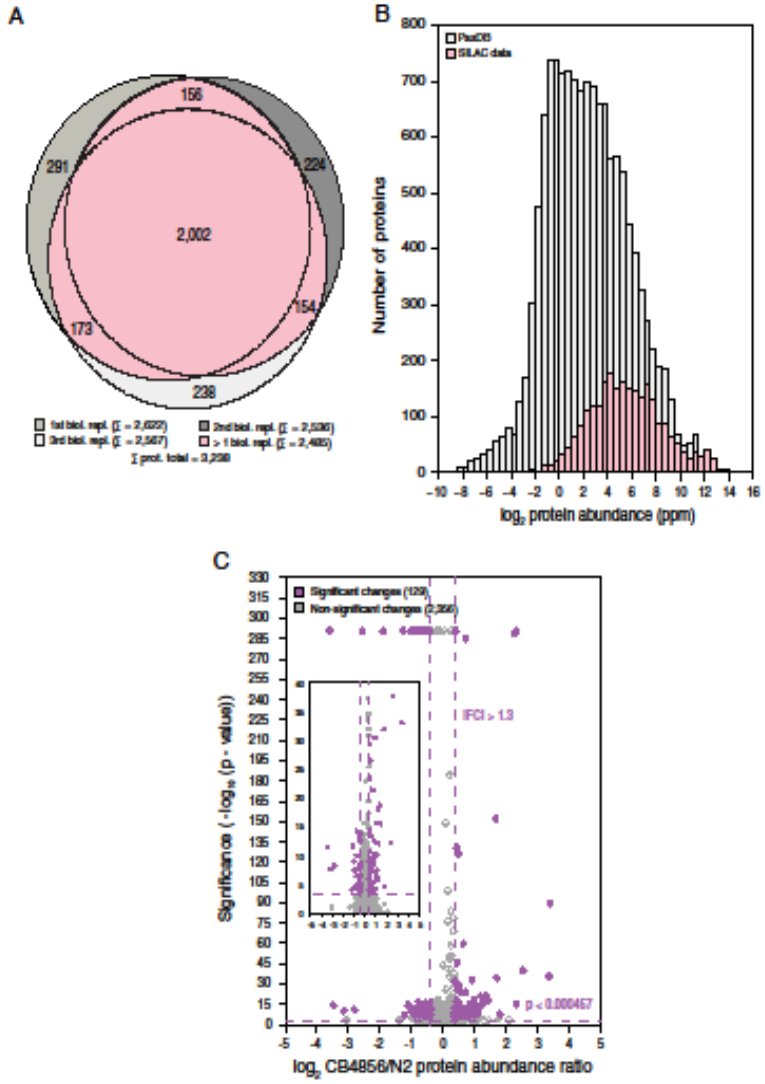


FIG. 2. **Proteins quantified in three CB4856/N2 SILAC experiments.** *A*, Venn diagram of the quantified proteins in three biological replicates. In total 3,238 proteins were quantified, and 2,002 (61.8%) proteins were quantified in all three biological replicates. Proteins quantified in at least two biological replicates (2,485; 76.7%) in the *pink sections* were used for further analysis. *B*, log2 MS intensity distribution of the proteins quantified at least twice (*pink section*) compared with the entire *C. elegans* proteome. *C*, volcano plot of protein abundance differences between N2 and CB4856. Differentially expressed proteins (129; 5.2%) are shown in *violet* (threshold: $p < 0.000457$, fold-change >1.3), and non-significant changes (2,356; 94.8%) are shown in *gray*. *Inset* represents the enlarged area from a $p$ value of 0.95 to $e^{-40}$. Proteins with a $p$ value of 0 were set to $e^{-2990}$ for plotting.

per SILAC experiment. 2,002 proteins (61.8%) were quantified in all three biological replicates and 2,485 proteins in at least two (protein FDR 5%, Fig. 2*A*, and supplemental Table 1). We compared our SILAC data to the integrated PaxDB dataset (65), which includes protein abundance data generated using various fractionation methods. We quantified 24.5% of the *C. elegans* proteins presented in PaxDB (13,224) in N2 and CB4856, distributed over 6 orders of magnitude, with a clear bias for high abundance proteins (Fig. 2*B*). Protein abundance between the two strains correlated very strongly

MCP MOLECULAR & CELLULAR PROTEOMICS ASBMB



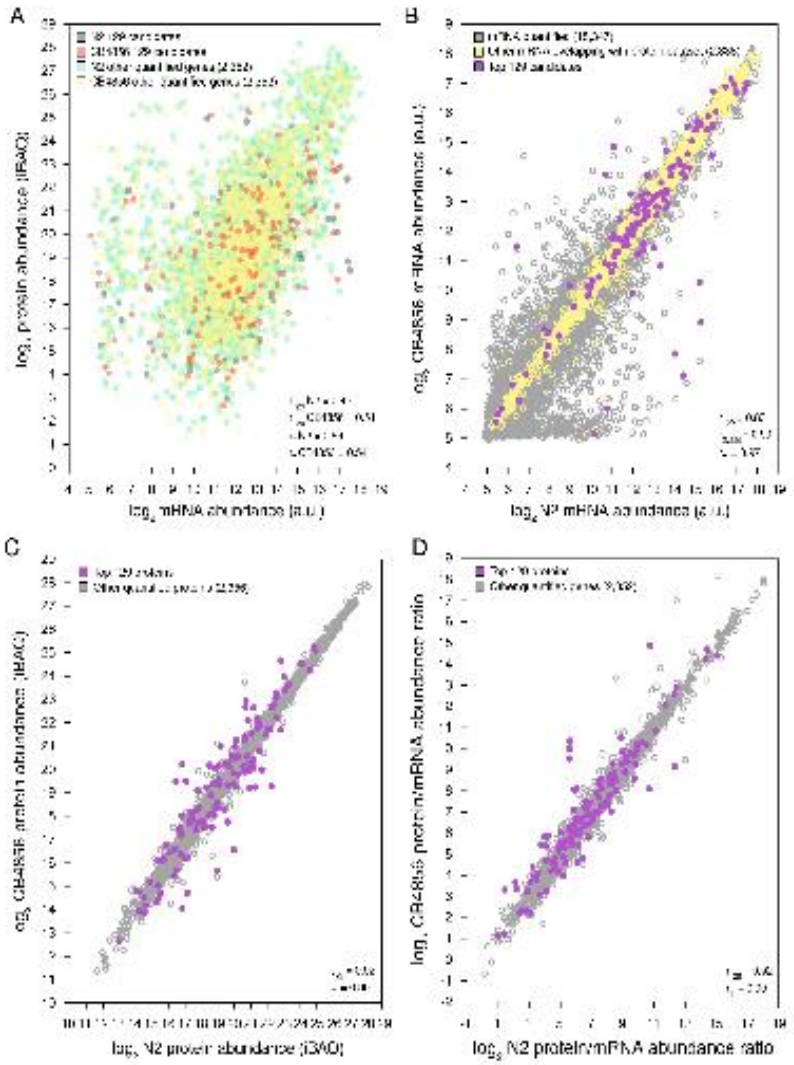


FIG. 3. **Correlations of mRNA and protein abundance between and within N2 and CB4856.** *A*, mRNA *versus* protein abundance. CB4856 in *yellow* and N2 in *green*, *orange*, and *dark green dots* represent the 129 differentially expressed proteins in CB4856 and N2. *B*, mRNA abundance of N2 compared with CB4856. The 129 differentially expressed proteins are shown in *violet*; 2,338 genes for which other unique mRNAs overlap with proteins are shown in *yellow*, and 18,347 genes for which only mRNA levels were quantified are shown in *gray*. *C*, protein abundance of N2 compared with CB4856. The 129 differentially expressed proteins are shown in *violet*, and other 2,356 quantified proteins are shown in *gray*. *D*, protein/mRNA ratio of N2 compared with CB4856. The 129 differentially expressed proteins are shown in *violet*, and other 2,352 quantified proteins (isoforms included) overlapping with mRNA dataset are shown in *gray*. $r_{129}$ is the Pearson correlation coefficient for the 129 differentially expressed proteins; $r_{2,338}$ is the Pearson correlation coefficient for other unique mRNAs overlapping with the protein dataset. For different protein isoforms, the same mRNA value was used for plotting. $r_T$ is the Pearson correlation coefficient for all genes quantified at mRNA and/or protein levels. (*a.u.*, arbitrary units).

($r = 0.99$, Fig. 3*C*). To identify proteins that are differentially expressed between N2 and CB4856, the combined SILAC data (3,238 proteins) were filtered for proteins that were quantified at least twice (2,485 proteins) with at least a 1.3-fold difference in abundance and a $p$ value $< 0.000457$ ($z$-test, FDR = 0.05, Fig. 2*C*). Using these criteria, 129

MCP MOLECULAR & CELLULAR PROTEOMICS ASBMB



proteins (5.2%) were found to be differentially expressed between the strains distributed over 5 orders of magnitude in expression. 70 proteins were up-regulated, and 59 proteins were down-regulated (Fig. 5).

*Local and Distant Regulation of the Conserved mRNA and Protein Expression*—In total, 2,481 quantified proteins (14 proteins with two isoforms each included) overlapped with 2,467 corresponding unique mRNAs in both strains (supplemental Table 3). The mRNA and protein expression patterns of N2 and CB4856 were very similar, whereas the correlation between mRNA and protein abundances within the strains was quite variable ($r = 0.54$ for both, Fig. 3*A*). By contrast, mRNA abundance, protein abundance, as well as protein-to-mRNA ratios correlated strongly between the strains ($r > 0.97$, Fig. 3, *B–D*). This suggests that for the detected genes both transcriptional and translational regulation of gene expression are well conserved between N2 and CB4856. The conservation of protein expression was also observed between distantly related species (26).

We also compared the protein abundance differences *versus* mRNA abundance differences between the two strains (Fig. 4). Of the 2,481 quantified genes, only 24 genes were found to be changed significantly at both the mRNA and protein levels between N2 and CB4856, and 105 proteins were different only at the protein level and 89 only at the mRNA level. To investigate the genetic loci possibly responsible for the mRNA and protein differences, we compared our data to eQTLs found in Vinuela *et al.* (9) and Rockman *et al.* (8). The vast majority of genes (16/23 and 23/25) found to be differentially expressed at both mRNA and protein levels had a QTL (*cis*- or *trans*) associated with them, with *cis*-eQTLs outnumbering *trans*-eQTLs with a ratio of about 2 to 1. By contrast, for the genes with no expression difference, eQTLs were relatively infrequent (~7–21%), with a slight bias toward *trans*-eQTLs. Genes varying at the protein or mRNA level only had intermediate eQTL frequencies, with the number of *trans*-eQTLs being higher for the genes differentially expressed only on a protein level (Table I).

*Aging and Stress Response-related Proteins Are Enriched among the 129 Differentially Expressed Proteins*—To characterize the function of the 129 differentially expressed proteins, we first analyzed their GO annotations. In our dataset, the categories carbohydrate metabolisms, innate immune response, defense response to bacterium, and cysteine biosynthesis from serine were over-represented. We have also found the NPL4 domain and domains involved in sugar metabolism over-represented among other enriched multiple protein domains (supplemental Table 4). Interestingly, *npl4* genes were shown to be involved in the life span of *C. elegans* (8, 66). As altered sugar metabolism, oxidative stress, and pathogen resistance pathways were shown to be associated with aging (67–70), and because the average life span of CB4856 is shorter than that of N2 (41, 50, 71), we compared our list with recently published aging and stress response transcriptome

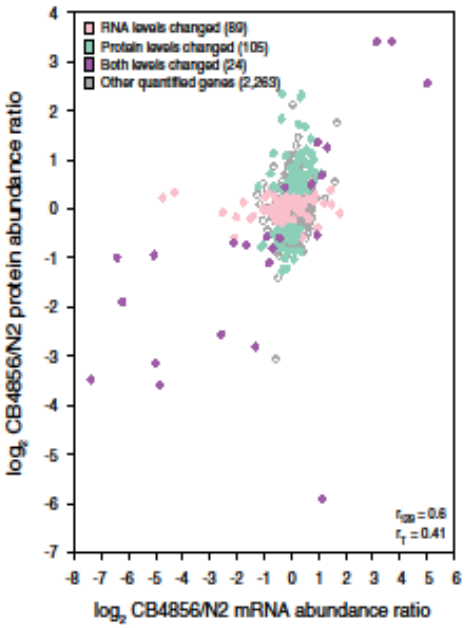


FIG. 4. **Variation in protein *versus* mRNA abundance ratios between CB4856 and N2.** 24 (1%) genes showed a significant change at both mRNA and proteins levels (*violet*); 105 (4.2%) genes showed a change only at the protein level (*green*); and 89 (3.6%) genes showed a change only at the mRNA level (*pink*). 2,263 (91.2%) genes without changes on protein and mRNA level (including the 13 proteins with isoforms, for which the same mRNA value was used for plotting) are shown in *gray*. $r_T$ is the Pearson correlation coefficient for all genes quantified at both mRNA and protein levels. $r_{129}$ is the Pearson correlation coefficient for the 129 differentially expressed proteins (*green* and *violet*).

datasets. Transcripts differentially regulated during aging ($p = 0.007$ (59) and transcripts responsive to the DAF-16 transcription factor ($p = 0.0002$ (60, 61)) were over-represented (Fig. 5 and supplemental Table 5). 2,485 proteins were used as the background list, and Benjamini-Hochberg multiple testing correction was applied. We further compared our data to a recent study that showed that the DAF-16-associated element-binding transcription factor PQM-1 complements DAF-16 aging-related functions (62). Genes transcriptionally regulated by PQM-1 alone were enriched in the 2,485 quantified proteins ($p < 2.15e^{-13}$, data not shown), whereas DAF-16 and PQM-1 targets were not ($p = 0.76$, data not shown). By contrast, among the 129 differentially expressed proteins, enrichment was found only for the DAF-16 and PQM-1 targets ($p = 0.0008$), whereas the PQM-1-specific targets were not enriched ($p = 0.24$, Fig. 5 and supplemental Table 5). This shows that highly abundant proteins have a higher chance to be PQM-1 targets, and the variation in protein abundance acts downstream of DAF-16 and PQM-1. In total, 51 proteins were enriched in at least one of the mentioned stud-

MCP MOLECULAR & CELLULAR PROTEOMICS ASBMB



TABLE 1
*Summary of the enriched eQTLs for the genes differentially expressed at mRNA and/or protein levels*

| Study/eQTL | No difference | mRNA levels changed | Protein levels changed | Both levels changed |
|---|---|---|---|---|
| Vinuela et al. 2010 all present in dataset | 2,270 | 91 | 103 | 23 |
| Vinuela et al. 2010 *cis*-eQTLs | 23 (1%) | 11 (12.1%) | 8 (7.8%) | 11 (47.8%) |
| Vinuela et al. 2010 *trans*-eQTLs | 130 (5.7%) | 9 (9.9%) | 20 (19.4%) | 5 (21.7%) |
| Rockman et al. 2010 all present in dataset | 2,288 | 86 | 109 | 25 |
| Rockman et al. 2010 *cis*-eQTLs | 209 (9.1%) | 40 (46.5%) | 20 (18.3%) | 18 (72%) |
| Rockman et al. 2010 *trans*-eQTLs | 266 (11.6%) | 13 (15.1%) | 28 (25.7%) | 5 (20%) |

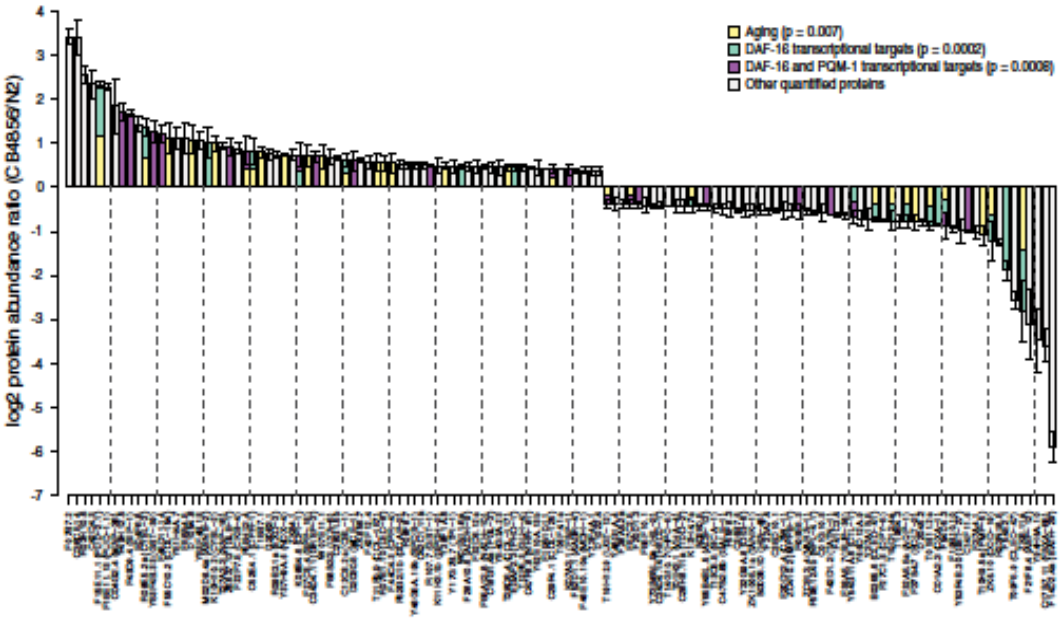


FIG. 5. **Functional categorization of the 129 differentially expressed proteins.** Differentially expressed proteins were significantly enriched in genes that are transcriptionally regulated during aging (yellow (59)), by the DAF-16 transcription factor (green (60, 61)), or by the PQM-1 and DAF-16 transcription factors (violet (62)) based on Benjamini-Hochberg-corrected two-sided Fisher exact and hypergeometric tests. Values shown at average ± S.D. of at least two biological replicates.

ies, and 18 proteins were identified in at least two of them (Fig. 5 and supplemental Table 5). Together, these observations suggest that the 129 differentially expressed proteins might contribute to the differences in life span of CB4856 and N2.

The 129 differentially expressed proteins were also enriched for eQTLs identified in aging worms (9) (47 proteins, $p \ll 1e^{-16}$) and for stage-specific eQTLs (8) (62 proteins, $p \ll 1e^{-16}$) (Table I). Eleven proteins were found to have an eQTL under mildly stressful conditions of 24 °C (Y37A1B.5, Y48G1A.4, SSP-16, GRSP-3, MCE-1, MPPB-1, TATN-1, T06F4.1a, NDX-4, SPDS-1, and LEC-8) (6). Combined, these eQTL enrichments provide further evidence suggesting that at least part of the protein expression level differences can be explained by mRNA expression level differences between CB4856 and N2, and they might play a role in aging.

MCP MOLECULAR & CELLULAR PROTEOMICS ASBMB



*Genes with eQTLs on the npr-1 Locus Are Enriched among the 129 Proteins*—CB4856 favors lower oxygen concentrations, mainly caused by an allelic difference in NPR-1 (39, 40), and this is reflected in its clumping behavior (72, 73). We found an enrichment for genes with an eQTL on the *npr-1* locus in the 129 candidates, suggesting that at least part of the gene expression differences lead to differences in protein levels. Furthermore, two cysteine synthases, CYSL-2 and CYSL-3, proposed sensors of cellular $H_2S$ levels upon hypoxia (74), showed up-regulated protein levels in CB4856 (Fig. 5). The oxygen-binding protein GLB-1, the transcript of which is up-regulated under hypoxic conditions and in *hif-1* mutants (75, 76), was also up-regulated in CB4856 (Fig. 5), as well as the oxygen-sensing globin protein GLB-5 (72, 73). These differences on protein level might contribute to the different oxygen responses of N2 and CB4856.

## DISCUSSION

In this paper, we analyzed the influence of genetic background and natural variation on the proteome and the transcriptome in two genetically highly divergent *C. elegans* wild-type strains, N2 (Bristol) and CB4856 (Hawaii). Using SILAC, we quantified in total 3,238 distinct proteins in three biological replicates; 2,485 proteins were quantified in at least two replicates. These numbers are comparable with other SILAC studies in *C. elegans*. More than 1,400 proteins were reliably quantified in worm samples using size exclusion chromatography (28), and 3,470 proteins were quantified using LysC digestion followed by hydrophilic interaction liquid chromatography separation of the peptides (29). Between 1,461 and 4,072 proteins were identified in different developmental stages of *C. elegans* and *C. briggsae* after separation on SDS gels (27). To quantify less abundant proteins, additional separation methods would be required, as was done for the quantitative comparison of distantly related species (26). In our study, primarily highly expressed proteins were quantified. These show relatively little variation between N2 and CB4856, also at the transcript level.

Among the 2,485 quantified proteins, 129 (5.2%) proteins distributed over 5 orders of magnitude in expression were differentially expressed between N2 and CB4856. By contrast, of all the genes, 1,532 genes (7.4%) were differentially expressed at the mRNA level. Of the 2,481 genes for which proteins were detected and that overlapped with the mRNA dataset, only 113 (4.6%) were different at the mRNA level. The overall correlations for both protein and mRNA abundances were close to one between the strains. This is consistent with the quantitative comparison of *C. elegans* and *C. briggsae* (27), but it is different for *C. elegans* and *D. melanogaster*, where the conservation in expression was found only on protein level (26). Thus, in this intraspecies comparison, we observed a strong selective pressure to maintain protein levels, an effect that was also shown for closely (27) and even distantly related species (26).

The 129 differentially expressed proteins were strongly enriched for downstream targets of the insulin-signaling pathway (DAF-16 and PQM-1 targets) (60, 61, 62). An increased expression divergence of DAF-16 targets was also observed in a quantitative comparison of gene expression between the two nematode species *C. briggsae* and *C. elegans* (27). These results imply that differential regulation of the insulin-signaling downstream targets can be observed already between strains of the same species, underlining the strong divergence of this signaling pathway in nematodes. Importantly, the genes differentially expressed between N2 and CB4856 were also strongly enriched in eQTLs associated with aging. These results suggest that at least a subset of our differentially expressed genes might contribute to the longevity differences between N2 and CB4856.

*Acknowledgments*—We thank Xiaoxue Li and Xue Zheng for carrying out pre-experiments in proteomics and Peter Hunziker for valuable advice. We thank Nikolaus Rajewsky and Nadine Thierfelder for kindly providing the SILAC labeling protocol and Jacob D. Jaffe for help with the correction of arginine-to-proline conversion. We also thank Morris Swertz and Joeri van der Velde for help in making the data accessible through WormQTL. We thank Christian Panse for help with MS/MS spectra annotation of the single peptide identifications.

* This work was supported by European Community Health Seventh Framework Programme FP7/2007-2013 under Grant PANACEA 222936, the Swiss National Science Foundation, and the Kanton of Zurich. L.B.S. was supported by Netherlands Organization for Scientific Research Project 823.01.001. R.J.M.V. was supported by the NWO-ALW Project 855.01.151. M.G.S. was funded by the Graduate School Production Ecology and Resource Conservation. The authors declare that they have no conflicts of interest with the contents of this article.

S This article contains supplemental material.

‡‡ To whom correspondence should be addressed: Laboratory of Nematology, Wageningen Universiteit, Droevendaalsesteeg 1, NL-6708 PB, Wageningen, The Netherlands. Tel.: 31-317-482996/482197; Fax: 31-317-484254; E-mail: jan.kammenga@wur.nl or Institute of Molecular Life Sciences, University of Zurich, Winterthurerstrasse 190, CH-8057 Zurich, Switzerland. Tel.: 41-44-6353112; E-mail: sabine.schrimpf@imls.uzh.ch.

¶ Both authors contributed equally to this work.

## REFERENCES

1. Oleksiak, M. F., Churchill, G. A., and Crawford, D. L. (2002) Variation in gene expression within and among natural populations. *Nat. Genet.* **32**, 261–266
2. Gaffney, D. J. (2013) Global properties and functional complexity of human gene regulatory variation. *PLOS Genet.* **9**, e1003501
3. Vinuela, A., Snoek, L. B., Riksen, J. A., and Kammenga, J. E. (2012) Aging uncouples heritability and expression-QTL in *Caenorhabditis elegans*. *G3* **2**, 597–605
4. Volkers, R. J., Snoek, L. B., Hubar, C. J., Coopman, R., Chen, W., Yang, W., Sterken, M. G., Schulenburg, H., Braeckman, B. P., and Kammenga, J. E. (2013) Gene-environment and protein-degradation signatures characterize genomic and phenotypic diversity in wild *Caenorhabditis elegans* populations. *BMC Biol.* **11**, 93
5. Brem, R. B., Yvert, G., Clinton, R., and Kruglyak, L. (2002) Genetic dissection of transcriptional regulation in budding yeast. *Science* **296**, 752–755
6. Li, Y., Alvarez, O. A., Gutteling, E. W., Tijsterman, M., Fu, J., Riksen, J. A., Hazendonk, E., Prins, P., Plasterk, R. H., Jansen, R. C., Breitling, R., and

Kammenga, J. E. (2006) Mapping determinants of gene expression plasticity by genetical genomics in *C. elegans*. *PLOS Genet.* **2**, e222
7. Li, Y., Breitling, R., Snoek, L. B., van der Velde, K. J., Swertz, M. A., Riksen, J., Jansen, R. C., and Kammenga, J. E. (2010) Global genetic robustness of the alternative splicing machinery in *Caenorhabditis elegans*. *Genetics* **186**, 405–410
8. Rockman, M. V., Skrovanek, S. S., and Kruglyak, L. (2010) Selection at linked sites shapes heritable phenotypic variation in *C. elegans*. *Science* **330**, 372–376
9. Viñuela, A., Snoek, L. B., Riksen, J. A., and Kammenga, J. E. (2010) Genome-wide gene expression regulation as a function of genotype and age in *C. elegans*. *Genome Res.* **20**, 929–937
10. Snoek, L. B., Terpstra, I. R., Doktor, R., Van den Ackervaken, G., and Peeters, A. J. (2012) Genetical genomics reveals large scale genotype-by-environment interactions in *Arabidopsis thaliana*. *Front. Genet.* **3**, 317
11. King, E. G., Sanderson, B. J., McNeil, C. L., Long, A. D., and Macdonald, S. J. (2014) Genetic dissection of the *Drosophila melanogaster* female head transcriptome reveals widespread allelic heterogeneity. *PLoS Genet.* **10**, e1004322
12. Jansen, R. C., and Nap, J. P. (2001) Genetical genomics: the added value from segregation. *Trends Genet.* 388–391
13. Bing, N., and Hoeschele, I. (2005) Genetical genomics analysis of a yeast segregant population for transcription network inference. *Genetics* **170**, 533–542
14. Kaurentjes, J. J., Fu, J., Terpstra, I. R., Garcia, J. M., van den Ackervaken, G., Snoek, L. B., Peeters, A. J., Vreugdenhil, D., Koornneef, M., and Jansen, R. C. (2007) Regulatory network construction in *Arabidopsis* by using genome-wide gene expression quantitative trait loci. *Proc. Natl. Acad. Sci. U.S.A.* **104**, 1708–1713
15. Terpstra, I. R., Snoek, L. B., Kaurentjes, J. J., Peeters, A. J., and van den Ackervaken, G. (2010) Regulatory network identification by genetical genomics: signaling downstream of the Arabidopsis receptor-like kinase ERECTA. *Plant Physiol.* **154**, 1067–1078
16. Cox, J., and Mann, M. (2007) Is proteomics the new genomics? *Cell* **130**, 395–398
17. Albert, F. W., Treusch, S., Shockley, A. H., Bloom, J. S., and Kruglyak, L. (2014) Genetics of single-cell protein abundance variation in large yeast populations. *Nature* **506**, 494–497
18. Foss, E. J., Radulovic, D., Shaffer, S. A., Goodlett, D. R., Kruglyak, L., and Bedalov, A. (2011) Genetic variation shapes protein networks mainly through non-transcriptional mechanisms. *PLoS Biol.* **9**, e1001144
19. Ghazalpour, A., Bennett, B., Petyuk, V. A., Orozco, L., Hagopian, R., Mungrue, I. N., Farber, C. R., Sinsheimer, J., Kang, H. M., Furlotte, N., Park, C. C., Wen, P. Z., Brewer, H., Weitz, K., Camp, D. G., *et al.* (2011) Comparative analysis of proteome and transcriptome variation in mouse. *PLoS Genet.* **7**, e1001393
20. Parts, L., Liu, Y. C., Tekkedil, M. M., Steinmetz, L. M., Caudy, A. A., Fraser, A. G., Boone, C., Andrews, B. J., and Rosebrock, A. P. (2014) Heritability and genetic basis of protein level variation in an outbred population. *Genome Res.* **24**, 1363–1370
21. Snoek, L. B., Van der Velde, K. J., Arends, D., Li, Y., Beyer, A., Elvin, M., Fisher, J., Hajnal, A., Hengartner, M. O., Poulin, G. B., Rodriguez, M., Schmid, T., Schrimpf, S., Xue, F., Jansen, R. C., *et al.* (2013) WormQTL–public archive and analysis web portal for natural variation data in *Caenorhabditis* spp. *Nucleic Acids Res.* **41**, D738–D743
22. Snoek, L. B., Joeri van der Velde, K., Li, Y., Jansen, R. C., Swertz, M. A., and Kammenga, J. E. (2014) Worm variation made accessible: take your shopping cart to store, link, and investigate! *Worm* **3**, e28357
23. van der Velde, K. J., de Haan, M., Zych, K., Arends, D., Snoek, L. B., Kammenga, J. E., Jansen, R. C., Swertz, M. A., and Li, Y. (2014) WormQTLHD–a web database for linking human disease to natural variation data in *C. elegans*. *Nucleic Acids Res.* **42**, D794–D801
24. Merrihew, G. E., Davis, C., Ewing, B., Williams, G., Kall, L., Frewen, B. E., Noble, W. S., Green, P., Thomas, J. H., and MacCoss, M. J. (2008) Use of shotgun proteomics for the identification, confirmation, and correction of *C. elegans* gene annotations. *Genome Res.* **18**, 1660–1669
25. Schrimpf, S. P., and Hengartner, M. O. (2010) A worm rich in protein: quantitative, differential, and global proteomics in *Caenorhabditis elegans*. *J. Proteomics* **73**, 2186–2197
26. Schrimpf, S. P., Weiss, M., Reiter, L., Ahrens, C. H., Jovanovic, M., Malmström, J., Brunner, E., Mohanty, S., Lercher, M. J., Hunziker, P. E., Aebersold, R., von Mering, C., and Hengartner, M. O. (2009) Comparative functional analysis of the *Caenorhabditis elegans* and *Drosophila melanogaster* proteomes. *PLoS Biol.* **7**, e48
27. Grün, D., Kirchner, M., Thierfelder, N., Stoecklus, M., Selbach, M., and Rajewsky, N. (2014) Conservation of mRNA and protein expression during development of *C. elegans*. *Cell Rep.* **6**, 565–577
28. Larance, M., Bailly, A. P., Pourkarimi, E., Hay, R. T., Buchanan, G., Coulthurst, S., Xirodimas, D. P., Gartner, A., and Lamond, A. I. (2011) Stable-isotope labeling with amino acids in nematodes. *Nat. Methods* **8**, 849–851
29. Fredens, J., Engholm-Keller, K., Giessing, A., Pultz, D., Larsen, M. R., Højrup, P., Møller-Jensen, J., and Færgeman, N. J. (2011) Quantitative proteomics by amino acid labeling in *C. elegans*. *Nat. Methods* **8**, 845–847
30. Snoek, L. B., Sterken, M. G., Volkers, R. J., Klatter, M., Bosman, K. J., Bevers, R. P., Riksen, J. A., Smant, G., Cossins, A. R., and Kammenga, J. E. (2014) A rapid and massive gene expression shift marking adolescent transition in *C. elegans*. *Sci. Rep.* **4**, 3912
31. van der Bent, M. L., Sterken, M. G., Volkers, R. J., Riksen, J. A., Schmid, T., Hajnal, A., Kammenga, J. E., and Snoek, L. B. (2014) Loss-of-function of β-catenin bar-1 slows development and activates the Wnt pathway in *Caenorhabditis elegans*. *Sci. Rep.* **4**, 4926
32. Capra, E. J., Skrovanek, S. M., and Kruglyak, L. (2008) Comparative developmental expression profiling of two *C. elegans* isolates. *PLoS One* **3**, e4055
33. Thompson, O., Edgley, M., Strasbourger, P., Flibotte, S., Ewing, B., Adair, R., Au, V., Chaudhry, I., Fernando, L., Hutter, H., Kieffer, A., Lau, J., Lee, N., Miller, A., Raymant, G., *et al.* (2013) The million mutation project: a new approach to genetics in *Caenorhabditis elegans*. *Genome Res.* **23**, 1749–1762
34. Thompson, O. A., Snoek, L. B., Nijveen, H., Sterken, M. G., Volkers, R. J., Brenchley, R., Van't Hof, A., Bevers, R. P., Cossins, A. R., Yanai, I., Hajnal, A., Schmid, T., Perkins, J. D., Spencer, D., Kruglyak, L., *et al.* (2015) Remarkably divergent regions punctuate the genome assembly of the *C. elegans* Hawaiian strain CB4856. *Genetics* **200**, 975–989
35. Barrière, A., and Félix, M. A. (2005) High local genetic diversity and low outcrossing rate in *Caenorhabditis elegans* natural populations. *Curr. Biol.* **15**, 1176–1184
36. Andersen, E. C., Gerke, J. P., Shapiro, J. A., Crissman, J. R., Ghosh, R., Bloom, J. S., Félix, M. A., and Kruglyak, L. (2012) Chromosome-scale selective sweeps shape *Caenorhabditis elegans* genomic diversity. *Nat. Genet.* **44**, 285–290
37. Barrière, A., and Félix, M. A. (2005) Natural variation and population genetics of *Caenorhabditis elegans*. *WormBook* 2005, 1–19
38. Maydan, J. S., Flibotte, S., Edgley, M. L., Lau, J., Selzer, R. R., Richmond, T. A., Pofahl, N. J., Thomas, J. H., and Moerman, D. G. (2007) Efficient high-resolution deletion discovery in *Caenorhabditis elegans* by array comparative genomic hybridization. *Genome Res.* **17**, 337–347
39. Sterken, M. G., Snoek, L. B., Kammenga, J. E., and Andersen, E. C. (2015) The laboratory domestication of *Caenorhabditis elegans*. *Trends Genet.* **31**, 224–231
40. Andersen, E. C., Bloom, J. S., Gerke, J. P., and Kruglyak, L. (2014) A variant in the neuropeptide receptor npr-1 is a major determinant of *Caenorhabditis elegans* growth and physiology. *PLoS Genet.* **10**, e1004156
41. Stastna, J. J., Snoek, L. B., Kammenga, J. E., and Harvey, S. C. (2015) Genotype-dependent lifespan effects in peptone deprived *Caenorhabditis elegans*. *Sci. Rep.* **5**, 16259
42. Schmid, T., Snoek, L. B., Fröhli, E., van der Bent, M. L., Kammenga, J., and Hajnal, A. (2015) Systemic regulation of RAS/MAPK signaling by the serotonin metabolite 5-HIAA. *PLoS Genet.* **11**, e1005236
43. Green, J. W., Snoek, L. B., Kammenga, J. E., and Harvey, S. C. (2013) Genetic mapping of variation in dauer larvae development in growing populations of *Caenorhabditis elegans*. *Heredity* **111**, 306–313
44. Duveau, F., and Félix, M. A. (2012) Role of pleiotropy in the evolution of a cryptic developmental variation in *Caenorhabditis elegans*. *PLoS Biol.* **10**, e1001230
45. Reddy, K. C., Andersen, E. C., Kruglyak, L., and Kim, D. H. (2009) A polymorphism in npr-1 is a behavioral determinant of pathogen susceptibility in *C. elegans*. *Science* **323**, 382–384
46. Glauser, D. A., Chen, W. C., Agin, R., Macinnis, B. L., Hellman, A. B., Garrity, P. A., Tan, M. W., and Goodman, M. B. (2011) Heat avoidance is

regulated by transient receptor potential (TRP) channels and a neuropeptide signaling pathway in *Caenorhabditis elegans*. *Genetics* **188**, 91–103
47. Gaertner, B. E., Parmenter, M. D., Rockman, M. V., Kruglyak, L., and Phillips, P. C. (2012) More than the sum of its parts: a complex epistatic network underlies natural variation in thermal preference behavior in *Caenorhabditis elegans*. *Genetics* **192**, 1533–1542
48. Bendesky, A., Pitts, J., Rockman, M. V., Chen, W. C., Tan, M. W., Kruglyak, L., and Bargmann, C. I. (2012) Long-range regulatory polymorphisms affecting a GABA receptor constitute a quantitative trait locus (QTL) for social behavior in *Caenorhabditis elegans*. *PLoS Genet.* **8**, e1003157
49. Bendesky, A., Tsunozaki, M., Rockman, M. V., Kruglyak, L., and Bargmann, C. I. (2011) Catecholamine receptor polymorphisms affect decision-making in *C. elegans*. *Nature* **472**, 313–318
50. Rodriguez, M., Snoek, L. B., Riksen, J. A., Bevers, R. P., and Kammenga, J. E. (2012) Genetic variation for stress-response hormesis in *C. elegans* lifespan. *Exp. Gerontol.* **47**, 581–587
51. Zahurak, M., Parmigiani, G., Yu, W., Scharpf, R. B., Berman, D., Schaeffer, E., Shabbeer, S., and Cope, L. (2007) Pre-processing agilent microarray data. *BMC Bioinformatics* **8**, 142
52. Cox, J., and Mann, M. (2008) MaxQuant enables high peptide identification rates, individualized p.p.b.-range mass accuracies and proteome-wide protein quantification. *Nat. Biotechnol.* **26**, 1367–1372
53. Panse, C. G., Grossman, J., and Oesterreicher, S. B. (2013) protViz: Visualizing and analyzing mass spectrometry related data in proteomics. *R Package*, version 3.0.2, Functional Genomics Center Zurich, Zurich
54. MacLean, B., Tomazela, D. M., Shulman, N., Chambers, M., Finney, G. L., Frewen, B., Kern, R., Tabb, D. L., Liebler, D. C., and MacCoss, M. J. (2010) Skyline: an open source document editor for creating and analyzing targeted proteomics experiments. *Bioinformatics* **26**, 966–968
55. Vihusola, A., Snoek, L. B., Riksen, J. A., and Kammenga, J. E. (2010) Genome-wide gene expression analysis in response to organophosphorus pesticide chlorpyrifos and diazinon in *C. elegans*. *PLoS One* **5**, e12145
56. Blagoev, B., Kratchmarova, I., Ong, S. E., Nielsen, M., Foster, L. J., and Mann, M. (2003) A proteomics strategy to elucidate functional protein-protein interactions applied to EGF signaling. *Nat. Biotechnol.* **21**, 315–318
57. Alexa, A., Rahnenführer, J., and Lengauer, T. (2006) Improved scoring of functional groups from gene expression data by decorrelating GO graph structure. *Bioinformatics* **22**, 1600–1607
58. Alexa, A., and Rahnenfuhrer, J. (2010) topGO: Enrichment analysis for gene ontology. *R package*, Version 2.23.0., Saarbrucken.
59. Budovskaya, Y. V., Wu, K., Southworth, L. K., Jiang, M., Tedesco, P., Johnson, T. E., and Kim, S. K. (2008) An elt-3/elt-5/elt-6 GATA transcription circuit guides aging in *C. elegans*. *Cell* **134**, 291–303
60. McElwee, J., Bubb, K., and Thomas, J. H. (2003) Transcriptional outputs of the *Caenorhabditis elegans* forkhead protein DAF-16. *Aging Cell* **2**, 111–121
61. Murphy, C. T., McCarroll, S. A., Bargmann, C. I., Fraser, A., Kamath, R. S., Ahringer, J., Li, H., and Kenyon, C. (2003) Genes that act downstream of DAF-16 to influence the lifespan of *Caenorhabditis elegans*. *Nature* **424**, 277–283
62. Tepper, R. G., Ashraf, J., Kaletsky, R., Kleemann, G., Murphy, C. T., and Bussemaker, H. J. (2013) PQM-1 complements DAF-16 as a key transcriptional regulator of DAF-2-mediated development and longevity. *Cell* **154**, 676–690
63. Rivals, I., Personnaz, L., Taing, L., and Potier, M. C. (2007) Enrichment or depletion of a GO category within a class of genes: which test? *Bioinformatics* **23**, 401–407
64. Vizcaino, J. A., Deutsch, E. W., Wang, R., Csordas, A., Reisinger, F., Rios, D., Dianes, J. A., Sun, Z., Farrah, T., Bandeira, N., Binz, P. A., Xenarios, I., Eisenacher, M., Mayer, G., Gatto, L., Campos, A., Chalkley, R. J., Kraus, H. J., Albar, J. P., Martinez-Bartolomé, S., Apweiler, R., Omenn, G. S., Martens, L., Jones, A. R., and Hermjakob, H. (2014) ProteomeXchange provides globally coordinated proteomics data submission and dissemination. *Nat. Biotechnol.* **32**, 223–226
65. Wang, M., Weiss, M., Simonovic, M., Haertinger, G., Schrimpf, S. P., Hengartner, M. O., and von Mering, C. (2012) PaxDb, a database of protein abundance averages across all three domains of life. *Mol. Cell. Proteomics* **11**, 492–500
66. Samuelson, A. V., Carr, C. E., and Ruvkun, G. (2007) Gene activities that mediate increased life span of *C. elegans* insulin-like signaling mutants. *Genes Dev.* **21**, 2976–2994
67. Lee, S. J., Murphy, C. T., and Kenyon, C. (2009) Glucose shortens the life span of *C. elegans* by downregulating DAF-16/FOXO activity and aquaporin gene expression. *Cell Metab.* **10**, 379–391
68. Priebe, S., Menzel, U., Zarse, K., Groth, M., Platzer, M., Ristow, M., and Guthke, R. (2013) Extension of life span by impaired glucose metabolism in *Caenorhabditis elegans* is accompanied by structural rearrangements of the transcriptomic network. *PLoS One* **8**, e77776
69. Garsin, D. A., Villanueva, J. M., Begun, J., Kim, D. H., Sifri, C. D., Calderwood, S. B., Ruvkun, G., and Ausubel, F. M. (2003) Long-lived *C. elegans* daf-2 mutants are resistant to bacterial pathogens. *Science* **300**, 1921
70. Papp, D., Csermely, P., and Sőti, C. (2012) A role for SKN-1/Nrf in pathogen resistance and immunosenescence in *Caenorhabditis elegans*. *PLoS Pathog.* **8**, e1002673
71. Doroszuk, A., Snoek, L. B., Fradin, E., Riksen, J., and Kammenga, J. (2009) A genome-wide library of CB4856/N2 introgression lines of *Caenorhabditis elegans*. *Nucleic Acids Res.* **37**, e110
72. McGrath, P. T., Rockman, M. V., Zimmer, M., Jang, H., Macosko, E. Z., Kruglyak, L., and Bargmann, C. I. (2009) Quantitative mapping of a digenic behavioral trait implicates globin variation in *C. elegans* sensory behaviors. *Neuron* **61**, 692–699
73. Persson, A., Gross, E., Laurent, P., Busch, K. E., Bretes, H., and de Bono, M. (2009) Natural variation in a neural globin tunes oxygen sensing in wild *Caenorhabditis elegans*. *Nature* **458**, 1030–1033
74. Qabazard, B., Ahmed, S., Li, L., Arif, V. M., Moore, P. K., and Stürzenbaum, S. R. (2013) *C. elegans* aging is modulated by hydrogen sulfide and the sulfhydrylase/cystaline synthase cysl-2. *PLoS One* **8**, e80135
75. Geuens, E., Hoogewijs, D., Nardini, M., Vinck, E., Pesce, A., Kiger, L., Fago, A., Tilleman, L., De Henau, S., Marden, M. C., Weber, R. E., Van Doorslaer, S., Vanfleteren, J., Moens, L., Bolognesi, M., and Dewilde, S. (2010) Globin-like proteins in *Caenorhabditis elegans*: *in vivo* localization, ligand binding and structural properties. *BMC Biochem.* **11**, 17
76. Hoogewijs, D., Geuens, E., Dewilde, S., Vierstraete, A., Moens, L., Vinogradov, S., and Vanfleteren, J. R. (2007) Wide diversity in structure and expression profiles among members of the *Caenorhabditis elegans* globin protein family. *BMC Genomics* **8**, 356

### A2.3 Reprint of the research article *Singh et al., 2016*

This section contains reprint of the research article entitled “Natural genetic variation influences protein abundances in *C. elegans* developmental signalling pathways” published in PLOS ONE journal on March 17, 2016 (volume 11, issue 3, e0149418). The supplemental materials are available at the online version of the research article under:
http://journals.plos.org/plosone/article?id=10.1371/journal.pone.0149418#sec023

PLOS | ONE

RESEARCH ARTICLE

# Natural Genetic Variation Influences Protein Abundances in *C. elegans* Developmental Signalling Pathways

**Kapil Dev Singh[1], Bernd Roschitzki[2], L. Basten Snoek[3], Jonas Grossmann[2], Xue Zheng[1], Mark Elvin[4], Polina Kamkina[1], Sabine P. Schrimpf[1], Gino B. Poulin[4], Jan E. Kammenga[3], Michael O. Hengartner[1]***

**1** Institute of Molecular Life Sciences, University of Zurich, Zurich, Switzerland, **2** Functional Genomics Center Zurich, University of Zurich and ETH Zurich, Zurich, Switzerland, **3** Laboratory of Nematology, Wageningen University, Wageningen, The Netherlands, **4** Faculty of Life Sciences, The University of Manchester, Manchester, United Kingdom

* michael.hengartner@uzh.ch

OPEN ACCESS

**Citation:** Singh KD, Roschitzki B, Snoek LB, Grossmann J, Zheng X, Elvin M, et al. (2016) Natural Genetic Variation Influences Protein Abundances in *C. elegans* Developmental Signalling Pathways. PLoS ONE 11(3): e0149418. doi:10.1371/journal.pone.0149418

**Editor:** Suzannah Rutherford, Fred Hutchinson Cancer Research Center, UNITED STATES

**Received:** October 18, 2015

**Accepted:** January 30, 2016

**Published:** March 17, 2016



**Data Availability Statement:** All SRM raw data, transition lists, MS/MS library and mProphet output files are available from the PeptideAtlas (http://www.peptideatlas.org) database (accession number PASS00748). QTL (protein and apoptosis) and processed transcriptomics data files are available from the WormQTL (http://www.wormqtl.org) database (accession numbers 70-75 and 80). All microarray data files are available from the Gene Expression Omnibus (GEO; http://www.ncbi.nlm.nih.gov/geo) database (accession number GSE77905).

## Abstract

Complex traits, including common disease-related traits, are affected by many different genes that function in multiple pathways and networks. The apoptosis, MAPK, Notch, and Wnt signalling pathways play important roles in development and disease progression. At the moment we have a poor understanding of how allelic variation affects gene expression in these pathways at the level of translation. Here we report the effect of natural genetic variation on transcript and protein abundance involved in developmental signalling pathways in *Caenorhabditis elegans*. We used selected reaction monitoring to analyse proteins from the abovementioned four pathways in a set of recombinant inbred lines (RILs) generated from the wild-type strains N2 (Bristol) and CB4856 (Hawaii) to enable quantitative trait locus (QTL) mapping. About half of the cases from the 44 genes tested showed a statistically significant change in protein abundance between various strains, most of these were however very weak (below 1.3-fold change). We detected a distant QTL on the left arm of chromosome II that affected protein abundance of the phosphatidylserine receptor protein PSR-1, and two separate QTLs that influenced embryonic and ionizing radiation-induced apoptosis on chromosome IV. Our results demonstrate that natural variation in *C. elegans* is sufficient to cause significant changes in signalling pathways both at the gene expression (transcript and protein abundance) and phenotypic levels.

## Introduction

Most complex traits, including many common diseases such as cancer, neurodegenerative, and autoimmune diseases are affected by multiple genes. There is overwhelming evidence that individuals with different genotypes have a different susceptibility to various complex diseases. For instance, the genetic background influences onset and progression of cancer in mice and

**Funding:** This work was supported by the Swiss National Science Foundation (grant No. 31003A_143932; http://www.snf.ch) to MOH and the European Community's Health Seventh Framework Programme under project PANACEA (project No. 222936; http://www.panaceaproject.eu) to JEK. LBS was funded by the Netherlands Organisation for Scientific Research (project No. 823.01.001; http://www.nwo.nl). The funders had no role in study design, data collection and analysis, decision to publish, or preparation of the manuscript.

**Competing Interests:** The authors have declared that no competing interests exist.

humans [1–3] and also plays an important role in other complex diseases such as renal failure [4], autoimmune diseases [5], and retinal degeneration [6]. Studying natural genetic variation is crucial for understanding the effect of allelic variation of gene expression and for determining the genetic basis of complex traits. However, the genetic mechanisms underlying these effects are often poorly understood.

To unravel how the genetic background affects signalling pathways that contribute to complex diseases, we used the model organism *Caenorhabditis elegans* [7]. Specifically, we selected genes involved in apoptosis [8], as well as genes involved in three pathways (MAPK [9], Notch [10], and Wnt [11]) that control vulva development, an important phenotypic readout in *C. elegans* for these pathways [12,13]. All four signalling pathways are evolutionarily conserved and many human homologs of these *C. elegans* signalling proteins [14] have been linked to various cancers, as well as neurodegenerative, cardiovascular, and other diseases [15–19].

Signalling pathways in *C. elegans* are usually studied in the canonical wild-type N2 (Bristol [20]) background through the screening for and characterization of induced mutations, which often lead to complete loss of gene function and show distinctive phenotypic defects. By contrast, natural variation usually causes more subtle phenotypic changes, as natural selection rapidly selects against mutations with strong negative impact.

To explore the effect of natural variation, we selected two highly divergent wild-type strains [21,22], N2 and CB4856 (Hawaii [23]), and a set of recombinant inbred lines (RILs) generated from them [24–27]. Previous transcriptome analysis of N2, CB4856, and RILs from this set showed significant heritable variation in gene expression at the transcript level, which could be mapped to several expression QTLs (eQTLs) [24,28–31], but very little is known about heritable variation at the protein level. Here we quantified the abundances of selected proteins from four cancer signalling pathways (apoptosis, MAPK, Notch, and Wnt) using selected reaction monitoring (SRM), a mass spectrometric technique for targeted quantitative proteomics that is characterized by its high specificity, sensitivity, and wide dynamic range [32,33]. We also measured apoptosis levels in both parental strains and RILs. We found that natural variation in *C. elegans* causes significant changes in signalling pathways both at the gene expression (transcript and protein abundance) and at the phenotypic levels.

## Results and Discussion

We selected 156 proteins (S1 Table) that have been implicated in one of four signalling pathways in *C. elegans*: apoptosis (62 proteins), MAPK (59 proteins), Notch (18 proteins), and Wnt (17 proteins). These 156 proteins span over three orders of magnitude in abundance [34], with approximately half of them being in the range of 1–20 ppm (S1A Fig and S1 Table), and show a similar abundance distribution as the overall *C. elegans* proteome (S1B Fig).

### SRM measurements

In a first step, we performed an experiment to find proteins that are differently abundant in the two parental strains N2 and CB4856. Out of 148 tested proteins (S2 Fig and S2 Table) we successfully measured the abundance of between 104 and 116 proteins in each sample; 71 proteins could be quantified in two biological replicates in both strains (S3 Fig). For most of these, the protein abundance difference was very small between the two strains (below our fold change cut-off, which we set at 1.3-fold, based on the variation in abundance that we measured between biological replicates of the same strain; S4 Fig) and also correlated poorly with the differences in transcript abundance levels (S5 Fig). The extent of conservation in protein abundance in the dataset of the four signalling pathways is very similar to the variation that can be observed at the level of the whole proteome using stable isotope labelling by amino acids in cell

culture (SILAC) based shotgun mass spectrometry data from [35] (Fig 1 and S4 Fig). Taken together, these observations suggest that for most of the measured proteins, the small variation in protein abundance observed between CB4856 and N2 is not due to genetic variation between the two strains, but rather comes from measurement errors or from the innate variation that also exists between biological replicates of the same strain (S4 Fig).

Previous work on wild isolates has shown that wild-type strains often contain hidden variation in gene expression due to compensatory mutations within the genome [37,38]. Crossing of two wild types followed by the generation of RILs can lead to significant variation due to shuffling of the parental genotypes and the segregation of compensatory mutations [30,37,38]. To test this concept at the proteome level, we analysed RILs generated from the two wild types. As was previously reported [24,28,29], many RILs show a higher level of variation in transcript abundance than either parental strain (Fig 2A). We selected four RILs (WN31, WN71, WN105, and WN186) that showed large variation in transcript abundance for the 148 selected proteins compared with the parental strains (Fig 2A) and that also showed great genetic diversity between them (Fig 2B and 2C).

Between 71 and 85 proteins (out of 148 proteins measured) were quantified by SRM in the four selected RILs; 44 proteins (represented by 114 peptides) were quantified in all four RILs. To gain more statistical confidence, we re-measured these 44 proteins (S2 Table) in the four

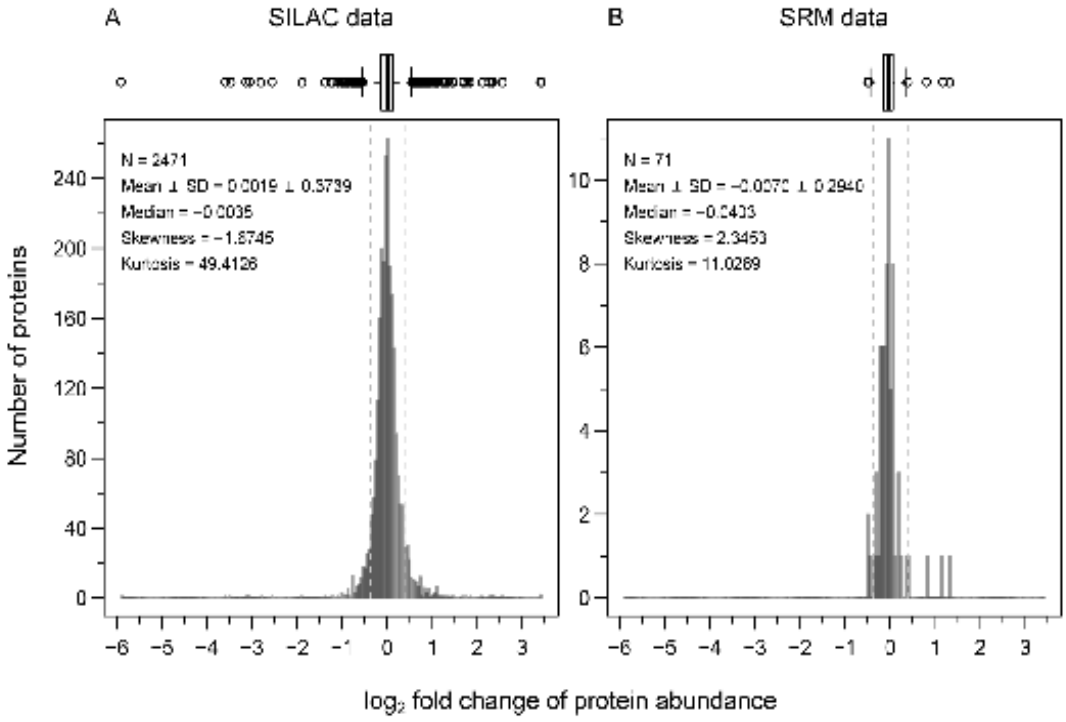


**Fig 1. Signalling pathway proteins show a similar variation in abundance between N2 and CB4856 as a *C. elegans* shotgun proteome dataset.** Histogram with Tukey-style box plot [36] on the top for protein abundances measured in CB4856 relative to N2. Vertical dashed lines represent the fold change cut-off of 1.3 (~ 0.38 on $\log_2$ scale). (A) The *C. elegans* shotgun proteome dataset was quantified using SILAC (data from [35]). (B) Signalling pathway proteins were quantified using SRM.

doi:10.1371/journal.pone.0149418.g001

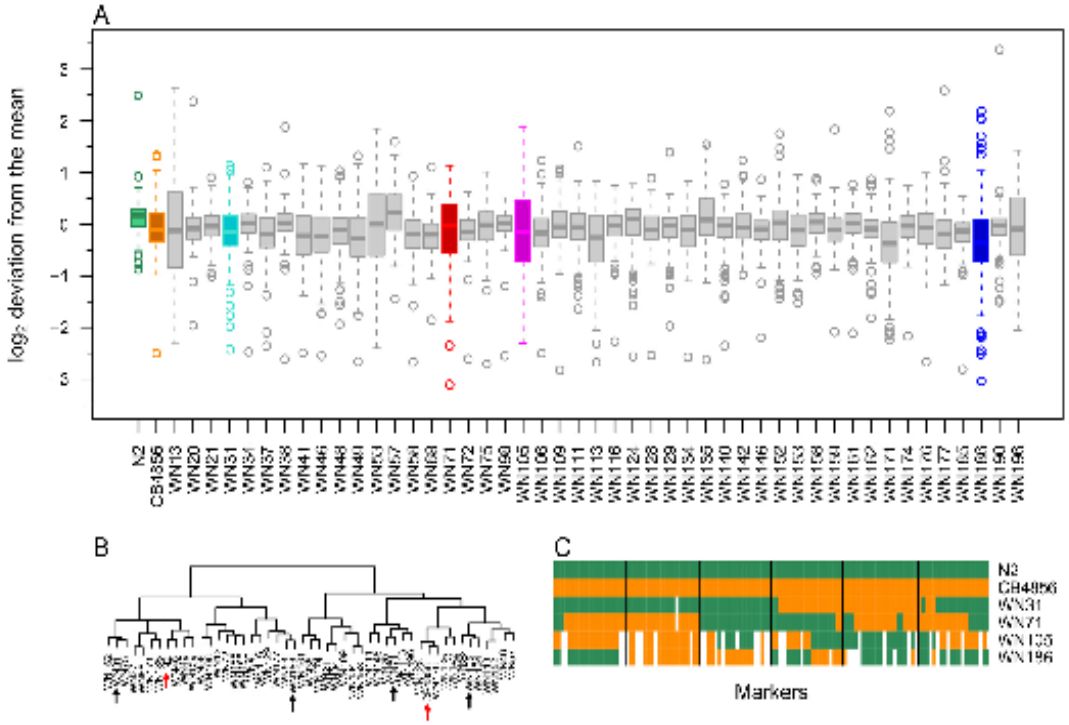


**Fig 2. Many RILs have a higher transcript expression level variation than the parental strains.** Gene expression at the transcript level was quantified in N2, CB4856, and 47 RILs by two-colour microarray analysis. (A) Tukey-style box plot representing $log_2$ scaled deviations of the gene expression value from the mean across all samples. Four genetically different RILs (WN31, WN71, WN105, and WN186) that showed large variation in transcript abundance were selected for proteome quantification. (B) Hierarchical clustering of the 47 RILs and the two parental strains based on their genotype (see "Additional file 1" of [25] for details). Clustering was done with R functions "dist" and "hclust" from the package stats (version 3.2.2) using "euclidean" distance and "ward.D2" method. Four RILs (black arrows) were chosen from different clusters to ensure maximum genetic diversity; red arrows indicate parental strains. (C) Genotype of the four selected RILs and the two parental strains. Vertical lines separate chromosomes I to V and X from left to right.

doi:10.1371/journal.pone.0149418.g002

selected RILs as well as in the two parental strains with three biological replicates (Fig 3A). Generally, the quantified proteins showed a trend to be up-regulated in CB4856 and in the RILs relative to N2 ($P \leq 0.01$; Fig 3A), and about a quarter of the protein abundance changes were both statistically significant ($P \leq 0.05$) and above the fold change cut-off of 1.3 (~ 0.38 on $log_2$ scale; Fig 3A and S6 Fig). To determine how much of the observed variation in protein levels could be attributed to genetic variation, we calculated the broad-sense heritability [39] for the 44 proteins and found that on average, about half of the measured protein level variation was due to genetic variation (Fig 3B and S1 Table). We tested the extent of variation in abundance of the 44 protein, at both the transcript and protein level (relative to N2) using the Fligner-Killeen test for homogeneity of variances. No significant variation could be detected except between CB4856 and WN105 at the transcript level (Fig 4). Indicating that for this smaller set of 44 genes, the tested RILs do not show greater overall levels of expression, at the transcript and protein levels compared to the parental strains.

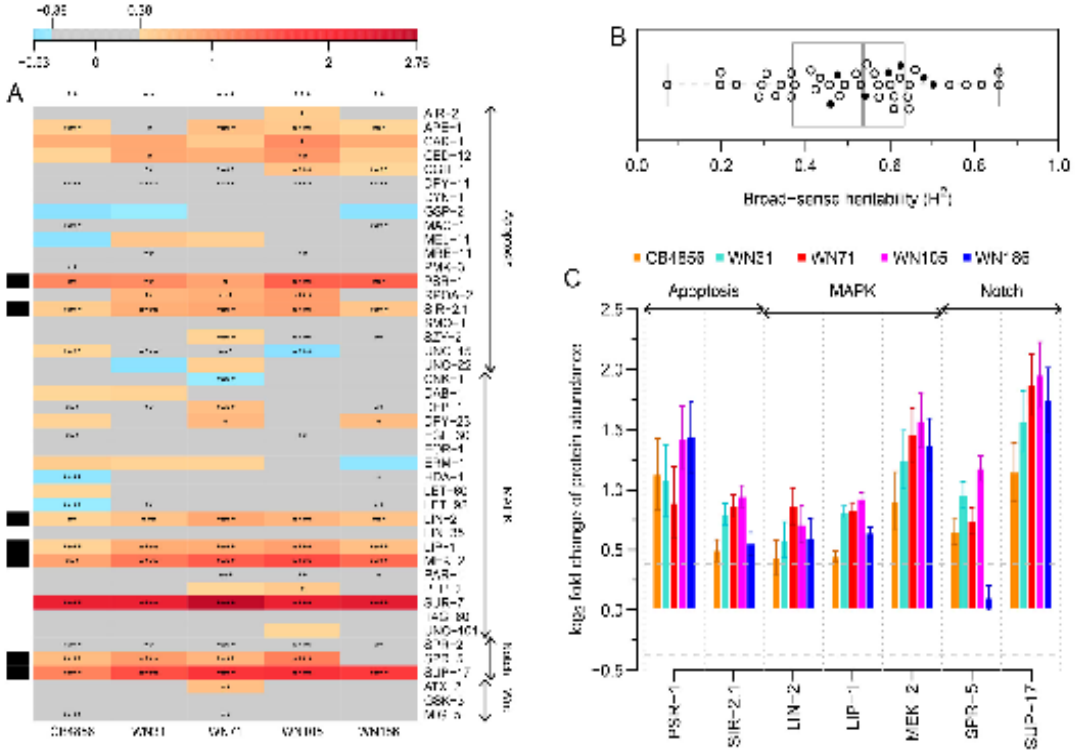


**Fig 3. Signalling pathway proteins tend to be up-regulated in CB4856 and in RILs compared to N2.** Protein abundance was quantified by SRM. Identification of the true peak group was performed using the mProphet software, followed by protein significance analysis using intensity-based linear mixed-effects model implemented in MSstats. (A) Heat map showing differential abundance of 44 proteins in CB4856 and four empirically selected RILs relative to N2. Blue and red shades represent $\log_2$ scaled fold changes, grey colour shows the fold change cut-off of 1.3 (~0.38 on $\log_2$ scale) and number of asterisks represent BH corrected *P*-values. Black bands on the left side indicate proteins selected for subsequent pQTL mapping. Number of asterisks on top of each column represent BH corrected *P*-values from one sample t-test ($H_0$: $\mu = 0$ and $H_1$: $\mu \neq 0$) on protein fold changes relative to N2; *$P \leq 0.05$; **$P \leq 0.01$; ***$P \leq 0.001$; ****$P \leq 0.0001$. (B) Tukey-style box plot of broad-sense heritability for the 44 proteins shown in panel A. Scatter points overlaid on the box plot represent the broad-sense heritability values for the individual proteins (solid black circles correspond to selected proteins). (C) Bar graph of selected proteins from panel A. Horizontal dashed lines represent the fold change cut-off of 1.3 (~0.38 on $\log_2$ scale). Error bars represent SEM between three biological replicates.

doi:10.1371/journal.pone.0149418.g003

## Protein QTL mapping

Most of the 156 proteins that we selected for SRM analysis have weak eQTLs at the transcript level (S1 Table) [27,40,41]. To explore the genetic basis of the protein abundance differences between parental strains and RILs, and to determine potential regulatory genes associated with the observed protein abundance differences, we performed protein quantitative trait locus (pQTL) mapping on seven proteins (PSR-1, SIR-2.1, LIN-2, LIP-1, MEK-2, SPR-5, and SUP-17; represented by 14 peptides; Figs 3A, 3C and S6) that showed significant abundance differences and fold changes above 1.3 among the six strains (two parental strains and four selected RILs). This mapping was used to determine whether genetic variation in the gene itself (or nearby location) was responsible for the observed protein abundance changes (local pQTL) or a change in another region away from the gene (distant pQTL) [42]. Mapping was done by linking the variation in abundances of the seven selected proteins (S2 Table) within the

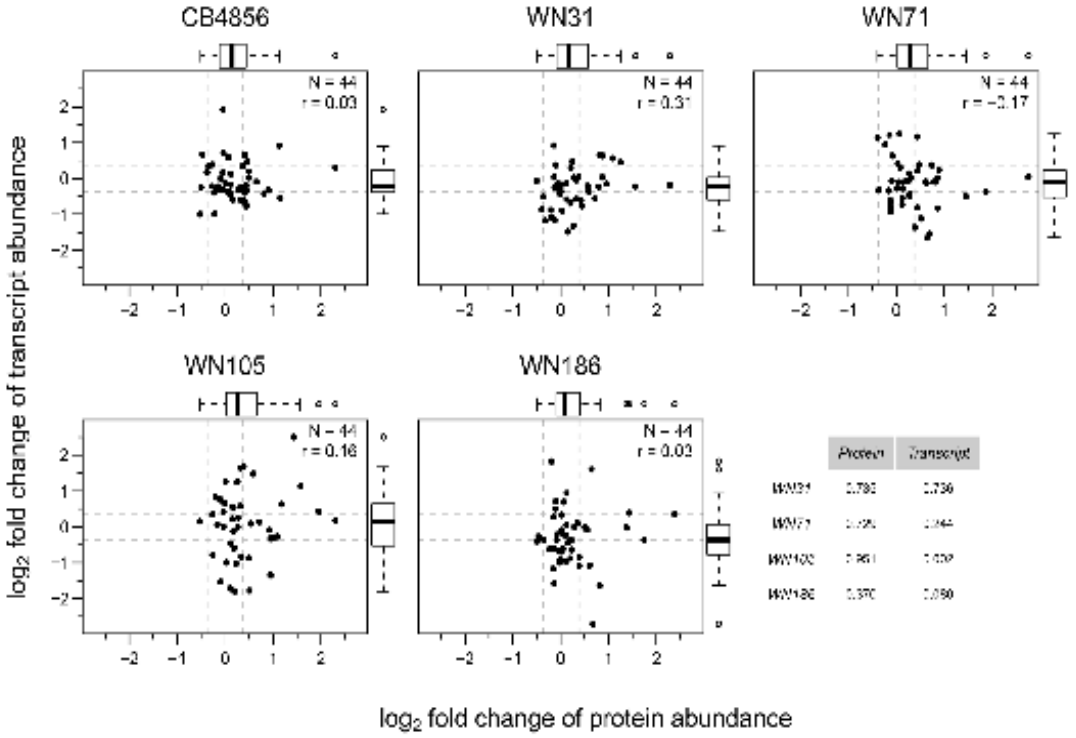


**Fig 4. RILs show similar protein and transcript abundance variation for the tested 44 genes as the parental strains.** Comparison of protein and transcript abundance ($log_2$ scaled fold changes relative to N2) for 44 signalling pathway proteins in CB4856 and four selected RILs. Horizontal and vertical dashed lines represent the fold change cut-off of 1.3 (~ 0.38 on $log_2$ scale). Tukey-style boxplot on top and right side represents variability in protein and transcript $log_2$ fold changes respectively. Pearson correlation coefficient is denoted by r. Table on bottom right represents the *P*-values from the Fligner-Killeen test for homogeneity of variances between protein (column 1) and transcript (column 2) data for RILs compared with CB4856.

doi:10.1371/journal.pone.0149418.g004

parental strains and 48 RILs (the four selected RILs and 44 additional ones; S7 Fig) with the genotypic variation in the same samples. For one of the seven proteins, PSR-1 (phosphatidylserine receptor), we found a significant distant pQTL on the left arm of chromosome II: the presence of the CB4856 allele at this position strongly correlated with a high PSR-1 protein abundance (Fig 5). Interestingly, this distant QTL is not apparent at the transcript level [24,29,43], suggesting that it likely affects a late step in the gene expression process (e.g. translation efficiency or protein stability). Early work in mouse [44] and yeast [45] showed that most of the pQTLs did not have corresponding variation at the transcript level, in contrast to this a much better agreement was found between eQTLs and corresponding pQTLs [46]. Recent studies in yeast using a new experimental design to overcome the sample size limitation of previous studies also suggest that over half of the previously reported eQTLs have corresponding pQTLs [47,48].

The large number of RIL measurements also allowed us to compare in more detail the relative variations in transcript and protein abundances for the seven selected proteins (Fig 6). Whereas some proteins (PSR-1, LIN-2, and MEK-2) showed a tendency for greater variation at

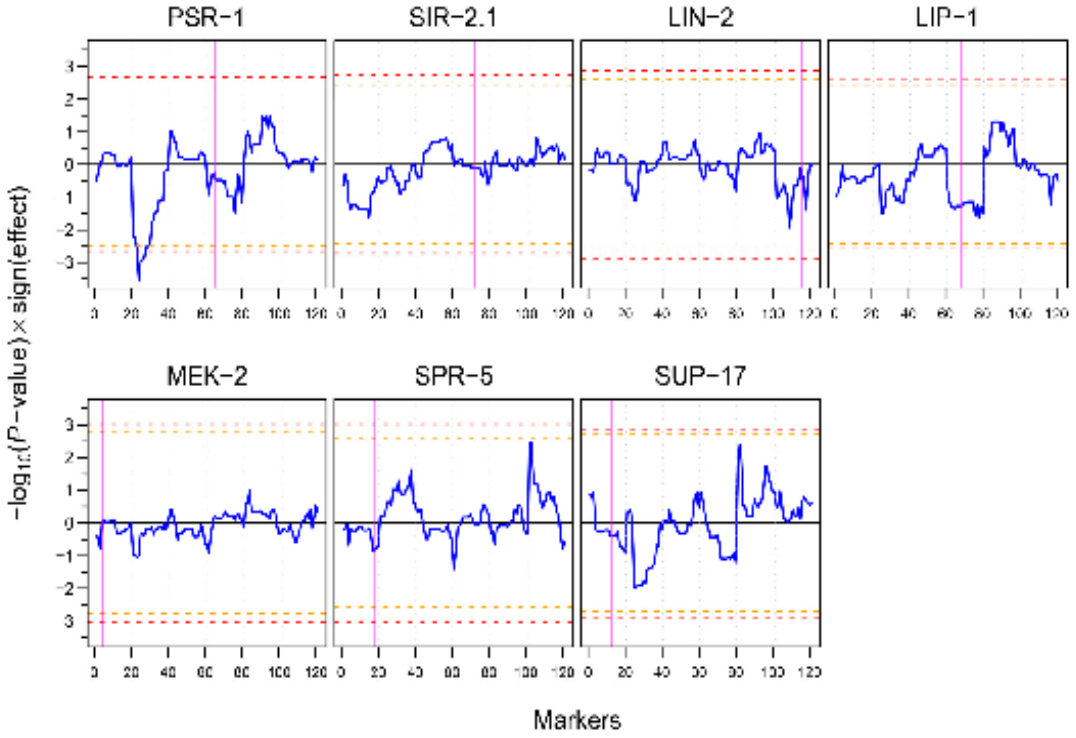


**Fig 5. pQTL profiles of seven selected signalling pathway proteins.** Blue curves show the significance of the pQTLs multiplied by the sign of the effect of the N2 allele (positive values of blue curve indicate higher protein abundance when the N2 allele is present, whereas negative values indicate higher protein abundance when the CB4856 allele is present). Horizontal orange and red dashed lines show 0.1 and 0.05 FDR thresholds respectively. Vertical dotted grey lines separate chromosomes I to V and X from left to right. Vertical magenta bands indicate the position of the gene in the genome. PSR-1 shows a significant pQTL on the left arm of chromosome II.

doi:10.1371/journal.pone.0149418.g005

the transcript level, SIR-2.1 showed a greater protein abundance variation while the remaining genes showed similar variation, at both protein and transcript levels.

## Natural variation in apoptosis levels

The PSR-1 protein has been implicated in the clearance of apoptotic cells in *C. elegans* [49,50]. To determine whether the changes in PSR-1 protein abundance might affect corpse clearance efficiency, we quantified both developmental [51] and germ line (physiological and DNA-damaged induced) [52] apoptosis levels, by counting apoptotic cell corpse numbers, both in embryos and in the adult germ line (Fig 7A–7C). Cell corpse numbers were consistently lower in CB4856 compared to N2. Although most RILs showed apoptotic cell corpse numbers between the two parental strains, some showed more extreme apoptotic levels than the parental strains (higher than N2, or lower than CB4856).

Unfortunately, we did not find any correlation between changes in PSR-1 protein abundance and apoptosis levels among the strains tested (Fig 7D–7F). Given that even the complete loss of PSR-1 function only results in a very mild change in cell corpse clearance [49], this

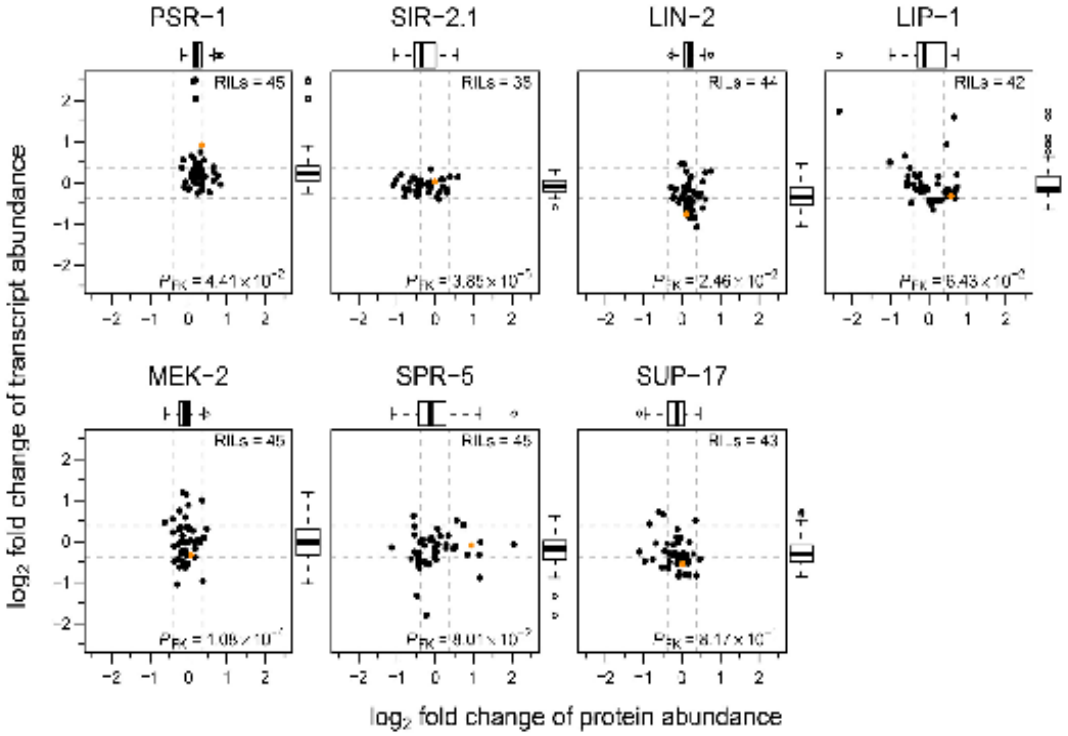


**Fig 6. Protein and transcript abundance variation of the signalling pathway proteins used in pQTL mapping in CB4856 and 45 RILs.** Comparison of protein and transcript abundance ($log_2$ scaled fold changes relative to N2) in CB4856 (solid orange circle) and RILs for the seven proteins used in pQTL mapping. Horizontal and vertical dashed lines represent the fold change cut-off of 1.3 (~0.38 on $log_2$ scale). Tukey-style box plot on top and right side represents variability in protein and transcript $log_2$ fold changes respectively. *P*-value from Fligner-Killeen test for homogeneity of variances between protein and transcript data is denoted by $P_{FK}$.

doi:10.1371/journal.pone.0149418.g006

result is not unexpected. We conclude that the variation in apoptosis observed between the RILs must arise from other genetic changes present between N2 and CB4856.

QTL mapping of the apoptosis levels revealed the presence of a QTL that affects ionizing radiation (IR)-induced apoptosis on chromosome IV and a QTL on the left arm of chromosome IV that affects embryonic cell death (in both cases, the presence of the N2 allele results in increased cell corpse numbers), whereas no QTLs were detected for physiological germ cell apoptosis (Fig 7G–7I). The QTL for IR-induced germ cell death is very broad, and might conceivably even consist of two (or more) linked QTLs on chromosome IV. By contrast, the embryonic cell corpse QTL is very sharp and maps close to, but can clearly be separated from, the physical position of *psr-1*. Interestingly, this region includes several genes that have been linked to apoptosis or cell corpse cleaning, including the engulfment gene *ced-10* [53] and the E3 ubiquitin ligase *eel-1* [54]. There are 8 and 20 SNPs between CB4856 and N2 for these two genes. While none of the *ced-10* SNPs change the protein sequence, one of the 20 SNPs in *eel-1* induces an amino acid change. Further analysis will be required to determine if any of those SNPs are responsible for the observed QTL in embryonic cell corpse apoptosis.

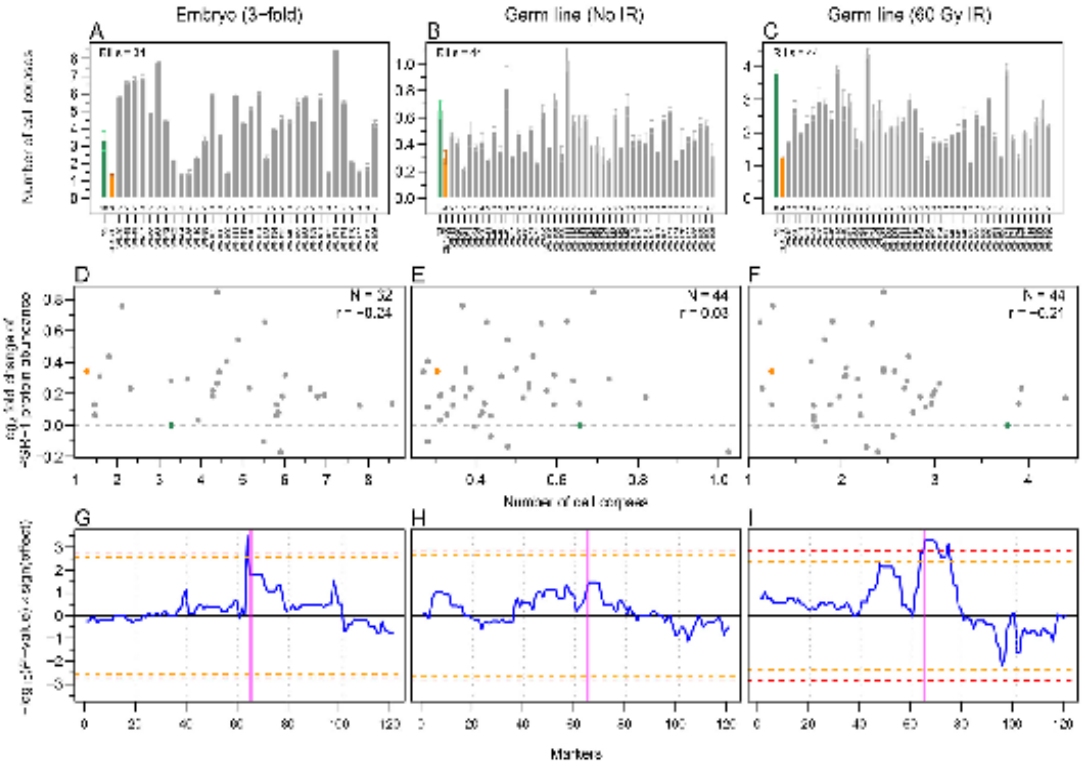


**Fig 7. Analysis of variation in embryonic and germ line apoptosis in parental strains and RILs.** (A-C) Quantification of apoptotic cell corpse numbers in embryos (A), germ line without ionizing radiation (IR; B), and with 60 Gy IR (C). Error bars represent SEM between numbers of biological replicates indicated at the bottom of each bar. (D-F) Natural variation in apoptosis levels of parental strains and RILs does not correlate with the PSR-1 protein abundance (relative to N2). Scatter plots (CB4856 in orange and N2 in green) of PSR-1 protein abundance and apoptotic levels in embryos (D), germ line without IR (E), and with 60 Gy IR (F). Pearson correlation coefficient is denoted by r. (G-I) Embryonic and IR-induced apoptosis shows a significant QTL on chromosome IV. QTL profiles of apoptotic phenotype in embryos (G), adult germ line without IR (H) and with 60 Gy IR (I). Blue curves show the significance of the QTLs multiplied by the sign of the effect of the N2 allele (positive values of blue curve indicate higher apoptosis level when the N2 allele is present, whereas negative values indicate higher apoptosis level when the CB4856 allele is present). Horizontal orange and red dashed lines show 0.1 and 0.05 FDR thresholds respectively. Vertical dotted grey lines separate chromosomes I to V and X from left to right. Vertical magenta band indicates the position of *psr-1* gene in the genome.

doi:10.1371/journal.pone.0149418.g007

## Conclusion

Here we developed and made available a SRM method for 148 *C. elegans* signalling pathway proteins represented by 295 peptides.

Our quantitative analysis of protein abundance changes across six strains revealed that statistically significant changes can be found at a fair frequency (in about half of the cases), but that most of these changes are very minor in magnitude (less than 1.3-fold). This is not surprising, as we assume that many of the tested proteins should be under significant evolutionary pressure, which likely precludes large changes in protein abundance. Nevertheless, we also identified a smaller number of genes that showed reproducible protein abundance changes in the two- to fourfold. QTL analysis on a selected set of seven proteins that showed particularly strong changes allowed us to identify a potential distant pQTL on the left arm of chromosome

II for PSR-1, a protein that intrinsically acts as receptor for phosphatidylserine exposed by apoptotic cells [49,50]. We also found two separate QTLs on chromosome IV affecting embryonic and IR-induced apoptosis levels, but failed to detect any correlation between PSR-1 abundance and apoptosis levels suggesting the involvement of other genes in these events.

## Materials and Methods

### Strains

We used *C. elegans* wild-type strains N2 [20] and CB4856 [23], and a set of 54 RILs (S3 Table) generated from them [24–27]. Unless otherwise stated all experiments were performed on synchronized developmental stage L4 worms, grown as previously described [7] on nematode growth medium (NGM) agar plates seeded with *Escherichia coli* strain OP50 at 20°C.

### Transcriptomics

From one sample of N2, CB4856 and 47 RILs (S3 Table) RNA extraction was done using RNEasy Micro Kit (Qiagen), as previously described (see "*RNA isolation*" from "Supplementary Materials and Methods" of [31]). Two-colour microarray was used to analyse the extracted RNA using 413 different hybridization probes (representing the 148 proteins of interest), as previously described (see "*Microarray sample preparation, scanning and normalization*" from "Supplementary Materials and Methods" of [31]) with the exception that we averaged normalised intensities from single channel for all probes of a gene, followed by the calculation of the $\log_2$ scale deviation of the gene expression value from the mean across all samples.

### Protein Extraction

Protein extraction was done as previously described [55] with minor changes. Briefly worm pellets were homogenized with glass-beads (G1277; Sigma-Aldrich) in lysis buffer (8 M urea, 50 mM Tris-HCl pH 8.3) in a 1:1:2 ratio using a benchtop homogenizer (FastPrep-24; MP Biomedicals) at 4°C, four times for 30 s at the speed of 5 m/s. After homogenization 0.125% SDS (v/v of buffer) was added and the homogenate was incubated at room temperature for 1 h to extract proteins. Proteins were separated from cell debris by centrifugation, and the protein concentration was determined using the Bradford reagent (B6916; Sigma-Aldrich).

### Database used for peptide spectrum matching

The *C. elegans* protein database wormpep212 (downloaded on March 2010, 24362 entries) was used for peptide spectrum matching. A decoy database generated by reversing the sequences was appended to forward database prior to the search, to facilitate the calculation of false discovery rate (FDR) [56], followed by addition of 259 common mass spectrometry contaminants yielding a total of 48983 entries.

### Sample Preparation for SRM

**Selection and solubilisation of hPTPs.** For each protein of interest, 1–5 tryptic proteotypic peptides (PTPs [57]; without cysteine and methionine; in total 377 PTPs; S2 Fig and S1 Table) were selected based on a *C. elegans* shotgun dataset [55]. These 377 PTPs were synthesized with isotopically labelled ($^{13}C$ and $^{15}N$) C-terminal Arginine and Lysine (SpikeTide L; JPT Peptide Technologies GmbH) as heavy labelled PTPs (hPTPs) for internal controls for SRM method development and SRM experiments. Prior to spike-in, hPTPs were dissolved in 180 µl of 20% ACN and 1% FA solvent. Either 0.4 nmol or 4 nmol of each peptide (depending on whether the abundance of the corresponding protein from PaxDb version 2.1 [34] is less

than 100 ppm or greater than 100 ppm) was mixed to generate a 100× hPTPs master-mix. Separate 100× hPTPs master-mixes were prepared for experiments targeting 148, 44, and 7 proteins with including only peptides corresponding to those proteins.

**Protein digestion and peptide pre-fractionation.** 250 μg of total worm protein from each sample was mixed with a 100 times diluted hPTP master-mix and digested overnight with trypsin (V5111; Promega) in the ratio of 50:1 (protein:trypsin) in digestion buffer (8 M urea, 50 mM Tris-HCl pH 8.3, 0.125% SDS, pH 7–8) at 37°C. Anionic SDS was removed after digestion using strong cation exchange (SCX). Samples were applied on SCX cartridges (Applied Biosystems) in loading buffer (10 mM $KH_2PO_4$, 25% ACN, pH < 3.0), and after washing peptides were eluted with 1 ml of elution buffer (10 mM $KH_2PO_4$, 25% ACN, 350 mM KCl, pH < 3.0). The cartridge was cleaned between subsequent samples using cleaning buffer (10 mM $KH_2PO_4$, 25% ACN, 1 M KCl, pH < 3). Salt was removed by solid phase extraction (SPE). Samples were applied on C18 SPE columns (Finisterre™, Teknokroma) in loading solution (5% ACN, 0.1% TFA), and after washing peptides were eluted with 1 ml of elution solution (60% ACN, 0.1% TFA). To circumvent the problem of inefficient ionization of target peptides in the complex background of the total worm protein extract, we used offline pre-fractionation by reversed phase-high pressure liquid chromatography (RP-HPLC) at pH 11.0 on an Agilent 1100 series HPLC system using a YMC Triart C18 column (150 mm × 4.6 mm ID, particle size 5 μm, pore size 12 nm) at a flow rate of 1 ml/min. Peptide samples were applied in buffer A (20 mM $K_2HPO_4$, 5% ACN, pH 11.0), and were eluted with a gradient between buffer A and buffer B (20 mM $K_2HPO_4$, 50% ACN, pH 11.0) into 47 fractions (pooled to 10 final fractions). The gradient profile was 2% buffer B between 0–20 min, 2%-50% buffer B between 20–50 min, 50%-98% buffer B between 50–55 min and 98% buffer B between 55–60 min followed by column re-equilibration to 2% buffer B in a total 80 min run. Buffer A and Buffer B were prepared from the stock solution (200 mM $K_2HPO_4$, pH 11.0).

For the pQTL experiments, peptide samples (directly after tryptic digestion) were pre-fractionated by hydrophilic interaction liquid chromatography (HILIC) on an Agilent 1100 series HPLC system using a YMC-pack polyamine II column (250 mm × 4 mm ID, particle size 5 μm, pore size 12 nm) at a flow rate of 0.85 ml/min. Peptide samples were applied in buffer A (8 mM $KH_2PO_4$, 75% ACN, pH 4.5), and were eluted with a gradient between buffer A and buffer B (100 mM $KH_2PO_4$, 5% ACN, pH 4.5) into 14 fractions (pooled to 3 final fractions). The gradient profile was 0% buffer B between 0–7.5 min, 0%-50% buffer B between 7.5–37.5 min, 50%-100% buffer B between 37.5–42.5 min and 100% buffer B between 42.5–47.5 min followed by column re-equilibration to 0% buffer B in a total 67.5 min run. Buffer A and buffer B were prepared from the stock solution (400 mM $KH_2PO_4$, pH 4.5).

To identify in which fractions the target peptides were eluted, all fractions were analysed by shotgun proteomics.

## SRM method development and analysis

**Generation of spectral library.** For each peptide two transitions were selected for doubly and triply charged precursor ions using Skyline [58] with the following transition settings (Precursor charges = 2 and 3, Ion charges = 1, Ion types = y, Product ions from = m/z > precursor, Product ions to = 2, and Always add = N-Terminal to Proline enabled). Transitions with |Q3-Q1| m/z < 40 were removed to reduce interferences. Remaining transitions were used to acquire MS/MS spectra triggered by SRM (SRM-triggered MS/MS [32,59]) on a TSQ Vantage (Thermo Scientific) triple quadrupole mass spectrometer (MS) coupled with a nanoLC-ultra chromatography instrument (Eksigent Technologies). Peptides were separated on a self-packed C-18 (Magic C18 AQ, particle size 3 μm, pore size 20 nm; Michrom) column (15 cm × 75 μm ID) at a flow rate of

200 nl/min. Peptides were loaded in 3% ACN, 0.1% FA and were eluted with a gradient between solvent A (water with 0.1% FA; Biosolves) and solvent B (ACN with 0.1% FA; Biosolves). The gradient profile was 5%-40% buffer B between 0–56 min, 40%-47% buffer B between 56–60 min, 47%-97% buffer B between 60–64 min and 97% buffer B between 64–71 min followed by column re-equilibration to 5% buffer B in a total 80 min run. The MS was operated in SRM mode ($Q1_{FWHM}$ = 0.40, $Q3_{FWHM}$ = 0.70, and dwell time = 20 ms with roughly 240 transitions per run), triggering MS/MS acquisition ($Q1_{FWHM}$ = 0.70, $Q3_{FWHM}$ = 0.70, and dwell time = 50 ms) if it detected counts higher than 300. MS/MS spectra were searched against the *C. elegans* protein database wormpep212 using the Mascot search engine (version 2.3.02; Matrix Science) [60], with the following search parameters (Type of search = MS/MS ion search, Enzyme = Trypsin with zero missed cleavage, Variable modifications = Arg10 and Lys8, Peptide mass-tolerance = 2 Da, and Fragment mass-tolerance = 0.8 Da). This resulted in the identification of 356 (94.4%) peptides with a 3.3% FDR at peptide level.

The Mascot search results in mascot DAT file format were used to build a MS/MS spectra library for 340 (90.2%) peptides corresponding to 154 proteins using Skyline with a score cut-off setting of 0.95. From this MS/MS spectra library, either doubly or triply charged precursor ions were selected for each peptide and for each selected precursor the five most intense y-ions fulfilling the following criteria (precursor $m/z > 400$ and $|Q3\text{-}Q1|$ $m/z > 5$) were selected to generate the final transition list 2950 transitions, including both heavy and light isoforms (S2 Fig and S2 Table).

**SRM.** After peptide pre-fractionation, ten fractions from RP-HPLC at pH 11.0 or three fractions from HILIC per strain were desalted by using ZipTip C18 (Millipore). Samples were applied at a speed of 1 drop/s in washing solution (5% ACN, 0.1% TFA; sample pH was adjusted below 3, if necessary with 5% ACN, 10% TFA), and after washing peptides were eluted with 80 μl of elution solution (60% ACN, 0.1% TFA) at a speed of 1 drop/s. Peptide samples were completely dried in a centrifugal evaporator and dissolved in 3% ACN, 0.1% FA solvent. SRM measurements were also performed on a TSQ Vantage (Thermo Scientific) coupled with a nanoLC-ultra (Eksigent Technologies). The setup was as described above except that the MS was operated in scheduled SRM (sSRM) mode ($Q1_{FWHM}$ = 0.40, $Q3_{FWHM}$ = 0.70, and cycle time = 2 s with a retention time window of 10 min for each peptide). For each off-line HPLC fraction a separate method containing only transitions for target peptides in that fraction was used. iRT kit (Biognosys) peptides were used as retention time standard [61].

## SRM data analysis

We used the mProphet software (version 1.0.4.1) [62] for the identification of true peak groups among each transition group record from SRM data, followed by a protein significance analysis using the intensity-based linear mixed-effects model [63] implemented in R [64] based on the package MSstats (version 0.99.0 for Fig 3A and version 1.99.0 for pQTL experiments) [65].

Briefly, at first raw data from the MS were converted into the mzXML file format [66] using command line tool ReAdW (version 4.0.2, ISB/SPC) with default options. Within mProphet, these mzXML files were mapped to transition lists using the mMap module (with parameter file = param_AQUA_heavy_stringent_ref_synthetic.def and machine type = QQQ) followed by peak picking using mQuest module (with parameter file = param_AQUA_heavy_stringent_ref_synthetic.def), and finally mQuest score optimization was done using the mProphet module (with workflow = SPIKE_IN). For each sample (based on mprophet_stat.xlsx file) an appropriate normalised discriminate score (d_score) cut-off was selected to keep the number of true positive peak groups higher and the number of false positive peak groups lower (for Fig 3A this was done by keeping a q-value of 0.05 and for

pQTL analysis by keeping a q-value of 0.01). Finally, identified peak groups with a d_score lower than the selected cut-off and dummy peak groups were filtered out from the final output file of mProphet software (mProphet_peakgroups.xlsx).

For MStats based analyses an input file (type "?RawData" in R console for details) with an intensity value for each transition of selected peak groups at both light and heavy isotopic level was generated using custom R scripts. To ensure that each peptide was analysed in the same fraction across all samples, we used fraction number concatenated with peptide as "PeptideSequence" in the input file. All fractions measured in one sample were considered to belong to the same "Run" under input file. Data analysis was done as previously described [63], considering interference in transitions and keeping "scope of biological variation" as restricted and "scope of technical variation" as expanded.

For S3 Fig, after mProphet analysis, Microsoft Excel and custom R scripts were used to sum intensity values for all transitions of a protein (including all detected peptides, if measured in all samples) at both light and heavy isotopic level separately for both replicates. These intensity values were appropriately scaled to make the median of resulted deconvoluted ratios $(CB4856_{Light}/CB4856_{Heavy})/(N2_{Light}/N2_{Heavy})$ for proteins in both biological replicates equal to 1. The ratios of averages of scaled intensities of CB4856 and N2 from both replicates represent the average protein fold change in CB4856 relative to N2. Whereas $\log_{10}$ transformed intensities were used to perform a two-sample equal variance t-test, resulting *P*-values were corrected for multiple hypothesis testing using the Benjamini-Hochberg (BH) procedure [67] (type "?p.adjust" in R console for details).

## QTL analysis

The QTLs were mapped using a custom R script applying linear regression on a single marker model as previously described [68]. For pQTLs, we used the $\log_2$ scale abundance of seven selected proteins in one sample of CB4856 and 48 RILs (S3 Table) relative to N2 as phenotypic data and genotypic variation in same samples using 121 markers [24]. Thresholds were determined per trait by 1000 permutations, where the trait values for the individual samples were randomly distributed before QTL mapping. Comparison to previously published eQTL data was done by extracting the data from WormQTL (http://www.wormqtl.org) [27,40,41]. QTL mapping of apoptosis levels was done as described above where average corpse number in N2, CB4856 and RILs were considered as phenotypic data.

## Apoptotic cell corpse counting

For embryonic cell corpse counting, between 6 and 23 embryos (3-fold stage) from N2, CB4856 and 34 RILs (S3 Table; Fig 7A for number of biological replicates) were counted in the head region using differential interference contrast (DIC) microscopy, as previously described [69] but instead of worms, mixed staged embryos were used. For germ line cell corpse counting, between 15 and 25 synchronized young adult hermaphrodites (12 h post L4/adult molts) from N2, CB4856 and 44 RILs (S3 Table; Fig 7B and 7C for number of biological replicates) were either exposed to no ionizing radiation (No IR) or 60 Gy ionizing radiation (60 Gy IR). After 24 h germ line apoptotic cell corpses were counted by using DIC microscopy, as previously described [69].

## Heritability

Broad-sense heritability [39] was calculated in R using the following formula $H^2 = msq.geno/(msq.geno + msq.error)$, where msq.geno was the mean sum of squares of genotype (between variation) and msq.error was the mean sum of squares of error (within variation).

### Statistical analysis

Unless otherwise stated all statistical tests were performed in R using the package stats (version 3.2.2). Specifically, function "t.test" (type "?t.test" in R console for details) was used for one sample t-test and function "fligner.test" (type "?fligner.test" in R console for details) was used for Fligner-Killeen test for homogeneity of variances.

## Supporting Information

**S1 Fig. Signalling pathway proteins used in this study show a similar abundance distribution as the whole *C. elegans* proteome.** Relative abundance data of *C. elegans* proteins were extracted from PaxDb version 2.1 [34]. (A) Data shown for 156 selected signalling pathway proteins. Each square represents a protein from one of four selected pathways, black squares (both solid and open) represent the 44 quantified proteins from Fig 3A; black open squares represent the 7 proteins (mostly under 20 ppm) selected for pQTL mapping. Parenthesis on top indicates number of proteins belonging to each pathway. (B) Histogram of all *C. elegans* proteins from PaxDb (top) and abundance distribution of the 156 selected signalling proteins (bottom, redrawn from A).
(TIF)

**S2 Fig. Outline of the SRM method development.** See Materials and Methods for details.
(TIF)

**S3 Fig. The N2 and CB4856 parental strains do not show any strong protein abundance variation of the tested signalling pathway proteins.** Protein abundance was quantified by SRM. Identification of the true peak group was performed using the mProphet software, followed by protein significance analysis using Microsoft Excel 2010 and custom R scripts. Horizontal dashed lines represent the fold change cut-off of 1.3 (~ 0.38 on $\log_2$ scale). Error bars represent SEM between two biological replicates. BH corrected *P*-values for all proteins from a two-sample equal variance t-test were above 0.9.
(TIF)

**S4 Fig. SILAC-based shotgun and SRM quantification show similar measurement accuracy.** Scatterplots with Tukey-style box plot representing variation in measurement of protein abundance in CB4856 relative to N2, within two biological replicates using SRM (A) and between the averages of two biological replicates using SRM with three biological replicates using SILAC-based shotgun mass spectrometry data from [35] (B) Horizontal and vertical dashed lines represent the fold change cut-off of 1.3 (~ 0.38 on $\log_2$ scale). Pearson correlation coefficient is denoted by r. (C) Tukey-style box plot for protein abundance of 71 proteins using SRM, indicating that variation in protein abundance between CB4856 and N2 is not greater than between two biological replicates of one of the two parental strains. Vertical dashed lines represent the fold change cut-off of 1.3 (~ 0.38 on $\log_2$ scale). N2-1 is 1$^{st}$ biological replicate of N2, N2-2 is 2$^{nd}$ biological replicate of N2, CB4856-1 is 1$^{st}$ biological replicate of CB4856, and CB4856-2 is 2$^{nd}$ biological replicate of CB4856.
(TIF)

**S5 Fig. Correlation between difference in protein and transcript abundances between the parental strains.** Scatterplots with Tukey-style box plot show $\log_2$ fold change for the tested signalling pathway proteins and transcripts in CB4856 relative to N2. Overall and pathway specific Pearson correlation coefficient is denoted by r.
(TIF)

**S6 Fig. Differential abundance of signalling pathway proteins in CB4856 and RILs relative to N2.** Tukey-style box plot of protein abundance ($log_2$ scaled fold changes relative to N2) redrawn from Fig 3A. Scatter points overlaid on the box plot represent the protein abundance values in CB856 and RILs. Most of the protein changes are either non-significant ($P > 0.05$) or below the fold change cut-off of 1.3 (~ 0.38 on $log_2$ scale; horizontal dashed lines). Seven proteins (unfilled black boxes) with significant abundance differences and fold changes above 1.3 were selected for pQTL mapping.
(TIF)

**S7 Fig. Differential abundance of proteins selected for pQTL mapping in CB4856 and 48 RILs.** Protein abundance was quantified by SRM. Identification of the true peak group was performed using the mProphet software, followed by protein significance analysis using an intensity-based linear mixed-effects model implemented in MSstats. Number of asterisks represent BH corrected *P*-values as follows, $^{*}P \leq 0.05$; $^{**}P \leq 0.01$; $^{***}P \leq 0.001$; $^{****}P \leq 0.0001$. Blue and red shades within heat map represent $log_2$ scaled fold changes in protein abundance relative to N2 (white boxes = no data).
(TIF)

**S1 Table. Proteins and peptides used in this study.** File with separate sheets for the list of 156 proteins (along with relative protein abundance data extracted from PaxDb version 2.1 and eQTL data extracted from WormQTL), broad-sense heritability values for 44 proteins, and the list of 377 PTPs.
(XLSX)

**S2 Table. SRM transitions used in this study.** File with separate sheets for SRM transition lists (targeting 148, 44, and 7 proteins) used in this study and a sheet with normalised retention time (iRT) of peptides.
(XLSX)

**S3 Table. Strains used in this study.** File with all the RILs along with parental strains N2 and CB4856 used in this study indicating (by "Yes") the experiments performed on them.
(XLSX)

**S4 Table. List of abbreviations.**
(XLSX)

## Acknowledgments

We thank Lukas Reiter from Biognosys for help with the mProphet software and Claudia Fortes from the Functional Genomics Center Zurich for help with offline HPLC.

## Author Contributions

Conceived and designed the experiments: KS BR LBS SPS JEK MOH. Performed the experiments: KS LBS XZ ME. Analyzed the data: KS LBS JG. Contributed reagents/materials/analysis tools: ME GBP JEK MOH. Wrote the paper: KS MOH. Helped develop SRM methods and provided SILAC-based shotgun data: PK.

## References

1. Freeman D, Lesche R, Kertesz N, Wang S, Li G, Gao J, et al. Genetic background controls tumor development in PTEN-deficient mice. Cancer Res. 2006; 66: 6492–6496. doi: 10.1158/0008-5472.CAN-05-4143 PMID: 16818619

2. Kristensen VN, Edvardsen H, Tsalenko A, Nordgard SH, Sorlie T, Sharan R, et al. Genetic variation in putative regulatory loci controlling gene expression in breast cancer. Proc Natl Acad Sci. 2006; 103: 7735–7740. doi: 10.1073/pnas.0601893103 PMID: 16684880
3. Seitz S, Korsching E, Weimer J, Jacobsen A, Arnold N, Meindl A, et al. Genetic background of different cancer cell lines influences the gene set involved in chromosome 8 mediated breast tumor suppression. Genes, Chromosom Cancer. 2006; 45: 612–627. doi: 10.1002/gcc.20325
4. Salido EC, Li XM, Lu Y, Wang X, Santana A, Roy-Chowdhury N, et al. Alanine-glyoxylate aminotransferase-deficient mice, a model for primary hyperoxaluria that responds to adenovirsl gene transfer. Proc Natl Acad Sci. 2006; 103: 18249–18254. doi: 10.1073/pnas.0607218103 PMID: 17110443
5. Tsuchiya N, Honda Z, Tokunaga K. Role of B cell inhibitory receptor polymorphisms in systemic lupus erythematosus: a negative times a negative makes a positive. J Hum Genet. 2006; 51: 741–750. doi: 10.1007/s10038-006-0030-4 PMID: 16946996
6. Thompson DA, Janecke AR, Lange J, Feathers KL, Hübner CA, McHenry CL, et al. Retinal degeneration associated with RDH12 mutations results from decreased 11-cis retinal synthesis due to disruption of the visual cycle. Hum Mol Genet. 2005; 14: 3865–3875. doi: 10.1093/hmg/ddi411 PMID: 16269441
7. Brenner S. The genetics of Caenorhabditis elegans. Genetics. 1974; 77: 71–94. PMID: 4366476
8. Conradt B. Programmed cell death. WormBook. 2005; 1–13. doi: 10.1895/wormbook.1.32.1
9. Sundaram M. RTK/Ras/MAPK signaling. WormBook. 2006; 1–19. doi: 10.1895/wormbook.1.80.1
10. Greenwald I. LIN-12/Notch signaling in C. elegans. WormBook. 2005; 1–16. doi: 10.1895/wormbook.1.10.1
11. Eisenmann DM. Wnt signaling. WormBook. 2005; 1–17. doi: 10.1895/wormbook.1.7.1
12. Sternberg PW. Vulval development. WormBook. 2005; 1–28. doi: 10.1895/wormbook.1.6.1
13. Schmid T, Hajnal A. Signal transduction during C. elegans vulval development: a NeverEnding story. Curr Opin Genet Dev. 2015; 32: 1–9. doi: 10.1016/j.gde.2015.01.006 PMID: 25677930
14. Shaye DD, Greenwald I. OrthoList: A Compendium of C. elegans Genes with Human Orthologs. PLoS One. 2011; 6: e20085. doi: 10.1371/journal.pone.0020085 PMID: 21647448
15. Saito RM, van den Heuvel S. Malignant Worms: What Cancer Research Can Learn from C. elegans. Cancer Invest. 2002; 20: 264–275. doi: 10.1081/CNV-120001153 PMID: 11901546
16. Favaloro B, Allocati N, Graziano V, Di Ilio C, De Laurenzi V. Role of apoptosis in disease. Aging (Albany NY). 2012; 4: 330–349.
17. Kim EK, Choi EJ. Pathological roles of MAPK signaling pathways in human diseases. Biochim Biophys Acta—Mol Basis Dis. 2010; 1802: 396–405. doi: 10.1016/j.bbadis.2009.12.009
18. Penton AL, Leonard LD, Spinner NB. Notch signaling in human development and disease. Semin Cell Dev Biol. 2012; 23: 450–457. doi: 10.1016/j.semcdb.2012.01.010 PMID: 22306179
19. Clevers H, Nusse R. Wnt/β-Catenin Signaling and Disease. Cell. 2012; 149: 1192–1205. doi: 10.1016/j.cell.2012.05.012 PMID: 22682243
20. Nicholas WL, Dougherty EC, Hansen EL. AXENIC CULTIVATION OF CAENORHARDITIS BRIGGSAE (NEMATODA: RHABDITIDAE) WITH CHEMICALLY UNDEFINED SUPPLEMENTS; COMPARATIVE STUDIES WITH RELATED NEMATODES*. Ann N Y Acad Sci. 1959; 77: 218–236. doi: 10.1111/j.1749-6632.1959.tb36902.x
21. Thompson OA, Snoek LB, Nijveen H, Sterken MG, Volkers RJM, Brenchley R, et al. Remarkably Divergent Regions Punctuate the Genome Assembly of the Caenorhabditis elegans Hawaiian Strain CB4856. Genetics. 2015; 200: 975–989. doi: 10.1534/genetics.115.175950 PMID: 25995208
22. Andersen EC, Gerke JP, Shapiro JA, Crissman JR, Ghosh R, Bloom JS, et al. Chromosome-scale selective sweeps shape Caenorhabditis elegans genomic diversity. Nat Genet. 2012; 44: 285–290. doi: 10.1038/ng.1050 PMID: 22286215
23. Hodgkin J, Doniach T. Natural variation and copulatory plug formation in Caenorhabditis elegans. Genetics. 1997; 146: 149–64. PMID: 9136008
24. Li Y, Álvarez OA, Gutteling EW, Tijsterman M, Fu J, Riksen JAG, et al. Mapping Determinants of Gene Expression Plasticity by Genetical Genomics in C. elegans. PLoS Genet. 2006; 2: e222. doi: 10.1371/journal.pgen.0020222 PMID: 17196041
25. Elvin M, Snoek LB, Frejno M, Klemstein U, Kammenga JE, Poulin GB. A fitness assay for comparing RNAi effects across multiple C. elegans genotypes. BMC Genomics. 2011; 12: 510. doi: 10.1186/1471-2164-12-510 PMID: 22004469
26. Rodriguez M, Snoek LB, Riksen JAG, Bevers RP, Kammenga JE. Genetic variation for stress-response hormesis in C. elegans lifespan. Exp Gerontol. 2012; 47: 581–587. doi: 10.1016/j.exger.2012.05.005 PMID: 22613270

27. Snoek LB, Van der Velde KJ, Arends D, Li Y, Beyer A, Elvin M, et al. WormQTL—public archive and analysis web portal for natural variation data in Caenorhabditis spp. Nucleic Acids Res. 2013; 41: D738–D743. doi: 10.1093/nar/gks1124 PMID: 23180786

28. Li Y, Breitling R, Snoek LB, van der Velde KJ, Swertz MA, Riksen J, et al. Global Genetic Robustness of the Alternative Splicing Machinery in Caenorhabditis elegans. Genetics. 2010; 186: 405–410. doi: 10.1534/genetics.110.119677 PMID: 20610403

29. Viñuela A, Snoek LB, Riksen JAG, Kammenga JE. Genome-wide gene expression regulation as a function of genotype and age in C. elegans. Genome Res. 2010; 20: 929–937. doi: 10.1101/gr.102160.109 PMID: 20488933

30. Viñuela A, Snoek LB, Riksen JAG, Kammenga JE. Aging Uncouples Heritability and Expression-QTL in Caenorhabditis elegans. G3. 2012; 2: 597–605. doi: 10.1534/g3.112.002212 PMID: 22670229

31. Snoek LB, Sterken MG, Volkers RJM, Klatter M, Bosman KJ, Bevers RPJ, et al. A rapid and massive gene expression shift marking adolescent transition in C. elegans. Sci Rep. 2014; 4: 3912. doi: 10.1038/srep03912 PMID: 24468752

32. Lange V, Picotti P, Domon B, Aebersold R. Selected reaction monitoring for quantitative proteomics: a tutorial. Mol Syst Biol. 2008; 4: 222. doi: 10.1038/msb.2008.61 PMID: 18854821

33. Gallien S, Duriez E, Domon B. Selected reaction monitoring applied to proteomics. J Mass Spectrom. 2011; 46: 298–312. doi: 10.1002/jms.1895 PMID: 21394846

34. Wang M, Weiss M, Simonovic M, Haertinger G, Schrimpf SP, Hengartner MO, et al. PaxDb, a Database of Protein Abundance Averages Across All Three Domains of Life. Mol Cell Proteomics. 2012; 11: 492–500. doi: 10.1074/mcp.O111.014704 PMID: 22535208

35. Kamkina P, Snoek LB, Grossmann J, Volkers RJM, Sterken MG, Daube M, et al. Natural genetic variation differentially affects the proteome and transcriptome in C. elegans. Mol Cell Proteomics. 2015; In press.

36. Krzywinski M, Altman N. Points of Significance: Visualizing samples with box plots. Nat Methods. 2014; 11: 119–120. doi: 10.1038/nmeth.2813 PMID: 24645192

37. Rieseberg LH, Archer MA, Wayne RK. Transgressive segregation, adaptation and speciation. Heredity (Edinb). 1999; 83: 363–372. doi: 10.1038/sj.hdy.6886170

38. Rieseberg LH, Widmer A, Arntz AM, Burke B. The genetic architecture necessary for transgressive segregation is common in both natural and domesticated populations. Philos Trans R Soc B Biol Sci. 2003; 358: 1141–1147. doi: 10.1098/rstb.2003.1283

39. Visscher PM, Hill WG, Wray NR. Heritability in the genomics era—concepts and misconceptions. Nat Rev Genet. 2008; 9: 255–266. doi: 10.1038/nrg2322 PMID: 18319743

40. Snoek LB, Joeri van der Velde K, Li Y, Jansen RC, Swertz MA, Kammenga JE. Worm variation made accessible: Take your shopping cart to store, link, and investigate! Worm. 2014; 3: e28357. doi: 10.4161/worm.28357 PMID: 24843834

41. van der Velde KJ, de Haan M, Zych K, Arends D, Snoek LB, Kammenga JE, et al. WormQTLHD—a web database for linking human disease to natural variation data in C. elegans. Nucleic Acids Res. 2014; 42: D794–D801. doi: 10.1093/nar/gkt1044 PMID: 24217915

42. Albert FW, Kruglyak L. The role of regulatory variation in complex traits and disease. Nat Rev Genet. Nature Publishing Group; 2015; 16: 197–212. doi: 10.1038/nrg3891

43. Rockman MV, Skrovanek SS, Kruglyak L. Selection at linked sites shapes heritable phenotypic variation in C. elegans. Science. 2010; 330: 372–376. doi: 10.1126/science.1194208 PMID: 20947766

44. Ghazalpour A, Bennett B, Petyuk VA, Orozco L, Hagopian R, Mungrue IN, et al. Comparative Analysis of Proteome and Transcriptome Variation in Mouse. Snyder M, editor. PLoS Genet. 2011; 7: e1001393. doi: 10.1371/journal.pgen.1001393

45. Foss EJ, Radulovic D, Shaffer SA, Goodlett DR, Kruglyak L, Bedalov A. Genetic Variation Shapes Protein Networks Mainly through Non-transcriptional Mechanisms. Eisen MB, editor. PLoS Biol. 2011; 9: e1001144. doi: 10.1371/journal.pbio.1001144 PMID: 21909241

46. Skelly DA, Merrihew GE, Riffle M, Connelly CF, Kerr EO, Johansson M, et al. Integrative phenomics reveals insight into the structure of phenotypic diversity in budding yeast. Genome Res. 2013; 23: 1496–1504. doi: 10.1101/gr.155762.113 PMID: 23720455

47. Albert FW, Treusch S, Shockley AH, Bloom JS, Kruglyak L. Genetics of single-cell protein abundance variation in large yeast populations. Nature. Nature Publishing Group; 2014; 506: 494–497. doi: 10.1038/nature12904

48. Parts L, Liu Y-C, Tekkedil MM, Steinmetz LM, Caudy AA, Fraser AG, et al. Heritability and genetic basis of protein level variation in an outbred population. Genome Res. 2014; 24: 1363–1370. doi: 10.1101/gr.170506.113 PMID: 24823668

49. Wang X, Wu Y-C, Fadok VA, Lee M-C, Gengyo-Ando K, Cheng L-C, et al. Cell corpse engulfment mediated by C. elegans phosphatidylserine receptor through CED-5 and CED-12. Science. 2003; 302: 1563–1566. doi: 10.1126/science.1087641 PMID: 14645848

50. Yang H, Chen Y-Z, Zhang Y, Wang X, Zhao X, Godfroy JI, et al. A lysine-rich motif in the phosphatidylserine receptor PSR-1 mediates recognition and removal of apoptotic cells. Nat Commun. 2015; 6: 5717. doi: 10.1038/ncomms6717 PMID: 25564762

51. Lettre G, Hengartner MO. Developmental apoptosis in C. elegans: a complex CEDnario. Nat Rev Mol Cell Biol. 2006; 7: 97–108. doi: 10.1038/nrm1836 PMID: 16493416

52. Gumienny TL, Lambie E, Hartwieg E, Horvitz HR, Hengartner MO. Genetic control of programmed cell death in the Caenorhabditis elegans hermaphrodite germline. Development. 1999; 126: 1011–22. PMID: 9927601

53. Reddien PW, Horvitz HR. CED-2/CrkII and CED-10/Rac control phagocytosis and cell migration in Caenorhabditis elegans. Nat Cell Biol. 2000; 2: 131–6. doi: 10.1038/35004000 PMID: 10707082

54. Page BD, Diede SJ, Tenlen JR, Ferguson EL. EEL-1, a Hect E3 ubiquitin ligase, controls asymmetry and persistence of the SKN-1 transcription factor in the early C. elegans embryo. Development. 2007; 134: 2303–2314. doi: 10.1242/dev.02855 PMID: 17537795

55. Schrimpf SP, Weiss M, Reiter L, Ahrens CH, Jovanovic M, Malmström J, et al. Comparative Functional Analysis of the Caenorhabditis elegans and Drosophila melanogaster Proteomes. Weissman JS, editor. PLoS Biol. 2009; 7: e48. doi: 10.1371/journal.pbio.1000048 PMID: 19260763

56. Käll L, Storey JD, MacCoss MJ, Noble WS. Assigning Significance to Peptides Identified by Tandem Mass Spectrometry Using Decoy Databases. J Proteome Res. 2008; 7: 29–34. doi: 10.1021/pr700600n PMID: 18067246

57. Kuster B, Schirle M, Mallick P, Aebersold R. Innovation: Scoring proteomes with proteotypic peptide probes. Nat Rev Mol Cell Biol. 2005; 6: 577–583. doi: 10.1038/nrm1683 PMID: 15957003

58. MacLean B, Tomazela DM, Shulman N, Chambers M, Finney GL, Frewen B, et al. Skyline: an open source document editor for creating and analyzing targeted proteomics experiments. Bioinformatics. 2010; 26: 966–968. doi: 10.1093/bioinformatics/btq054 PMID: 20147306

59. Picotti P, Rinner O, Stallmach R, Dautel F, Farrah T, Domon B, et al. High-throughput generation of selected reaction-monitoring assays for proteins and proteomes. Nat Methods. 2010; 7: 43–46. doi: 10.1038/nmeth.1408 PMID: 19966807

60. Perkins DN, Pappin DJC, Creasy DM, Cottrell JS. Probability-based protein identification by searching sequence databases using mass spectrometry data. Electrophoresis. 1999; 20: 3551–3567. doi: 10.1002/(SICI)1522-2683(19991201)20:18<3551::AID-ELPS3551>3.0.CO;2-2 PMID: 10612281

61. Escher C, Reiter L, MacLean B, Ossola R, Herzog F, Chilton J, et al. Using iRT, a normalized retention time for more targeted measurement of peptides. Proteomics. 2012; 12: 1111–1121. doi: 10.1002/pmic.201100463 PMID: 22577012

62. Reiter L, Rinner O, Picotti P, Hüttenhain R, Beck M, Brusniak M-Y, et al. mProphet: automated data processing and statistical validation for large-scale SRM experiments. Nat Methods. 2011; 8: 430–435. doi: 10.1038/nmeth.1584 PMID: 21423193

63. Chang C-Y, Picotti P, Hüttenhain R, Heinzelmann-Schwarz V, Jovanovic M, Aebersold R, et al. Protein Significance Analysis in Selected Reaction Monitoring (SRM) Measurements. Mol Cell Proteomics. 2012; 11: M111.014662. doi: 10.1074/mcp.M111.014662 PMID: 22190732

64. R Core Team. R: A Language and Environment for Statistical Computing. R Foundation for Statistical Computing, Vienna, Austria; Available: http://www.r-project.org/

65. Choi M, Chang C-Y, Vitek O. MSstats: Protein Significance Analysis in DDA, SRM and DIA for Label-free or Label-based Proteomics Experiments. 2014.

66. Pedrioli PGA, Eng JK, Hubley R, Vogelzang M, Deutsch EW, Raught B, et al. A common open representation of mass spectrometry data and its application to proteomics research. Nat Biotechnol. 2004; 22: 1459–1466. doi: 10.1038/nbt1031 PMID: 15529173

67. Benjamini Y, Hochberg Y. Controlling the False Discovery Rate: A Practical and Powerful Approach to Multiple Testing. J R Stat Soc Ser B. 1995; 57: 289–300.

68. Snoek LB, Orbidans HE, Stastna JJ, Aartse A, Rodriguez M, Riksen JAG, et al. Widespread Genomic Incompatibilities in Caenorhabditis elegans. G3. 2014; 4: 1813–1823. doi: 10.1534/g3.114.013151 PMID: 25128436

69. Sendoel A, Maida S, Zheng X, Teo Y, Stergiou L, Rossi C-A, et al. DEPDC1/LET-99 participates in an evolutionarily conserved pathway for anti-tubulin drug-induced apoptosis. Nat Cell Biol. 2014; 16: 812–820. doi: 10.1038/ncb3010 PMID: 25064737

# POLINA KAMKINA

Ukraine
polina.kamkina@uzh.ch
08.09.1987

## EDUCATION

| | |
|---|---|
| 10/2012 - today | **PhD candidate** at University of Zurich, Life Science Zurich Graduate School |
| 09/2011 - 09/2012 | **Master of Science (M. Sc.)**, University of Zurich<br>„Quantitative proteome analysis of natural variation in human cancer pathways in *C. elegans*"<br>major subject: mass spectrometry, quantitative traits, genetics |
| 09/2009 - 03/2011 | **Bachelor of Science (B.Sc.)**, University of Zurich |
| 08/2006-08/2009 | Bachelor of Arts, Zurich University of the Arts |
| 09/2004 - 07/2006 | Assessments in Biology, National University 'Ivan Franko', Lviv, Ukraine |
| 09/1994 – 06/2004 | University entrance diploma, High School in Lviv, Ukraine |

## PUBLICATIONS DURING DOCTORAL STUDIES

Kamkina, P., Snoek, L.B., Grossmann, J., Volkers, R.J.M., Sterken, M.G., Daube, M., Roschitzki, B., Fortes, C., Schlapbach, R., Roth, A., et al. (2016). Natural Genetic Variation Differentially Affects the Proteome and Transcriptome in Caenorhabditis elegans. Mol. Cell. Proteomics 15, 1670–1680.

Singh, K.D., Roschitzki, B., Snoek, L.B., Grossmann, J., Zheng, X., Elvin, M., Kamkina, P., Schrimpf, S.P., Poulin, G.B., Kammenga, J.E., et al. (2016). Natural Genetic Variation Influences Protein Abundances in C. elegans Developmental Signalling Pathways. PLOS ONE 11, e0149418.

## LANGUAGES

| | | | |
|---|---|---|---|
| Ukrainian | native speaker (C2) | Russian | native speaker (C2) |
| German | advanced (C1) | Englisch | advanced (C1) |